Regulation of Vascular Endothelial Growth Factor-A (VEGF) in Human Endometrial Stromal Cell Decidualisation

LING TING

A thesis submitted to University of Birmingham for the degree of DOCTOR OF PHILOSOPHY

Institute of Cardiovascular Sciences
College of Medical and Dental Sciences
University of Birmingham

Nov 2018

ABSTRACT

Decidualisation of the endometrium is essential for successful implantation and pregnancy. Central to this is the progesterone-driven differentiation of human endometrial stromal cells (hESC) to secretory decidual cells which is dependent on the up-regulation of the Forkhead box O1 (FOXO1) transcription factor. Vascular endothelial growth factor-A (VEGF) is essential for vascular remodelling in the endometrium and perturbation of VEGF activity can lead to infertility, recurrent miscarriage and preeclampsia. However, little is known about the factors that regulate VEGF activity during ESC decidualisation. To investigate this, primary hESC and the St-T1b cell line were differentiated *in vitro* to decidual cells, confirmed by the up-regulation of decidual markers including FOXO1. VEGF mRNA and protein production was strongly induced with decidualisation leading to increased angiogenic activity. Interestingly, secretion of soluble Flt-1 receptor (sFlt-1), the physiological inhibitor of VEGF, decreased significantly upon hESC decidualisation. FOXO knock-down or over-expression in hESC showed that FOXO1 up-regulates VEGF, whilst FOXO3A inhibits its expression. FOXO1 increased *VEGF* promoter activity and in chromatin immunoprecipitation assays bound directly to three sites identified in the *VEGF* gene promoter in decidual hESC. In contrast, FOXO3A bound the same regions in the *VEGF* promoter in proliferative and decidual hESC. The Flt-1 receptor was detected on the surface of hESC and maintained during decidualisation. VEGF induced Akt and MAPK kinase signalling and promoted hESC migration and invasion. Collectively, these findings demonstrate that the increased VEGF activity of decidual hESC is a result of FOXO1-driven *VEGF* expression and concomitant decrease in sFlt-1 secretion. They also highlight an antagonist relationship between FOXO1 and FOXO3A in the control of *VEGF* expression which may have implications for endometrial and pregnancy associated disorders.

DEDICATION

Apart from self-efforts, every challenging work needs guidance of elders especially those who were close to our heart.

My humble effort I dedicate to my sweet and loving

Mom & Dad,

Mr. Ting Sing Kong & Mrs. Chuo Teck Iyen

Whose love, encouragement, support and prays of day and night make me able to get such success and honour.

Brothers, sister, and sister in laws,

Chuong, Chii, Chang, da sao, er sao

For their external love, suggesting and motivating until the last of this thesis.

And

IN MEMORY OF

my grandparents,

Mr. Chou Kuoh Tung and Mrs. Ling Ngiik Sieng

whose inspired me to be strong despite of many obstacles in life. I miss them every day, but I am glad to know they saw this process through to its completion.

I do expect this thesis can make all of you proud.

ACKNOWLEDGEMENTS

First, I would like to thank my supervisors, Dr. Peter Hewett and Dr. Sarah Conner for their never-ending support, encouragement, patience, and ideas. Dr. Peter Hewett has helped me tremendously in structuring my research and guiding me in my project's development. Dr. Sarah Conner who has fulfilled an advisory role during my Ph.D. studies. Both of them have guided me, gave me not only the chance to develop research skills, but also attend conferences. I would not be the scientist I am today without them as my supervisors. I will always be grateful for their mentorship and support.

I give a very special thank you to Dr. Phillip Kitchen, who helped me a great deal in performing a variety of laboratory skills especially ChIP and was always there when I needed help. My PhD studies would have taken a significantly longer time if I would have not received help from him. I would like to give special thanks to Professor Janesh Gupta from Birmingham Women's Hospital who helped in consenting the endometrial tissues from the patient. I am extremely grateful to all the women who consented to donate endometrial samples for my research purposes. And also Dr. Victoria Health for help in performing the tube formation assay.

Last but not least, I thank to my family and friends. My parents, Ting Sing Kong and Chuo Teck Iyen for them believe in me. Without their love and guidance, I would not be the person I am today. Also, special thanks go out to my hang out buddies especially, Josephine and Katrina who made life interesting at UOB these past four years. In the end, I would like to thank UOB Taekwondo Club, an amazing club where I know awesome instructors and friends, found another passion in my life and am as fit as I can be mentally and physically today.

TABLE OF CONTENTS

LIST OF FIGURES

LIST OF TABLES

LIST OF ABBREVIATIONS

NO	ABBREVIATION	MEANING
1	Ab	Antibody
2	AKT	Serine/threonine kinase
3	APS	Ammonium Persulphate
4	ART	Assisted Reproductive Technology
5	BMP2	Bone Morphogenetic Protein 2
6	BSA	Bovine Serum Albumin
7	C/EBPβ	CCAAT enhancer binding protein β
8	cAMP	Cyclic Adenosine Monophosphate
9	cDNA	Complementary DNA
10	ChIP	Chromatin Immunoprecipitation
11	CM	Conditioned Medium
12	CO_2	Carbon Dioxide
13	CRE	Cre Recombinase
14	CREB	cAMP Response Element-Binding Protein
15	CREM	cAMP Response Element Modulating protein
16	CRH	Corticotrophin Releasing Hormone
17	DAPI	4',6-Diamidino-2-phenylindole
18	ddH_2O	Double Distilled Water
19	DEPC	Diethyl Pyrocarbamate
20	Depp	Decidual protein induced by Progesterone
21	DMEM	Dulbecco's Modified Eagle's Medium
22	DMEM/F-12	Dulbecco's Modified Eagle's Medium and Ham's F-12 nutrient mixture
23	DMSO	Dimethyl Sulfoxide
24	dPRL	Decidual Prolactin
25	E2	17β-Oestradiol
26	ECL	Enhanced Chemiluminescence
27	ECM	Extracellular Matrix
28	EDTA	Ethylenediaminetetraacetic Acid
29	ELISA	Enzyme-Linked Immunosorbent Assay
30	EMT	Epithelial-Mesenchymal Transition
31	EPAC	Exchange Protein directly Activated by cAMP
32	ER	Oestrogen receptor
33	ESC	Endometrial Stromal Cell
34	EVT	Extravillous Trophoblast
35	FACS	Fluorescence-Activated Cell Sorting
36	FBS	Foetal Bovine Serum
37	FHRE	Forkhead Response Element
38	FHRE-luc	FHRE luciferase reporter construct
39	FITC	Fluorescein Isothiocyanate
40	Flt-1	Fms-like Tyrosine Kinase-1/ VEGFR-1
41	FOXO	Forkhead Box protein
42	FSH	Follicle Stimulating Hormone

43	GFP	Green Fluorescence Protein
44	GOI	Gene of Interest
45	H_2O	Water
46	H_2O_2	Hydrogen Peroxide
47	HB-EGF	Heparin-Binding Epidermal Growth Factor
48	hCG	Human Chorionic Gonadotrophin
49	hESC	Human endometrial stromal cell
50	HIF-1	Hypoxia Inducible Factor-1
51	HMEC-1	Human Microvessels Endothelial Cell
52	HBP-1	HMG Box protein-1
53	HOX	Homeobox Transcription Factors
54	HOXA10	Homeobox A10
55	HRE	Hypoxia Response Element
56	HRP	Horseradish Peroxidase
57	HUVEC	Human Umbilical Vein Endothelial Cell
58	IF	Immunofluorescence
59	IGF-1	Insilin-like growth factor-1
60	IGFBP-1	Insulin Growth Factor Binding protein -1
61	IKK	IkB kinase
62	IL-11	Interleukin-11
63	IP	Immunoprecipitation
64	IUGR	Intrauterine Growth Restriction
65	IVF	*In vitro* Fertilisation
66	JNK	c-Jun N-terminal Kinase
67	LH	Luteinizing Hormone
68	LIF	Leukemia Inhibitor Factor
69	MET	Mesenchymal-Epithelial Transition
70	MMP	Matrix Metalloproteinase
71	MMP	Matrix Metalloproteases
72	MOI	Multiplicity of Infection
73	MPA	Medroxy-Progesterone Acetate
74	MST1	Mammalian Sterile 20-Kinase-1
75	NACI	Sodium Chloride
76	NRP	Neuropilin
77	PBS	Dulbecco's phosphate buffered saline (Ca^{2+}-/Mg^{2+}- free)
78	PCOS	Polycystic Ovarian Syndrome
79	PCR	Polymerase Chain Reaction
80	PDVF	Polyvinylidene Fluoride
81	PEI	Polyethylenimine
82	Pen/Strep	Penicillin/Streptomycin
83	p*Flt-1*-Luc	Full-length Flt-1 promoter luciferase reporter construct
84	pGL-*VEGF*-Luc	VEGF promoter luciferase reporter construct
85	PI	Propidium Iodine
86	PI3K	Phosphatidylinositol-4,5-bisphosphate 3-kinase
87	PIGF	Placenta Growth Factor

88	PKA	Protein kinase A
89	PLZF	Promelocytic Leukemia Zinc Finger
90	PR	Progesterone receptor
91	PRE	Progesterone Response Elements
92	PRL	Prolactin
93	qPCR	Real-Time Quantitative Polymerase Chain Reaction
94	RIPA	Radioimmunoprecipitation Assay Buffer
95	ROS	Reactive Oxygen Species
96	RPMI	Roswell Park Memorial Institute
97	RT-PCR	Reverse Transcriptase Polymerase Chain Reaction
98	SDS	Sodium Dodecyl Sulfate
99	SDS-PAGE	Sodium Dodecyl Sulfate–Polyacrylamide Gel Electrophoresis
100	sFlt-1	Soluble Flt-1/ Soluble VEGFR-1
101	SGK	Serum-and Glucocorticoid-inducible Kinase
102	SOD2	Superoxide Dimutase
103	STAT3	Signal Transducer and Activator of Transcription 3
104	TAE	Tris-Acetate-EDTA
105	TEMED	N.N.N'N' Tetramethylethylenediamine-1,2-Diamine
106	TGF	Transforming Growth Factor
107	uNK	Uterine Natural Killer Cell
108	VEGF	Vascular Endothelial Growth Factor -A
109	VEGFR	Vascular Endothelial Growth Factor Receptor

CHAPTER 1:
GENERAL INTRODUCTION

1.1 Introduction

Pregnancy is a complex process that requires decidualisation of the maternal endometrium, blastocyst implantation, and placentation (Okada *et al.,* 2017). The endometrium is the most crucial determinant of successful embryo implantation (Gellersen & Brosens, 2014). Decidualisation is one of the most critical events occurring within the human endometrium throughout the pregnancy. Failure of this process results in infertility (Lee *et al.,* 2007). Whereas, impairment of decidualisation alters embryo-maternal interactions, which may lead to recurrent pregnancy loss, preeclampsia, and poor embryo selection (Salker *et al.,* 2010; Macklon & Brosens, 2014). Although many anatomical, endocrine, immunological, and genetic perturbations have been associated with pregnancy complications like recurrent miscarriage, none of these are specific to the condition. The limitation of IVF is largely due to the endometrial function and receptivity which lead to lower implantation rates (Shapiro *et al*., 2011; Penzias, 2012). An improved understanding of normal endometrial-receptivity and the molecular mechanisms involved should enhance embryo implantation and therefore increase pregnancy to successful delivery rates (Aplin, 2006). It may also lead to a greater understanding of other pathologies of pregnancy like recurrent miscarriage, early pregnancy loss, preeclampsia, intrauterine growth restriction (IUGR), preterm birth and ectopic pregnancy (Venners *et al*., 2004; Brosens *et al*., 2011).

Menstrual pre-conditioning and the repeated inflammatory activities associated with each cycle may be crucial to sensitize the endometrium to environmental signals and coordinate a specific spatial-temporal decidual response (Brosens *et al.,* 2009). Understanding the regulation of gene expression during decidualisation as well as their specific function is important to overcome various pregnancy complications. Vascular endothelial growth factor A (VEGF) is a potent stimulator of vascular remodelling of the maternal blood supply to

support the conceptus, but the precise role(s) of VEGF on the route to successful pregnancy is still unknown.

1.2 The endometrium and the menstrual cycle

1.2.1 The human endometrium

The human uterus consists of three layers: the outer perimetrial layer which is composed of epithelial cells covering the uterus; the middle myometrial muscular layer which contains a highly organised network of arteries and veins; and the inner endometrial layer (**Figure 1.1**). The endometrial lining of the uterus is a unique and dynamic multi-layered tissue consisting of functional and basal layers overlaying the myometrium (Johnson and Everitt, 2007) (**Figure 1.1**). The endometrium is composed of a single layer of luminal epithelium which overlies a network of connective tissue and a multicellular stromal compartment (Gilbert, 2010). The endometrial blood supply enters via the arteries arising from the myometrium, which then split to form basal arteries and spiral arterioles to supply the functional and basal layers (Rogers, 1996) (**Figure 1.1**). A new functional layer regenerates each month from the permanent basal layer and is shed during menstruation if implantation does not occur. Studies have identified epithelial progenitor cells (Chan *et al.*, 2004; Verdi *et al.*, 2014) and mesenchymal stem cells in the human endometrium, which are thought to play a role in the regeneration and maintenance of the endometrium (Masuda *et al.*, 2010).

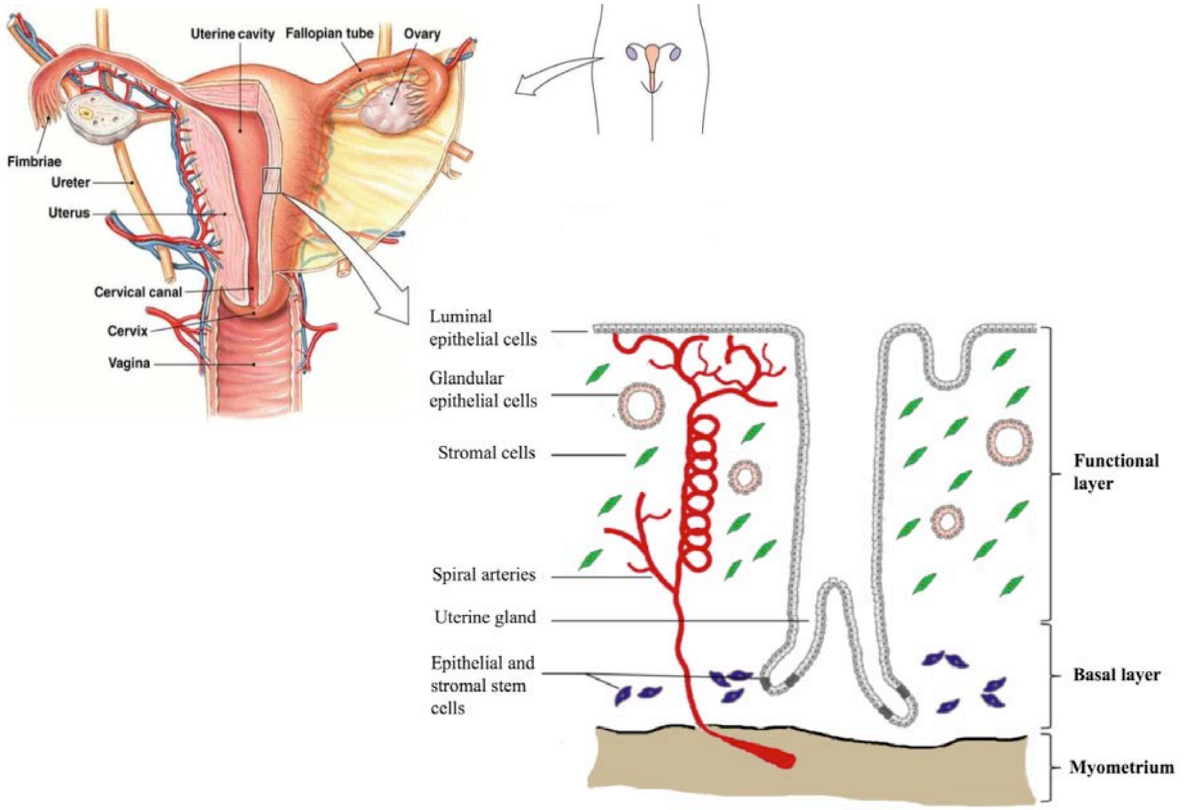

Figure 1.1: The structure of the human endometrium. The functional layer is composed of endometrial luminal and glandular epithelium and stromal cells receiving a blood supply from the spiral arterioles. The basal layer contains stem and progenitor cells which are important for regeneration of the functional layer during the menstrual cycle (adapted from https://www.grepmed.com/images/2497).

1.2.2 Cyclical changes of the endometrium

The endometrium undergoes phases of proliferation, differentiation, tissue degeneration and regeneration with an average full cycle spanning 28 days under the control of ovarian steroid hormones (Gellersen and Brosens, 2014). The ovaries undergo a monthly cycle concurrent with the endometrial cycle to coordinate the release an oocyte with the preparation of the endometrium for implantation of an embryo. The ovarian cycle consists of the follicular and luteal phases. During the follicular phase, follicular granulosa cells produce a large amount of oestrogen initiated by the stimulation of follicle stimulating hormone (FSH), reaching a peak of circulating oestrogen prior to ovulation which induces positive feedback to trigger

the luteinizing hormone (LH) surge and ovulation (Johnson and Everitt, 2007). During the luteal phase (day 14-28), the corpus luteum forms and becomes highly vascularised and begins to secrete high levels of progesterone. If pregnancy occurs, human chorionic gonadotrophin (hCG) secreted by the syncytiotrophoblast of an implanting blastocyst maintains the corpus luteum. Otherwise, the corpus luteum degenerates at the end of luteal phase leading to a decline in both oestrogen and progesterone levels (Critchley and Saunders, 2009) (**Figure 1.2**). The length of the menstrual cycle is variable ranging from 26 to 34 days (Mihm *et al*., 2011) and a typical woman has more than 400 cycles during their reproductive life.

During days 1-5 of the menstrual cycle, the endometrium breaks down and is sloughed off in menses. During the proliferative phase (days 5-13) under the influence of oestrogen, there is growth of the endometrial functional layer through rapid epithelial and stromal cell proliferation. The secretory phase (days 15-28) begins following the onset of progesterone production from corpus luteum. During the mid-secretory phase (days 20-23), the endometrium becomes receptive (**Figure 1.2**). With the rising levels of progesterone, the endometrium stops proliferating and the endometrial stromal cells (ESC) undergo differentiation, via a process called decidualisation (Gellersen and Brosens, 2014; Gellersen *et al.*, 2007) (**Figure 1.2**).

The process of decidualisation is marked by the transformation of elongated spindle-like stromal cells into rounded, enlarged epithelial-like decidual cells (Wynn, 1974; Gellersen *et al.*, 2007). Decidualisation begins around day six post-ovulation in the humans, independent of the presence of a blastocyst (de Ziegler *et al.,* 1998, Gellersen and Brosens, 2014) which is at the onset of the window of implantation (**Figure 1.2**). Decidualisation in the human is very pronounced and includes changes in all compartments of the uterus such as junctional

zone monocytes, local immune cells, spiral arteries, epithelial and major changes in the stromal compartment (Gellersen *et al.*, 2007).

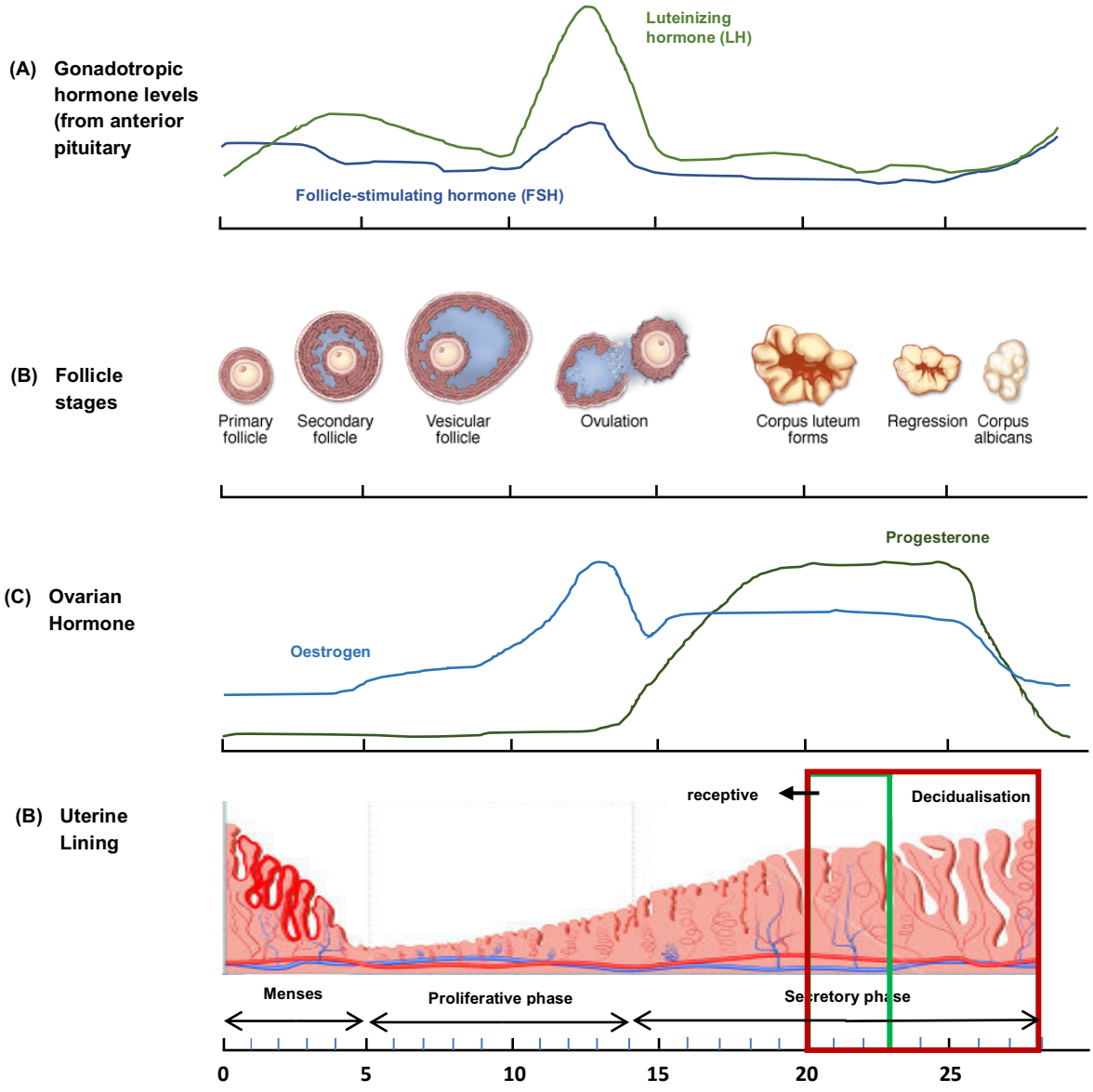

Figure 1.2: Hormone levels through the menstrual cycle. A series of degenerative and regenerative endometrial changes occur on a monthly basis in response to the influence of ovarian hormones. Following ovulation (day 14), progesterone is produced by the newly formed corpus luteum. In the absence of pregnancy, the corpus luteum breaks leading to withdrawal of ovarian hormones resulting in menstruation. The cyclical changes involve transformation of the endometrium into a state where it is most receptive to embryo implantation termed the 'window of implantation' (days 20-23). The elevated progesterone level elevated during the mid-secretory phase triggers decidualisation.

1.3 Decidualisation of human endometrial stromal cells

Decidualisation of human endometrial stromal cells (hESC) is an example of mesenchymal-to-epithelial transition (MET). The interconversion between epithelial and mesenchymal phenotype through MET and the epithelial-mesenchymal transition (EMT) processes is essential for embryogenesis and wound healing during differentiation (Micalizzi *et al.*, 2010; Choi and Diehl, 2009). Undifferentiated hESC are mesenchymal cells with an elongated spindle-shaped fibroblastic appearance (Gellersen & Brosens, 2003; Gellersen *et al.*, 2007). Decidualised hESC are characterised by a marked cell enlargement, rounded nucleus with an increase of nucleoli, expansion of the secretory machinery consisting rough endoplasmic reticulum and the Golgi complex, and cytoplasmic accumulation of glycogen and lipid droplets (Oliver *et al.,* 1999; Christian *et al.,* 2002). This transformation is accompanied by profound biochemical changes. Microarray studies have reported that decidualisation involves sequential reprogramming of functionally related genes involved in extracellular matrix organisation, metabolism, stress response, cell cycle progression, differentiation and apoptosis (**Figure 1.3**) (Giudice, 2004). Therefore, through decidualisation, hESC acquire new biochemical functions that are critical for embryo implantation and successful pregnancy. Upon decidualisation, hESC acquire a secretory phenotype releasing various cytokines, growth factors and proteins that are important for maintaining the decidual phenotype and regulating trophoblast invasion and placental formation (Giudice, 2004). Decidual prolactin (dPRL) and insulin-like growth factor binding protein-1 (IGFBP-1) are the most commonly used markers of decidualisation (Gellersen *et al.*, 2007; Oliver *et al.*, 1999; Tseng *et al.*, 1992).

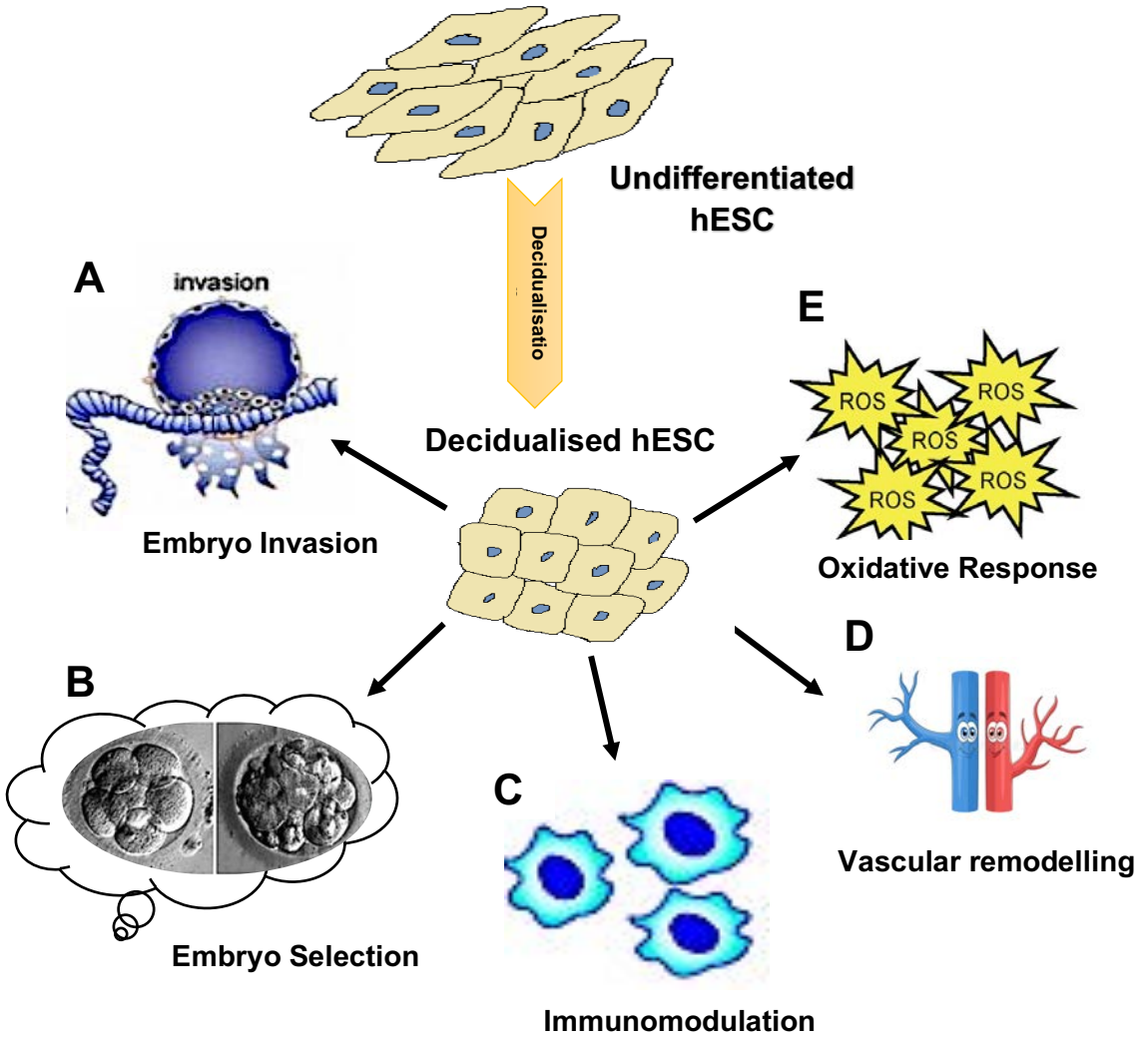

Figure 1.3: Functions of decidualised hESC. Decidualised hESC acquire a secretory phenotype and become specialised epithelioid cells that regulate various biological functions for successful pregnancy: **(A)** Blastocyst/ embryo invasion; **(B)** Selection of high-quality embryos; **(C)** Immune responses to protect the fetal-maternal interface; **(D)** Angiogenesis and vascular remodelling of endometrial spiral arteries to support the growing conceptus; **(E)** Increased resistance to the oxidative stress.

1.3.1 The importance of hESC decidualisation in embryo implantation

Pregnancy relies upon dynamic cross-talk between the embryo and receptive endometrium. In order for successful implantation to occur the endometrium has to undergo changes which optimise the environment to receive and support the developing blastocyst (Hannan *et al.*, 2010; Lee and DeMayo, 2004; Dey *et al.*, 2004). The implantation process can be divided

into three main steps: apposition, attachment and invasion (**Figure 1.4**) (Lee *et al.*, 2011; Norwitz *et al.*, 2001). There are many factors that can lead to implantation failure such as uterine abnormalities, hormonal disorders, immunological factors and infections (Timeva *et al.*, 2014). Recently, changes in the levels of autocrine and paracrine factors during the menstrual cycle have been identified as critical to uterine function (Dimitriadis *et al.*, 2010; Singh *et al.*, 2011; Okada *et al.*, 2014).

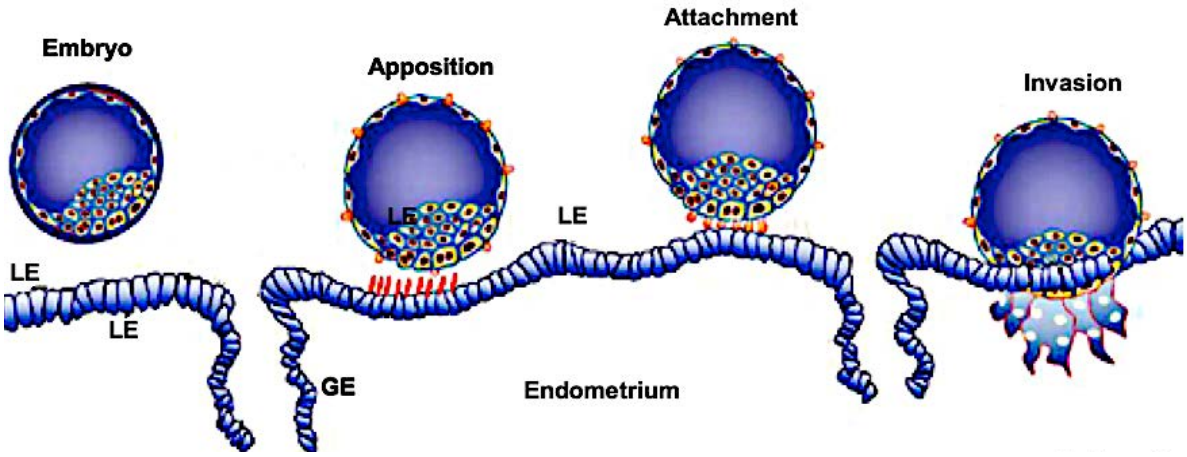

Figure 1.4: Human embryo implantation. The embryo enters the uterus approximately 4 days after fertilisation as a morula. Apposition begins when the blastocyst hatches from the zona pellucida and associates with the endometrial epithelial layer to form an unstable adhesion. This is followed by the firm attachment of blastocyst to the endometrium. Invasion occurs when the embryo invades through the luminal epithelium (LE) and basal lamina deeper into the stroma of uterine lining to reach maternal blood vessels (adapted from Greening *et al.,* 2016).

1.3.1.1 The window of implantation

It is now well-established that endometrial receptivity is a vital part of successful implantation. The receptive period is known as the 'window of implantation' and usually occurs at around day 20-23 of the menstrual cycle, coinciding with the mid-secretory phase (**Figure 1.2**) (Harper, 1992; Achache and Revel, 2006). Deficiencies of endometrial receptivity or the failure of a blastocyst to attach to the endometrium at the right time can cause infertility and there is a strong correlation between implantation occurring beyond the

normal receptivity period and early pregnancy loss (Wilcox *et al.*, 1999). Many studies have attempted to find the useful biomarkers which signify endometrial receptivity including histological dating, immunohistochemistry, and microarray analysis, several genes have been found but the number of common genes that were identified was minimal (Haouzi *et al.,* 2012; Sugawara *et al.,* 2014). However, it was shown that local factors produced during the receptive period including cytokines, growth factors and transcription factors serve to specify endometrial receptivity.

1.3.1.2 Embryo invasion

As discussed earlier, embryo implantation involves embryo apposition and attachment to the endometrial surface, breaching of the luminal epithelium and invasion into the ESC (Loke *et al.,* 1995). Understanding of this process in the human is somewhat limited as it is restricted to the use of animal models and *in vitro* co-culture systems for ethical and practical reasons. Decidualised hESC secrete a number of matrix metalloproteases (MMPs), transforming growth factor β (TGFβ) on the trophoblast (Anacker *et al.*, 2011), which are able to promote embryo invasion due to the chemoattractant ability of their secreted leukocytes (Salamonsen *et al.,* 2007).

1.3.1.3 Embryo selection

It has been reported that secretion of cytokines, chemokines and growth factors from the supernatants of decidualised hESC co-cultured with blastocysts are different if the blastocyst displays signs of developmental arrest and inhibition of interleukins and growth factors (Teklenburg *et al.,* 2010). A few studies have reported that decidual hESC can act as biosensors in recognising compromised embryos and prevent their implantation (Salker *et al.*, 2010; Teklenburg *et al.*, 2010). Decidualised hESC have been shown to migrate more in

the presence of high-quality embryos compared to low-quality embryos using the time-lapse microscopy (Gonzalez *et al.*, 2011; Weimar *et al.*, 2012). However, a mechanism of how hESC contribute to discrimination between high- and low-quality embryos remains unknown.

1.3.1.4 Immunomodulation

Pregnancy is an inflammatory-related process which requires complex immunoregulation to prevent the fetal antigens being recognised by cytotoxic T-cells and to protect the fetal-maternal interface (Cloke *et al.*, 2010). During decidualisation, an influx of innate immune cells (uNK) takes place to tolerate the semi-allogenic embryo and these cells also regulate trophoblast invasion and vascular remodelling through the expression of angiogenic factors, endothelial cell mitogens and chemokines (Koopman *et al.*, 2003; Ledee *et al.*, 2008).

Decidualised ESC also modulate the immune responses at the fetal-maternal interface. Decidual cells play a critical role to ensure sufficient balance of specialised macrophages and uNK to prevent the priming of maternal T cells to paternal anti-allogens (Hanna *et al.*, 2006; Lash *et al.*, 2006). The importance of uNK cells in angiogenesis has also been highlighted by studies in mice lacking uNK cells which show impaired angiogenesis (Greenwood *et al.*, 2000) and develop conditions such as preeclampsia and fetal growth restriction (Zhang *et al.*, 2011).

1.3.1.5 Oxidative stress responses

During early pregnancy, there is vascular remodelling and as a consequence oxygen concentrations fluctuate profoundly at the fetal-maternal interface (Burton *et al.*, 1999; Brosens *et al.*, 2009). Due to these changes and inflammatory responses, reactive oxygen species (ROS) including hydroxy radicals, superoxide anions and hydrogen peroxide are produced. ROS, when not attenuated by antioxidative defences, cause nucleic acid and

protein damage and subsequent cell death (Valko *et al.,* 2007). Decidualised hESC acquire resistance to oxidative cell death by producing ROS scavengers such as superoxide dismutase 2 (SOD2), which is up-regulated by the forkhead box protein O1 (FOXO1) transcription factor (Takano *et al.*, 2007). In contrast, ROS are reported to up-regulate forkhead box protein O3A (FOXO3A) in undifferentiated cells which triggers apoptosis under oxidative stress (Kajihara *et al.*, 2006). Silencing of FOXO3A in ESC can prevent apoptosis (Kajihara *et al.,* 2006). Therefore, ESC only adopt pro-survival behaviour upon decidualisation.

1.4 Use of hESC *in vitro* to model decidualisation and its ethical limitations

A failure or impairment of decidualisation can result in infertility or altered embryo-maternal interactions which can cause poor embryo selection, recurrent pregnancy loss and preeclampsia (Salker *et al.,* 2010; Macklon & Brosens, 2014). Determining the regulation and roles of differentially expressed genes during decidualisation may be important to overcome these conditions. Human ESC (hESC) obtained from endometrial biopsies or after hysterectomy for gynaecology disorders are used widely to study decidualisation (Gellersen and Brosens, 2003). However, ethical restrictions and the limited proliferation of primary hESC *in vitro* has led to the establishment of various immortalised hESC lines through retroviral transduction of telomerase (Krikun *et al.*, 2004; Samalecos *et al.*, 2009; Yuhki *et al.*, 2011) or SV40 large T antigen (Chapdelaine *et al.*, 2006) which provide good models for decidualisation (Samalecos *et al.*, 2009). Moreover, using hESC *in vitro* has greatly advanced our understanding of implantation. Mouse models have also been widely utilised to investigate the process of decidualisation *in vivo*. Non-primate mammals have an oestrus cycle and, in the species, decidualisation of the endometrium only occurs following a signal from an implanting blastocyst. Despite this, the regulation of murine uterine function is

sufficiently similar to the human to allow some relevant information to be gained from mouse models (Paria *et al.*, 2002).

1.5 Clinical perspective: Disorders associated with impaired decidualisation

Humans are a relatively sub-fertile species compared to other mammals with a 20% average monthly fertility rate (Evers, 2002; Gnoth *et al*., 2005). Assisted reproductive techniques (ART) have subsequently been used widely (Diedrich *et al*., 2007). However, despite the rapid improvement, the implantation rate is only 20-30% for *in vitro* fertilisation (IVF) (Scott *et al*, 2013; Schoolcraft and Katz-Jaffe, 2013; Shapiro *et al,* 2011). Successful implantation requires a receptive endometrium and a viable embryo. Failure of decidualisation results in infertility (Gellersen and Brosens, 2014), whereas, impairment of decidualisation alters embryo-maternal interactions. This can cause recurrent pregnancy loss, preeclampsia, and diminished embryo selection (Salker *et al.,* 2010; Macklon and Brosens, 2014). In order to improve pregnancy rates and prevent miscarriage, researchers have been focused on gaining a clearer understanding of the mechanisms involved during the dynamic process of ESC decidualisation and implantation.

1.5.1 Endometriosis

Endometriosis is a female reproductive disorder that results from abnormal extra-uterine growth of endometrial tissue mainly the outer surface of the ovaries, or Fallopian tubes. The cause of endometriosis is still unknown and as yet there is no cure for this disorder. It is associated with serious pelvic pain, heavy menstrual periods and 35-50% of infertile women are diagnosed with endometriosis (Macer and Taylor, 2012). Eutopic endometrium was found to be the underlying cause of infertility and has been shown to exhibit an impaired decidual response. Microarray studies have identified various genes involved in decidualisation and implantation that are aberrantly expressed in the endometrium of women

with endometriosis (Kao *et al.*, 2003). In addition, the expression of decidualisation markers is also altered in endometriosis (Aghajanova *et al.*, 2009; Aghajanova *et al.,* 2010; Su *et al.*, 2015). Lower expression of dPRL and IGFBP-1 mRNA and IGFBP-1 secretion were observed in primary hESC isolated from women with endometriosis compared to cells from healthy women (Aghajanova *et al.*, 2011). FOXO1 mRNA expression was reported to be significantly decreased in endometriosis compared to the healthy endometrium in the secretory phase (Shazand *et al.*, 2004; Burney *et al.*, 2007) which may be due to defective notch signalling (Su *et al.*, 2015).

HOXA10 expression was also found to be reduced in mid-secretory phase hESC from women with endometriosis compared to healthy women (Matsuzaki *et al.*, 2009; Taylor *et al.,* 1999). Taken together, these findings suggest that women with endometriosis show changes in the decidual response including the expression of PRL, IGFBP-1, FOXO1 and HOXA10 which may in part explain the increased infertility associated with this disorder.

1.5.2 Recurrent miscarriage

Recurrent miscarriage is a prevalent cause of reproductive failure. Although many anatomical, endocrine, immunological, and genetic perturbations have been implicated as causes of recurrent miscarriage, none are definitive (Saravelos *et al.*, 2014). Several studies have reported that women with recurrent miscarriages show impaired decidualisation (Teklenburg *et al.,* 2010; Salker *et al.,* 2010). One study found that hESC from women with recurrent miscarriage failed to transition between a pro-inflammatory and anti-inflammatory decidual response (Salker *et al.*, 2012). A large body of research has investigated endometrial defects including the interaction of fetal-maternal endometrial interface and how these lead to the recurrent miscarriage. Decidual cells act as biosensors of embryo viability by recognising, selecting and eliminating defective embryos (Teklenburg *et al.,*

2010). Consistent with this hESC from recurrent miscarriage patients are also reported not to be able to distinguish between high or low-quality embryos (Weimar *et al.*, 2012).

1.5.3 Preeclampsia

Preeclampsia is a severe pregnancy complication which affects ~8% of pregnancies worldwide (Winn *et al*., 2011; Fisher, 2015). This disorder is mainly characterised by hypertension, proteinuria and other signs of maternal vascular damage (Roberts and Cooper, 2001). Currently, there is no cure for preeclampsia other than delivery of the placenta and consequently, the fetus which increases the rate of preterm births (Goldenberg *et al.*, 2008; Duley, 2009). Despite decades of research, a full understanding of preeclampsia pathogenesis remains elusive due to the difficulties in the identification of predictive biomarkers for the development of targeted therapies. The pathogenesis of preeclampsia has been investigated in many studies which have shown that placenta plays a central role (Khong *et al.*, 1986, Zhou *et al.*, 1997). The endometrial contribution to the aetiology of preeclampsia has received little attention. Global transcriptional profiling of chorionic villus samples has demonstrated that defective decidualisation in pregnancies may lead to preeclampsia (Rabaglino *et al.*, 2015). Furthermore, Garrido-Gomez *et al.* (2017) showed the failure of *in vitro* decidualisation in primary hESC isolated from women with previous preeclamptic pregnancies with 129 genes differentially expressed and the conditioned medium (CM) from decidual cells failing to promote trophoblast invasion. This study concluded that PRL and IGFBP-1 could be potential biomarkers for preeclampsia (Garrido-Gomez *et al.*, 2017).

1.5.4 Intrauterine Growth Restriction

Intrauterine growth restriction (IUGR) is a common pregnancy complication that increases the risk for perinatal morbidity and mortality (Pallotto and Kilbride, 2006), diabetes and cardiovascular disease in later life (Gluckman *et al*., 2008). Placental insufficiency resulting in decreased fetal oxygen and nutrient availability is believed to be the most common cause of IUGR (Krishna and Bhalerao, 2011). Abnormal increase in utero-placental blood flow, as a result of inadequate trophoblast invasion into the maternal decidua, has been suggested to cause placental insufficiency leading to IUGR (Gagnon, 2003). However, the molecular mechanisms underlying the development of IUGR remain poorly understood. There are no clinically useful biomarkers for the early detection of IUGR, and currently no specific treatment is available for IUGR once diagnosed (Poljak *et al.*, 2017). Insulin-like growth factor (IGF)-binding protein 1 (IGFBP-1) is the predominant IGFBP that determines IGF-1 bioavailability during pregnancy (Hills *et al.*, 1996). The decidua is also believed to be the primary source of IGFBP-1 in the maternal circulation during pregnancy, thereby regulating the bioavailability of maternal IGF-1, a positive regulator of placental function and growth (Sferruzzi-Perri *et al.*, 2007). Human IUGR is associated with increased IGFBP-1 levels and IGFBP-1 hyperphosphorylation in umbilical cord plasma (Shehab *et al.*, 2014). The decidua synthesizes and secretes IGFBP-1 locally in the maternal-fetal interface regulating the actions of IGF-1, which is known to promote trophoblast invasion and placental function (Lacey *et al*., 2002). A very recent study in hESC following decidualisation *in vitro* demonstrated that hypoxia and leucine deprivation markedly increased IGFBP-1 phosphorylation and decreased IGF-1 bioavailability (Shehab *et al.*, 2017). These findings are consistent with increased of IGFBP-1 phosphorylation in decidualised stromal mesenchymal cells in human IUGR (Singal *et al.*, 2018), which possibility constitutes a link between decreased decidual oxygen and nutrient availability and reduced fetal growth due

to diminished IGF-1 bioavailability, leading to inhibition of trophoblast invasion and placental function. Therefore, maternal IGFBP-1 phosphorylation may constitute a sensitive early pregnancy biomarker for IUGR (Gupta *et al.*, 2019).

1.6 Decidualisation cues

1.6.1 Endocrine cues

Progesterone plays an essential role in gland development, ovulation, decidualisation, implantation, menstruation and maintenance of pregnancy (Brosens *et al.*, 2009). Prior to ovulation, ESC are predominantly under the influence of oestrogen and mount the decidual response following the rise of progesterone levels. It is reported the morphological signs of decidualisation are not seen until nine days following ovulation, indicating that other factors are important to initiate this process (Gellersen and Brosens, 2003). Consistent with these findings, studies with primary hESC show that induction of decidual markers takes 7-10 days of stimulation with progesterone analogues and can be accelerated by other factors for example, relaxin (Tseng *et al.*, 1992; Telgmann *et al.*, 1997). This indicates that progesterone, although is critical for the development and maintenance of the decidualised ESC, is not the primary initiating factor in ESC differentiation (Gellersen and Brosens, 2014).

1.6.2 Paracrine and autocrine signals

A number of growth factors, cytokines, peptides and lipids are secreted following the onset of ESC decidualisation which further promote decidualisation. The heparin-binding epidermal growth factor (HB-EGF) is known to be up-regulated during the mid-secretory phase of the cycle and in hESC decidualisation *in vitro* (Lessey *et al.*, 2002). It is reported that blockade of HB-EGF during decidualisation reduced decidual marker expression in hESC (Chobotova *et al.*, 2005). Transforming growth factor-β1 (TGFβ1) inhibits the

expression of decidualisation markers such as dPRL, IGFBP-1 and tissue factor in isolated primary hESC (Kane *et al.*, 2010). Activin A is a secretory, dimeric glycoprotein of the TGF family which is an early inducer of decidualisation through the up-regulation of MMPs and promotes angiogenesis, inflammation and trophoblast differentiation and adhesion (Jones *et al.*, 2002 & 2006; Menkhorst *et al.*, 2010; Rocha *et al.*, 2012).

Other paracrine factors involved in decidualisation are the interleukin family of cytokines, such as interleukin-11 (IL-11), which is a pro-inflammatory cytokine up-regulated during decidualisation (Dimitriadis *et al.*, 2005). IL-11 receptor knock-out mice are infertile due to a lack of sustained decidualisation resulting in implantation failure (van Mourik *et al.,* 2009). Other interleukins include IL-1β which is important for complete decidualisation and embryo implantation (Strakova *et al.*, 2005) and IL-6, which is mostly produced by endometrial epithelial and stromal cells during implantation and its expression reaches a peak during the secretory phase. Deficiency of IL-6 during decidualisation and placenta development causes recurrent miscarriage (van Mourik *et al.*, 2009). Leukaemia inhibitor factor (LIF), a member of the IL-6 class of cytokines, is an important cytokine for endometrial epithelial cell function. Although it is unclear whether LIF is involved in hESC decidualisation, the LIF receptor is up-regulated in hESC and may be important in pregnancy (Shuya *et al.* 2011).

1.6.3 Cyclic adenosine monophosphate signalling

Activation of the cyclic adenosine monophosphate (cAMP) pathway is essential to initiate decidualisation (Gellersen & Brosens, 2003). Many pieces of evidence suggest that the decidual process is initiated by increased cAMP signalling and sustained activation of the protein kinase A (PKA) pathway (Gellersen & Brosens, 2003; Telgmann *et al.*, 1997). Levels of cAMP increase following exposure of the endometrium to relaxin, prostaglandins,

corticotrophin releasing hormone (CRH) and pituitary gonadotropins following ovulation via activation of α-subunits ligands of G-protein coupled receptors (GPCRs) leading to the catalytic conversion of adenosine triphosphate (ATP) into cAMP by adenylate cyclase (Christian *et al.*, 2002; Dimitriadis *et al.*, 2005). Cyclic AMP predominantly activates the protein kinase A (PKA) by binding to its two regulatory subunits, causing a conformational change that leads to the release of two catalytic subunits to regulate several target proteins in cytoplasm and nucleus (Chen *et al.*, 2008). Several studies show that elevated cAMP levels sensitise hESC to progesterone signalling. First, it is reported that higher levels of cAMP are detected in the endometrial tissues obtained from patients in the secretory phase than in the proliferative phase of the menstrual cycle (Tanaka *et al.*, 1993). Second, basal and prostaglandin-stimulated adenylate cyclase activity is higher in the secretory phase than the proliferative phase (Tanaka *et al.*, 1993). Finally, progesterone treatment of hESC *in vitro* increases intracellular cAMP levels (Brar *et al.*, 1997). In addition, studies on the effect of cAMP or progesterone alone or in combination revealed that cAMP is a potent inducer of the decidual phenotype (**Figure 1.5**) (Tang *et al.*, 1993; Gao *et al.*, 1994; Brosens *et al.*, 1999; Reem *et al.*, 1999).

In the nucleus of hESC, the catalytic subunit of PKA activates a number of target proteins including the cAMP response element binding protein (CREB), cAMP response element modulating protein (CREM), signal transducer and activator of transcription 3 (STAT3), CCAAT-enhancer binding protein (C/EBPβ) and FOXO1 (Christian *et al.*, 2002; Gellersen and Brosens, 2003; Brosens and Gellersen, 2006; Gellersen *et al.*, 2007). The maintenance of cAMP signalling during decidualisation is highlighted by the studies which demonstrate that inhibition of PKA prevents decidual gene expression in hESC (Brar *et al.*, 1997;

Matsuoka *et al.*, 2010). The siRNA-mediated knock-down of the exchange protein directly activated by cAMP (EPAC) also prevents decidualisation in hESC (Kusama *et al.*, 2013).

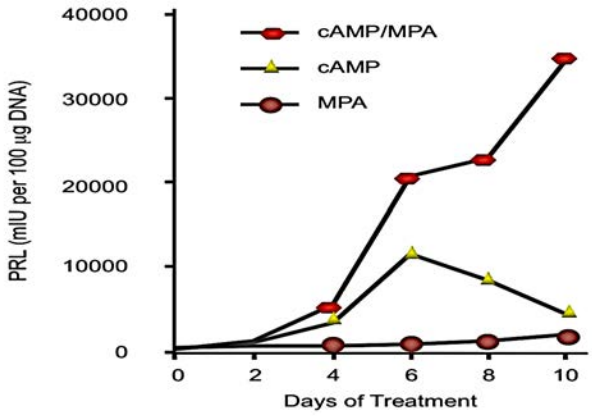

Figure 1.5: Initiation of decidual process is primarily dependent on cAMP. hESC treated with cAMP alone show marked induction of decidual marker PRL but fail to maintain the decidual phenotype. Treatment with medroxyprogesterone (MPA) alone induces PRL after 8 to 10 days of stimulation. The combination of cAMP and MPA has a synergistic effect on PRL production and maintenance of the decidual phenotype (adapted from Brosens *et*

1.6.4 Progesterone signalling

Progesterone acts primarily through activation of the progesterone receptor (PR). PR knock-out in mice leads to diverse reproductive defects including changes in sexual behaviour and implantation (Rider, 2002; Lydon *et al.*, 1995). There are two isoforms of PR, PR-A and PR-B, as a result of alternative promoter usage and translation at two distinct start codons (Wen *et al.*, 1994). Progesterone receptor expression is driven by oestrogen acting on the oestrogen receptor α (ERα) during the proliferation phase (Schultz *et al.*, 2003). It is therefore essential when culturing hESC to have oestrogen present not only to promote growth but to ensure progesterone receptor expression is maintained. PR-A is known to be expressed in stromal cells throughout the menstrual cycle, whereas PR-B is expressed in the mid-proliferative phase (Mote *et al.*, 1999). PR-A is the predominant PR in hESC (Brosens *et al.*, 1999). On binding progesterone, PRs undergo a conformational change leading to phosphorylation,

dimerisation and binding to promoter and enhancer elements of specific target genes (Patel *et al.*, 2015; Jones *et al.*, 2006). PR is able to control the expression of various genes involved in decidualisation even if they lack a progesterone response element (PRE) by hijacking other transcription factors and binding to response elements indirectly (Maruyama and Yoshimura, 2008).

1.6.5 cAMP and progesterone cross-talk

The human endometrium is exposed to progesterone for 7-10 days before decidualisation is observed and only a few genes respond to short-term progesterone exposure; decidual protein induced by progesterone (Depp) and promelocytic leukaemia zinc finger protein (PLZF) (Watanabe *et al.*, 2005). Depp is up-regulated within 30 min of progesterone treatment, however, its function still remains to be determined (Watanabe *et al.*, 2005). PLZF is rapidly induced by progesterone and is indispensable for progesterone-dependent decidualisation (Kommagani *et al.*, 2016).

Treating stromal cells with both cAMP and progesterone *in vitro* enhances decidualisation (Samalecos *et al.*, 2009). However, it has recently become apparent that progesterone does not trigger the decidual response but is required for maintenance of the decidual phenotype and cAMP, via activation of PKA pathway, is the initiating factor sensitising the stromal cells to progesterone signalling leading to the convergence of cAMP-PKA and progesterone pathways as shown in **Figure 1.6**. Firstly, cAMP signalling activates the expression of transcription factors such as STAT3, FOXO1, and C/EBPβ (Christian *et al.*, 2002; Mak *et al.*, 2002) which have the ability to bind to the PR and facilitate PR modulation of gene transcription without the need for a PRE (Gellersen and Brosens, 2003). Second, progesterone-dependent hESC decidualisation occurs simultaneously with intracellular cAMP elevation and is blocked in the presence of PKA inhibitor (Brar *et al.*, 1997).

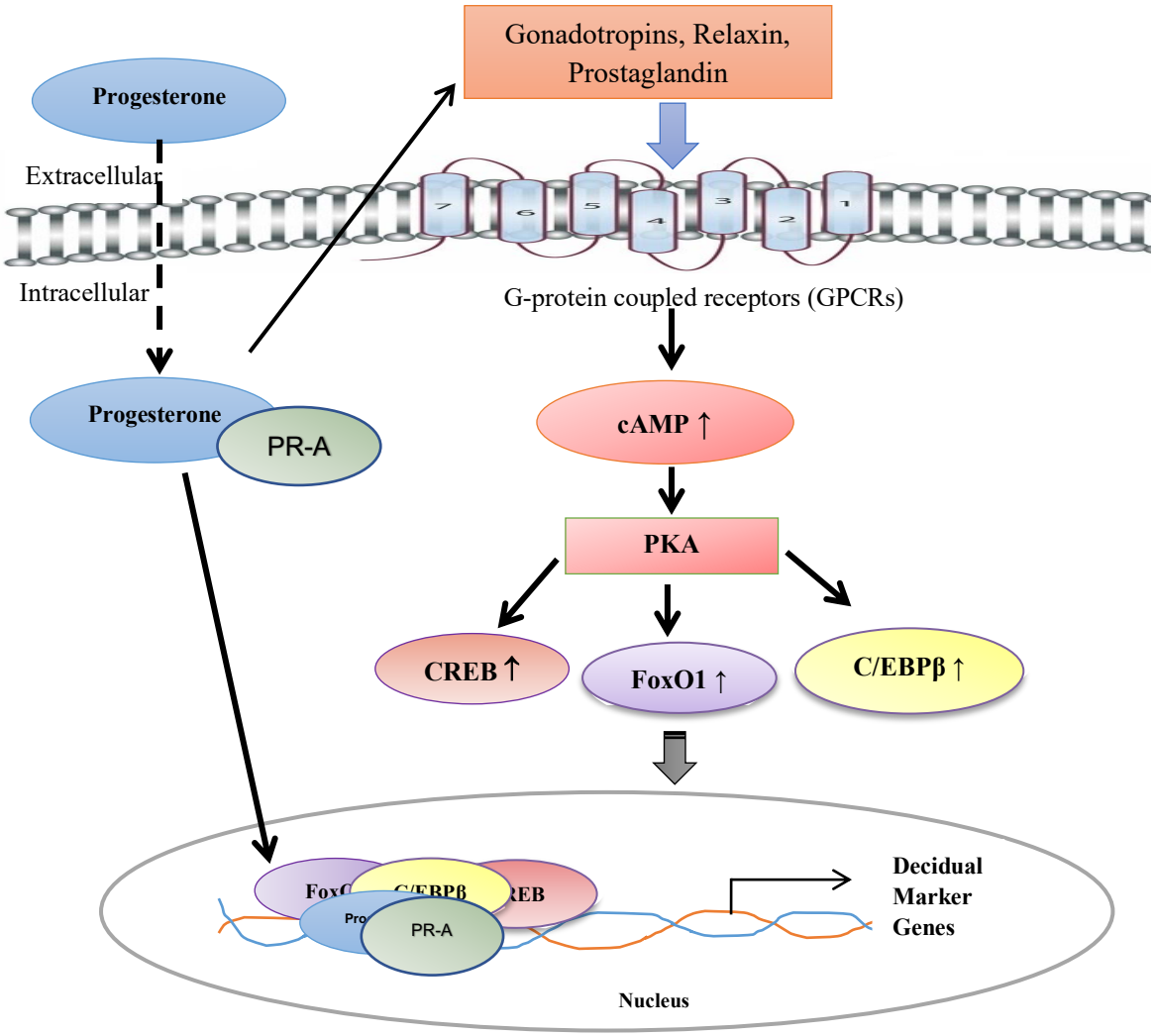

Figure 1.6: Crosstalk between cAMP and progesterone signalling. The activation of G-protein coupled receptors (GPCRs) by ligands such as relaxin, prostaglandin and corticotrophin releasing hormone (CRH) increases cellular cAMP levels. Consequently, there is an accumulation of transcription factors within the nuclei of stromal cells which form a complex with the activated progesterone receptor PR-A, resulting in activation of a number of decidua-specific genes such as prolactin (PRL).

1.6.6 Hormones, cytokines and growth factors that are associated with decidualisation

No	*Abbreviation*	*Protein Name*	*Functions*	*References*
(A) Hormones				
1	E2	Oestrogen	Induces progesterone receptors	Lydon *et al.*, 1995
2	ER-α	Oestrogen receptor-α	Mediates up-regulation of progesterone receptors, endometrial proliferation and differentiation	Kurita *et al.*, 2001
3	ER-β	Oestrogen receptor-β	Up-regulates progesterone receptors; regulates vascular function	Lecce *at al.*, 2001
4	P4	Progesterone	Inducing and maintaining complete decidualisation	Kurita *et al.*, 2001
5	PR-A	Progesterone receptor A	Predominant PR in decidualisation; represses transcriptional activity of PRB	Cheon *et al.*, 2002
6	CRH	Corticotropin-releasing hormone	Auto-immune reaction to an inflammatory component of decidualisation	Kalantaridou *et al*., 2003
7	FSH	Follicle stimulating hormone	Induces cAMP to promote decidualisation	Tang and Gurpide, 1993
8	LH	Luteinizing Hormone	Induces cAMP to initiate decidualisation	Tang and Gurpide,1993
9	hCG	Human chorionic gonadotropin	Prevents degeneration of corpus luteum; variety functions in and outside of embryo-endometrium	Licht *et al.*, 2001
10	PTHLH	Parathyroid hormone-like hormone	Inhibits decidualisation and stimulates stromal cell apoptosis	Sherafat-Kazemzadeh *et al.*, 2011
11	PGE2	Prostaglandin E2	Synergistic with E2/P4 to enhance differentiation and PRL expression	Frank *et al.*, 1994
12	Relaxin	Relaxin	Induces cAMP and PKA pathway to initiate decidualisation	Bartscha and Ivell, 2004
(B) Growth factors				
1	Activin A	Activin A	Trophoblast invasion, promotes decidualisation	Jones *et al.*, 2002
2	EGF	Epidermal growth factor	Mediates the actions of oestrogen and progesterone on the proliferation and differentiation in human endometrium	Watson *et al.*, 1996
3	VEGF	Vascular endothelial growth factor	Stimulates angiogenesis and vasculogenesis	Sugino *et al.*, 2002
4	TGFβ1	Transforming growth factor β1	Pro-apoptotic effect via FasL/Fas system; inhibits decidualisation	Chatzaki *et al.*, 2003
5	Decorin	Decorin	Binds to TGFβ to inhibit trophoblast invasion	Xu *et al.*, 2002
6	BMP2	Bone morphogenetic protein 2	Induces Wnt4 and mediates progesterone to induce decidualisation	Li *et al.*, 2007

7	TNFα	Tumor necrosis factor-α	Activin A mediator; modulates menstruation, proliferation, implantation and decidualisation	Mangioni *et al*., 2005
(C) Cytokines				
1	IL-1β	Interleukin-1β	Pro-inflammatory cytokine stimulates IL-8 and IL-8; inhibits cAMP-mediated decidualisation	Yoshino *et al.*, 2003b
2	IL-8	Interleukin-8	Stimulates trophoblast secretion of progesterone to maintain embryo-endometrium interaction and successful pregnancy	Tsui *et al.*, 2004
3	IL-11	Interleukin-11	Induction of prostaglandins and relaxin to induce decidualisation	Dimitriadis *et al.*, 2005b
4	IL-15	Interleukin-15	Modulates uNK and decidualisation	Ashkar *et al.*, 2003; Godbole and Modi, 2010
5	LIF	Leukaemia inhibitory factor	Enhances decidualisation and up-regulates IL-6 and IL-15, essential for implantation and decidualisation	Shuya *et al.,* 2011
6	MMP2/3/9	Matrix Metallopeptidase 2/3/9	Connective tissue controlling, Extracellular matrix remodelling and trophoblast invasion	Curry and Osteen, 2003
7	TIMP3	Tissue inhibitor metallopeptidase 3	Inhibits MMP9 and regulates trophoblast invasion	Vassilev *et al.*, 2005
8	CBR-1	Cannabinoid receptor 1	Inhibits human decidualisation and encourages apoptosis by a cAMP-dependent mechanism	Kessler *et al.*, 2005
9	SRC-1	steroid receptor coactivator-1	Involved in functional and morphological decidualisation	Maruyama *et al.*, 2004
(D) Signalling				
1	Akt	AKT1 kinase	Intracellular mediator of cAMP/PKA pathway	Yoshino *et al.*, 2003
2	Wnt4/5	Wingless-type MMTV integration	Progesterone mediator of cAMP by up-regulating SOD2 anti-apoptosis	Matsuoka *et al.*, 2010
3	PKA	Protein kinase A	Phosphorylates prolactin promoter and induces prolactin during decidualisation	Tierney *et al.*, 2003
4	Notch1	Notch1	Dual function in the window of implantation: Initially mediates a hCG survival signal for endometrium from the blastocyst and subsequently down-regulated for decidualisation	Afshar *et al.*, 2012

Table 1.1: Hormones, cytokines, growth factors and signalling intermediates that regulate ESC decidualisation via progestereone and cAMP signalling.

1.7 Decidualisation markers

1.7.1 Decidual Prolactin

Decidual prolactin (PRL) is detected around day 22 of the menstrual cycle (Maslar *et al.*, 1986) and reaches a peak during the secretory phase of the menstrual cycle and is an established marker for decidualisation (Tseng *et al.*, 1992). Secretion of PRL during *in vitro* ESC decidualisation is induced by progesterone, cAMP and combination of these, with a prominent role of the PKA signalling pathway in activating transcription of *PRL* (Telgmann and Gellersen, 1998; Tang *et al.*, 1993; Brosens *et al.*, 1999) (**Figure 1.5**). MPA treatment increases PRL mRNA and protein expression in secretory phase of the endometrium (Reis *et al.*, 1999). Whereas, the anti-progestin RU 486 reduces mRNA expression of PRL and PRL receptor in ESC *in vitro* (Tseng and Mazella, 1999) showing that PRL expression is regulated by progesterone. The expression of PRL receptor has been detected in stromal cells in the mid- to late-secretory endometrium (Jones *et al.*, 1998) consistent with its role in decidualisation. Mice deficient in PRL or its receptor are infertile due to a failure in embryo implantation (Horseman *et al.*, 1997; Bole-Feysot *et al.*, 1998). PRL is essential for trophoblast growth and invasion, angiogenesis, cytotoxic activity of uNK cells, as well as regulation of water transport to the maternal compartment (Corbacho *et al.*, 2002; Stefanoska *et al.*, 2013). Consistent with these findings, PRL deficiencies during the window of implantation can cause unexplained infertility in women (Garzia *et al.*, 2004).

1.7.2 Insulin-like growth factor binding protein-1

Insulin-like growth factor binding protein-1 (IGFBP-1) (a.k.a placental protein 12) is induced in secretory phase endometrium and decidua and its expression is used to assess the extent of decidualisation *in vitro* (Bell *et al.*, 1991; Giudice *et al.*, 1991; Bryant-Greenwood

et al., 1993). Studies using *IGFBP-1* promoter-reporter constructs in primary hESC have identified PR-A as the dominant transactivator of the *IGFBP-1* promoter (Gao *et al.*, 2000). Dysregulation of IGFBP-1 is associated with pregnancy complications like intrauterine growth restriction (IUGR), pre-eclampsia and polycystic ovarian syndrome (PCOS) (Crossey *et al.*, 2002). High levels of IGFBP-1 in early pregnancy appear to be beneficial but promote obstetrical disorders in late pregnancy (Giudice, 2002; Fazleabas *et al.*, 2004). IGFBP-1 triggers trophoblast invasion interacting with the invading extravillous trophoblasts (EVT) and regulating the insulin-like growth factor (IGFs) activity during decidualisation (Gleeson *et al.*, 2001; Giudice *et al.*, 1998). Oestrogen stimulates IGF-1 and facilitates endometrial growth and is expressed during proliferative and early secretory phases. Whereas, IGF-II is expressed by EVT during the secretory phase and early pregnancy (Zhou *et al.*, 1994). IGF-1 and IGF-II knockout mice show impaired placenta growth and develop IUGR (Crossey *et al*., 2002). Furthermore, the addition of recombinant IGF-1 leads to failure of primary hESC decidualisation *in vitro* (Matsumoto *et al.*, 2008).

1.7.3 Homeobox A10 (HOXA10)

Homeobox (HOX) transcription factors play a crucial role in embryonic development and reproductive tract in the developing human and mouse embryo (Taylor *et al.*, 1997). HOXA10 is also an important decidualisation associated transcription factor in both human (Taylor *et al.*, 1998) and mouse (Lim *et al.*, 1999) endometrium. HOXA10 expression is increased in the primary hESC treated with oestrogen and progesterone during the secretory phase (Taylor *et al.*, 1998). HOXA10 has been reported to regulate the expression of several genes involved in the differentiation process such as IGFBP-1 (Kim *et al.*, 2003), integrin-β3 (Daftary *et al.*, 2002) and MMP26 (Jiang *et al.*, 2014) to promote embryo adhesion during the window of implantation. HoxA10 knock-out mice are sub-fertile due to endometrial

dysfunction (Satokata *et al.*, 1995) and HOXA10 expression is decreased in the secretory ESC of women with unexplained infertility (Wu *et al.*, 2005; Matsuzaki *et al.*, 2009).

1.7.4 CCAAT- enhancer binding protein β

During the early phase of decidualisation, increased levels of CCAAT- enhancer binding protein β **(**C/EBPβ) are detected in ESC. C/EBPs are members of basic leucine-zipper (bZIP) superfamily of transcription factors (Lekstrom and Xanthopoulos, 1998). C/EBPβ has been detected in the nuclei of decidual cells during mid-secretory phase of the menstrual cycle (Plante *et al.*, 2009). There is also evidence indicating that C/EBPβ is implicated in IL-11 and cell cycle regulation during decidualisation (Wang *et al.*, 2012). C/EBPβ deficiency impairs ESC decidual transformation leading to infertility in mice (Mantena *et al*., 2006). Loss of C/EBPβ also decreases the expression of bone morphogenetic protein 2 (BMP2), which plays an important role in mouse and human ESC decidualisation (Wang *et al.*, 2012).

1.7.5 Forkhead box O (FOXO) transcription factors

The FOXO subfamily of forkhead transcription factors were first identified in Drosophila melanogaster (Weigel *et al.*, 1989). In mammals, there are four members: FOXO1, FOXO3A, FOXO4 and FOXO6. FOXOs show similar DNA binding specificity and bind with high affinity to the forkhead recognition element (FHRE) DNA consensus sequence (5'-TTGTTTAC-3') due to the high conservation within the DNA-binding domain (Furuyama *et al.*, 2000). FOXOs bind DNA via a 100 amino acid forkhead DNA-binding domain which has a winged-helix domain (Kaestner *et al.*, 2000) to either activate or repress gene transcription. They increase the accessibility of genomic regions within chromatin to promote transcription factor recruitment and binding to a region of DNA (Lalmansingh *et al.*, 2012). FOXOs are important in the regulation of several diverse processes including the

cell cycle, apoptosis, responses to oxidative stress, DNA damage and repair and tumour suppression (Zhang *et al.*, 2011). The transcriptional activity of FOXO1, 3A and 4 is regulated by multiple post-translational modifications including phosphorylation, acetylation, ubiquitination and methylation (Calnan and Brunet, 2008). In the absence of growth factor signalling, FOXOs are predominantly located in the nucleus (Brownawell *et al.*, 2001). Phosphorylation of FOXOs by serine/threonine protein kinase B (AKT) on three conserved residues: threonine 24; serine 256; and serine 319, inhibits FOXO transcriptional activity by blocking DNA-binding and relocalising FOXOs to the nucleus. The presence of three highly conserved phosphorylation sites was predicted based on a consensus motif for Akt phosphorylation (Arg-X-Arg-X-X-(Serine/Threonine)) (Alessi *et al.*, 1996). Phosphorylation of serine-256 is critical for nuclear exclusion of FOXOs (Zhang *et al.*, 2002) and its phosphorylation can limit gene transactivation by FOXOs independent of threonine-24 and serine-319 phosphorylation (Zhang *et al*., 2002). FOXO phosphorylation induces 14-3-3 proteins to bind to the first two FOXO1 phosphorylated sites and subsequently block the DNA binding (Boura *et al.*, 2007; Brunet *et al.*, 1999). In addition, 14-3-3 protein binding to FOXOs causes a shift from the nucleus to the cytoplasm (**Figure 1.7)** (Obsilova *et al.*, 2005). Multiple kinases have been identified to regulate FOXO transcriptional activity in both a positive and negative manner including serum-and glucocorticoid-inducible kinase (SGK), IkB kinase (IKK), c-jun N-terminal kinase (JNK) and mammalian sterile 20-kinase-1 (MST1) (Calnan and Brunet, 2008). JNK is activated by oxidative stress in mammalian cells and subsequently phosphorylates FOXOs on multiple alternative residues leading to nuclear accumulation (Esser *et al.*, 2004; Kawamori *et al.*, 2006). Similarly, MST1 is activated by cellular stress and reduces 14-3-3 binding to FOXO leading to nuclear translocation (Yuan *et al.*, 2009).

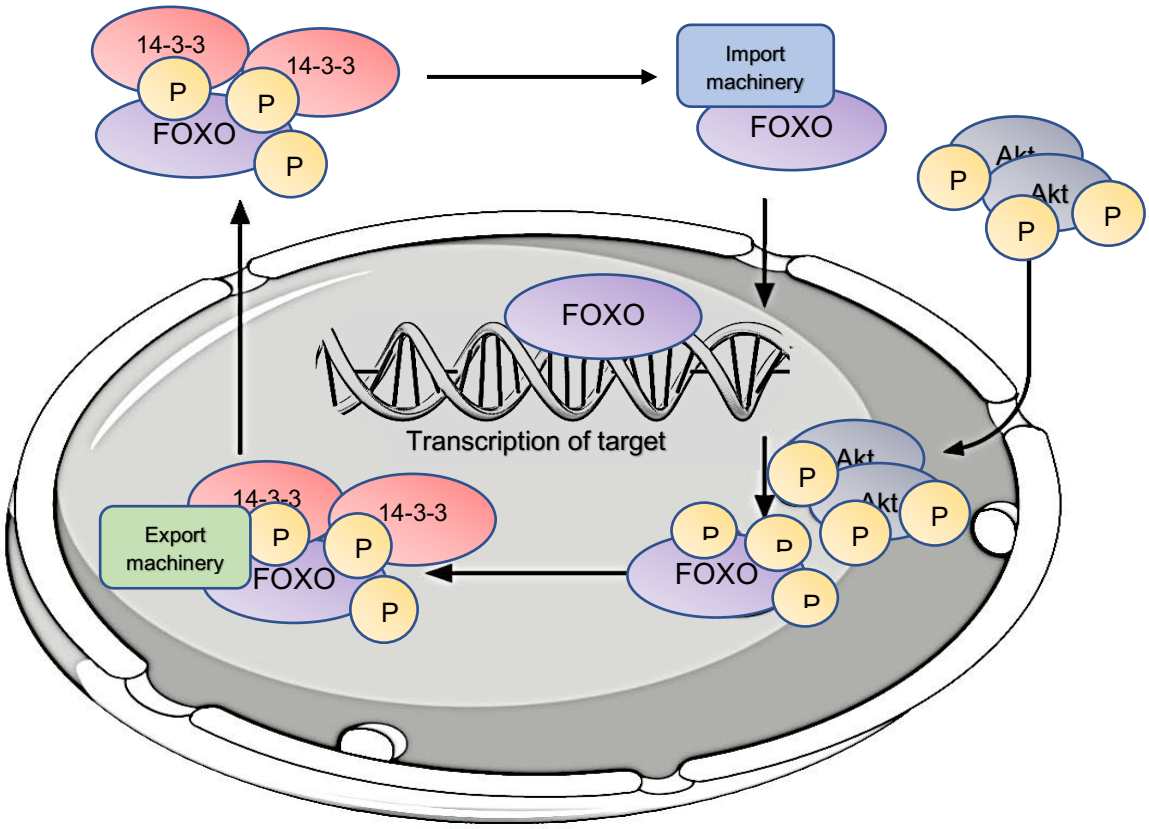

Figure 1.7: Translocation of FOXO transcription factors regulates their transcriptional activity. In the presence of growth factor/survival signals activated Akt, which translocates to the nucleus and phosphorylates FOXO releasing it to bind to the 14-3-3 chaperone proteins transporting it out of the nucleus. In the absence of growth factor/survival signals, FOXO is dephosphorylated, 14-3-3 is released and it re-enters nucleus (modified from Zhang *et al.*, 2011).

1.7.5.1 FOXO1

FOXO1 is critical for the induction of decidualisation (Grinius *et al.*, 2006; Kajihara *et al.*, 2013) regulating various key genes such as dPRL (Lynch *et al.*, 2009; Christian *et al.*, 2002) and IGFBP-1 (Kim *et al.*, 2003). Immunohistochemical studies show that FOXO1 expression increases in human endometrial tissues during the secretory phase with only cytoplasmic epithelial staining during the early secretory phase and both cytoplasmic and nuclear epithelial and stromal cell staining during the late secretory phase (Christian *et al.*, 2002). It is known that cAMP and progesterone signalling positively regulate FOXO1

expression upon *in vitro* decidualisation of hESC. Activation of FOXO1 protects the decidual cells from oxidative stress (Brosens and Gellersen, 2006; Buzzio *et al.*, 2006; Takano *et al.*, 2007). In response to progesterone withdrawal, FOXO1 translocates to the nucleus of decidual ESC (Labied *et al.*, 2006). Various genes involved in hESC decidualisation are regulated by FOXO1, overexpression of FOXO1 increased the expression of PRL, IGFBP-1 and TIMP3, while FOXO1 deletion significantly reduced their expression (Buzzio *et al.*, 2006; Grinius *et al.*, 2006). In summary, increased levels of progesterone in ESC during secretory phase of menstrual cycle activate the phosphatidylinositol-4,5-bisphosphate 3-kinase (PI3K)/Akt pathway which causes localisation to FOXO1 in the cytoplasm. However, progesterone stimulation also increases the levels of intracellular cAMP in hESC which activates the PKA pathway and inactivates PI3K/Akt pathway causing FOXO1 to enter the nucleus and regulate gene transcription (**Figure 1.8**).

1.7.5.2 FOXO3A

FOXO3A acts to protect the cells from oxidative stress, apoptosis and plays an essential role in follicular development and oocyte growth (Wang *et al.*, 2014; Christian *et al.*, 2011). FOXO3A was found to be down-regulated during hESC decidualisation and silencing of FOXO3A reduces apoptosis in hESC (Kajihara *et al.*, 2006). A very recent study reported that FoxO3a expression increased in the decidualisation of mouse primary stromal cells, and siRNA-mediated FoxO3a knock-down reduced the apoptosis (Long *et al.*, 2018).

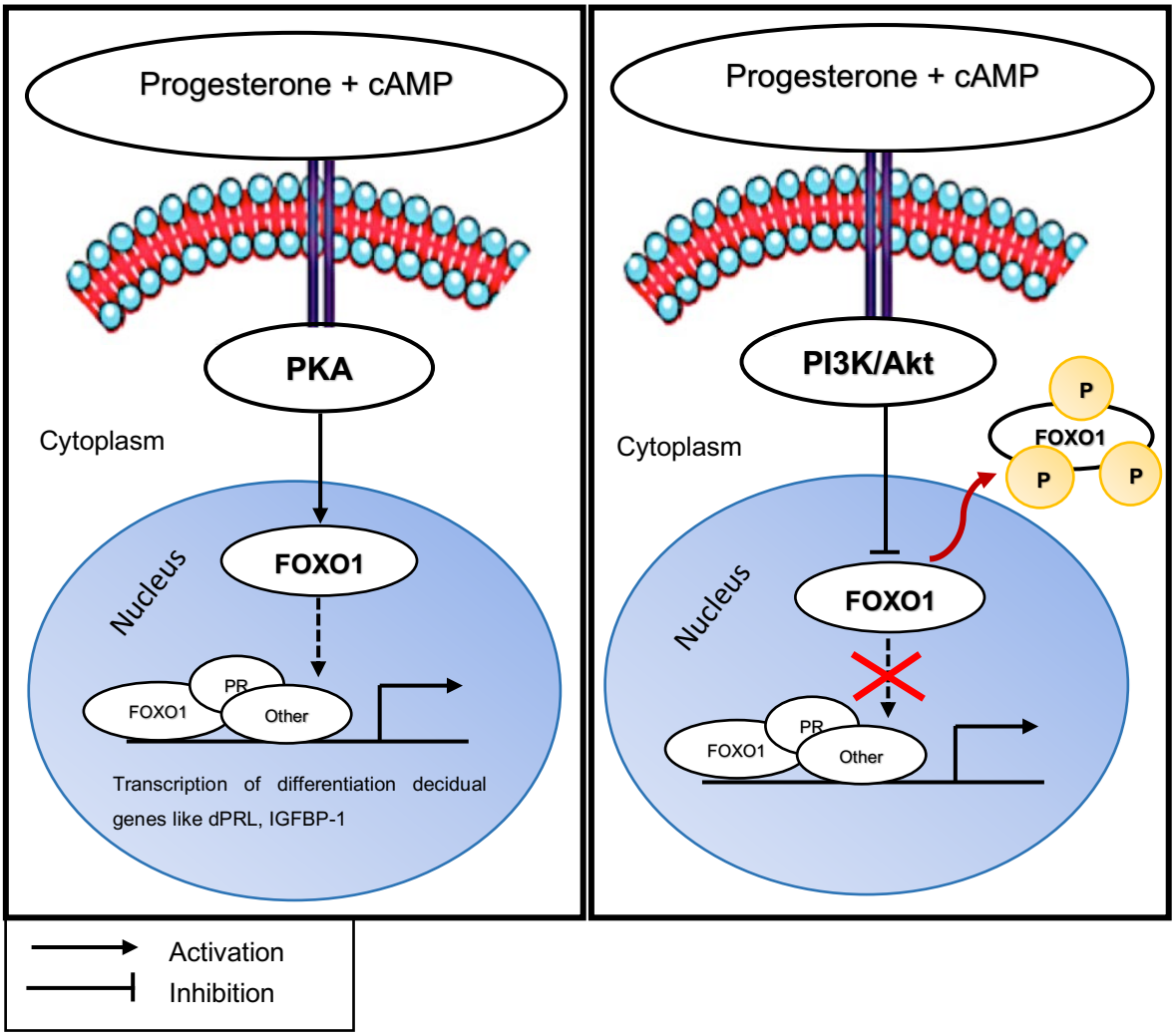

Figure 1.8: Model of the regulation of FOXO1 transcriptional activity in a progesterone-dependent manner in ESC through the PI3K/Akt and PKA pathways. The rise of progesterone levels in hESC during secretory phase of menstrual cycle activates the PI3K/Akt pathway which stimulates localisation of FOXO1 in the cytoplasm to prevent its transcriptional activity (right). However, progesterone stimulation also increases the levels of intracellular cAMP in hESC which activates the PKA pathway, up-regulates FOXO1 expression and inactivates PI3K/Akt pathway causing FOXO1 to enter the nucleus to increase target gene transcription (left).

1.7.6 Transcription factors associated with hESC decidualisation

No	*Abbreviation*	*Protein Name*	*Functions*	*References*
1	FOXO1	Forkhead box O1	Induces dPRL during decidualisation, protects against reactive oxygen species apoptosis	Labied *et al.*, 2006
2	C/EBPβ	CCAAT/enhancer-binding protein β	Cooperates with FKHR in the regulation of decidual specific-genes expression e.g. dPRL	Christian *et al.*, 2002
3	PLZF	Promelocytic leukemia zinc finger protein	Progesterone-induced transcription factor in decidualisation	Komangani *et al.*, 2016
4	HOXA10	Homeobox A10	Essential for uterine receptivity during the window of implantation	Gui *et al.*, 1999
5	FOXM1	Forkhead Box M1	Downstream of HOXA10 in decidualisation	Gao *et al.*, 2015
6	STAT3	signal transducer and activator of transcription 3	Downstream of FOXM1 in decidualisation	Jiang *et al.*, 2015
7	TWIST1	TWIST homolog 1	Associated with FOXO1 and ETS1	Schroeder *et al.*, 2011
8	ETS1	v-ets erythroblastosis virus E26	Enhances decidual markers e.g. PRL, IGFBP-1	Kessler *et al.*, 2005
9	HAND2	Heart and neural crest derivatives expressed transcript 2	Regulated by progesterone, important in decidualisation	Huyen and Bany, 2011
10	CREB	cAMP response element binding protein	Central transcription factor downstream of cAMP signalling	Yoshie *et al.*, 2015
11	p300/CBP	p300/CREB-binding protein	Forms complex with progesterone receptor in the secretory phase	Shiozawa *et al.*, 2003
12	KLF-9	Kruppel-like factor 9	Progesterone receptor-interacting protein, loss of KLF-9 leads to subfertility	Pabona *et al.*, 2012
13	LEFTY	LEFTY	Inhibits induction of decidualisation	Tabibzadeh, 2011; Li *et al.* 2014; Tang *et al.*, 2010

Table 1.2: Transcription factors associated with decidualisation of hESC.

1.8 Angiogenesis in the endometrium

1.8.1 Angiogenesis

The vascular system forms through two independent processes: vasculogenesis and angiogenesis. Vasculogenesis is the *de novo* formation of blood vessels from endothelial progenitors which is important for embryo development and in adults (Kolte *et al.*, 2016).

Angiogenesis is the process by which new blood vessels are formed from pre-existing vessels. It is essential in various physiological processes, for example, embryo development, reproductive function, wound healing and pathological conditions such as tumorigenesis (Ribatti, 2005). Angiogenesis is a complex and coordinated process requiring sequential activation of receptors by numerous families of ligands in endothelial and mural cells (Ferrara, 2009; Carmeliet and Jain, 2011).

1.8.2 Angiogenesis and vascular remodelling in the endometrium

Angiogenesis occurs in normal tissues during wound healing and in the ovary and endometrium during female reproductive life (Fraser and Wulff, 2003). Angiogenesis is important in the development and differentiation of human endometrium in preparation for implantation and pregnancy (Gordon *et al.*, 1995). As discussed earlier, there is dynamic remodelling of the vasculature in the endometrium during the menstrual cycle. A complex process of proliferation, differentiation, regeneration of vascular, stromal and glandular cells occurs each month during female reproductive life. The endometrium is supplied by the spiral arterioles arising from arteries in the myometrium supplying the basal and functional layer (Farrer-Brown *et al.*, 1970). Upon decidualisation, the endometrial spiral arteries become increasingly tortuous (Kaiserman-Abramof and Padykula, 1989; Rogers and Gargett, 1998), and undergo dynamic remodelling/transformation if pregnancy occurs to ensure adequate nutrient supply for the growing fetus (Plasier, 2011; Smith, 2001). Many pro-angiogenic factors such as VEGF (-A), VEGF-C, placenta growth factor (PIGF) and angiopoietins have been identified in the endometrium (Li *et al.*, 2001; Smith, 2001).

1.8.3 Angiogenesis and VEGF

VEGF and its receptors are essential for blood vessel development. Mice lacking a single allele of *Vegf* die *in utero* between day 11 and 12 due to inadequate vascular development

(Ferrara *et al.*, 1996; Carmeliet *et al.*, 1996). Whereas, the over-expression of VEGF causes severe abnormalities in heart development and embryonic lethality at day 12.5 to day 14 (Miquerol *et al.*, 2000). This indicates that the level of VEGF present is critical and that it needs to be tightly regulated for normal development. VEGF and PIGF are known to regulate early placental vascular development and are important factors in implantation success (Andraweera *et al.*, 2012). In addition, studies in transgenic mice have shown that VEGF is a prime regulator of angiogenesis during decidualisation (Douglas *et al.*, 2009).

It is interesting that the loss of PIGF and VEGF-B does not cause embryonic lethality. Mice deficient in PIGF are viable and fertile, and only show some impairment of wound healing (Carmeliet *et al.*, 2001). Inactivation of *Vegf-b* reduces heart size and impairs the coronary vasculature (Bellomo *et al.*, 2000). VEGF-C plays an essential role in vascular development and deletion of VEGF-C causes embryonic lethality due to a failure of lymphatic development (Karkkainen *et al.*, 2004).

1.9 Vascular endothelial growth factor-A (VEGF)

1.9.1 VEGF structure

VEGF was identified in 1983 as a vascular permeability factor (VPF), secreted by a guinea pig tumour cell line (Senger *et al.*, 1983). In 1989, an endothelial-specific mitogen was isolated from the conditioned medium of bovine pituitary follicular cells by Ferrara and Hanzel and named VEGF (Ferrara and Hanzel, 1989). Subsequently, Connolly *et al.* (1991) independently isolated and sequenced the VPF from U937 cells. The cloning and sequencing of VEGF (Leung *et al.*, 1989) and VPF (Keck *et al.*, 1989) cDNAs was reported in 1989, which concluded that VEGF and VPF were the same protein. VEGF is also known as VEGF-A following the discovery of its homologues: PIGF, VEGF-B, VEGF-C, VEGF-D.

VEGF is a highly conserved, heparin binding small disulfide-linked ~46 kDa homodimeric glycoprotein (Ferrara and Henzel, 1989). There are several VEGF isoforms that differ in their degree of extracellular matrix binding capacity affecting their distribution and bioavailability (Park *et al.*, 1993) (**Figure 1.9**). The human *VEGF* gene is located on chromosome 6p21.3 (Vincenti *et al.*, 1996), which composed of eight exons and separated by seven introns (Houck *et al.*, 1991). The main human VEGF isoforms are $VEGF_{121}$, $VEGF_{145}$, $VEGF_{165}$, $VEGF_{189}$, and $VEGF_{206}$ formed by alternative mRNA splicing (**Figure 1.9**) (Cross *et al.*, 2003; Ferrara, 2009). $VEGF_{121}$ and $VEGF_{165}$ are the most abundant isoforms (Neufeld *et al.*, 1999). $VEGF_{121}$ is a freely diffusible protein with poor extracellular matrix (ECM) binding capacity as it lacks exons 6 and 7 which confer heparin-binding properties (Park *et al.*, 1993). $VEGF_{165}$ is the predominant biologically active isoform which lacks exon 6 and is secreted and partially bound to the cell surface and ECM. $VEGF_{189}$ and

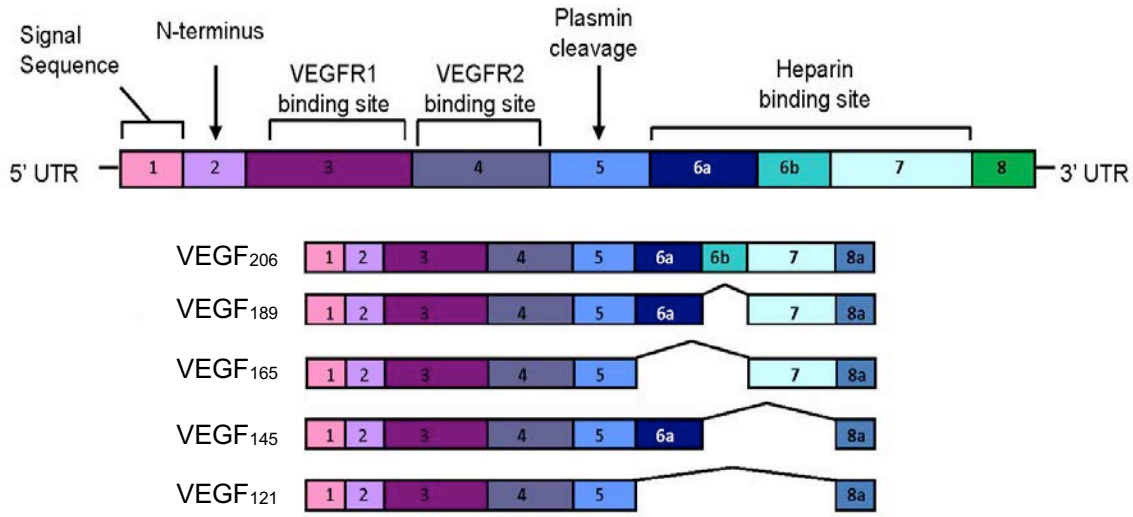

Figure 1.9: Exon structure of the *VEGF* gene. The *VEGF* gene consists of eight exons. Exon 6 and 7 encode heparin binding domains responsible for determining whether VEGF is membrane bound or soluble. $VEGF_{206}$ and $VEGF_{189}$ contain all eight exons and are predominantly membrane bound. $VEGF_{165}$, the most abundant isoform, and lacks exon 6 and $VEGF_{145}$ lacks exon 7. Whereas, $VEGF_{121}$ diffuses freely lacking exons 6 and 7. Domains 1 to 5 are conserved between all VEGF isoforms and are the VEGFR-1 and VEGFR-2 binding domains (modified from Fearnley *et al.*, 2013).

$VEGF_{206}$ are found tightly bound to ECM, because they contain all eight exons (Ferrara, 2009). $VEGF_{145}$ is detected in placental tissue and is the major VEGF produced by cell lines derived from carcinomas of the female reproductive tract (Poltorak *et al.*, 1997).

1.9.2 *VEGF* gene regulation

VEGF expression is regulated by many factors including hormones, growth factors and primarily oxygen tension (**Figure 1.10**). VEGF mRNA expression is up-regulated in low oxygen tensions in a variety of pathological conditions (Semenze, 2003; Dor *et al.*, 2001). Hypoxia inducible factor-1α (HIF-1α) is a key regulator of *VEGF* gene expression in response to hypoxia and binds to the hypoxia-responsive element (HRE) in the *VEGF* gene promoter region increasing its expression and mRNA stabilisation (Wenger *et al.*, 2005; Kietzmann *et al.*, 2016). Growth factors including platelet-derived growth factor (PDGF), fibroblast growth factor (FGF), transforming growth factor β (TGFβ) are reported to regulate *VEGF* expression (Frank *et al.*, 1995; Pertovaara *et al.*, 1994). Ovarian hormones such as oestrogen and progesterone have also been reported to induce VEGF in endometrium both *in vivo* (Ferrara *et al.*, 1998) and *in vitro* (Classen-Linke *et al.*, 2000).

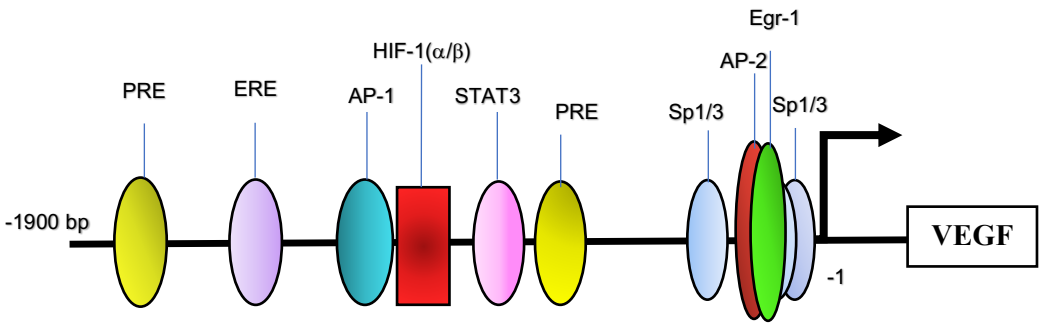

Figure 1.10: Schematic representation of the VEGF promoter region. The arrow indicates the transcriptional start site. **PRE**: progesterone response element; **ERE**: oestrogen response element; **HIF-1α/β**: hypoxia inducible factor-1 α/β; **STAT3**: signal transducer and activator of transcription 3 (adapted from Pagès and Pouysségur, 2004).

1.9.3 VEGF receptors

VEGF binds to two closely related receptor tyrosine kinases (RTK); VEGFR-1 and VEGFR-2 primarily via the second and third immunoglobulin-like domains of VEGFR-1 and VEGFR-2 (Fuh *et al.*, 1998). These receptors contain seven immunoglobulin-like domains in the extracellular domain, a single transmembrane region and other receptor tyrosine kinase sequences. Flt-1 and VEGFR-2 are necessary for embryonic vascular development in mice (Fong *et al.*, 1999; Shalaby *et al.*, 1995). A third member of this RTK family, VEGFR-3 (Flt-4), is not a receptor for VEGF, but instead binds specifically to VEGF-C and VEGF-D (**Figure 1.11**). In addition, neuropilin-1 & 2 (NRP1 & 2) have also been identified as co-receptors for VEGF (Soker *et al.*, 1998).

1.9.3.1 Vascular endothelial growth factor receptor-2 (VEGFR-2/KDR)

VEGFR-2 is a 230 kDa protein is also known as kinase insert domain receptor (KDR) in human, and fetal liver kinase-1 (Flk-1) in mouse (Ferrara, 2009). VEGFR-2 is expressed mostly in vascular endothelial cells from early fetal development (Cortés *et al.*, 1999). VEGF activates VEGFR-2 inducing dimerisation and phosphorylation at various tyrosine residues resulting in a chemotactic, mitogenic and pro-survival signal (Ferrara, 2009). This stimulates phosphorylation of various downstream mediators including PI3K, phospholipases Cγ, ras GTPase activating protein, Src tyrosine kinases, protein kinase C and MAPK-ERK pathway (Ferrara, 2009). The role of VEGFR-2 in angiogenesis and haematopoiesis was demonstrated through the study of Flk-1 null mice led to the death *in utero* due to the lack of vasculogenesis and failure in blood vessel development (Shalaby *et al.*, 1995). Therefore, VEGFR-2 is a key mediator of the angiogenic and permeability-enhancing effect of VEGF.

1.9.3.2 Vascular endothelial growth factor receptor-1 (VEGFR-1/Flt-1)

Flt-1 (a.k.a the fms-like tyrosine kinase-1/ VEGFR-1) is a 180 kDa protein that was the first VEGF receptor identified (Ferrara, 2004). However, the full functional activity of this receptor remains unclear. Studies indicate that the function and signalling properties of Flt-1 vary depending on the cell type and developmental stage at which it is acting (Ferrara, 2004). Flt-1 binds to the VEGF, PIGF and VEGF-B (**Figure 1.11**) (Park *et al.*, 1994; Olofsson *et al.*, 1998). Flt-1 is also produced in a soluble form, sFlt-1 (sVEGFR-1), which is a potent physiological inhibitor of VEGF activity (**Figure 1.11**) (Kendall and Thomas, 1993).

There are many studies that report Flt-1 acts as a VEGF ligand-trap or "decoy receptor" which negatively regulates the access of VEGF to VEGFR-2 (Park *et al.*, 1994; Fong *et al.*, 1995). Flt-1 knockout mice die at embryonic day (E) 8.5 to E9.5 due to the increased proliferation of endothelial progenitor cells resulting in a disorganised vasculature (Fong *et al.*, 1999). However, transgenic mice which have the tyrosine kinase domains of Flt-1 deleted develop a normal vasculature and are viable (Hiratsuka *et al.*, 1998) suggesting that Flt-1/sFlt-1 acts mainly as a decoy receptor modulating embryonic development by sequestering VEGF and preventing over-activation of VEGFR-2.

Our understanding of the role of the Flt-1 receptor has deepened with findings indicating the involvement of PIGF signalling in angiogenesis (Carmeliet *et al.*, 2001; Autiero *et al.*, 2003). Carmeliet *et al.* (2001) showed that PIGF binds to Flt-1 to promote angiogenesis by displacing VEGF and consequently enhancing VEGFR-2 activation. Autiero *et al.* (2003) demonstrated that PIGF can also initiate intermolecular signalling through binding to Flt-1 leading to transphosphorylation of VEGFR-2. The direct inhibition of Flt-1 signalling was found to inhibit endothelial cell migration (Gille *et al.*, 2000) and it is also reported to produce weak mitogenic signals (Maru *et al.*, 1998). Our laboratory has shown that Flt-1 can

negatively regulate VEGFR-2 signalling via heterodimerisation (Cudmore *et al.*, 2011). In addition, Flt-1 is also present in other cell types including retinal pericytes (Takagi *et al.*, 1996) and monocytes (Barleon *et al.*, 1996) where it mediates positive migratory responses to VEGF.

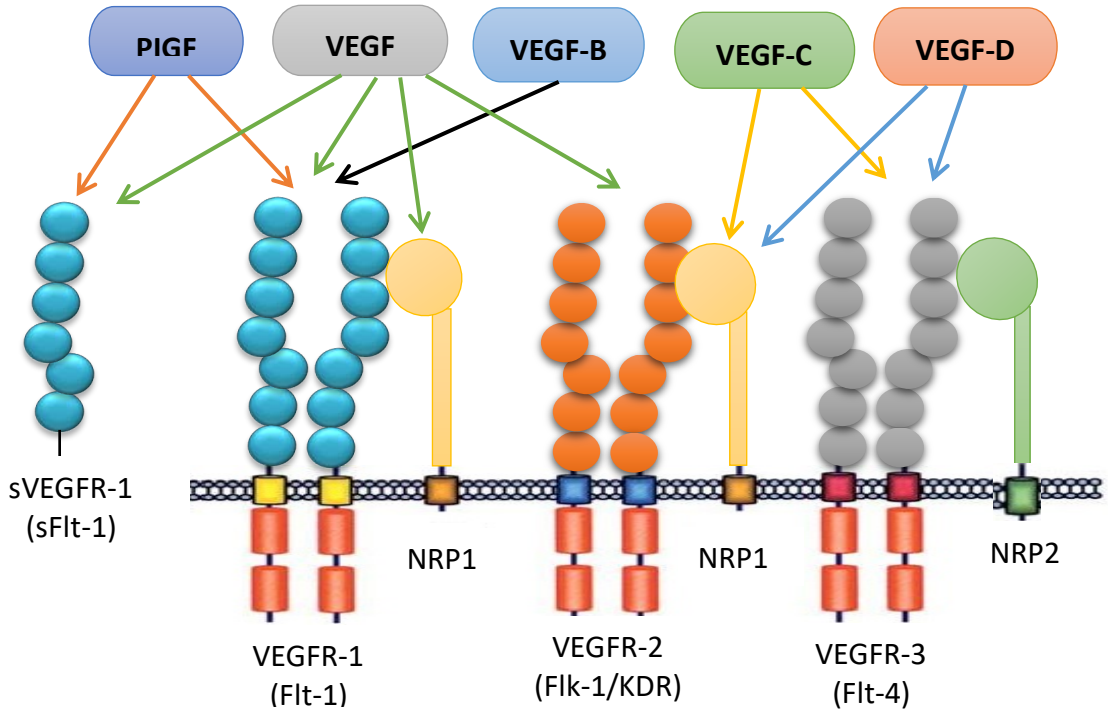

Figure 1.11: Schematic illustration of the VEGF family members and their specific interactions with VEGF receptors. VEGF receptors (VEGFR-1, VEGFR-2 and VEGFR-3) contain seven immunoglobulin-like domains in the extracellular region, a single transmembrane domain and split intracellular tyrosine kinase domains. *Arrows* indicate which ligands are capable of binding to each receptor. VEGF can bind to two cell surface receptors VEGFR-1/Flt-1 and VEGFR-2/KDR. VEGF binds to Flt-1 with higher affinity than VEGFR-2/KDR. Alternatively, spliced soluble forms of Flt-1, sFlt-1 act as inhibitors of VEGF, VEGF-B and PIGF activity. Neuropilin co-receptors (NRP1 & 2) bind specific VEGF ligand splice variants to enhance VEGFR-2 mediated signalling.

1.9.3.3 Neuropilin-1/2

Neuropilins 1 & 2 (NRP1 & 2) were originally discovered as semaphorins II receptors which are involved in neuronal growth and axonal guidance (Kolodkin *et al.*, 1997). NRP1 was shown to bind VEGF acting as a co-receptor to enhance VEGFR-2 signalling in response to

VEGF (Soker *et al.*, 1998; Gelfand *et al.*, 2014). *NRP1* knock-out mice die *in utero* with seriously disorganised vasculature (Kawasaki *et al.*, 1999; Takashima *et al.*, 2002). NRP1 may positively regulate the level of Flt-1 within the cell as NRP-1 knock-down leads to reduced Flt-1 expression (Quante *et al.*, 2009).

1.9.4 Flt and sFlt-1 structure and function

The *Flt-1* gene expresses one long mRNA form of approximately 8 kb which encodes the full-length receptor and shorter truncated mRNAs encoding most of the extracellular domain of between 2.5 to 3.0 kb. The sFlt-1 isoforms contain the N-terminal six immunoglobulin-like (Ig-like) domains and lack a transmembrane domain and so are freely soluble (Shibuya *et al.*, 1999). As sFlt-1 contains the same extracellular domain as Flt-1, sFlt-1 competes with Flt-1 to bind VEGF and PIGF, subsequently reducing free VEGF and PIGF levels and blocking their interaction with and signalling from membrane bound VEGF receptors (**Figure 1.12**).

The role of sFlt-1 is further complicated by the existence of multiple mRNA splice variants (**Figure 1.13**). The two most abundant splice variants, sFlt-1-i13 (a.k.a sFlt1_v1) and sFlt-1-e15a (a.k.a sFlt1_v2), are differentially expressed in human tissues (Thomas *et al.*, 2007; Heyderian *et al.*, 2009; Rajakumar *et al.*, 2009; Whitehead *et al.*, 2011; Jebbink *et al.*, 2011). sFlt-1-i13 was the first sFlt-1 identified (Kendal and Thomas, 1993) and comprises of the first 13 exons of Flt-1 with an extension of exon 13 into the intronic sequence (**Figure 1.13**) (Heydarin *et al.*, 2009). It shares 657 amino acids of full-length Flt-1, encoding a unique 31 amino acid C-terminus producing an 85-95 kDa protein (**Figure 1.13**) and is expressed in most tissues including brain, heart, and kidney (Thomas *et al.*, 2007).

In comparison, sFlt-1-e15a is specific to primates and mainly expressed in the placenta (Whitehead *et al.*, 2011; Jebbink *et al.,* 2011). sFlt-1-e15a encodes the first 14 exons of Flt-

1 followed by a 480 nucleotide stretch of an intronic sequence which forms an alternative exon (15a) (**Figure 1.13**) (Sela *et al.*, 2008; Thomas *et al.*, 2007; Gu *et al.*, 2008). More than 80% of all Flt-1 transcripts are spliced to become sFlt-1-e15a in the human placenta which indicates that sFlt-1-e15a may be the major isoform involved in preeclampsia (Jebbink *et al.,* 2011). Whereas sFlt-1-i14 is generated by skipped mRNA splicing and extension of exon 14, and sFlt-1-e15b contains the alternative exon 15b derived from another intronic sequence. sFlt-1-i14 and sFlt-1-e15b are expressed at low levels compared to sFlt-1-i13 and sFlt-1-e15a and so were not investigated in this study.

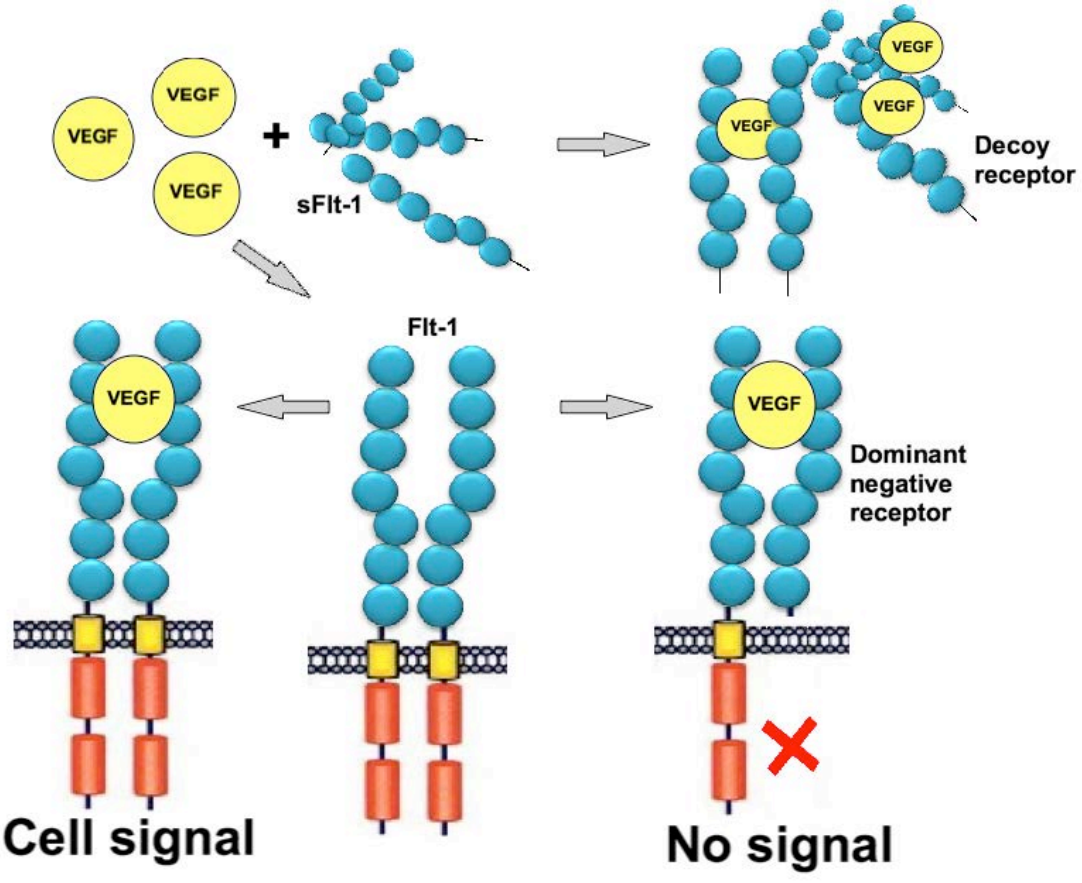

Figure 1.12: sFlt-1 blocks VEGF signalling. Soluble Flt-1 sequesters free VEGF and prevents it from binding to full length VEGFRs. sFlt-1 also forms dominant-negative complexes with VEGFRs so that no signal can be initiated (adapted and modified from Ahmed and Cudmore, 2009).

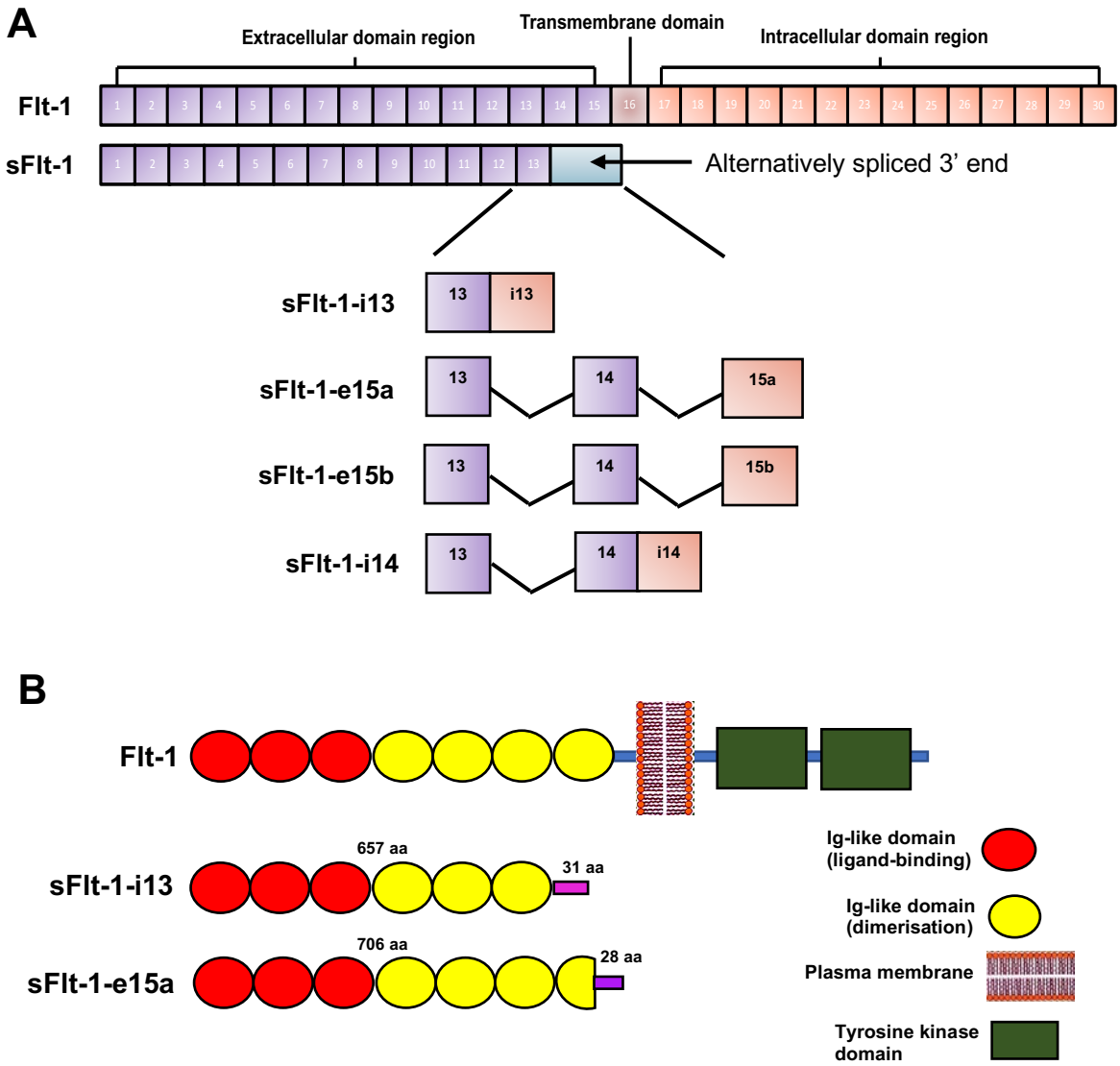

Figure 1.13: The *Flt-1* and *sFlt-1* gene exon arrangement and protein structure. The full-length Flt-1 receptor is encoded by an mRNA transcript of 30 exons which composed of seven extracellular Ig-like domains containing the ligand-binding regions, a transmembrane domain and intracellular tyrosine kinase domains. sFlt-i13 contains the first six Ig-Like domains, 657 amino acids (aa) of Flt-1 and it is generated by skipped splicing and extension of exon 13, while, sFlt-1-e15a diverges from Flt-1 after 706 aa and alternatively spliced exon derived from intronic sequences (exon 15a). sFlt-1-i14 is generated by skipped splicing and extension of exon 14 and sFlt-1-e15b encodes the alternative spliced exon of 15b derived from an intronic sequence (adapted from Palmer *et al.*, 2016).

The oxygen-sensing Jumonji domain containing protein 6 (JMJD6) directly affects the splicing pattern of Flt-1 to produce sFlt-1 in endothelial cells (Palmer *et al.,* 2016; Boeckel *et al.,* 2011). JMJD6 was able to hydroxylate U2 small nuclear ribonucleoprotein auxiliary factor 65-kDa subunit (U2AF65), a component of the splicing machinery under normal conditions to produce the full-length Flt-1 receptor transcripts (Boeckel *et al.,* 2011). However, under hypoxic conditions JMJD6 activity decreases which reduces its ability to hydroxylate U2AF65, leading the splicing machinery to produce shorter alternatively spliced sFlt-1 transcripts (Boeckel *et al.*, 2011).

sFlt-1 is suspected to act as a biochemical barrier between the fetal and maternal circulation in the placenta by stopping excess angiogenesis and abnormal vascular permeability. Patients with preeclampsia have abnormally high plasma levels of sFlt-1 (Maynard *et al.*, 2003). The placental trophoblasts are the major cell type producing large amounts of sFlt-1 in preeclampsia (Maynard *et al.*, 2003). The suppression of VEGF activity by sFlt-1 in the maternal circulation causes hypertension and proteinuria in patients. Over-expression of sFlt-1 in pregnant mice induces hypertension and proteinuria, showing that sFlt-1 is, at least in part, the cause of the maternal preeclamptic syndrome (Maynard *et al.*, 2003; Roberts and Rajakumar, 2009).

1.10 VEGFs in the endometrium

VEGF is expressed in both endometrial epithelial and stromal cells (Perrot-Applanat *et al.*, 2000). Immunohistochemical studies in human endometrial epithelial and stromal cells have demonstrated that the expression of VEGF is highest during the mid-secretory phase of cycle (Sugino *et al.*, 2002). In addition, the expression of VEGF in stromal cells was also detected in decidua in early pregnancy, but not in epithelial cells in the late secretory phase and early pregnancy (Sugino *et al.*, 2002). In the human endometrium, Flt-1 and VEGFR-2 are

detected mainly in vascular endothelial cells (Meduri *et al.*, 2000). Flt-1 is reported to be present only in stromal and endothelial cells in early pregnancy but not during the normal menstrual cycle (Sugino *et al.*, 2002). However, VEGFR-2 was readily detected in epithelial and endothelial cells throughout the menstrual cycle, in stromal cells during the secretory phase and in early pregnancy (Sugino *et al.*, 2002). In addition, oestrogen and progesterone treatment in primary hESC *in vitro* increased VEGFR-2 mRNA expression (Sugino *et al.*, 2002).

VEGF transcription was reported to be regulated by oestrogen via oestrogen receptor (ER) in human endometrial epithelial and stromal cells (Mueller *et al.*, 2000). ERα knock-out in mice was reported to lead to a failure of angiogenesis (Johns *et al.*, 1996). Furthermore, VEGF is the most prominent pro-angiogenic factor in endometriosis and is found at higher levels in the peritoneal fluid and lesions of endometriosis patients compared to healthy controls (McLaren *et al.*, 1996). This has led to an interest in the development of anti-VEGF therapies for endometriosis (Hull *et al.*, 2003, Rein *et al.*, 2010).

1.11 Rationale and Aims

hESC decidualisation is a highly regulated event and is crucial for the maintenance of a successful pregnancy. It encompasses various morphological changes underpinned by extensive biochemical changes, and the signalling pathways involved in this cell differentiation are complex. Research into the process of decidualisation may lead to greater understanding of endometriosis, female infertility, recurrent miscarriage as well as pregnancy complications like preeclampsia and intrauterine growth restriction (IUGR). VEGF family members are essential for maintaining the cycling endometrium under normal hormonal regulation and for a successful pregnancy. VEGF is up-regulated in hESC by

cAMP and levels of VEGF and sFlt-1 in the endometrium are linked to fertility and successful pregnancy.

We propose that VEGF activity is under the direct control of the PKA/FOXO1 pathway in hESC undergoing decidualisation and may modify the functional activity of these cells in addition to promoting vascular remodelling and trophoblast migration. Therefore, the aim of this thesis is to identify the pathways regulating VEGF activity during the decidualisation of ESC and how this may impact on vascular remodelling/angiogenesis.

The specific objectives are:

- To establish and characterise the *in vitro* decidualisation of primary hESC and St-T1b cell line and determine changes in pro-angiogenic activity.
- To examine the relative levels of VEGF, Flt-1 and sFlt-1 expression and secretion during hESC decidualisation.
- To determine whether FOXO1 directly regulates *VEGF* and *Flt-1* gene expression during hESC decidualisation.
- To assess the relative activity of decidual hESC-derived VEGF on endothelial cell and hESC function.

CHAPTER 2:
MATERIALS AND METHODS

2.1 Cell culture

2.1.1 Isolation of Primary Cells

2.1.1.1 Human Endometrial Stromal Cells (hESC) Isolation

The endometrial tissues were collected in accordance with the University of Birmingham approved ethics protocol numbered 10-014. Endometrial cell isolation was based on a modification of previous methods (Zhang *et al.*, 1995; Chen and Roan, 2015). The endometrial tissues from pipelle biopsies was collected in Dulbecco's phosphate buffered saline (PBS) containing Penicillin/Streptomycin (Pen/Strep) (100 U/ml Penicillin and 100 µg/ml of Streptomycin (Gibco)) and processed immediately or stored at 4^{o}C. The tissue was transferred to a Petri dish and minced into 1 mm^3 pieces between scalpel blades. The pieces were transferred to a 15 ml tube and were centrifuged at 300 x g for 2 min to pellet the tissue cells. The supernatant was discarded, and pellet resuspended in 10 ml of 1 x digestion media (2 x concentration: 6.4 mg/ml Collagenase Type 1 (Worthington Biochemical Corporation) and 125 U/ml hyaluronidase (Sigma) in Dulbecco's modified eagle's medium and Ham's F-12 (DMEM/F12) supplemented with Pen/Strep (100 U/ml Penicillin and 100 µg/ml of Streptomycin (Gibco)). The tissues were incubated on a rotator for 2 h at 37^{o}C. The digest was then passed through a 100 µm cell strainer placed on top of an opened 50 ml tube. The flow-through was centrifuged at 300 x g for 5 min to remove the digestion media and the pellet resuspended in growth medium comprising DMEM/F-12 (Gibco), 10% (v/v) of Foetal Bovine Serum (FBS) (Sigma), 1 nM 17-β-Oestradiol (E2), 1 µg/ml insulin (Gibco), 2 mM L-glutamine (Sigma) and Pen/Strep (100 U/ml Penicillin and 100 µg/ml of Streptomycin (Gibco)). The cells were then plated in a T-25 flask and incubated overnight. On the next day, the cells were washed with PBS and fresh medium added.

2.1.1.2 Mouse Endometrial Epithelial and Stromal Cells Isolation

The endometrial cell isolation was based on the modification of previously published methods (Grant *et al*., 2003; Inada *et al.*, 2006). The uteri from three mice were opened lengthwise and cut into ~ 0.5 cm^2 pieces. The tissue was pooled together and incubated in 5 ml of 0.25% of trypsin-EDTA (Gibco) for 2 h in 4^oC followed by 30 min at room temperature. The DMEM/F12 medium with 10% (v/v) FBS (Sigma) was added and the mixture vortexed three times to release the sheets of epithelial cells. The digested uteri were then passed through a 100 µm nylon mesh and the supernatant collected was centrifuged for 10 min at 500 x g. The pellet was re-suspended in the complete growth medium (DMEM/F12 supplemented with 10% FBS, 1 nM E2, 1 µg/ml insulin (Gibco), 2 mM L-glutamine (Sigma) and Pen/Strep (100 U/ml Penicillin and 100 µg/ml of Streptomycin (Gibco)). The cells were seeded on a 6-well plate.

The remaining digested uterine material transferred to the universal tube containing DMEM/F12 medium with collagenase (1 mg/ml) and incubated at 37^oC for 40 min to isolate the stromal cells. The digest was dispensed onto a 40 µm nylon mesh and gently washed through with fresh medium. The supernatant collected was centrifuged for 10 min at 500 x g and the pellet was re-suspended in complete growth medium. The cells were seeded on 6-well plate. The cells were observed every day and the medium changed after 48 h.

2.1.1.3 Mouse Embryonic Fibroblast preparation

Floxed FoxO mice were kindly provided by Prof Domineco Acilli, Columbia University, New York USA and described previously (Paik *et al.*, 2007). Timed pregnant mice were used to prepare mouse embryonic fibroblasts (MEFs) (Lengner *et al.*, 2004). E14 embryos were removed from the uterus, dissected out from yolk sac and transferred into a sterile dish containing PBS. The head, tail and internal organs of each foetus were removed carefully

and washed with sterile PBS to remove as much blood as possible. The foetuses were then minced between scalpel blades and transferred to 1 ml of 0.25% trypsin/EDTA followed by 10 min incubation at 37°C. The trypsin was neutralised with fresh growth medium (below) and the digest was filtered through 70 μm mesh. The cells were pelleted at 1,700 x g for 5 min and plated on 10 cm^2 culture dishes. The cells were incubated at 37°C, 6% CO_2 with humidified atmosphere. The medium was changed the next day and cells grown to confluence and then cryopreserved. MEFs were cultured in DMEM supplemented with 10% (v/v) FBS (Sigma), 2 mM L-glutamine, Pen/Strep (100 U/ml Penicillin and 100 μg/ml of Streptomycin (Gibco)), 1 mM sodium pyruvate (Sigma, S8636), 1% of MEM non-essential amino acid 100 x (Sigma, M7145).

2.1.2 Cell Culture

2.1.2.1 St-T1b hESC Line

St-T1b, a telomerase-immortalised hESC line (Samalecos *et al.*, 2009) was provided by Dr. Birgit Gellersen (Endokrinologikum, Hamburg, Germany). St-T1b cells were cultured in growth medium comprising DMEM/F-12 (Gibco), 10% (v/v) FBS (Sigma), 1 nM E2, 1 μg/ml insulin (Gibco), 2 mM L-glutamine (Sigma) and Pen/Strep (100 U/ml Penicillin and 100 μg/ml of Streptomycin (Gibco)). The cells were used between passage 22 and passage 35 in all the experiments.

2.1.2.2 Human embryonic kidney cells (HEK-293)

HEK-293, human embryonic kidney cells (Graham *et al.*, 1977) and the SV40 large T antigen transformed HEK-293T cell line (DuBridge *et al.*, 1987) were provided by Dr. Philip Kitchen (University of Birmingham, United Kingdom) and cultured in DMEM with high

glucose (Sigma) supplemented with 10% (v/v) FBS, 2 mM L-glutamine and Pen/Strep (100 U/ml Penicillin and 100 μg/ml of Streptomycin (Gibco)).

2.1.2.3 Human Umbilical Vein Endothelial cells (HUVEC)

Human Umbilical Vein Endothelial Cells (HUVEC) were purchased from PromoCell and cultured on 0.2 % gelatin-coated plates in Endothelial Cell Growth Medium 2 (EGM-2, PromoCell), which is a low serum cell culture medium for endothelial cells from large blood vessels, free from bovine hypothalamic extract. HUVEC were used between passage 2 and passage 6 in experiments.

2.1.2.4 Human microvascular endothelial cell line (HMEC-1)

The human microvascular endothelial cell line, HMEC-1 (Ades *et al.*, 1992) were cultured in MCDB 131 medium (Gibco) supplemented with 10% (v/v) FBS, 2 mM L-glutamine and Pen/Strep (100 U/ml Penicillin and 100 μg/ml of Streptomycin (Gibco)).

2.1.3 Maintenance of Cells

All the cell lines were grown in T-75 flasks and passaged once confluent. Culture medium was removed, and cells washed gently with PBS (Ca^{2+}-/Mg^{2+}-free) before incubation with 0.25% Trypsin-EDTA (1X) (Gibco) at 37ºC for 1-2 min. Cells were re-suspended in an appropriate volume of culture medium to inactivate the trypsin. Cell number was calculated using haemocytometer and the cells plated at the desired density. All the cells were incubated under standard culture condition at 37ºC with 6% CO_2 and humidified atmosphere.

2.1.4 Cell Viability

50 μl of cell suspension was placed in a 1.5 ml Eppendorf tube. An equal part of 0.4% trypan blue dye (Gibco™) was added to the cell suspension to obtain a 1:2 dilution. The mixture was mixed by pipetting up and down. The haemocytometer counter was filled with the cell

suspension (10 µl) by placing the tip of the pipette at the notch. The viable cells (clear) and non-viable cells (blue) were counted. The percentage of viable cells was calculated by dividing the number of viable cells by the number of total cells and multiplying by 100 using the formula below.

$$Cell\ viability\ (\%) = \frac{viable\ cells}{Total\ cells} \times 100$$

2.1.5 Cell Culture Media

Media	*Ingredients*
E2 medium (Maintenance media)	DMEM/F-12 with: 10% (v/v) FBS 2 mM L-Glutamine 100 U/ml penicillin 100 µg/ml streptomycin 1 µg/ml Insulin 1 nM β-Estradiol (E2)
MM1 medium (Differentiation media)	DMEM/F-12 with: 2% (v/v) Charcoal-stripped FBS 2 mM L-Glutamine 100 U/ml penicillin 100 µg/ml streptomycin 1 µM Medroxyprogesterone (MPA) 0.5 mM 8-Br-cAMP
HEK293/293T	DMEM (high glucose) with: 10% (v/v) FBS 2 mM L-glutamine 100 U/ml penicillin 100 µg/ml streptomycin
HMEC-1	MCDB 131 with: 10% (v/v) FBS 2 mM L-glutamine 100 U/ml penicillin 100 µg/ml streptomycin
MEFs	DMEM (high glucose) with: 10% (v/v) FBS 2 mM L-glutamine 100 U/ml penicillin 100 µg/ml streptomycin 1 mM sodium pyruvate 1% MEM non-essential amino acid 100 x

Table 2.1: Lists of cell culture medium.

2.1.6 Cryopreservation of Cells

Freezing of cells was routinely performed to maintain cell stocks for later research. The cells were detached by exposure to trypsin as described in section 2.1.3 and then transferred to a 15 ml centrifuge tube and pelleted at a low speed (200 x g) for 5 min. The supernatant was then discarded, and cell pellets were re-suspended in freezing medium, consisting of 10% (v/v) dimethyl sulphoxide (DMSO) (Sigma) in their respective growth medium. The cells were aliquoted in cryovials (1 ml) and placed in a "Mr Frosty" (BDH) at room temperature and transferred to a -80^{o}C freezer. The cells were then transferred to liquid nitrogen storage within 3 days for long term storage.

2.1.7 Thawing cells

Frozen cells were thawed at 37^{o}C. Immediately, the contents were removed into 9 ml of pre-warmed complete medium in a 15 ml Falcon tube. The cells were re-suspended, and the tube was centrifuged at 200 x g for 5 min. The supernatant was discarded, and the cell pellet was re-suspended in 5 ml complete medium. The suspended cells were transferred into a 75 cm^2 flask and complete medium was added to a final volume of 15 ml. Cells were incubated at 37^{o}C in humidified conditions supplemented with 6% CO_2. The medium was changed the next day and the cell condition and viability was observed.

2.1.8 Mycoplasma Test

To ensure the absence of mycoplasma, the cells were tested using the EZ-PCR Mycoplasma Test Kit (Biological Industries) according to the manufacturer's instructions. Briefly, cell culture supernatants (1 ml) were centrifuged at 16,000 x g for 10 min to sediment mycoplasma. The supernatant was discarded, and the pellet re-suspended in 50 µl of buffer and heated at 95^{o}C for 3 min. PCR was performed with the following conditions:

denaturation 94ºC, 30 secs; amplification 94ºC, 30 secs; annealing 60ºC, 2 min; 72ºC for 1 min, with 35 cycles. The PCR product was loaded on a 2% agarose gel electrophoresis.

2.2 *In Vitro* Decidualisation of hESC

In vitro decidualisation of primary hESC and St-T1b cells was induced as described previously (Samalecos *et al*., 2009). The hESC were plated onto 6-well plates at 3 x 10^5 cells/well, or 10 cm Ø Petri dishes at 1 x 10^6 cells/dish and allowed to grow until confluent. The growth medium was aspirated, and cells were washed once with PBS. The cells were then treated with decidualisation medium (MM1) comprising DMEM/F-12, 2% charcoal-stripped FBS (Biosera, South America), 0.5 mM 8-Br-cAMP (Enzo Life Sciences), 1 µM medroxyprogesterone acetate (MPA) (Sigma) and Pen/Strep (100 U/ml Penicillin and 100 µg/ml of Streptomycin (Gibco)). Non-decidualised control cells were maintained in a proliferative state by culturing in E2-containing medium (E2 medium) (DMEM/F-12, 10% (v/v) of charcoal-stripped FBS, 1 nm E2, 1 µg/ml insulin and Pen/Strep (100 U/ml Penicillin and 100 µg/ml of Streptomycin (Gibco)). The cells were re-stimulated with fresh medium 24 h prior to harvesting (**Figure 2.1**). Conditioned medium (CM) was collected from the cells after various time periods. CM was centrifuged at 1,000 x g to remove cells and the supernatant frozen at -20ºC.

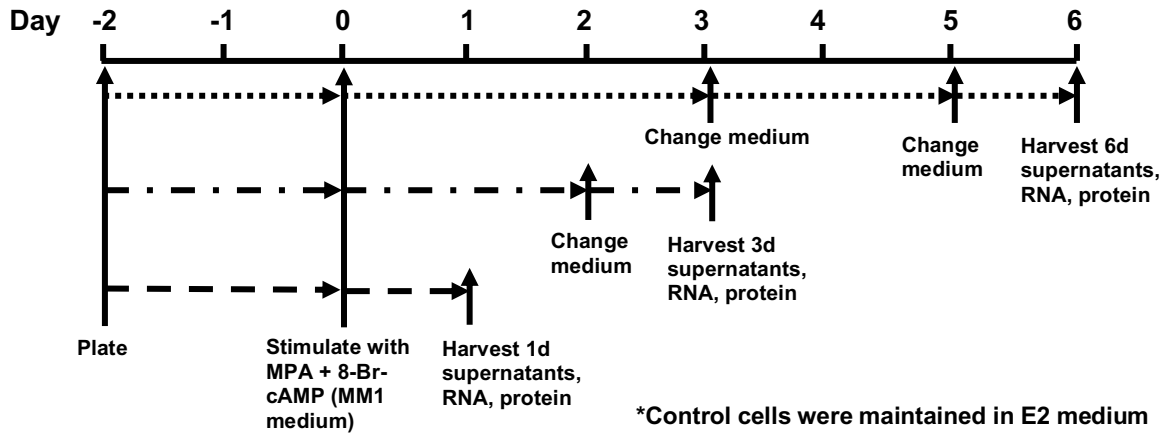

Figure 2.1: Stimulation of hESC for decidualisation. The incubation of primary hESC and St-T1b cells is outlined. Cultures were treated with E2 or MM1 medium for 1, 3 or 6 days. Supernatants were collected from each time point, and RNA, as well as protein, was collected.

2.3 Total RNA Extraction

Total RNA was extracted using Total RNA plus Extraction Kit (Norgen, Biotek Corporation, Canada) according to the manufacturer's instructions. Cells grown on 6-well plates were washed with PBS twice and incubated with 120 µl Lysis Buffer per well for 5 min at room temperature. The lysate from three wells was combined and stored at -20°C. Samples were passed through the gDNA column by centrifugation at 13,000 x g for 1 min to remove genomic DNA. The flow-through then mixed with 210 µl molecular-grade ethanol and transferred to RNeasy columns followed by centrifugation at 13,000 x g for 1 min. The flow through was discarded, and the columns were washed with 400 µl of wash buffer three times. RNA was eluted with 50 µl of elution buffer and centrifuged at 2,000 x g for 2 min followed by 14,000 x g for 1 min at 4°C. The RNA concentration was measured by a spectrophotometer and the purity assessed by 260:280nm absorbance ratio greater than 1.8. The purified RNA was either used immediately for cDNA synthesis or stored at -80°C.

2.4 cDNA Synthesis

A stock solution of cDNA reaction mix was prepared using the Tetro cDNA synthesis kit (Bioline, UK) according to the manufacturer's guidelines. RNA concentrations were normalised so that all cDNA reactions contained the same amount of RNA (1 µg). The priming premix (1 µg of total RNA, 1 µl Oligo $(dT)_{18}$ primer, 1 µl of 10 mM dNTP were made up in diethyl pyrocarbamate (DEPC)-treated water to a total volume of 12 µl) and incubated at 65°C for 5 min to denature any secondary structures of RNA formed in samples followed by 2 min on ice. The reaction premix (for one reaction: 4 µl 5x RT buffer, 1 µl Ribosafe RNase inhibitor, 1 µl of Tetro Reverse Transcriptase and 2 µl of DEPC-treated water) were prepared. The mixture was incubated at 42°C for 30 min and followed by 55°C for 30 min. The samples were then stored at -20°C or used immediately for polymerase chain reaction (PCR).

2.5 Reverse Transcription PCR

A reaction master mix was made using the MangoTaq PCR kit (Bioline) and prepared as following per sample : 4 µl 5x MangoTaq™ Reaction Buffer, 2 µl of $MgCl_2$ (50 mM), 0.3 µl of dNTP mix (100 mM), 0.3 µl of primer mix (50 µM), 0.3 µl of Mango Taq polymerase (1000 units) and PCR grade water was added to a total volume to 19 µl/reaction. The master mix (19 µl) was aliquoted into 0.2 ml PCR tubes followed by adding 1 µl of cDNA. The samples were mixed, centrifuged and placed into the PCR instrument (SensiQuest Labcycler). PCR amplification conditions were as follows: Denaturation at 95°C for 10 min followed by 35-40 cycles of denature 95°C, 30 sec; annealing (refer to **Table 2.2**), 30 sec; extension 72°C, 1 min and final extension step at 72°C for 10 min. The PCR products were separated on 1 to 2% (w/v) agarose gels.

Primers	*Forward/Reverse Primer*	*Annealing Temperature*	*Product Size*	**References / Sources**
dPRL	5'-GAGACACCAAGAAGAATCGGAACA TACAGG-3' 5'-TCGGGGGTGGCAAGGGAAGAA-3'	60^{O}C	416 bp	Samalecos *et al*., 2009
IGFBP-1	5'-TGCTGCAGAGGCAGGGAGCCC-3' 5'-AAGGATCCTCTTCCCATTCCA-3'	63^{O}C	378 bp	Samalecos *et al*., 2009
GAPDH	5'-GGAGTCCACTGGCGTCTTCAC-3' 5'-GAGGGGCCATCCACAGTCTTCT-3'	51^{O}C	159 bp	Samalecos *et al.*, 2009
Uni-Cre	5'- ACCTGAAGATGTTCGCGATTATCT-3' 5'- ACCGTCAGTACGTGAGATATCTT-5'	58ºC	~400 bp	Paik *et al.*, 2007

Table 2.2: Oligonucleotide primers and amplification conditions for RT-PCR.

2.5.1 Agarose Gel Electrophoresis

Agarose gels were prepared by mixing molecular grade agarose (Bioline) into 100 ml of 1x TAE electrophoresis buffer (**Table 2.3**) and heating using a microwave to dissolve the agarose. The gel was then allowed to cool to 50ºC before adding 5 µl of 10 mg/ml Midori Green Advance DNA Stain (Nippon Genetics Europe GmbH). Immediately, the gel was poured into a casting tank and left to solidify for 10 min. The gel was placed in a electrophoresis tank and filled with 1 x TAE buffer. Samples and DNA Hyperladder IV or V marker (Bioline) were loaded and the gel was run to 100 V for approximately 30 min. Gel images were captured using a SyngeneII gel doc system.

Buffer	*Recipe*
50 X TAE	For 1 L: 242.2 g Tris base 57.1 ml glacial acetic acid 100 ml 0.5 M Ethylenediaminetetraacetic Acid (EDTA), pH 8.0 Bring the volume up to 1L with ddH_2O
0.5 M EDTA, pH 8.0	For 500 ml: 93.05 Na_2•EDTA•$2H_2O$ (disodium dyhydrate) 9 g solid NaOH Adjust the pH to 8 Bring the volume up to 500 ml with ddH_2O

Table 2.3: Buffers for agarose gel electrophoresis

2.6 Real-Time Quantitative PCR

The cDNA was diluted with polymerase chain reaction grade water (PCR.H_2O) in a 1:3 ratio. The master mix for one reaction: 7.5 µl of 2x SensiMix™ SYBR® No-ROX (Bioline), 0.1 µl primer (50 pmol/µl), 1 µl of diluted cDNA and PCR.H_2O added to a final volume of 15 µl was prepared. Primers were designed or verified using Primer Blast (http://www.ncbi.nlm.nih.gov/tools/primer-blast/). Correct amplicon size was confirmed by running product on an agarose gel and the standard curves were run with genomic DNA (gDNA) to ensure suitable amplification efficiency. Samples were amplified under the following conditions: denaturation 95ºC 10 min followed by 40-45 cycles of denature 95ºC, 10 secs; annealing temperature (*see* **Table 2.4** and **Table 2.5**), 15 secs; extension 72ºC, 20 secs on a Rotor-Gene Q (Qiagen). Reactions were run in duplicate and repeated twice. CT values were extracted to Microsoft Excel format and target gene values normalised to the control β-actin values using the comparative ΔΔCt method ($\Delta\Delta\mathrm{Ct} = \Delta\mathrm{Ct\ sample} - \Delta\mathrm{Ct}$ β-actin) (Pfaffl, 2004). Fold change was then calculated using the equation $2^{-\Delta\Delta\mathrm{Ct}}$.

Primers	***Forward/Reverse Primer***	***Annealing Temperature***	***Product Size***	***References / Sources***
β-actin	5'-TCACCCACACTGTGCCCATCTACGA-3' 5'-CAGCGGAACCGCTCATTGCCAATGG-3'	58ºC	295 bp	Mälarstig *et al.*, 2003
FOXO1	5'-TTGAATTCACCCAGCCCAAACT-3' 5'-GCTACCCCAGGATCAACTGGTG-3'	58ºC	215 bp	Tanaka *et al.*, 2009
FOXO3A	5'-TGACTGATATGGCAGGCACCAT-3' 5'-CCGTGCTGTTAAAGGAGCTGGT-3'	58ºC	211 bp	Tanaka *et al.*, 2009
HOXA10	5'-GGTGGACGCTGCGGCTAATCTC-3' 5'-GCCCCTTCCGAGAGCAGCAAAG-3'	61ºC	211 bp	Yang *et al.*, 2012
SOD-2	5'-TCAGCGGTAGCACCAGCACT-3' 5'- ATCTGCGCGTTGATGTGAGG -3'	65ºC	163 bp	Araujo *et al.*, 2011
VEGF	5'- CCTTGCCTTGCTGCTCTACC-3' 5'- ACACTCCAGGCCCTCGTCATTG-3'	58ºC	250 bp	In house

sFlt-i13	5'- ACAATCAGAGGTGAGCACTGCAA-3' 5'- TCCGAGCCTGAAAGTTAGCAA-3'	56ºC	180 bp	Whitehead *et al*., 2011
sFlt-e15a	5'-CTCCTGCGAAACCTCAGTG-3' 5'-GACGATGGTGACGTTGATGT-3'	54ºC	158 bp	Whitehead *et al*., 2011
Flt-1	5'-TGGCAGCGAGAAACATTCTTTTATC-3' 5'-CAGCAATACTCCGTAAGACCACAC-3'	58ºC	200 bp	In house
C/EBPβ	5'- AACTCTCTGCTTCTCCCTCTG-3' 5'- TGCGTCAGTCCCGTGTAC-3'	59ºC	113 bp	Jiang *et al*., 2015
EGR-1	5'-AGCACCTGACCGCAGAGTCT-3' 5'-AGATGGTGCTGAGGACGAGG-3'	60ºC	236 bp	Kommagani *et al*., 2016
FOXM1	5'-GACATCAGCTTTCCTGGCCT-3' 5'-CAGTGGCTAGGGTGTGACTG-3'	60ºC	248 bp	Jiang *et al*., 2015
PLZF	5'- TAGGGTGCACACAGGTGAGA-3' 5'- GTGCAGATGGTGCACTGGTA-3'	60ºC	129 bp	Kommagani *et al*., 2016
c-Myc	5'-TCGGATTCTCTGCTCTCCTCG-3′ 5'-CTGCGTAGTTGTGCTGATGTGTG -3′	60ºC	274 bp	McConnell *et al*., 2015
STAT3	5'- GAGAAGGACATCAGCGGTAAG -3' 5'- AGTGGAGACACCAGGATATTG -3'	60ºC	137 bp	Turton *et al*., 2015
Akt-1	5'-AGGCTCCCCTCAACAACTTC-3' 5'-CTCCTCCTCCTCCTGCTTCT-3'	58ºC	206 bp	Ericson *et al*., 2016
CREB-1	5'-TTAACCATGACCAATGCAGCA-3' 5'-TGGTATGTTTGTACGTCTCCAGA-3'	58ºC	203 bp	Primer bank (ID:215490111c3)
IRF4	5'-ACCCGGAAATCCCGTACCA-3' 5'-GGCAACCATTTTCACAAGCTG-3'	58ºC	84 bp	Vasquez *et al*., 2015

Table 2.4: Human real-time qPCR primers.

Primers	*Forward/Reverse Primer*	*Annealing Temperature*	*Product Size*	*References / Sources*
β-actin	5'-GTATGCCTCGGTCGTACCA-3' 5'-CTTCTGCATCCTGTCAGCAA-3'	58ºC	62 bp	In house
FoxO1	5'-TTCAATTCGCCACAATCTGTCC-3' 5'-GGGTGATTTTCCGCTCTTGC-3'	58ºC	118 bp	Tanaka *et al.*, 2009
Vegf	5'-GAGTACCCCGACGAGATAGAGT-3' 5'-GGTGAGGTTTGATCCGCATGA-3'	58ºC	148 bp	In house
FoxO3a	5'- TGAACTCCTTGCGTCAGTCACC-3' 5'- CGGTGCTAGCCTGAACATCAA-3'	58ºC	177 bp	Tanaka *et al*., 2009

Table 2.5: Mouse real-time qPCR primers.

2.7 Western Blot

2.7.1 Protein Extract and Protein Assay

Confluent cells plated on 6-well dishes were washed with PBS and harvested using Pierce™ Radioimmunoprecipitation Assay Buffer (RIPA) lysis buffer (Fisher Scientific) with 20 µl/ml 50 X protease inhibitor (cOmplete mini EDTA free, Roche Diagnostics GmbH). The cells were incubated on ice for 2 min, scraped off the dish and transferred to a cold Eppendorf tube and stored at -20°C for later analysis or centrifuged at 13,000 x g for 30 min at 4°C prior to Western Blotting. Protein concentrations were measured using the Bradford protein assay according to the manufacturer's instructions (Bio-rad). 20 µg of protein was aliquoted and an equal volume of 2 x Laemmeli loading buffer (Bio-rad) was added. The samples were boiled for 5 min at 95°C, centrifuged at 12,000 x g for 1 min and loaded onto 10% sodium dodecyl sulfate–polyacrylamide gel electrophoresis (SDS-PAGE) gel.

2.7.2 SDS-PAGE

The mini gel plates (1.0 mm) (Geneflow) were cleaned with distilled water and assembled. A 10% (w/v) resolving gel (2.5 ml of 1.5 M Tris pH 8.8, 3.3 ml of 30% acrylamide, 4 ml of dH_2O, 100 µl 10% SDS, 90 µl 10% ammonium persulphate (APS) and 10 µl N.N.N'N' tetramethylethylenediamine-1,2-diamine (TEMED)) was poured and isopropanol was added immediately over the top to prevent oxidation. Once the gels were set, the isopropanol was poured off and a 5% stacking gel (3 ml dH_2O, 700 µl 30% acrylamide, 1.25 ml 0.5 M Tris pH 6.8, 50 µL 10% SDS, 50 µl of freshly prepared 10% APS and 10 µl TEMED) was added. Combs were inserted and the gels left to set. Gels were placed into electrophoresis tanks containing 1 x running buffer (0.1 M Tris pH 8.0, 0.1 M glycine, 0.1% (w/v) SDS) and the combs removed carefully. The pre-stained protein markers (GeneFlow) and samples (20 µg

total protein) were loaded, and the gels were run at 200V for 45 min to allow separation of proteins.

2.7.3 Immunodetection

Polyvinylidene fluoride (PVDF) membrane (Immobilon, Merck Millipore) was activated with 100 % methanol for 30 secs, then transferred to dH_2O for 5 min and placed in the transfer buffer (25 mM Tris-HC1, 150 mM glycine and 10% methanol). The SDS-PAGE gel was removed from the glass plates and transferred onto a Scotch pad and pre-soaked filter paper in a transfer cassette before the membrane was placed on top with another layer of filter paper and Scotch pad before closing the cassette. The cassette and a cool block were then placed in a tank filled with transfer buffer and left to transfer at 100 V for 1 h.

After transfer, the membrane was removed from the tank and stained with 0.1% Ponceau S solution to visualise the protein. The membrane was then de-stained with PBS in a tray on the shaker at room temperature and the membrane was blocked with 20% (w/v) dried skimmed milk powder (Marvel) in PBS whilst shaking for 1 h at room temperature, or overnight at 4^{o}C. After blocking, the membrane was washed three times in PBS with 0.1% Tween-20 (PBS-T) for 5 min each on a shaker at room temperature. The membrane was then incubated with the appropriate concentration of primary antibody (*see* **Table 2.6**) in 5% bovine serum albumin (BSA) (Millipore) in PBS-T on a roller stirrer at 4^{o}C overnight (**Table 2.6)**. The membrane was washed three times with PBS-T, for 5 min each, on the shaker and then incubated with agitation at room temperature with the appropriate secondary antibody diluted in 5% (w/v) skimmed milk powder (Marvel) in PBS for an hour followed by three washes with PBS-T. EZ-ECL (Biological Industries) (1 ml/membrane) was added to the membranes, which were then wrapped in Saran Wrap and exposed to Amersham Hyperfilm^{TM} ECL (GE Healthcare) and developed.

Antibody	*Species raised in*	*Dilution factor*	*Code No/Clove*
Primary Antibody (monoclonal)			
α/β- Tubulin Antibody	Rabbit	1:1000	#2148, CST
FOXO1	Rabbit	1:1000	C29H4, CST
FOXO1	Mouse	1:1000	D7C1H, CST
Anti-Phospho-FOXO1 (Ser256)	Rabbit	1:1000	#9461, CST
Flt-1	Mouse	1:500	V4262, Sigma
Akt Antibody	Rabbit	1:1000	#9272, CST
Phospho-Akt (Ser473) Antibody	Rabbit	1:1000	#9271, CST
P44/42 MAPK (Erk1/2) Antibody	Rabbit	1:1000	#9102, CST
Phospho-p44/42 MAPK (Erk1/2)(Thr202/Tyr204)	Rabbit	1:1000	#9101, CST
FOXO3A	Rabbit	1:1000	D19A7, CST
Neuropilin-1	Rabbit	1:1000	D62C6, CST
Secondary Antibody			
Anti-rabbit IgG, HRP-linked Antibody	Rabbit	1:3000	# 7074, CST
Anti-mouse IgG, HRP-linked Antibody	Mouse	1:3000	# 7076, CST

Table 2.6: Details of primary and secondary antibodies used for Western Blotting including dilution factors, incubation conditions and suppliers.

2.7.4 Stripping and re-probing membranes

After the signal development, the membrane was washed twice in PBS and placed in 20 ml of stripping buffer (*see* **Table 2.7**) for 15 min twice at room temperature. The membrane was then washed twice in PBS-T for 10 min each and re-blocked for further use.

Buffer	*Recipe*
1.5 M Tris, pH8.8 (Resolving gel)	90.8 g Tris Base 500 ml ddH_2O 2g SDS
0.5 M Tris, pH6.8 (Stacking gel)	6.06 g Tris Base 100 ml ddH_2O 0.4 g SDS
2X Sample Loading Buffer	1M Tris-HCI, pH 8 10 % SDS 1M DTT 20% Glycerol 1% Bromophenol Blue ddH_2O
10 X Running Buffer	30.3 g Tris Base 144 g Glycine 10 g SDS 1L ddH_2O

10 X Transfer Buffer	30.3 g Tris Base 144 g Glycine 1L ddH_2O
1 X Transfer Buffer	100 ml 10 X Transfer Buffer 200 ml Methanol 700 ml ddH_2O
Stripping Buffer, pH 2.2	7.5 g Glycine 0.5 g SDS 5 ml Tween-20 Bring the volume up to 500 ml with ddH_2O

Table 2.7: Buffers for SDS-PAGE and Western blotting.

2.8 Cell Staining

2.8.1 FITC Phalloidin Staining

Cells were plated onto 8-well glass microculture slides (Nunc) at 2 x 10^4 cells/well in 300 µl of growth medium and incubated at 37°C, 6% CO_2 in a humidified atmosphere. Primary hESC and St-T1b cell were used. The cells were stimulated with MM1 medium for 5 days then re-stimulated for 24 h and then fixed with 4% formaldehyde (Pierce) in PBS for 20 min in room temperature. Cells were washed twice with PBS for 5 min each, permeabilised with 0.1% Triton X-100 for 15 min and then washed twice with PBS. The cells were then stained with a 1:500 dilution Phalloidin-iFluor 488 Reagent CytoPainter (ab176753, Abcam) with PBS in a volume of 200 µl for 1 h at room temperature with gentle rocking. Cells were washed with PBS and counterstained with Hoescht (33342) at 1:500 dilution in PBS (200 µl/well) for 45 min with gentle rocking and washed twice in PBS. The cells were visualised under a confocal microscope LSM 780 at 10 X magnification. All the incubations were performed in the dark due to the light sensitivity of fluorescent dye.

2.8.2 Immunofluorescence Staining

Cells were plated onto 8-well glass microculture slides (Nunc) at a density of 2 x 10^4 cells/well in 300 µl growth medium and incubated at 37°C, 6% CO_2 and a humidified

atmosphere. Primary hESC and St-T1b cell were stimulated with MM1 medium for 3 days and re-stimulated for 24 h prior to staining. Cells were rinsed with PBS and fixed with 4% formaldehyde in PBS for 20 min in a fume hood at room temperature. The cells were rinsed with PBS, incubated with methanol for 10 min and then washed twice with PBS. The cells were then blocked with 5% goat serum (Sigma, D9663) in PBS for 20 min, followed by overnight incubation at 4ºC with 1:50 dilution of primary antibody (Anti-FOXO1(C29H4); Anti-FOXO3A (D19A7); Flt-11 and C/EBPβ (H-7)) in 1% BSA and 0.3% Triton X-100 in PBS. The cells were then washed twice with PBS and incubated with 1:1000 dilution of Alexa Fluor™ 594 F(ab')2 fragment of goat anti-rabbit IgG (H+L) or Alexa Fluor™ 488 F(ab')2 fragment of goat anti-mouse IgG (H+L) secondary antibody (Invitrogen, Thermo Fisher Scientific) in 1.5% blocking serum in PBS for another 1 h in dark. The cells were washed again with 1 X PBS, mounted with Vectashield mounting medium H-1500 (Vector Laboratories) and visualised under LSM 780 confocal microscope.

2.8.3 Indirect Flow Cytometry (FACS)

Cells were plated on the 10 cm Ø dishes, grown to confluence and stimulated with E2 or MM1 medium for up to 6 days. Cells were re-stimulated with fresh medium 24 h and the total cell number determined. Cells (1 x 10^6 cells/ml) were re-suspended in ice-cold PBS and fixed with 4% formaldehyde for 20 min then washed three times with PBS and incubated with 1:100 dilution of anti-Flt-1 monoclonal antibody (Sigma) or relevant IgG control antibody in 3% BSA in PBS for 1 h on ice with agitation. The cells were centrifuged at 500 x g for 5 min and re-suspended in ice-cold PBS three times. The cells were then incubated with diluted Alexa Fluor-488 labelled secondary antibodies in 3% BSA in PBS and incubated for 1 h on ice with agitation. The PI stain was added to label DNA. The cells were analysed in a 5 ml sterile non-pyrogenic FACS tubes with FACSCalibur Flow Cytometer

(Becton-Dickinson). The Flowing software 2 (free online software - http://flowingsoftware.btk.fi) was used to analyse the data for all experiments.

2.9 Enzyme-Linked Immunosorbent Assay (ELISA)

The conditioned media (1 ml/well) collected from stimulated cells were assayed for VEGF and sFlt-1 levels using the commercial human VEGF and Flt-1 DuoSet ELISA kits (DY293B & DY321B, R&D Systems) following the manufacturer's guidelines. Immuno^{TM} 96-well plates (Nunc) were coated with 100 µl capture antibody overnight at room temperature. The plates were aspirated and washed three times with 400 µl wash buffer (PBS with 0.05% Tween-20) and blocked with 300 µl of Reagent Diluent (0.22 µm filtered 1% (w/v) BSA in PBS) 1 h at room temperature. The wells were washed three times with wash buffer. 100 µl of protein standards or culture samples was added to the wells in duplicate and incubated for 2 h followed by three washes with wash buffer. 100 µl/well of detection antibody was added and incubated for 2 h at room temperature. The plates were washed three times again and 100 µl/well of Streptavidin-HRP was added and incubated for 20 min in the dark. The Substrate solution (100 µl/well) following three washes for 20 min in the dark. Stop solution (2N H_2SO_4) (50 µl/well) was added and the optical density read immediately at 450 nm with background correction at 540 nm using BioTek Synergy HT Microplate reader. Sample concentrations were calculated with Microsoft Excel from the standard curve.

2.10 Proteome Profilling

2.10.1 Human Angiogenesis Array

hESC were plated at density of 2.5 x 10^6 cells on 10 cm Ø dishes overnight. The cells were then stimulated with E2 and MM1 medium for 5 days. The cells were detached by exposure

to trypsin and re-plated onto 6-well plates with a seeding density of 8 x 10^5 cells/well in 1 ml DMEM/F12 containing 2% FBS or MM1 medium overnight and re-stimulated with fresh medium for 24 h. Cell supernatants were collected and aliquots stored at -20ºC. Human Angiogenesis Proteome Profiller Array kits (R&D Systems) were used according to the manufacturer's instructions. Briefly, 1 ml of CM was used per membrane. Each membrane, which carries capture antibodies to 55 angiogenesis-related factors spotted in duplicate, was treated with a cocktail of biotinylated detection antibodies and binding detected using streptavidin-HRP and chemiluminescence reagent. The signal density from each spot on the film was quantified using ImageJ software after exposure to film. Integrated densities for each spot were corrected using the negative control spots and normalised to the positive controls.

2.10.2 Human Phospho-Kinase Array

The St-T1b cells were plated in 10 cm Ø dishes at a cell density of 2.5 x 10^6 cells. After 24 h, the medium was changed to DMEM/F12 with 2% FBS overnight. The cells were treated with 2% charcoal-stripped FBS medium or MM1 medium for 6 h and re-treated with their respective fresh medium 1 h prior to harvesting. The cells were rinsed with PBS, scraped into 1 ml of PBS and centrifuged at 200 x g for 5 min. The supernatants were discarded, and the cell pellet was solubilised at ~ 1 x 10^7 cells/ml of lysis buffer (Buffer 6) and incubated at 4ºC for 30 min on a shaker. The lysate was centrifuged at 14,000 x g for 5 min and the supernatant transferred into a clean tube. The protein concentration in the lysates was quantified using the Bradford assay as described in section 2.7.1. Aliquots were stored at -20ºC before analysis using Human Phospho-Kinase profiler array kits (ARY003B, R&D Systems) according to the manufacturer's instructions. The phospho-kinase array detects 43 kinase phosphorylation sites and 2 related total proteins, each spotted in duplicate. A total

of 400 µg of cell lysate per membrane was mixed with a cocktail of biotinylated detection antibodies and the signal was detected with streptavidin-HRP and chemiluminescence reagent. Signal densities on the film were quantified using ImageJ software. Integrated densities of each spot were corrected using the negative control spots and normalised to the positive controls.

2.11 Plasmids

2.11.1 Recovery of plasmids stored on the filter paper

Plasmids that had been archived on filter paper were extracted by cutting out the region carefully where the DNA had been spotted and placing it in 30 µl of QIAGEN elution buffer in an Eppendorf tube. The tube was warmed at 37ºC for 15 min and centrifuged at 1,000 x g for 1 min to elute the plasmid.

2.11.2 Transformation of plasmids into *E.Coli*

TOP10 competent cells (Alpha-select gold efficiency, Bioline) were thawed on ice and plasmids (3 µl) was added gently and incubated on ice for 30 min. The cells were heat shocked for 45 secs at 42ºC and placed on ice for 2 min before adding 500 µl of Luria Broth (LB) (Sigma). The cells were incubated at 37ºC for 1 h in a shaking incubator. Between 20 µl and 100 µl of bacterial culture was spread onto LB agar plates containing the appropriate antibiotics (100 µg/ml ampicillin or 50 µg/ml kanamycin (**Table 2.8**) and incubated at 37ºC overnight.

2.11.3 Plasmid Mini preparation

A single bacterial colony was selected and inoculated into 5 ml LB medium containing the appropriate antibiotic and left to grow overnight at 37ºC in a shaking incubator. 1 ml of culture was transferred to an Eppendorf tube and centrifuged at 12,000 x g for 1 min

according to QIAprep Miniprep protocol (Qiagen). The supernatant was discarded, and the pellet re-suspended in 250 µl of Buffer P1 and transferred to a centrifuge tube. Buffer P2 (250 µl) was added and mixed thoroughly by inverting the tube a few times. Buffer N3 was immediately added and mixed by inverting a few times. The mixture was centrifuged at 13,000 x g for 10 min and the supernatant transferred to a QIAprep 2.0 spin column followed by a quick spin at 13,000 x g. The column was washed with 0.5 ml Buffer PB, centrifuged for 1 min and then 0.75 ml Buffer PE, centrifuged for 1 min followed by an additional 1 min centrifugation after discarding the flow through. The column was placed in a clean 1.5 ml Eppendorf tube and 50 µl Buffer EB added, allowed to stand for 1 min and centrifuged for 1 min to elute the DNA.

2.11.4 Restriction digests to confirm the correct plasmid

Plasmids isolated from bacteria clones were examined by restriction digestion to ensure the correct insert was present. All restriction digests were performed in a final volume of 20 µl. Restriction enzyme master mix was prepared by adding 2 µl Restriction enzyme buffer (NEB), 0.2 µl 100 x BSA, 1 µl of restriction enzyme (**Table 2.8**) and 5 µg of digesting fragment size determined on 1% agarose gels.

2.11.5 Plasmid Maxi Preparation

After verification, 500 µl of the overnight bacterial cultures was added to 200 ml of LB Broth with antibiotic and grown up overnight in a shaker at 500 rpm at 37ºC. The plasmids were extracted using an Endotoxin-free Maxi DNA kit (QIAGEN). Briefly, the bacterial culture was harvested by centrifuging at 6,000 x g for 15 min at 4ºC and the pellet re-suspended in 5 ml of Buffer P1 followed by 5 ml of Buffer P2. The lysate was then mixed by inverting the tube until viscous and then incubated at room temperature for 3 min.

Immediately, the pre-chilled Buffer P3 (10 mL) was added, mixed and transferred to a QIAfilter cartridge. The lysate was incubated at room temperature for 10 min and then filtered into a 50 ml tube. The Buffer ER (5 ml) was added, mixed and incubated on ice for 30 min. While a QIAGEN-tip 500 was equilibrated with 25 ml of buffer QBT. The lysate was then passed through the QIAGEN-tip 500 under gravity. The QIAGEN-tip was then washed twice with 30 ml of Buffer QC and the DNA was eluted in 10 ml of Buffer QN. The DNA was precipitated by adding an equal volume of isopropanol and centrifuging at 15,000 x g for 30 min at 4ºC. The DNA pellet was washed with 70% ethanol and centrifuged at 15,000 x g, 10 min then allowed to air-dry and dissolved in 100 µl of endotoxin-free Tris-EDTA (TE) buffer. The DNA concentration and purity was determined using a spectrophotometer by measuring 260:280nm absorbance.

2.11.6 Cryopreservation of bacterial stocks

Bacterial glycerol stocks were established for long-term storage. 500 µl of overnight bacterial culture was added to 500 µl of autoclaved 50% glycerol in PBS in a cryovial and mixed gently. The glycerol stocks were frozen at -80ºC.

Plasmids	***Antibiotic Resistant***	***Restriction Enzymes***	***Provider/supplier***
FHRE-luc	Ampicillin	*BamHI and Bgl II*	Michael Greenberg (plasmid #1789)
pcDNA3.1-EGFP	Ampicillin	*Bgl II and Xbal*	Doug Golenbock (Addgene plasmid # 13031
pVEGF-Luc	Ampicillin		Dr Padma-Sheela Jayaraman, University of Birmingham, UK
pFlt-1-Luc	Ampicillin		Dr Peter Hewett, University of Birmingham, UK
pFOXO1(-AAA)	Ampicillin		William Sellers (Addgene # 9022)
pFOXO3(-AAA)	Ampicillin		William Sellers (Addgene # 10709)
pBABE-GFP	Ampicillin	*BamHI and Xbal*	William Hahn (Addgene # 10668)

pBABE-puroL HA FKHR AAA	Ampicillin	*BamHI and Xhol*	William Sellers (Addgene # 9025)
pBABE-puroL FKHR AAA delta DB	Ampicillin	*BamHI and Xhol*	William Sellers (Addgene # 10697)
pLenti-FOXO1 AAA	Ampicillin	*BamHI and SalI*	Prof. Khandror, Boston University, USA
pLenti-FOXO1 Wild Type	Ampicillin	*BamHI and SalI*	Prof. Khandror, Boston University, USA
pUMVC	Kanamycin	*NotI and SalI*	Bob Weinberg (Addgene # 8449)
pWPT-GFP	Ampicillin	*Bgl II*	Dr Samir Sissaoui, University of Worcester, Cambridge, USA
pMD2.G	Ampicillin	*Bgl II*	Didier Trono (Addgen plasmid # 12259)
psPAX2	Ampicillin	*Xbal and SalI*	Didier Trono (Addgen plasmid # 12260)

Table 2.8: Lists of plasmids used in this study.

2.12 Viral Production and Infection

2.12.1 Lentivirus and pBABE retrovirus production

HEK293T cells were plated at density 1 x 10^6 cells/well in a 6-well plate for 24 h. After 24 h, a ratio of 2:2:1 of the plasmid carrying the gene of interest, psPAX2 (packaging plasmid) and pMD2.G (envelope plasmid) was used to make up the lentivirus with various transfection reagents such as PEI, $CaPO_4$, TransIT-2020 and TransIT-LT1. The transfected cells were topped up with fresh medium after 24 h of transfection. After 48 h of transfection, the supernatant was collected and aliquoted into sterile 1.5 ml tubes and centrifuged for 10 min at 1,500 x g. The supernatant was then transferred to a new tube and stored at -80^{o}C, used immediately for infection.

Similar procedures were employed to produce retroviral vectors using pBABE. A ratio of 4:3:1 of pBABE carrying the gene of interest (GOI) plasmid, pUMVC (packaging plasmid) (Stewart *et al.*, 2003) and pMD2.G (envelope plasmid).

2.12.2 Viral Transduction

The HEK293 cells were plated onto 6-well plates at a density of 1 x 10^6 cells/well and St-T1b cells with 1 x 10^5 cells/well at least 24 h before infection. The growth medium was aspirated and replaced with fresh medium. The appropriate amount of virus was added to the well with 8 µg/ml of polybrene and incubated for 48-72 h. The medium was collected after every 24 h of infection. The GFP expression level was visualised under a fluorescence microscope. After 48-72 h of infection, the RNA, or protein lysates was harvested for later analysis.

To select cells expressing the gene of interest (GOI) following viral infection, puromycin was used for negative selection. The lowest concentration of puromycin required to kill cells was established by treating the cells with different concentration of puromycin and incubated for 10-12 days. The medium containing puromycin was changed every 2-3 days.

2.12.3 Puromycin Kill Curve

A 10 mg/ml puromycin (Gibco, Life Technologies) stock solution was used. The cells were plated at 1 x 10^6 cells/well into a 6-well tissue culture plate. Once the cells were 60-80% confluent they were incubated in a range of 0 to 1.0 µg/ml of puromycin and incubated for 5 days. After 5 days, the lowest concentration of puromycin in which 100% of cells died was the optimal concentration to use for transduced cell selection.

2.13 Transient Transfection

Transient plasmid transfections were carried out in St-T1b cells. The transfection efficiency was optimised using various reagents: Lipofectamine® 2000 (Invitrogen), JetPRIME (Polyplus Transfection), K2 (Biontex), HappyFect, polyethyleneimine (PEI), TransIT-X2 (Mirus, Gene Flow), TransIT-2020 (Mirus, Gene Flow), Viromer Red (Lipocalyx) (*see* **Appendix A**). The cells were plated onto 12-well plates with appropriate cell density

according to TransIT-2020 manufacturer's guidelines and incubated overnight. Transfections were performed with 1 µg of pcDNA3-EGFP gift from Doug Golenbock (AddGene) and the DNA complexes added dropwise to each well following manufacturer's guideline. The plates were incubated for 24 h at 37°C and transfection medium replaced with fresh growth medium.

2.13.1 Dual-luciferase reporter assay

Dual-Luciferase Reporter Assays (Promega) were performed with various reporter vectors (*see* **Table 2.7**) and pRL-CMV Renilla control plasmid. TransIT-2020 transfection reagent was used. The cells were co-transfected with 1 µg of firefly luciferase test plasmid and ~50 ng pRL-CMV Renilla control plasmid into cells overnight followed by 24 h stimulation with E2 or MM1 medium. The firefly reporter activity was determined using the Dual-Luciferase assay (Promega) in transfected cells following manufacturer's guidelines, and the results normalised to Renilla luciferase reading measured using a Berthold Sirius Single Tube Luminometer.

2.13.2 siRNA-mediated knock-down of genes expression in hESC

hESC were plated at a density of 2.2 x 10^5 cells per well in 6-well plates and transfected with 50 nM of siRNAs targeting FOXO1 (siFOXO1), FOXO3A (siFOXO3A), Akt-1 (siAkt-1), Flt-1 (siFlt-1), VEGF (siVEGF) or control (siControl) in Viromer Blue (4 µl/well) following the manufacturer's guidelines. siRNA sequences are shown in **Table 2.9**. After 24 h transfection, cells were stimulated with E2 or MM1 medium for another 24 h before harvesting.

Target	*Sequences*	*References*
Universal Control	5'- UACCCCAUGGCAUUGUCAUtt-3' 5'-AUGACAAUGCCAUGGGGUAtt-3'	Dharmacon
FOXO1	5'-GAGCGUGCCCUACUUCAAGGAtt-3' 5'-UCCUUGAAGUAGGGCACGCUCtt-3'	Potente *et al*., 2005
AKT-1	5'-GGAGGGUUGGCUGCACAAAtt-3' 5'-UUUGUGCAGCCAACCCUCCtt-3'	Jiang *et al*., 2005
FOXO3A	5′- GAGCUCUUGGUGGAUCAUCtt-3′ 5'- GAUGAUCCACCAAGAGCUCtt-3'	Potente *et al.*, 2005
Flt-1	5'-UGAUGGCCUUACACUGAAAtt-3' 5'-UUUCAGUGUAAGGCCAUCAtt-3'	Dharmacon
VEGF	5'-GGAGUACCCUGAUGAGAUtt-3' 5'-AUCUCAUCAGGGUACUCCtt-3'	Takei *et al*., 2004

Table 2.9: siRNA duplex used in this study.

2.13.3 FoxO Knock-out MEFs

To generate the FoxO knock-out in MEFs, the cells were infected with an adenovirus expressing Cre recombinase (Ad-Cre), a kind gift of Dr Chris Kantos, Durham University, USA. Briefly, Ad-Cre viral supernatant was added onto 90% confluent HEK-293 cells (T-75 flask). The supernatant was harvested after the cells had rounded up resembling bunches of grapes and the medium changed to bright yellowish colour. The viral supernatant was stored at -80^{o}C.

The MEFs were passaged and split onto T-75 flasks to be ~ 90% confluent on the next day. The cells were treated with Ad-Cre virus in 8 ml of serum-free MEFs medium and incubated overnight. The plate was rocked gently every 10-15 min for the first hour.

2.14 Adenoviral-mediated transduction of hESC

hESC cells (2.5 x 10^5 cells/well) were plated on 6-well plates and incubated overnight. The cells were then transduced with a multiplicity of infection (MOI) of 50 infection units (ifu)/ cell of recombinant adenovirus expressing HA-tagged murine FoxO1 (Ad-FoxO1) or empty

control virus (Ad-CMV) for 24 h and incubated in E2 medium for another 24 h prior to harvesting. The Ad-FoxO1 was kindly provided by Prof. Domenico Acilli (Columbia University, New York, USA). Cell supernatants, RNA and protein lysate were harvested.

2.15 Immunoprecipitation (IP) of Flt-1 from cell supernatants

St-T1b cells were plated on 150 cm Ø tissue culture dishes and grown to confluence and stimulated with E2 or MM1 medium for 6 days. The cells were re-stimulated with fresh medium 24 h prior to harvesting. The supernatants were collected in clean Eppendorf tubes and centrifuged at 1,000 x g for 5 min to remove the cells and debris. Anti-Flt-1 antibody (3 µg, Flt-11 mouse mAb, Sigma) was added and incubated at room temperature for 2 h on a rotary stirrer. The protein A/G magnetic beads (50 µl) were washed with 1 ml of reduced serum medium three times and the beads re-suspended with 100 µl of serum-reduced medium. The beads were then added into the antibody mixture and incubated overnight at 4ºC on a rotary stirrer. Magnetic separation was used to wash the pellet with 300 µl of Wash Buffer three times. The supernatants were collected in clean Eppendorf tubes and stored at -20ºC Antibody-protein complexes were eluted with 100 µl of 4 X SDS Lysis Buffer (**Table 2.10**) at 95ºC for 10 min and analysed by SDS-PAGE and Western blotting.

Buffer	***Recipe***
Wash Buffer	10 mM Tris, pH 7.4 1 mM EDTA 1 mM EGTA, pH8.0 150 mM NaCI 1% Triton-X-100 0.2 mM sodium orthovanadate + Protease Inhibitor (1X)
4 X SDS Lysis Buffer	60 mM Tris-HCI, pH6.8 2% SDS 20% Glycerol 100 mM DTT 0.001% Bromphenol blue

Table 2.10: Buffers for Immunoprecipitation (IP)

2.16 Chromatin Immunoprecipitation-quantitative PCR (ChIP-qPCR)

For ChIP, ~ 1 x 10^7 cells were used per condition. The cells were fixed on the plates by adding methanol-free formaldehyde (Pierce™ (28906), Thermo Scientific) directly to the culture medium to a final concentration of 1% and incubated for 10 min at room temperature in a fume hood with agitation. The formaldehyde was then quenched by adding 2 M glycine (Sigma) to a final concentration of 0.4 M. The cells were scraped into ice-cold PBS and pelleted by centrifugation at 300 x g, 4ºC for 5 min and washed twice with ice-cold PBS. The cells were then resuspended in ice-cold Buffer A (**Table 2.11**) and incubated for 10 min at 4ºC with end-over-end mixing on a rotary stirrer. The nuclei were pelleted by centrifugation and resuspended with ice-cold Buffer B (**Table 2.11**) and incubated for another 10 min at 4ºC with rotation then pelleted and snap frozen on dry ice and stored at -80ºC or processed further. The nuclei were re-suspended in ice-cold ChIP buffer (300 µl/ 1 x 10^7 cells) and transferred to clean low-binding tube (Axygen).

The chromatin was sonicated by using a Bioruptor (Diagenode, USA) set at high=240W; 30 secs ON; 30 secs OFF. The degree of sonication was optimised using a series of cycles (0, 15, 20, 25, 30, 35 and 40 cycle) for each cell type to ensure that the majority of fragments were around 200 – 500 bp. The sonicated material was then centrifuged for 10 min at 16,000 x g at 4ºC and the supernatants transferred to fresh tubes. Chromatin was diluted with 3x ChIP-dilution buffer (1:3 ratio) and 50 µL was kept as "input" control sample.

Protein A/G Magnetic Beads (Pierce; Thermo Scientific), 10 µl per IP were washed twice with phosphate buffer (pH 8.0) and resuspended in 100 mM phosphate buffer (10 µl per sample). 10 µg of primary antibody (FOXO1A – ab39670 rabbit polyclonal, Abcam; FoxO1 (C29H4) rabbit monoclonal; FKHR (H-128) sc-11350 Rabbit polyclonal; Anti-FOXO3A – ab12162 rabbit polyclonal, Abcam; Anti-Pol II – ab26721 rabbit polyclonal, Abcam) and BSA (0.5% (w/v) final concentration) was added to the Protein A/G Dynabeads. A non-

specific rabbit IgG sc-2027 (Santa Cruz Biotechnology, Inc) was used as the negative control antibody. The antibody-Dynabeads mixture was incubated for 2 h at 4°C with rotation then washed with 100 mM phosphate buffer with 0.5% BSA and re-suspended in 10 µl of 100 mM phosphate buffer. The diluted chromatin (400 µl) was added into the antibody-Dynabead mixture and incubated for another 3 h at 4°C with rotation. The beads were washed with 1 ml of wash buffer 1, twice with wash buffer 2, once with LiCl buffer and finally twice with TE/NaCl. Each was for 10 minutes at 4°C. The beads were then transferred to a new tube and incubated with 50 µl of elution buffer twice for 15 min at room temperature with shaking. The chromatin cross-links were reversed by adding 1 µl of RNase A (10 mg/ml) and incubated for 30 min incubation at room temperature. The chromatin was then incubated overnight at 55°C in a water bath with 4 µl of 5 M NaCl, 2 µl of 0.5 M EDTA and 1 µl of proteinase K (50 mg/mL).

The DNA was isolated by adding AxyPrep Mag™ PCR clean-up beads (Axygen, Biosciences) [(Volume AMPure) =1.8 x reaction volume]. The DNA was mixed thoroughly by pipetting up and down and incubated at room temperature for 10 min. The beads were washed with 200 µl of 80% ethanol twice and air dried for 10 to 20 min. The DNA was eluted with 50 µl of 0.1 x TE buffer and the supernatant transferred carefully to new tubes. Real-time qPCR was run to determine the level of binding to sites in target genes. **Table 2.12** shows the lists of primers sequences and conditions used for amplification.

The percentage of Input which represents the amount of DNA pulled down using the antibody of interest in the ChIP reaction relative to the amount of starting material (Input DNA) was calculated. The average Ct values for each antibody used were averaged and the delta Ct (the difference in Ct values between the input and the antibody of interest) was

calculated. Finally, the percentage of input was calculated based on the delta Ct using the formula below.

$$\%\ input = 100 \times \left(\frac{50}{total\ sonicated\ material}\right) \times 2^{(Delta\ Ct)}$$

Fold enrichment was calculated by normalised to Negative control (NegC).

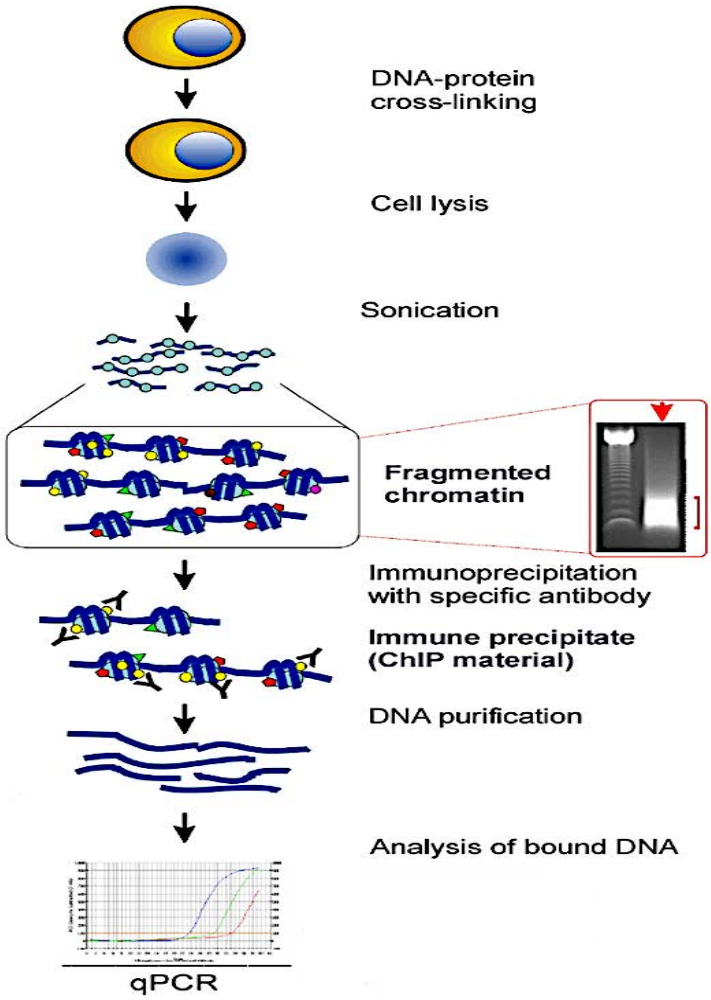

Figure 2.2: Illustration of the key steps in ChIP-qPCR (Collas and Dahl, 2008).

2.16.1 Identification of putative FOXO transcription factor binding sites and ChIP primer design

The *VEGF* and *Flt-1* reference sequences were obtained from University of California Santa Cruz (UCSC) genome browser (http://genome.ucsc.edu/) and then analysed using rVista (http://rvista.dcode.org/) (Loots and Ovcharenko, 2004) and Genomatix MatInspector

(http://www.genomatix.de/) (Cartharius *et al.*, 2005) for the presence of FHRE consensus sequences. Primers were then designed using Primer3 (http://primer3.wi.mit.edu/) (Koressaar and Remm, 2007) and Primer-Blast (http://www.ncbi.nlm.nih.gov/tools/primer-blast/) to amplify 80-200bp containing the sites of interest.

Buffer	***Recipe***
Buffer A	10 mM HEPES, pH 8.0 10 mM EDTA 0.5 mM EGTA 0.25 % Triton X-100 (+ protease inhibitor cocktail (PIC) 1X) optional: 10 mM Na-butyrate
Buffer B	10 mM HEPES, pH 8.0 200 mM NaCl 1mM EDTA 0.5 mM EGTA 0.01 % Triton X-100 (+ PIC 1X) optional: 10 mM Na-butyrate
ChIP Buffer	25 mM Tris-HCl, pH 8.0 150 mM NaCl 2 mM EDTA 1 % Triton X-100 0.25 % SDS (+ PIC (1:1000), 0.1 mM PMSF) optional: 10 mM Na-butyrate
3 X ChIP Dilution Buffer	25 mM Tris-HCl, pH 8.0 150 mM NaCl 2 mM EDTA 1 % Triton X-100 7.5 % Glycerol (+ PIC (1:1000), 0.1 mM PMSF) optional: 10 mM Na-butyrate
Phosphate Buffer, pH 8.0	2 ml 1M Na_2HPO_4 6 ml 1M NaH_2PO_4
Wash Buffer 1	20 mM Tris-HCl (pH 8.0) 150 mM NaCl 2 mM EDTA 1 % Triton X-100 0.1 % SDS
Wash Buffer 2	20 mM Tris-HCl (pH 8.0) 500 mM NaCl 2 mM EDTA 1 % Triton X-100 0.1 % SDS
LiCI Buffer	10 mM Tris-HCl (pH 8.0) 250 mM LiCl

	1 mM EDTA 0.5 % NP-40 0.5 % Na-deoxycholate
TE/NaCI Buffer	10 mM Tris-HCl (pH 8.0) 50 mM NaCl 1 mM EDTA
Elution Buffer	100 mM $NaHCO_3$ 1 % SDS

Table 2.11: Buffers used for ChIP.

Primers	***Forward/Reverse Primer***	***Annealing Temperature***	***Amplicon***	***References / Sources***
IGFBP-1	5'-CTGGACCTGGGCTGTCTTT-3' 5'-ACACAGCGCGCACCTTAT-3'	58°C	287 bp	Tamura *et al*., 2012
HBP1	5'-TGTCCCAGACACCAAAACAA -3' 5'-CGGGGAAGAGCTGGACTAC-3'	55°C	112 bp	Coomans *et al*., 2014
ERAG-1	5'-GCACTGCAAATGGCCTGTGAAC-3' 5'-TAGAGACCAGAGGGCTTAACATT-3'	58°C	197 bp	Chen *et al*., 2011
IGFBP-1	5'-TGATGAAGGACACTGCTTGG-3' 5'-CTGTGCTCCTCCTGTGTTTAG-3'	57°C	143 bp	Vasquez *et al*., 2012
IGF-1	5'-AACTTAAAGCTGTTTGGCTTCTC-3' 5'-GGCTGACATTATGCTGTTGTG-3'	57°C	103 bp	Vasquez *et al*., 2012
VEGFProx	5'-GGTCGAGCTTCCCCTTCA-3' 5'-GATCCTCCCCGCTACCAG-3'	58°C	202 bp	Clifford *et al*., 2012
VEGFdist	5'-GCGTGTCTCTGGACAGAGTTT-3' 5'-AGCCTCAGCCCTTCCACA-3'	58°C	160 bp	Clifford *et al*., 2012
NegC	5'-ATGGTTGCCACTGGGGATCT-3' 5'-TGCCAAAGCCTAGGGGAAGA-3'	58°C	174 bp	Active Motif
VEGF-FOXM1	5'-TCCGGGTTTTATCCCTCTTC-3' 5'-TCTGCTGGTTTCCAAAATCC-3'	55°C	165 bp	Karadedou *et al*., 2012
VEGF-ChIP-1	5'-CACACAGCTTCCCGTTCT-3' 5'-CCTCTGACAATGTGCCATCT-3'	56°C	~160 bp	Jeon *et al*., 2018
VEGF-ChIP-3	5'-ATCCCGTTCATCAGCCTAGA-3' 5'-ACCCTCCCTTTCCATCATTC-3'	58°C	172 bp	In House
VEGF-ChIP-4	5'-GGAGTGACTGGTGATGGCTA-3' 5'-TCAGCCCCTAAAAGAGCCAA-3'	60°C	123 bp	In House
VEGF-ChIP-5	5'-GGAGGTGGGCCATACTTTCT-3' 5'-GGTACCCAGCAAGGTGTGTT-3'	58°C	172 bp	In House
Flt-1-ChIP-1	5'-CCAAGTTGCAGGAGCAGTTT-3' 5'-GCCCAAGTCATTTCCTCAGT-3'	60°C	103 bp	In House
Flt-1-ChIP-2	5'-GAGCCATCACAGTCCCTTGT-3' 5'-GAGCAGCCCAGTCTTGTCTC-3'	60°C	97 bp	In House

Flt-1-ChIP-3	5'-TCTCCTGAGAAGCCCTCCTT-3' 5'-ACTTGAAGTGGCTGCAGGA-3'	60°C	120 bp	In House
Flt-1-ChIP 4	5'-CGACATGCTGGAAAGACAGA-3' 5'-GCTATCTGGCTGCCCTTGT-3'	60°C	109 bp	In House

Table 2.12: ChIP primer sequences and conditions for PCR amplification.

2.17 *In Vitro* Angiogenesis Assays

2.17.1 Scratch-wound Migration Assay

Cells (2 x 10^5) were seeded into 12-well plates and allowed to grow in their respective growth medium until they reached confluence. The cells were starved with serum-free medium for 4 h. Cell monolayers were then scratched with a sterile 200 µl pipette tip and the dislodged cells were washed away with PBS. Cells were then incubated in DMEM/F12 containing 2% FBS with, or without, growth factors (50 ng/ml VEGF-165, 50 ng/ml PIGF-2 or 100 ng/ml EGF) or with various CM. Eight images of cells per condition were captured on 0 and 24 h with an EVOS inverted phases microscope at 10 X objective as shown in **Figure 2.3.** The wound closure was quantified by ImageJ with Trainable Weka Segmentation and Voxel Counter plugins (Arganda-Carreras *et al.*, 2017). The area of cell migration was calculated by the difference between time 24 h and 0 h.

2.17.2 Tube Formation Assay

Growth factor-reduced, phenol red-free Matrigel (Corning® Matrigel® Matrix USA) was stored at -80°C and thawed on ice. A 12-well plate was rinsed with PBS and 70 µl of Matrigel was immediately pipetted into each well and left to set at room temperature. HUVEC were harvested and 180,000 cells were mixed with 1 ml of medium pipetted into each well. The tube formation was visualised using an IncuCyte ZOOM® system control (Essen BioScience) under 4 X objective and the images were taken every 6 h. The tube networks were quantified using Angiogenesis Analyser, ImageJ (plugin software) (Gilles, 2012).

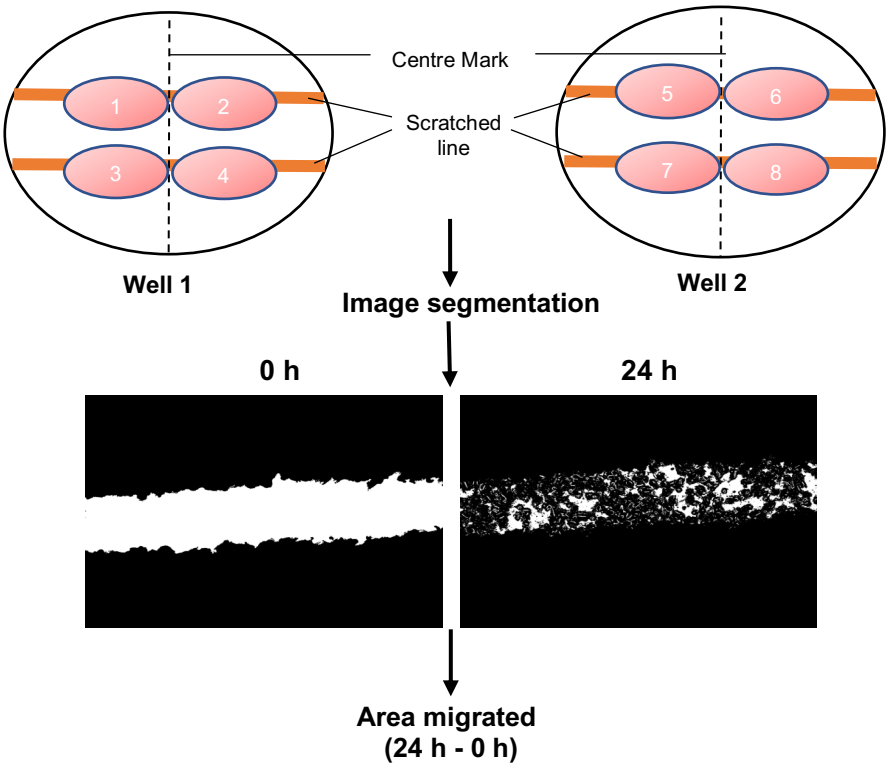

Figure 2.3: Illustration of the Wound healing assay plate layout. Confluent cell monolayers were scratched with a 200 µl tip and images were taken at 0 and 24 h according to the areas labelled.

2.17.3 Spheroid Sprouting Assay

hESC spheroids (5,000 cells/spheroid) or mixed cell spheroids (HUVEC and St-T1b cell with a ratio 1:1) were seeded on 96-well round bottom non-TC-treated plates in DMEM/F12 medium supplemented with 2% FBS and 0.25% methylcellulose (Polymer). The cells were incubated overnight at 37ºC to allow aggregation and formation of the spheroid.

Growth factor-reduced Matrigel (200 µl) was added to each well of a pre-cooled 24-well plate and incubated at 37ºC and 5% CO_2 for 45 min to set. Spheroids were harvested by rinsing with PBS and 12 spheroids were rapidly transferred to a well and covered 200 µl of Matrigel. The gel was mixed very carefully with a pipette tip without breaking the bottom layer of Matrigel to achieve an even distribution of the spheroids in the gel and incubated for 30 min at 37ºC to let the gel set fully. CM (250 µl) was added on top (**Figure 2.4**) and

spheroids sprouting observed under phase contrast with 10 X objective up to 24 h. Images of 10 spheroids per condition were taken and the mean length of the sprouts was measured using skeleton analysed (Skeleton analysis Plugins) in ImageJ.

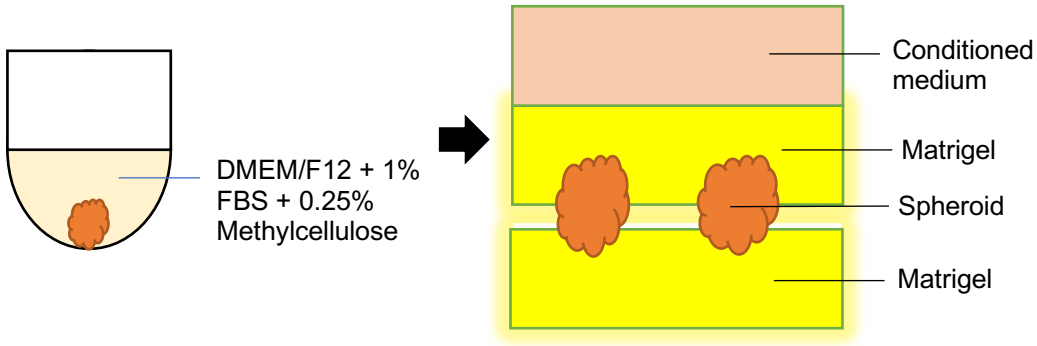

Figure 2.4: Formation and embedding of spheroids in Matrigel for sprouting assays. The spheroids were formed in a round bottom non-tissue culture plate and embedded in growth factor-reduced Matrigel on 24-well plate and conditioned medium (CM) or control medium added.

2.18 Statistical Analysis

The statistical significance of the data was determined using GraphPad Prism; two-tailed t-tests (Nonparametric Tests), one-way and two-way ANOVA with multiple comparisons using the Dunnett test. All data are expressed as means and standard error (+/- SEM). Overall, $p < 0.05$ was considered to be statistically significant.

CHAPTER 3:

ISOLATION OF HUMAN ENDOMETRIAL STROMAL CELL AND CHARACTERISATION OF THEIR DECIDUALISATION

3.1 INTRODUCTION

Unlike most adult tissues, uterine endometrium undergoes cyclic growth and tissue remodelling throughout the reproductive years to prepare for blastocyst implantation. During the mid-secretary phase of the cycle, the endometrial stromal cells (ESC) differentiate into decidual cells (decidualisation) regulated by ovarian steroids such as oestrogen, progesterone and various cytokines, beginning a few days after ovulation, at the onset of the window of implantation (Gellersen and Brosens, 2014). Impaired decidualisation can cause miscarriage independently of the quality of the blastocysts, or even lead to preeclampsia and IUGR later in pregnancy (Zhang *et al.*, 2013; Large *et al.*, 2014).

In humans, the decidualisation process is maternally controlled and is initiated independently of a signal from an implanting blastocyst, by progesterone and increased intracellular cAMP levels. *In vivo*, rising progesterone levels in the secretory phase of the menstrual cycle stimulate stromal cells, increasing intracellular cAMP and activating downstream PKA signalling leading to the expression of decidual genes (Telgmann *et al.*, 1997) such as PRL and IGFBP1 accompanied with morphological changes (Samalecos *et al.*, 2009). Both oestrogen and progesterone have been widely used to induce *in vitro* decidualisation for up to 14 days (Dimitriadis *et al.*, 2002; Sakai *et al.*, 2003). However, *in vitro* decidualisation can also be induced by the addition of progesterone analogues such as MPA, which has a much longer half-life in aqueous solution than progesterone and/or cAMP (Tawadros *et al.*, 2007; Samalecos *et al.*, 2009).

To date, accumulating data have shown that numbers of genes including cytokines, growth factors, and transcription factors are involved in decidualisation (Zhang *et al.*, 2013; Tamura *et al.*, 2014a). FOXO1 is an important regulator of various integral cell functions including apoptosis and metabolism (Samalecos *et al.*, 2009; Gellersen and Bronsens, 2003). The activity of FOXO1 is regulated by the PI3K via Akt-mediated phosphorylation of FOXO1

leading to its nuclear translocation (Tang *et al.*, 1999). Decidualised ESC support the remodelling and development of the endometrial vasculature and play a critical role in embryonic growth and survival in response to female sex hormones such as oestrogen and progesterone which act indirectly via many regulators (Girling and Rogers, 2005; Smith, 2001). Decidualised ESC play a role in protecting the embryo from oxidative stress (Okada *et al.*, 2017). Decidualised ESC are known to be more resistant to oxidative cell death compared to the undifferentiated ESC through increased expression of copper, zinc (SOD1) and manganese superoxide dismutases (SOD2) in early pregnancy (Kajihara *et al.*, 2006).

Despite advances in assisted reproductive technology (ART), many couples experience infertility due to the failed or defective implantation of the fertilised embryo into the uterus leading to pregnancy loss (Venners *et al.*, 2004; Brosens *et al.*, 2011). Therefore, knowledge of the mechanism of decidualisation is important to help in improving the success rate of ART and to lay a foundation for the development of the new treatments in reproductive clinical practice. In addition, impairment of ESC decidualisation may be a factor in preeclampsia, IUGR, recurrent miscarriage and other pregnancy disorders. In order to investigate the molecular mechanisms regulating human decidualisation, cultured hESC are critical tools due to the ethical issues associated with *in vivo* human studies. In this chapter, primary hESC and the established St-T1b hESC line (Samalecos *et al.*, 2009) were used to establish conditions for *in vitro* decidualisation, characterise changes that occur during this process and to investigate the secretion of angiogenesis associated factors.

3.2 RESULTS

3.2.1 Characterisation of hESC

In order to induce decidualisation, primary hESC and St-T1b cells were stimulated with MPA and 8-Br-cAMP at various time points over 7 days. The cell lysates and supernatants were collected depending on the type of experiment as shown in **Figure 3.1**. The Trypan Blue dye exclusion was used to determine the cell viability in a cell suspension. The expression of angiogenic factors and various decidual marker genes was examined. Differentiation of the cells was confirmed by observing cell morphology (**Figure 3.2**) and the expression of PRL, IGFBP-1 and FOXO1 (**Figure 3.3**).

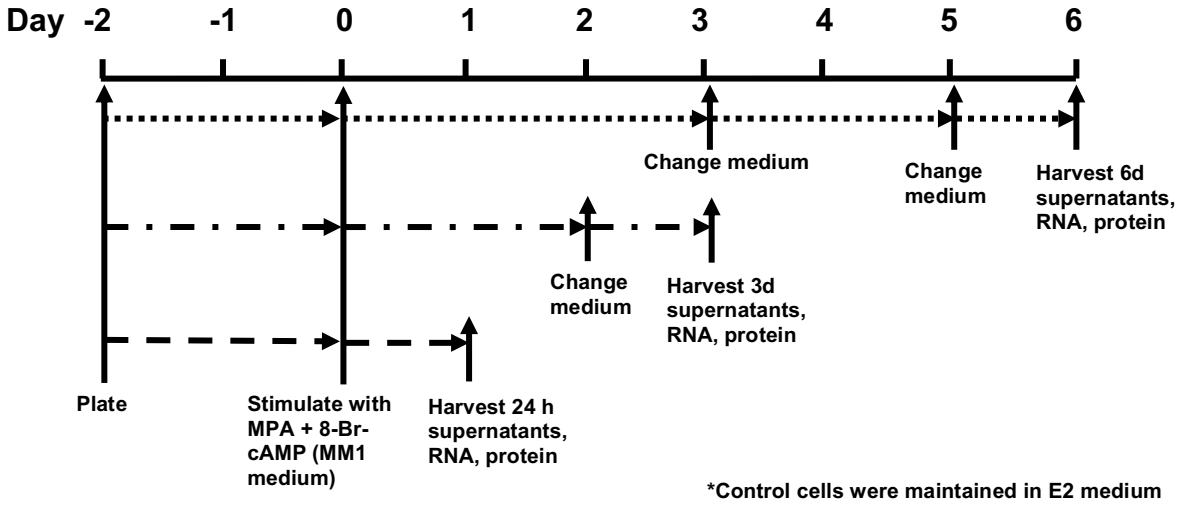

Figure 3.1: Protocol for stimulation of hESC decidualisation *in vitro*. Primary hESC and St-T1b cells were incubated as outlined in the scheme. Cultures were treated with E2 or MM1 medium for 1, 3 or 6 days. Supernatants were collected at each time point, RNA or protein lysates were harvested as described (**Section 2.3**).

3.2.1.1 Morphological Changes of hESC with decidualisation

Primary hESC and St-T1b cells were incubated with E2 or MM1 medium and harvested at a range of time point up to 7 days and the cell viability was greater than 90%. In order to determine whether the cells had undergone decidualisation, the morphology of the cells was monitored under bright field illumination on the phase contrast microscope every 24 h. The

cell morphology started to change from an elongated, fibroblast-like appearance to a more rounded epithelial cell appearance after 24 h (**Figure 3.2A**).

In order to determine the changes in the actin cytoskeleton arrangement of the cells, the cells were incubated with E2 or MM1 medium, for 6 days followed by Phalloidin staining. The localisation of F-actin filaments in decidualised hESC showed the expected cytoskeletal reorganisation and the changes of shape that were consistent with the transformation from fibroblast to a polygonal shape phenotype in St-T1b cells as seen in primary hESC (**Figure 3.2B**).

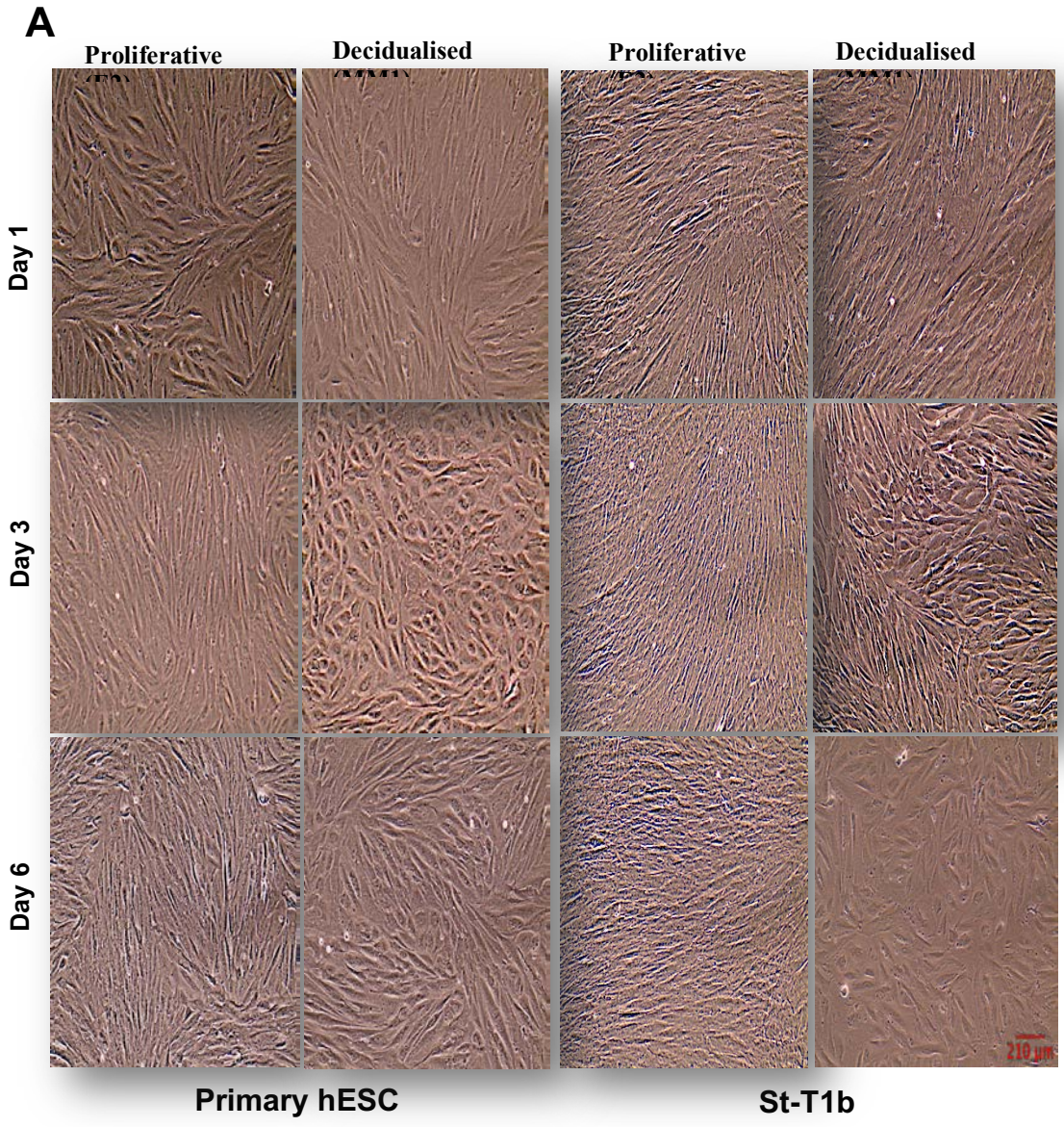

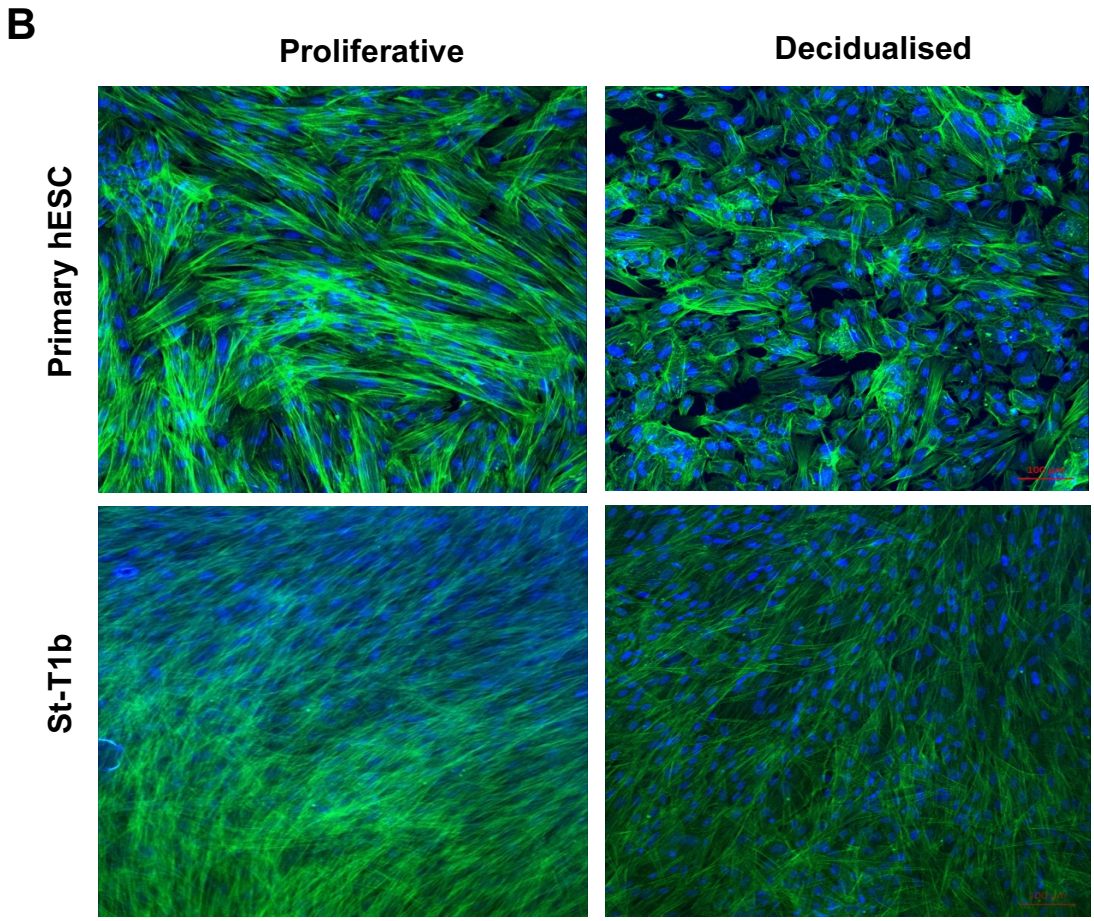

Figure 3.2: Changes in hESC actin cytoskeleton following *in vitro* decidualisation. (A) Primary hESC and St-T1b cells were seeded on 6-well plates and stimulated with E2 or MM1 medium over 6 days. Images were taken using EVOS phase contrast microscope at 10 X objective magnification. **(B)** Primary hESC and St-T1b were decidualised on culture slides for 5 days and stained with rhodamine phalloidin (green) and Hoescht 33342 (blue). The images were taken using LSM 780 Confocal Microscope under 10 X objective magnification.

3.2.1.2 Biochemical Changes of hESC with decidualisation

Decidualisation of ESC with cell viability >95% was confirmed by checking the expression of decidual-specific markers PRL and IGFBP1 (Samalecos *et al.*, 2009) with GAPDH as control by RT-PCR. The expression of PRL and IGFBP-1 were increased with decidualisation. Interestingly, both PRL and IGFBP-1 expression decreased from day 3 to day 6 of stimulation in primary hESC (**Figure 3.3A**). St-T1b cells also behaved as primary

hESC where PRL and IGFBP-1 were increased with decidualisation and the expression was observed as early as 24 h after stimulation (**Figure 3.3B**).

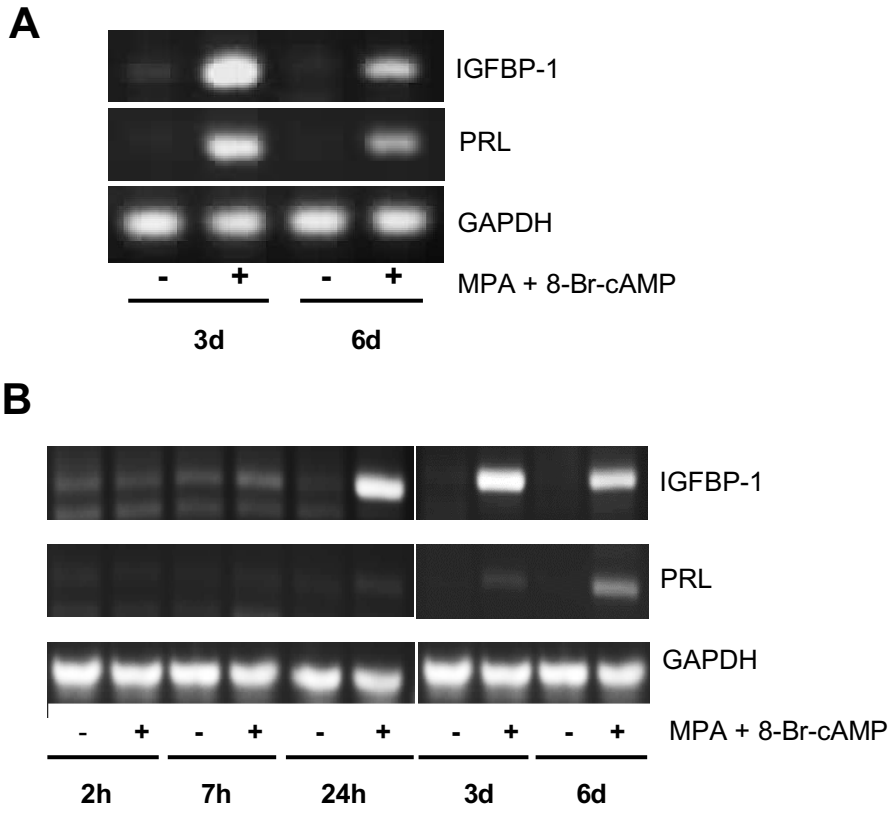

Figure 3.3: Induction of PRL and IGFBP-1 in hESC. (A) Primary hESC and **(B)** St-T1b cells were cultured in 6-well plates and stimulated with E2 (-) and MM1 medium (+) for 3 days (3d) and 6 days (6d). Induction of transcripts for decidualisation markers PRL and IGFBP-1 was demonstrated by RT-PCR; GAPDH used as a housekeeping control.

3.2.2 Regulators of decidualisation

3.2.2.1 Expression and activity of FOXO1 transcription factor in hESC during *in vitro* decidualisation

The FOXO1 transcription factor is a key regulator of ESC decidualisation (Gellersen and Brosens, 2003). Changes in FOXO1 mRNA expression were examined by real-time qPCR as well as protein levels by Western blotting. The expression of FOXO1 mRNA and protein was examined in primary hESC. FOXO1 mRNA and protein were increased dramatically during decidualisation in primary hESC (**Figure 3.4A&B**). The FOXO1 mRNA and protein

expression were also examined in St-T1b cells. The results obtained from St-T1b cells validated the increased of FOXO1. There was a large increase in FOXO1 mRNA levels from day 3 which was maintained to day 6 of decidualisation in St-T1b cells (**Figure 3.5A**). The expression of FOXO1 mRNA was detected as early as 2 h (**Figure 3.5B**). The FOXO1 protein levels mirrored the expression of mRNA. There was no increase in FOXO1 expression in control cells incubated in E2 medium (**Figure 3.5B**).

As FOXO1 activity is also subject to post-translational regulation, a FHRE promoter firefly luciferase reporter construct (FHRE-Luc) was used to investigate FOXO1 activity in St-T1b cells during decidualisation. St-T1b cells were co-transfected with FHRE-Luc plasmid and the pRL-CMV Renilla luciferase control plasmid for 24 h, followed by 24 h stimulation with E2 or MM1 medium containing 2% charcoal-stripped FBS and 0.5 mM 8-Br-cAMP. Luciferase activity was determined by dual luciferase reporter assay and the data was normalised to Renilla luciferase control readings. A 4-fold increase of FHRE promoter activity was detected in the cells stimulated with 8-Br-cAMP compared to control and the increase in activity was independent on the concentration of cAMP (**Figure 3.6**).

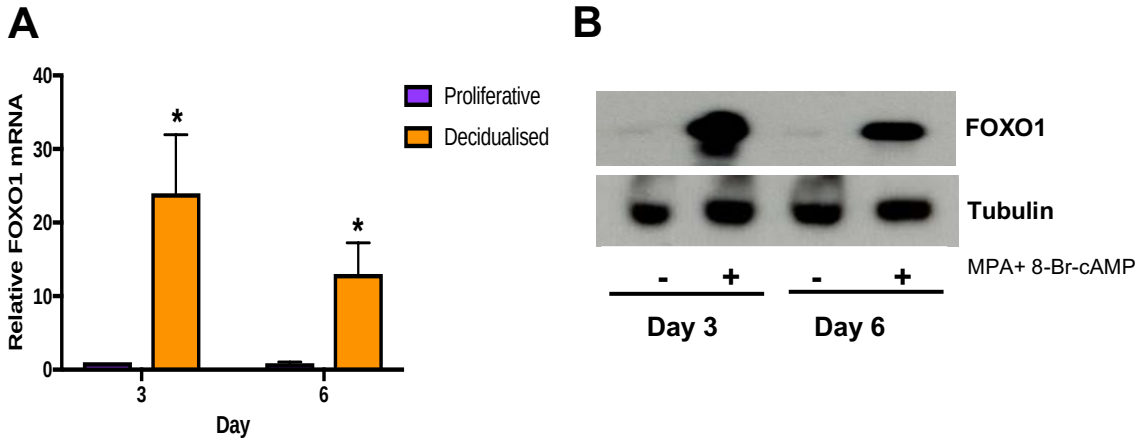

Figure 3.4: FOXO1 expression in primary hESC during *in vitro* decidualisation. **(A)** Real-time qPCR analysis of FOXO1 mRNA normalised to β-actin in primary hESC treated with E2 or MM1 medium for 3 and 6 days. **(B)** Representative Western blot showing of FOXO1 in whole-cell lysates with tubulin as a control. Results are the mean (+/- SEM) of 3 experiments and analysed using an unpaired, non-parametric t-test; *p<0.05.

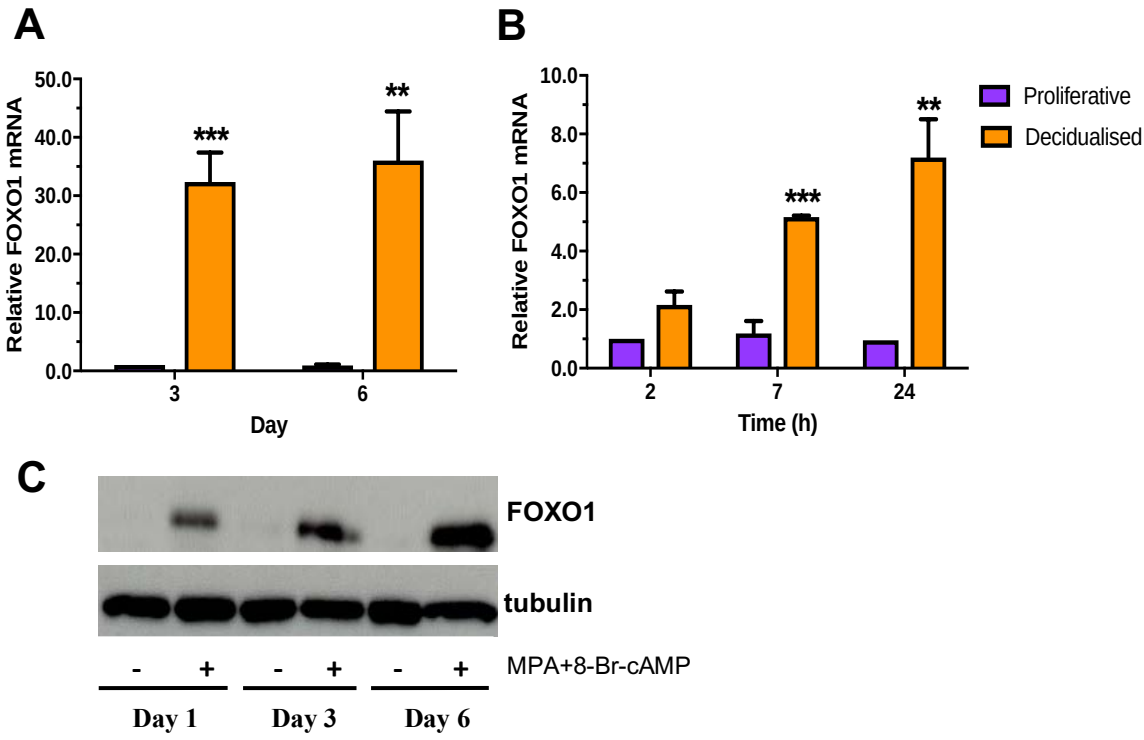

Figure 3.5: FOXO1 expression in St-T1b cells during *in vitro* decidualisation. Real-time qPCR analysis of FOXO1 mRNA normalised to β-actin in St-T1b cells treated with E2 or MM1 medium **(A)** for 3 and 6 days, and **(B)** short-term stimulation. **(C)** Representative Western blot showing of FOXO1 in whole-cell lysates with tubulin as a control. Results are the mean (+/- SEM) of 3 experiments analysed using an unpaired t-test; **p<0.01; ***p<0.001.

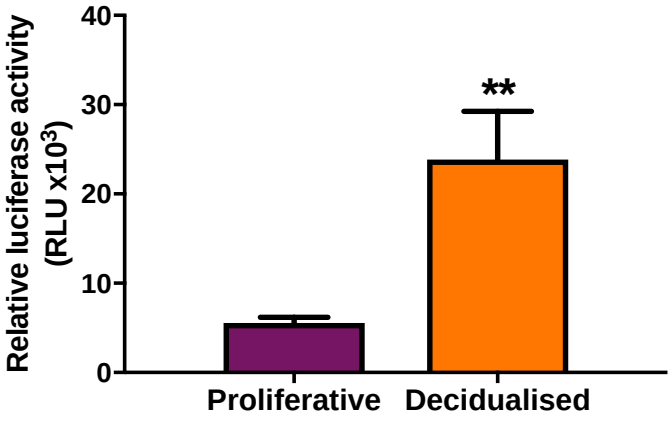

Figure 3.6: FOXO1 activity in St-T1b cells during *in vitro* decidualisation. St-T1b cells were plated on 12-well plates overnight and co-transfected with a FOXO1 luciferase reporter (FHRE) and pRL-CMV Renilla luciferase control plasmid. FHRE activity was normalised to pRL-CMV Renilla activity to control for differences in transfection efficiency. Results are the mean (+/- SEM) of 3 experiments and analysed using an unpaired t-test, **p<0.01.

3.2.2.2 Characterisation in changes of key decidualisation-related genes in primary hESC and St-T1b

Other key decidualisation-related genes including C/EBPβ, SOD2, HOXA10, FOXM1, IRF-4 and PLZF expression were investigated in primary hESC and St-T1b cells under our *in vitro* decidualisation conditions. C/EBPβ plays an important role in regulating decidual marker gene expression in association with FOXO1 transcription factors (Tamura *et al.*, 2014b). C/EBPβ mRNA dramatically increased by ~ 6-fold during decidualisation in both primary hESC (**Figure 3.7A**) and St-T1b cells (**Figure 3.7B**).

Superoxide dismutase-2 (SOD2) and Interferon regulatory factor 4 (IRF-4) which is reported to be a direct target of FOXO1 (Ujavri *et al.*, 2017; Vazquez *et al.*, 2015), was found to significantly increase in the decidualised St-T1b cells (**Figure 3.8A&D**). In addition, the increasing of HOXA10, PLZF, and FOXM1 also detected in St-T1b cells (**Figure 3.8B-D**).

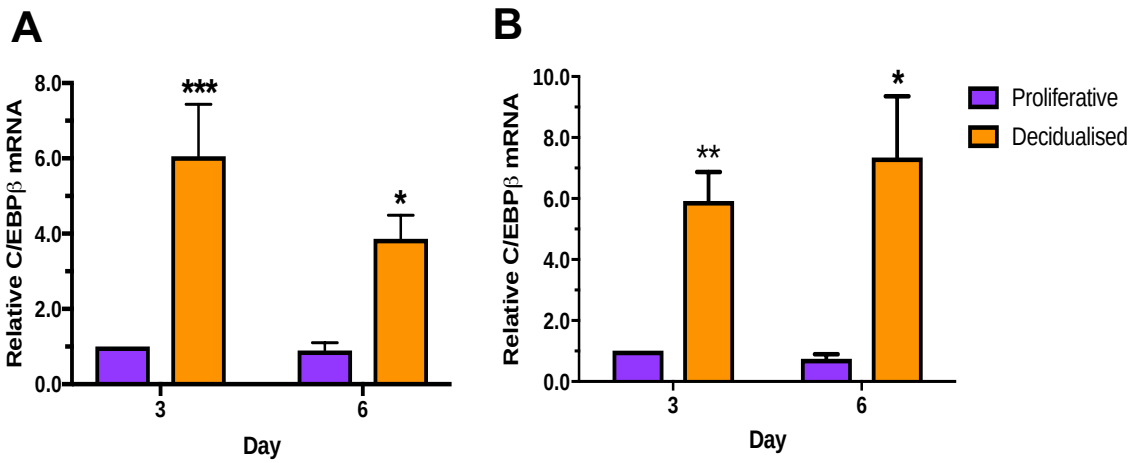

Figure 3.7: Up-regulation of C/EBPβ during decidualisation in hESC. Real-time qPCR analysis of C/EBPβ mRNA expression normalised to β-actin in **(A)** primary hESC and **(B)** St-T1b cells treated with E2 or MM1 medium after 3 and 6 days. Results are the mean (+/- SEM) of 3 experiments and analysed using an unpaired, non-parametric t-test; *p<0.05; **p<0.01; ***p<0.001.

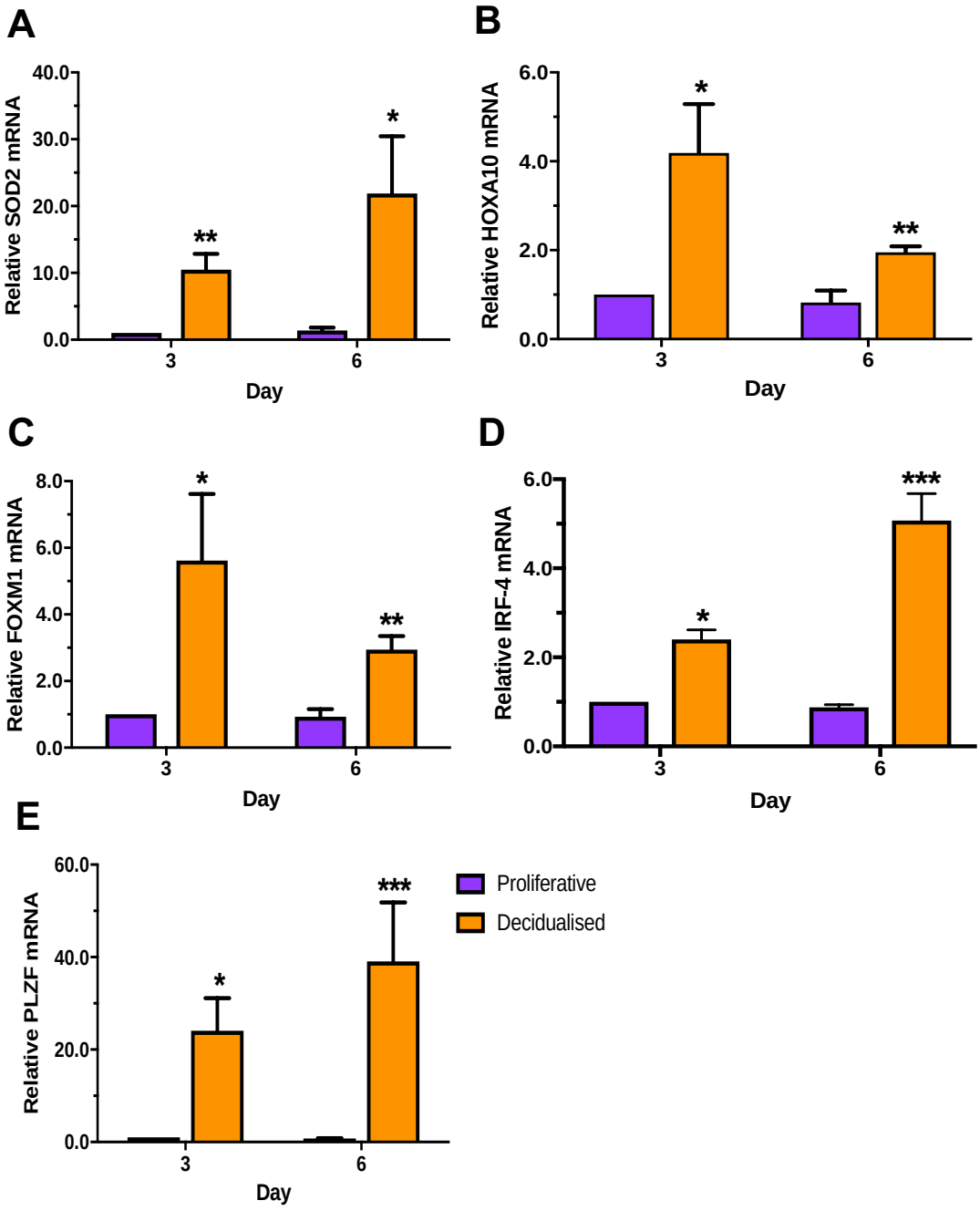

Figure 3.8: Up-regulation of various decidual factor during decidualisation in St-T1b cells. Real-time qPCR analysis of **(A)** SOD2, **(B)** HOXA10; **(C)** FOXM1; (**D**) IRF-4 and **(E)** PLZF expression normalised to β-actin in St-T1b cells treated with E2 or MM1 medium after 3 and 6 days. Results are the mean (+/- SEM) of 3 experiments and analysed using an unpaired, non-parametric t-test; *p<0.05; **p<0.01; ***p<0.001.

3.2.3 Secretion of angiogenic factors by hESC during decidualisation

Decidualised hESC are known to play a critical role in angiogenesis in the endometrium (Okada *et al.*, 2017). Therefore, human proteome profiler angiogenesis arrays were used to determine the profile of angiogenic factors secreted by hESC during decidualisation. Primary hESC and St-T1b cells were incubated with E2 or MM1 medium for 5 days and then re-plated with DMEM/F12 medium containing 2% FBS or MM1 medium overnight, the cells were re-stimulated with E2 or MM1 medium 24 h prior to harvesting and the supernatants analysed using the angiogenesis array. The results were analysed by measuring the mean spot density normalised to spots reference using ImageJ as described in **Section 2.11.1**.

As shown in **Table 3.1**, we found that in primary hESC angiopoeitin-1, amphiregulin, EG-VEGF, HB-EGF, MCP-1, MMP-8, MMP-9, PRL, TIMP-4 and VEGF were changed during decidualisation compared to proliferative cells while in St-T1b cells, the factors like endoglin, GM-CSF, HB-EGF, HGF, IGFBP-1, MCP-1, MMP-9, PDGF-AA, PF4, PRL, TIMP-4, and VEGF were changed during decidualisation. However, only angiopoeitin-1, MCP-1, MMP-8, MMP-9, PRL, and VEGF were significantly increased with decidualisation in primary hESC (**Figure 3.9B**). The secretion of GM-CSF, HB-EGF, and PDGF-AA were significantly decreased with decidualisation, while, HGF, IGFBP-1, MCP-1, PRL and VEGF secretion were significantly increased in St-T1b cells (**Figure 3.9D**). There were only three identical factors, PRL, VEGF, and MCP-1 that were significantly up-regulated in both primary hESC and St-T1b cells. Surprisingly, IGFBP-1 which is a commonly used decidual marker was significantly increased in St-T1b cells during decidualisation, which is consistent with the previous as shown in **Figure 3.3**. However, low IGFBP-1 mRNA detected at day 6 in primary hESC did not show the changes of IGFBP-1

secretion. There are many angiogenic factors that were highly expressed in hESC (**Table 3.2**), but, did not change with decidualisation compared to proliferative cells.

Angiogenesis	***Primary hESC***		***St-T1b***	
Associated Factors	**Proliferative**	**Decidualised**	**Proliferative**	**Decidualised**
Angiopoietin-1	0.66	0.89	0.79	0.88
Amphiregulin	0.32	0.49	0.12	0.17
EG-VEGF	0.27	0.39	0.29	0.30
Endoglin	0.83	0.91	0.42	0.30
GM-CSF	0.60	0.68	0.64	0.18
HB-EGF	0.27	0.40	0.84	0.19
HGF	0.47	0.59	0.29	0.91
IGFBP-1	0.85	1.00	0.45	1.00
MCP-1	0.16	0.47	0.17	1.00
MMP-8	0.39	0.79	0.29	0.33
MMP-9	0.34	0.86	0.53	0.35
PDGF-AA	0.26	0.31	0.97	0.44
Platelet Factor 4 (PF4)	0.19	0.31	0.16	0.37
Prolactin	0.45	0.97	0.14	0.73
TIMP-4	0.30	0.37	0.46	0.96
VEGF	0.71	1.00	0.42	0.78

Table 3.1: Lists of angiogenesis involved proteins differentially expressed during decidualisation in primary hESC and St-T1b cells.

Angiogenesis	*Primary hESC*		*St-T1b*	
Associated Factors	**Proliferative**	**Decidualised**	**Proliferative**	**Decidualised**
Activin	0.89	0.99	0.99	0.99
ADAMTS-1	0.14	0.18	0.29	0.23
Angiogenin	0.90	0.99	1.00	0.98
Angiopoietin-2	0.79	1.00	0.49	0.47
Angiostatin/Plasminogen	0.14	0.17	0.20	0.16
Artemin	0.27	0.28	0.17	0.13
Coagulation Factor III	0.89	0.92	0.87	0.77
CXCL16	0.31	0.35	0.28	0.38
DPPIV	0.85	0.91	0.22	0.32
EGF	0.09	0.13	0.17	0.17
Endostatin/Collagen XV	0.88	0.90	0.63	0.56
Endothelin-1	0.66	0.65	0.65	0.42
FGF acidic	0.26	0.26	0.22	0.27
FGF basic	0.35	0.41	0.14	0.17
FGF-4	0.22	0.23	0.10	0.27
FGF-7	0.22	0.33	0.10	0.28
GDNF	0.21	0.26	0.19	0.21
IGFBP-2	0.87	0.97	0.48	0.32
IGFBP-3	0.83	0.99	1.00	1.00
IL-1β	0.12	0.15	0.21	0.18
IL-8	0.89	1.00	0.72	0.92
TGF-β1	0.53	0.50	0.22	0.19
Leptin	0.17	0.19	0.11	0.24
MIP-1a	0.38	0.40	0.25	0.23
NRG1-β1	0.15	0.24	0.29	0.42
Pentaxin 3 (PTX3)	0.54	0.72	0.98	1.00
PD-ECGF	0.29	0.37	0.27	0.26
PDGF-AB/BB	0.10	0.11	0.18	0.13
Persephin	0.30	0.34	0.34	0.39
PIGF	0.20	0.25	0.17	0.26
Serpin B5	0.35	0.56	0.25	0.23
Serpin E1	0.99	1	0.97	0.98
Serpin F1	0.96	0.98	0.99	0.98
TIMP-1	0.98	1.00	1.00	1.00
Thrombospondin-1	1.00	1.00	0.99	1.00
Thrombospondin-2	0.57	0.58	0.36	0.34
μPA	1.00	1.00	0.99	0.96
Vasohibin	0.45	0.46	0.11	0.11
VEGF-C	0.39	0.41	0.09	0.14

Table 3.2: List of angiogenesis involved proteins expressed in primary hESC and St-T1b cells without showing any differences in decidualisation.

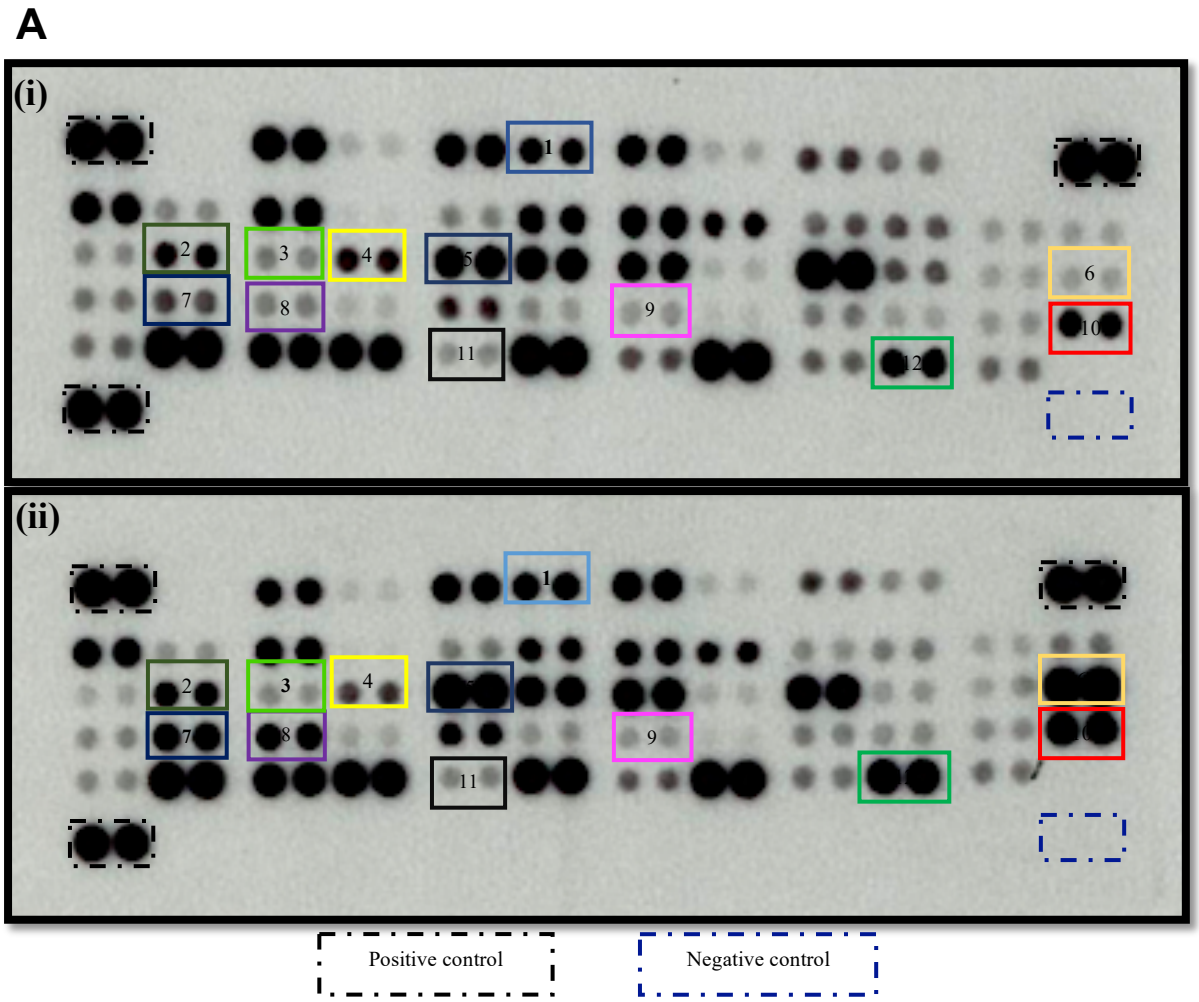
A
(i)
1
2
3
4
5
6
7
8
9
10
11
12
(ii)
1
2
3
4
9
11
Positive control
Negative control

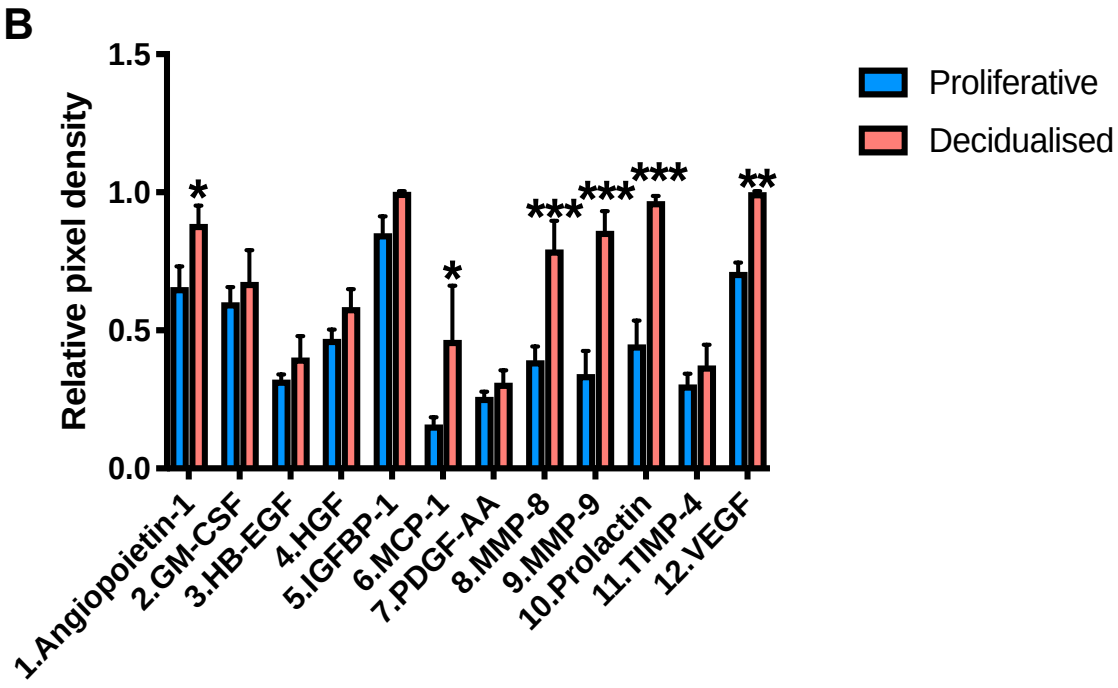
B
Relative pixel density
1.5
1.0
0.5
0.0
Proliferative
Decidualised
*
*
***
***
***
**
1.Angiopoietin-1
2.GM-CSF
3.HB-EGF
4.HGF
5.IGFBP-1
6.MCP-1
7.PDGF-AA
8.MMP-8
9.MMP-9
10.Prolactin
11.TIMP-4
12.VEGF

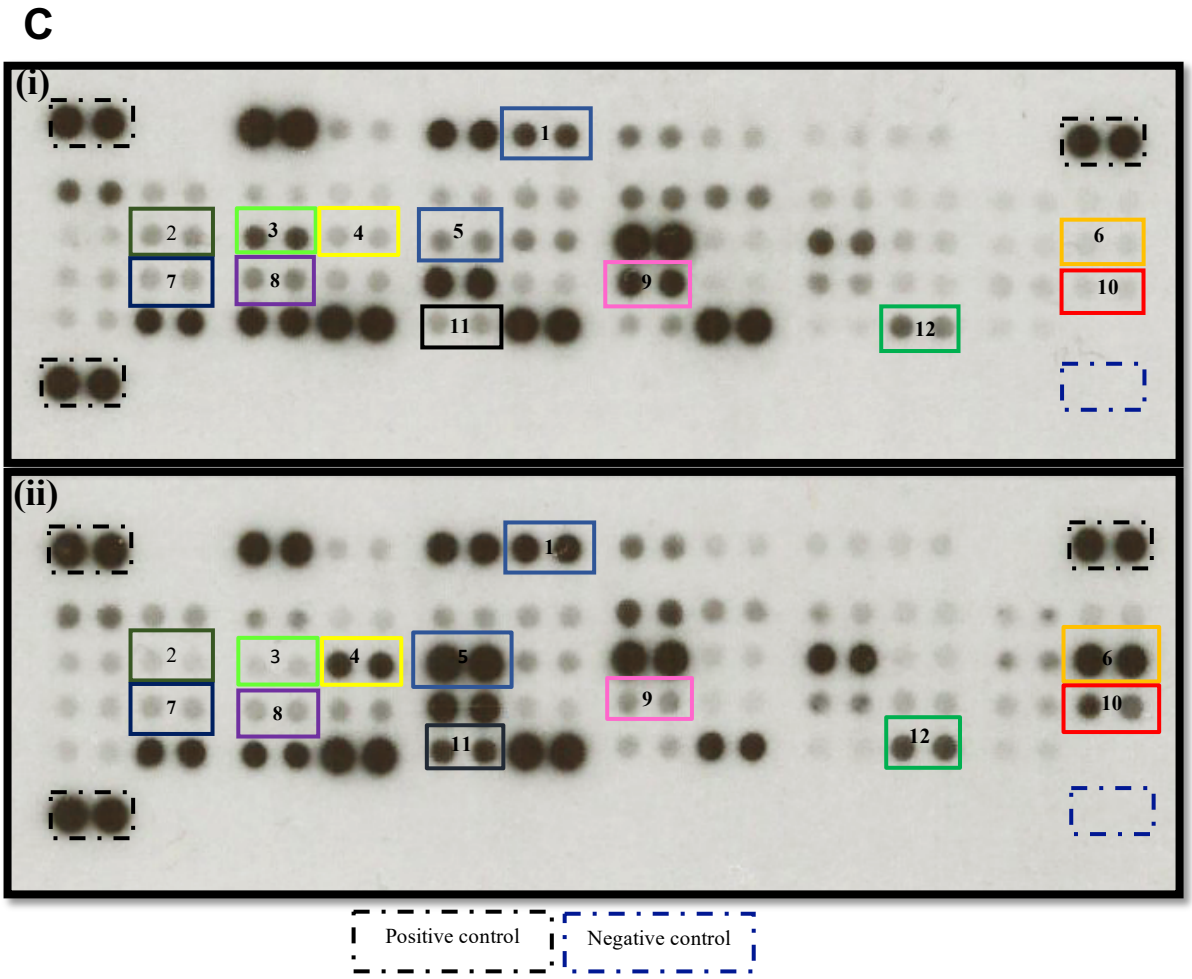
C
(i)
1
2
3
4
5
6
7
8
9
10
11
12
(ii)
1
2
3
4
5
6
7
8
9
10
11
12
Positive control
Negative control

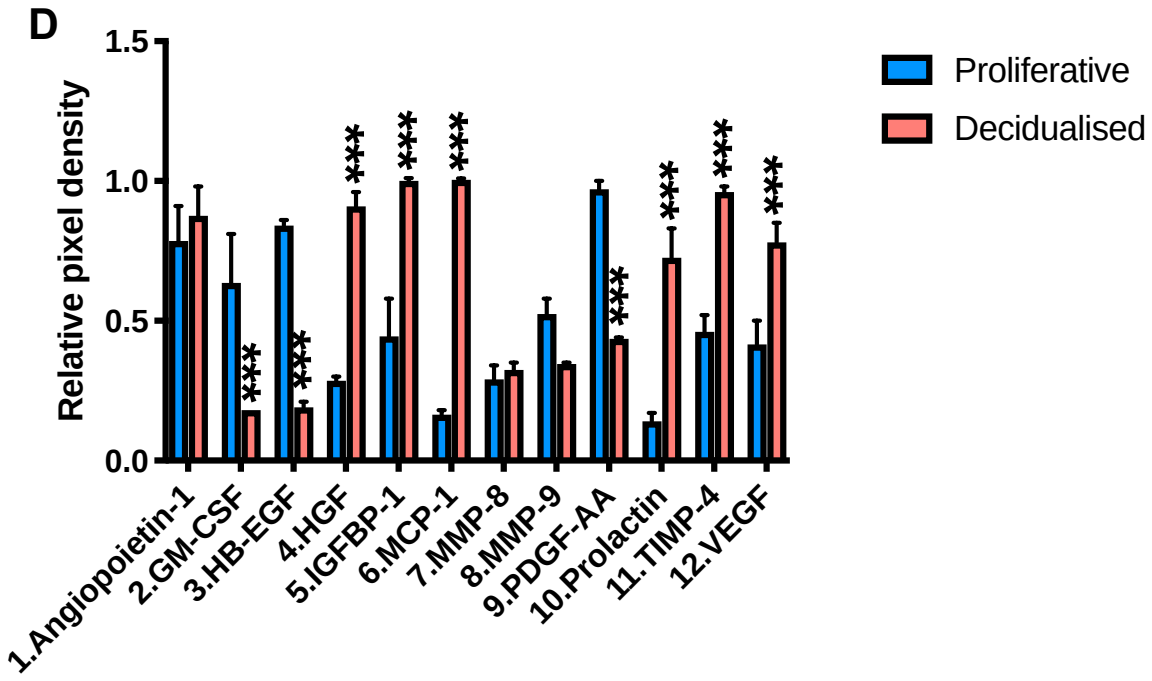
D
Relative pixel density
1.5
1.0
0.5
0.0
Proliferative
Decidualised
1.Angiopoietin-1
2.GM-CSF
3.HB-EGF
4.HGF
5.IGFBP-1
6.MCP-1
7.MMP-8
8.MMP-9
9.PDGF-AA
10.Prolactin
11.TIMP-4
12.VEGF

Figure 3.9: Summary of primary hESC and St-T1b cell analysis using the angiogenesis proteome profiler arrays. The **(A)** primary hESC and **(C)** St-T1b cells were treated with (**i**) E2 and (**ii**) MM1 medium for 5 days in 10 cm culture dishes and re-plated on 6-well plate with cell density 8.0 x 10^5 cells/well for another 48 h. The cells were re-stimulated with fresh medium after 24 h and the supernatants were analysed using Human Proteome Profiler Angiogenesis Arrays. The density was measured by densitometry using ImageJ and the results were normalised to positive reference control spots following subtraction of the negative control spots. All the significant changes of angiogenic factors in both **(B)** Primary hESC, and **(D)** St-T1b cells were shown in the graph. The results are the mean (+/- SEM) of 4 experimental repeats and analysed using student t-test; *p<0.05; **p<0.01; ***p<0.001.

3.3 DISCUSSION

3.3.1 Up-regulation of decidual markers, PRL and IGFBP-1

In the present study, St-T1b cell line was confirmed as having similar characteristics as primary hESC following the induction of decidualisation by MPA and cAMP (Samalecos *et al.*, 2009). Primary hESC and St-T1b cells stimulated with 8-Br-cAMP and MPA showed a dramatic increase of both common decidual markers, PRL and IGFBP-1 mRNA transcripts supporting the previous findings (Samalecos *et al.,* 2009). Surprisingly, unlike the mRNA expression, IGFBP-1 protein was highly secreted in both proliferative and decidualised primary hESC and these results are consistent with the earlier findings in T-HESC cells during decidualisation (Gellersen *et al.,* 2013).

3.3.2 Up-regulation of transcription factors during hESC decidualisation

FOXO1 has been identified as a key transcriptional regulator of decidualisation (Gellersen and Brosens, 2003; Samalecos *et al.,* 2009; Christian *et al.*, 2011). The activation of protein kinase A (PKA) results in the up-regulation and nuclear localisation of FOXO1 and is accompanied by the induction of C/EBPβ expression (Christian *et al.*, 2011). C/EBPβ is another transcription factor that regulates the expression of a number of decidualisation related genes. As shown in **Figure 3.4 & 3.5**, FOXO1 and C/EBPβ were up-regulated from

day 3 to day 6 during the decidualisation in both primary hESC and St-T1b cells, while no changes were observed in proliferative cells. Studies show that dPRL and IGFBP-1 are induced by cAMP through the recruitment of C/EBPβ during decidualisation of ESC (Christian *et al.,* 2002; Tamura *et al.*, 2014b). Furthermore, Manganese superoxide dismutase (Mn-SOD/SOD2), an anti-oxidant enzyme is expressed in hESC at basal levels without decidualisation stimulus, and its expression increases with decidualisation, contributing to cell survival by scavenging superoxide radicals produced by decidualisation stimulus in primary hESC (Kajihara *et al.*, 2006). Previous studies also demonstrated the increase of SOD2 in primary hESC decidualisation (Brar *et al.,* 2001; Garrido-Gomez *et al.,* 2011). In this study, SOD2 mRNA was detected and its expression was dramatically increased during decidualisation in St-T1b cells (**Figure 3.6**) which supports the previous studies in primary hESC (Brar *et al.,* 2001; Kajihara *et al.*, 2006; Garrido-Gomez *et al.,* 2011). IRF4 was reported to be regulated by FOXO1 in hESC (Vasquez *et al*., 2015) which is consistent with my results showing an increase of IRF4 in hESC during decidualisation.

HOXA10 is one of the known homeobox gene family that is essential in development. HOXA10 is up-regulated in the response to steroid hormones including oestrogen and progesterone and its expression rises dramatically during the mid-secretory phase of the menstrual cycle (Taylor *et al.*, 1997). The HOXA10 deficient mice are infertile due to the impairment of endometrial decidualisation (Benson *et al.*, 1996), and HOXA10 expression was found at high levels in the late secretory phase of implantation (Cakmak and Taylor, 2011). In addition, the injection of antisense oligonucleotides to HOXA10 into the mouse uterus leads to a reduction of implantation rates (Bagot *et al.*, 2000). However, the exact role of HOXA10 in uterine stromal cell differentiation remains unclear. HOXA10 has been found to cooperate with FOXO1 in the regulation of IGFBP-1 expression during decidualisation

(Kim *et al.*, 2003). However, it has also been reported that HOXA10 acts as an inhibitor to IGFBP-1 expression during decidualisation, where knock-down of HOXA10 was found to increase IGFBP-1 expression (Kim *et al.*, 2007). Moreover, HOXA10 has been reported to play a role in proliferation by regulating 494 genes during decidualisation in primary hESC (Lu *et al.*, 2008). As shown in the present study, the expression of HOXA10 mRNA was up-regulated with decidualisation in St-T1b cells (**Figure 3.8**), which is consistent with the previous findings in primary hESC.

FOXM1 plays an important role in cell cycle progression and differentiation (Laoukili *et al.*, 2007). It is expressed in hESC and its inhibition is found to prevent decidualisation (Jiang *et al.*, 2015). In agreement with these findings in hESC, the conditional deletion of FOXM1 in the mouse led to the implantation failure with decidualisation defects (Gao *et al.*, 2015). In our study, FOXM1 mRNA levels increased during decidualisation in St-T1b cells consistent with previous studies in primary hESC (Gao *et al.,* 2015; Jiang *et al.,* 2015).

PLZF has been reported recently as a direct target of the progesterone receptor and it is up-regulated during decidualisation of St-T1b cells (Samalecos *et al.,* 2009) and primary hESC (Kommagani *et al.,* 2016; Szwarc *et al.*, 2018). In this study, PLZF expression was significantly up-regulated with decidualisation in St-T1b cells as the previous findings in primary hESC (Kommagani *et al.,* 2016; Scwarc *et al.,* 2018). No PLZF was detected in the cells treated with just cAMP alone.

3.3.3 Changes of angiogenic factors during hESC decidualisation

Adequate angiogenesis is reported to be the most critical factor during decidualisation to ensure successful implantation and placentation (Tory *et al.*, 2007). Our protein array results show that *in vitro* decidualisation not only up-regulates major angiogenic factors and regulators such as angiopoietin-1, VEGF, MMP-8, MMP-9, but also other cytokines and

chemokines such as MCP-1. Monocyte chemoattractant protein-1 (MCP-1) is important for angiogenesis, tissue remodelling, embryo implantation, early pregnancy and trophoblast invasiveness (Houser, 2012; Bourdiec *et al.*, 2016). Angiopoietin-1, MMP-8, and MMP-9 secretion increased during decidualisation of primary hESC, but not in St-T1b cells. While, MCP-1 was increased with decidualisation in both primary hESC and St-T1b cells. Many studies have reported the up-regulation of MCP-1 expression in primary decidual ESC (Lockwood *et al.,* 2006; He *et al.,* 2007) and St-T1b cells (Schwenke *et al.,* 2013) supporting the findings in this study.

In this study, VEGF secretion was increased during decidualisation in both primary hESC and St-T1b cells. The up-regulation of VEGF expression has been reported in primary hESC under decidualisation conditions supporting my findings (Sugino *et al.,* 2002; Schwenke *et al.,* 2013). However, very little is known about the significance of the contribution of VEGF produced by decidual cells during decidualisation in hESC. Further studies are needed to investigate the contribution of VEGF in decidualisation which will be discussed in the later chapter in this thesis.

Angiopoietins are another key factor in promoting angiogenesis and vessel remodelling in the endometrium. The balance between angiopoietin-1 and angiopoietin-2 expression is important for angiogenesis in the endometrium (Tsuzuki *et al.,* 2013). Angiopoitein-1 expression was suppressed by hypoxia and oestrogen which increase angiopoietin-2/angiopoietin-1 ratio appears to favour the remodelling of endometrial blood vessel in primates (Albrecht and Pepe, 2010). Whereas, angiopoietin-2 expression was suppressed by MPA for maturation and maintenance of newly formed vessels in endometrium (Tsuzuki *et al.,* 2013). In this study, high expression of angiopoietin, angiopoietin-1 and angiopoietin-2 were detected in both primary hESC and St-T1b cells. The expression of angiopoietin-1 was

found to increase in primary hESC during decidualisation which may be influenced by the oestrogen and MPA.

Furthermore, a large amount of MMPs are secreted in normal early pregnancy, while simultaneously producing TIMPs to inhibit MMPs to maintain the dynamic balance of MMPs/TIMPs (Singh *et al.*, 2017). A significant increase of MMP-9 expression was found in the endometrium of women with spontaneous abortion (Skrzypczak *et al.,* 2007; Jiang and Qi, 2015). In addition, the earlier study reported the increase of MMP-8 and MMP-9 during decidualisation in T-HESC cells (Gellersen *et al.,* 2013). It is known that MMPs are important in decidual development, but the information is very limited due to the actions of individual MMPs and also the interaction of MMPs and TIMPs. Therefore, it is difficult to explain the differential expression of MMPs between primary hESC and St-T1b cells in this study. Further study is needed to investigate the expression levels of MMPs and TIMPs during decidualisation.

Heparin-binding epidermal growth factor (HB-EGF) plays a critical role in the human female reproductive system during the menstruation cycle, implantation, ESC decidualisation (Lim and Dey, 2009; Simone *et al.*, 2012) as well as blastocyst adhesion and development (Leach *et al.*, 2004). HB-EGF mRNA is expressed predominantly in the stromal compartment of the endometrium (Leach *et al.,* 2004) and promotes decidualisation via increased levels of decidual markers, dPRL and IGFBP-1 *in vivo* (Chobotova *et al.*, 2005) and *in vitro* (Lessey *et al.,* 2002). However, one study recently reported that there was a higher expression level of HB-EGF in endometrium in women with missed abortion (Ozbilgin *et al.*, 2015). In the present study, the proteome profiler angiogenesis arrays showed a reduction of HB-EGF during decidualisation in St-T1b cells which support the earlier finding that no HB-EGF secretion was detected in decidualised St-T1b cells

(Schwenke *et al.*, 2013) with limited information on the expression in proliferative St-T1b cells. Surprisingly, HB-EGF expression was insignificantly increased in primary hESC which supporting the earlier study that HB-EGF expression was increased in *in vitro* decidualisation (Lessey *et al.,* 2002).

Previous studies reported PDGF-AA is a novel trophoblast-derived chemoattractant for ESC (Gellersen *et al.,* 2013). However, only a few studies have looked at the expression of PDGF-AA during hESC decidualisation. Our studies show that levels of PDGF-AA secreted by St-T1b cells decreased during decidualisation, while, PDGF-AA is not expressed in primary hESC which is consistent with the previous studies in the T-hESC line (Gellersen *et al.*, 2013). PDGF-BB was not detected in St-T1b cells or primary hESC in the angiogenesis profiler array (**Table 3.2**). In the present study in angiogenesis array, there are changes in expression between primary hESC and St-T1b cells during decidualisation. This difference could due to the limitation in measuring the density of each spot. For example, IGFBP-1, 2 and 3 secretions highly expressed in both proliferative and decidualised primary hESC which may lead to the difficulties in determining the changes. In addition, there are also factors that have a low expression which is under the detection limit.

3.3.4 Conclusion

In conclusion, changes in the St-T1b cells were characterised by morphology, mRNA and protein expression during decidualisation confirming and extending the previous findings (Samalecos *et al.,* 2009), and with primary hESC showing that the St-T1b cell is a good model to use in the present study. Various angiogenic factors were found to express in the hESC decidualisation. MCP-1 and VEGF were the factors that were expressed in both primary hESC and St-T1b and will be focused in the next chapter. The next results chapter will focus more on the FOXO transcription factor, VEGF expression and its regulation during hESC decidualisation.

CHAPTER 4:

THE FOXO TRANSCRIPTION FACTORS IN HUMAN ENDOMETRIAL STROMAL CELL DECIDUALISATION

4.1 INTRODUCTION

The FOXO transcription factor family consists of four members, namely FOXO1, FOXO3A, FOXO4 and FOXO6, in mammals (Zhang *et al.*, 2011). FOXO1 is one of the earliest transcription factors induced upon decidualisation of stromal cells (Gellersen and Brosens, 2003; Brar *et al.*, 2001; Christian *et al.*, 2002), a process that can be mimicked *in vitro* by cAMP and progesterone treatment (Labied *et al.,* 2006). FOXO1 is important in the regulation of various integral cell functions including metabolism (Tzivion *et al.,* 2011), while, FOXO3A is known to regulate inflammation and like FOXO1, FOXO3A also acts to protect the cells from oxidative stress and they both can promote apoptosis (Wang *et al.*, 2014). The deletion of FOXO3A in female mice leads to infertility due to the impairment of oocyte growth follicular development (Christian *et al.*, 2011). FOXO1 has been shown to up-regulate various key genes in hESC decidualisation, for example, IGFBP-1, PRL, IRF-4, TIMP3 and decorin (Vasquez *et al.*, 2015; Kim *et al.*, 2005; Buzzio *et al.*, 2006). It is known to co-operate with other transcription factors such as C/EBPβ and IRF-4 to promote decidual gene expression including PRL and IGFBP-1 expression (Christian *et al.,* 2002; Vasquez *et al.*, 2015).

The transcriptional activity of FOXO transcription factors is dependent on their localisation in the nucleus, which is controlled mainly by post-translational modifications such as phosphorylation, acetylation and ubiquitination (Brunet *et al.,* 1999; Zhang *et al.*, 2011) (*see* **Figure 1.7**). Activation of the PI3K pathway leads to phosphorylation of Akt which in turn phosphorylates downstream target genes including FOXO transcription factors (Brunet *et al.*, 1999; Tang *et al.*, 1999; Barthel *et al.*, 2005). The Akt-dependent phosphorylation of nuclear FOXO at threonine 24; serine 256; and serine 319 then generates binding sites for the 14-3-3 chaperone protein which causes FOXO to be exported from the nucleus and localised in the cytoplasm to inhibit its transcriptional activity (Brunet *et al*., 1999; Brosens

and Gellersen, 2006). There are three Akt isoforms: Akt-1, Akt-2, and Akt-3. Deficiency of Akt-1 in mice leads to increased neonatal mortality and reduced body mass (Cho *et al.,* 2001), mice deficient for Akt-2 exhibited glucose metabolism syndrome (Garofalo *et al.,* 2003), whereas Akt-3 deficient mice show reduced brain size (Easton *et al.,* 2005). Studies have shown that progesterone activates the PI3K /Akt pathway causing localisation of FOXO1 in the cytoplasm (Ujvari *et al*., 2017).

Little is known about the expression and function of FOXO3A in hESC decidualisation. FOXO3A was reported to be down-regulated in decidualised stromal cells but oxidative stress increased FOXO3A expression during decidualisation (Kajihara *et al.,* 2006). Due to the up-regulation of FOXO1 in hESC during decidualisation and their similar, but not completely overlapping function in many processes, FOXO1 and FOXO3A expression and activity in hESC during in *vitro* decidualisation were investigated further.

4.2 RESULTS

4.2.1 FOXO1 activity in hESC during decidualisation

FOXO1 transcription factor activity increases in hESC following 8-Br-cAMP treatment (**Section 3.3.3.1**). To investigate FOXO activity following cAMP or/and MPA stimulation in hESC, St-T1b cells were plated on 12-well plates overnight and co-transfected with 1 µg of FHRE Luciferase-reporter (FHRE-Luc) (Brunet *et al.*, 1999) and pRL-CMV plasmid for 24 h followed by various treatments (0.5 mM or 0.25 mM 8-Br-cAMP, and 10 µM MPA) for a further 24 h.

To demonstrate that the FHRE-Luc reporter was working, St-T1b cells were co-transfected with FHRE-Luc reporter construct which contains FOXO3A genes with constitutively active FOXO1 (caFOXO1) or FOXO3A (caFOXO3A) mutant plasmids (Ramaswamy *et al.*, 2002), or the pcDNA3.1 parent plasmid as a control. The FHRE-firefly luciferase reading was

normalised to the pRL-CMV Renilla activity to determine the relative FHRE reporter activity. FHRE-Luc reporter activity increased with co-transfection of both caFOXO1 and caFOXO3A plasmids by 4- to 5-fold (**Figure 4.1A**) confirming successful co-transfection and the activity of the FHRE reporter and its response to both FOXO1 and FOXO3A.

The FHRE firefly luciferase activity was determined after 24 h by dual-luciferase assay. **Figure 4.1B** shows a large increase in FOXO activity following 8-Br-cAMP treatment. while MPA (5 μM) alone did not affect FOXO activity compared to control. Furthermore, FOXO activity in the cells treated with both 8-Br-cAMP and MPA did not show greater FOXO activity than those treated with 8-Br-cAMP alone (**Figure 4.1C**).

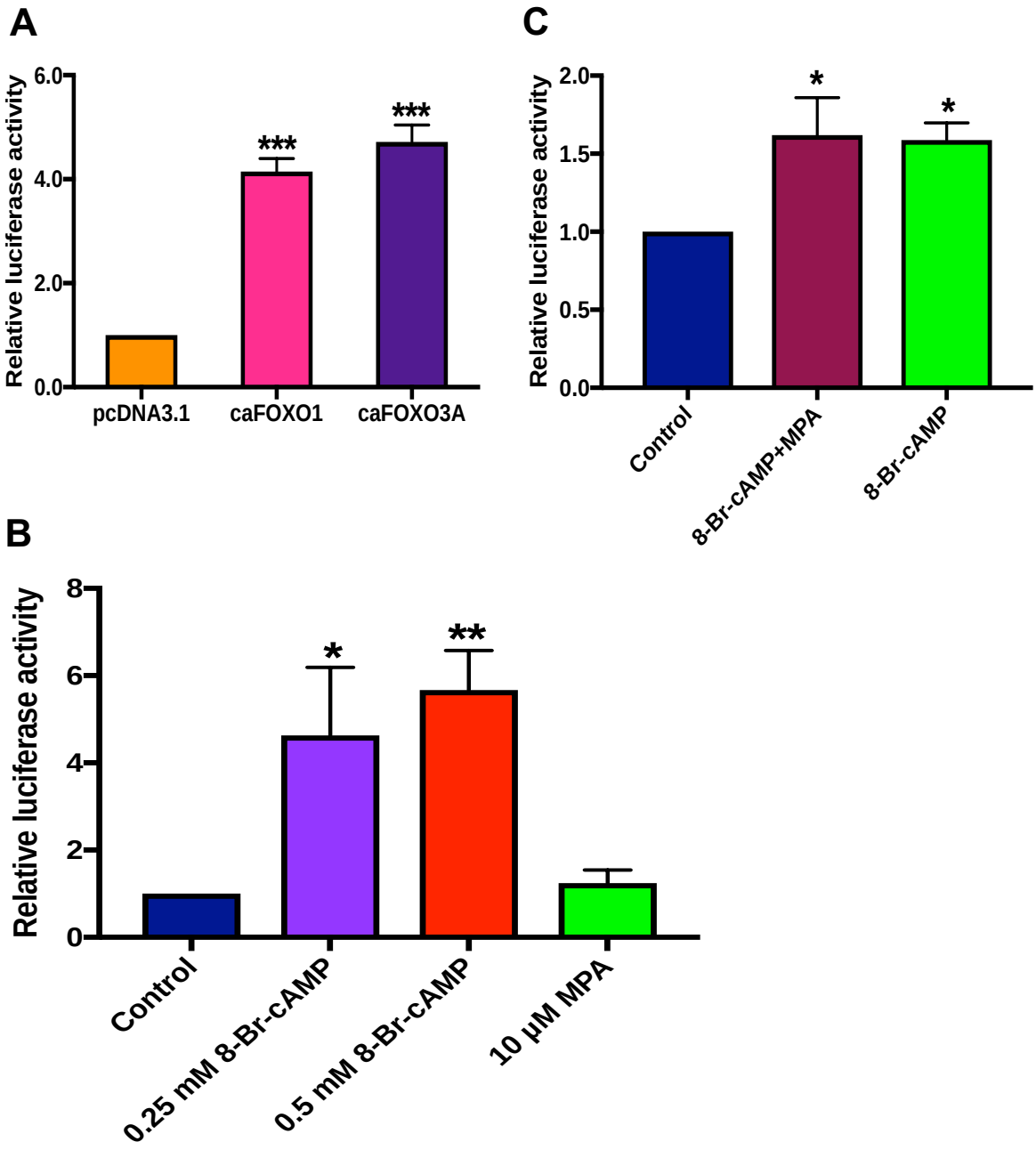

Figure 4.1: Relative FOXO activity determined using Forkhead responsive luciferase reporter. St-T1b cells were co-transfected with forkhead responsive element (FHRE) luciferase-reporter construct (FHRE-luc) and **(A)** constitutively active mutant FOXO1 (caFOXO1) or FOXO3A (caFOXO3A) mutant plasmids or pcDNA3.1 as control for 24 h or stimulated with DMEM/F12 supplemented with 2% FBS and combinations of **(B and C)** 8-Br-cAMP and 10 µM MPA for 24 h. The firefly luciferase readings were normalised to Renilla activity. Results are the mean (+/- SEM) of 3 experiments and analysed using one-way ANOVA; *p<0.05; **p<0.01; ***p<0.001.

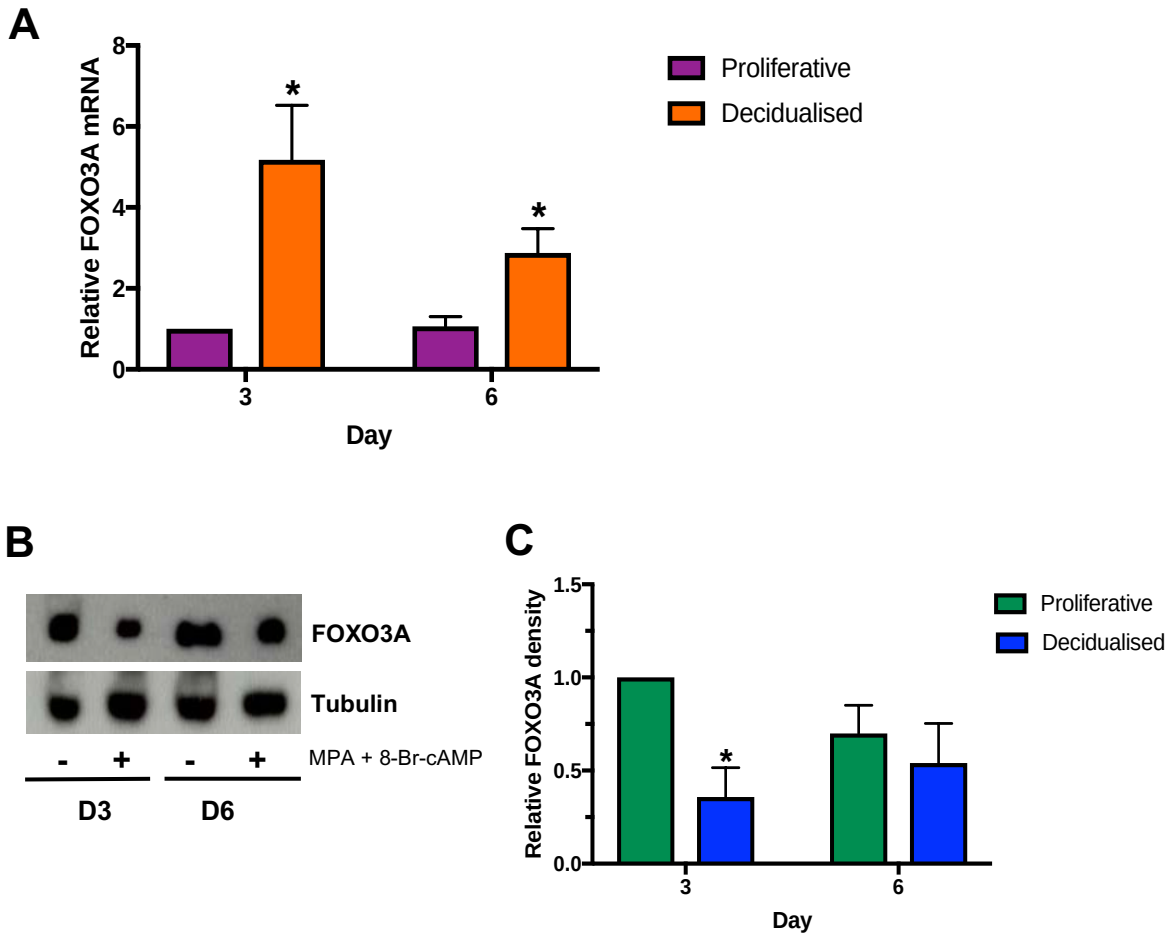

Figure 4.2: FOXO3A transcription factor expression in primary hESC decidualisation. Primary hESC were grown to confluence and incubated in E2 or MM1 medium over 6 days. **(A)** Real-time qPCR analysis of FOXO3A mRNA expression normalised to β-actin**. (B)** Representative Western blot showing FOXO3A expression in whole-cell lysates with tubulin as a loading control. **(C)** Graph of densitometry analysis of relative FOXO3A protein levels normalised to tubulin control. Results are the mean (+/- SEM) of 3 experiments and analysed using unpaired t-test; *p<0.05; **p<0.01; ***p<0.001.

4.2.2 Expression of FOXO3A transcription factor in hESC decidualisation

FOXO3A was previously reported to be down-regulated in decidualised stromal cells following the up-regulation of FOXO1 (Kajihara *et al.*, 2006). To confirm this, primary hESC and St-T1b cells were plated and stimulated with E2 or MM1 medium over 6 days. FOXO3A mRNA and protein expression level were measured using real-time qPCR and Western blotting. Surprisingly, FOXO3A mRNA increased with decidualisation in the primary hESC (**Figure 4.2A**) and St-T1b cells (**Figure 4.3A**) over 6 days. In addition, shorter-term stimulation over 24 h also showed significant up-regulation of FOXO3A mRNA expression in St-T1b cells (**Figure 4.3B**). However, examination of FOXO3A by Western blotting showed that FOXO3A protein levels were decreased with decidualisation compared to proliferative cells on day 3, but not at day 6 in primary hESC (**Figure 4.2C**). While, in St-T1b cells, the FOXO3A protein remained at similar levels following decidualisation and did not change compared to proliferative cells **(Figure 4.3D**).

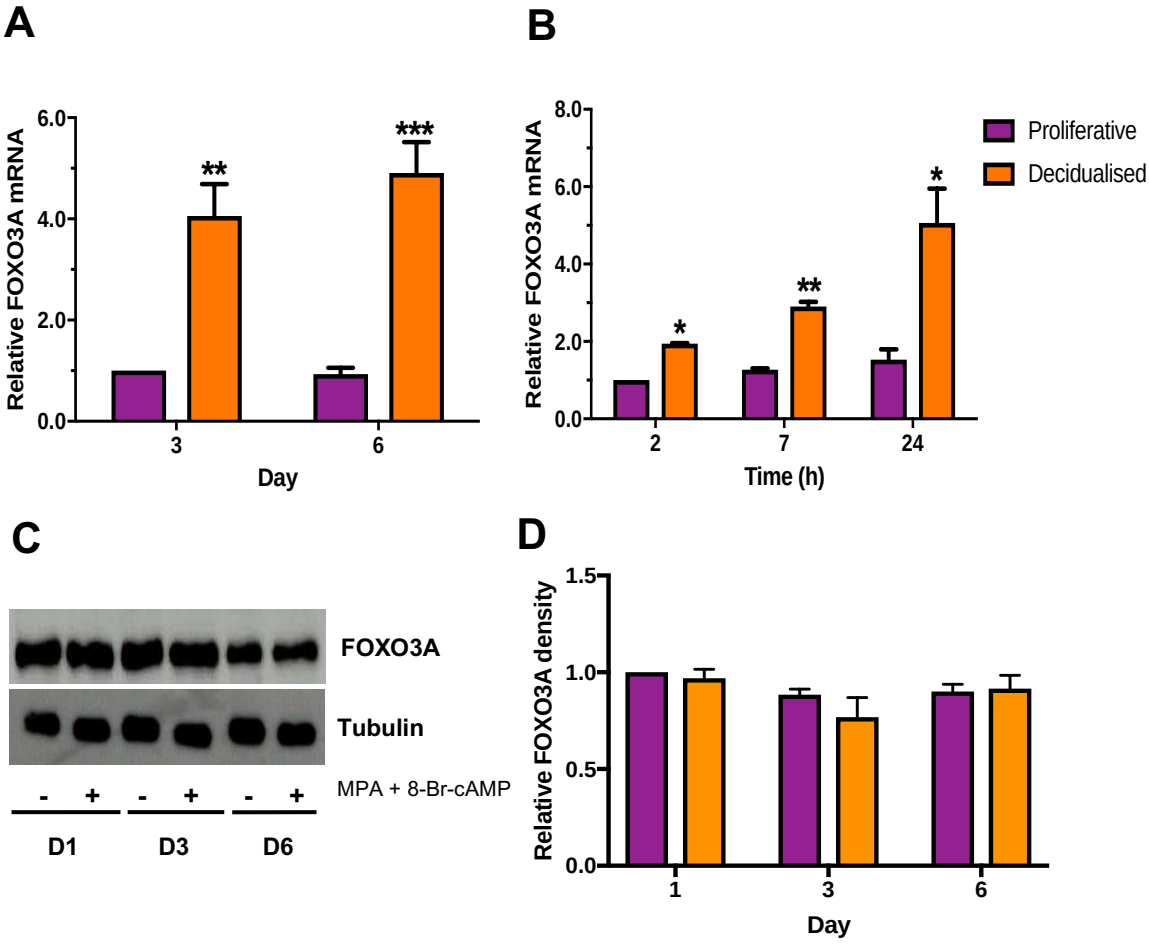

Figure 4.3: FOXO3A transcription factor expression in St-T1b decidualisation. ST-T1b cells were grown to confluence and incubated in E2 or MM1 medium over 6 days. Real-time qPCR analysis of FOXO3A mRNA expression normalised to β-actin **(A)** over 6 days, and **(B)** over 24 h (2, 7, 24 h). **(C)** Representative Western blot showing FOXO3A expression in whole-cell lysates with tubulin as a loading control. **(C)** Graph of densitometry analysis of relative FOXO3A protein levels normalised to tubulin control. Results are the mean (+/- SEM) of 3 experiments and analysed using unpaired t-test; *p<0.05; **p<0.01; ***p<0.001.

4.2.3 FOXO1 regulates FOXO3A expression in hESC

4.2.3.1 Deletion of FOXO1 suppresses FOXO3A expression in hESC

The relationship between FOXO1 and FOXO3A was investigated to identify whether FOXO1 regulates FOXO3A or vice versa in hESC by using siRNA knock-down. The primary hESC and St-T1b cells were plated at a density of 2.2 x 10^5 cells/well on 6-well plates overnight and transfected with siRNAs targeting FOXO1 (siFOXO1), FOXO3A (siFOXO3A) (Potente *et al.*, 2005) or a universal control (siControl) (Dharmacon) followed by stimulation with E2 or MM1 medium for 24 h. Knock-down of FOXO1, or FOXO3A (**Figures 4.4 & 4.5**) was confirmed by real-time qPCR and Western blotting (**Figure 4.4A & Figure 4.5A**). Both FOXO1 and FOXO3A mRNA and protein expression upon FOXO1 or FOXO3A knock-down were analysed. FOXO1 knock-down was found to reduce FOXO3A mRNA and protein expression in both primary hESC (**Figure 4.4**) and St-T1b cells (**Figure 4.5**). Interestingly, FOXO3A knock-down significantly decreased the FOXO1 mRNA (**Figure 4.4C**), but there were no changes in FOXO1 protein levels in primary hESC (**Figure 4.4B**). FOXO3A knock-down did not affect FOXO1 mRNA (**Figure 4.5 D&E**), or protein expression (**Figure 4.5 B&C**) in St-T1b cells. Collectively, these results show that FOXO1 promotes FOXO3A during decidualisation.

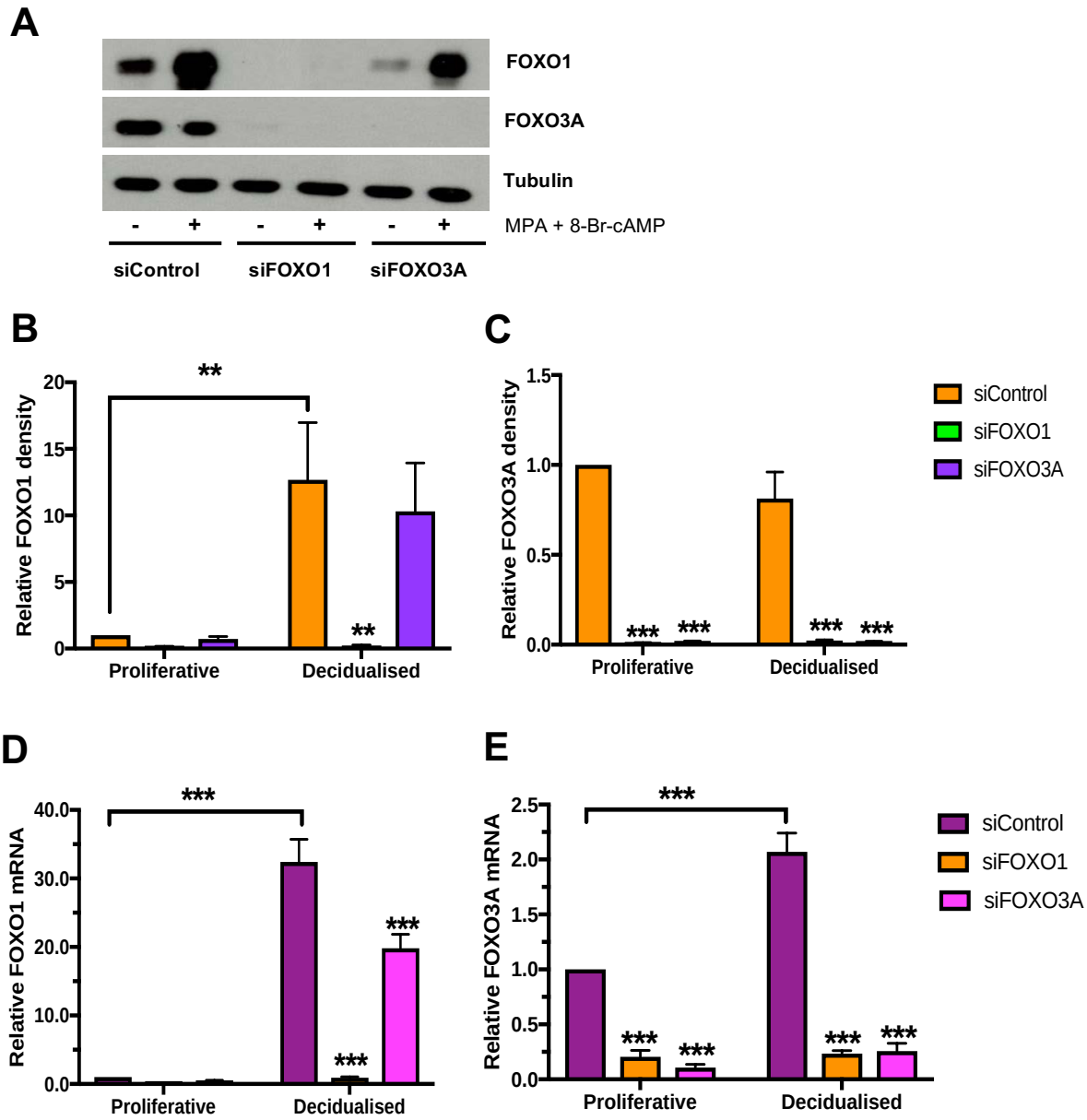

Figure 4.4: Knock-down of FOXO1 suppresses FOXO3A expression in primary hESC. Primary hESC were transfected with siRNAs targeting FOXO1 (siFOXO1), FOXO3A (siFOXO3A) or control (siControl) overnight followed by stimulation with E2 or MM1 medium for 24 h. **(A)** Representative Western blots showing FOXO1 and FOXO3A expression in whole-cell lysates and tubulin as a control. Graph of densitometry analysis of relative **(B)** FOXO1 and **(C)** FOXO3A protein levels normalised to tubulin control. Real-time qPCR analysis of **(D)** FOXO1 and **(E)** FOXO3A normalised to β-actin. Results are the mean (+/- SEM) with 3 experiments and analysed using two-way ANOVA; *p<0.05; **p<0.01; ***p<0.001.

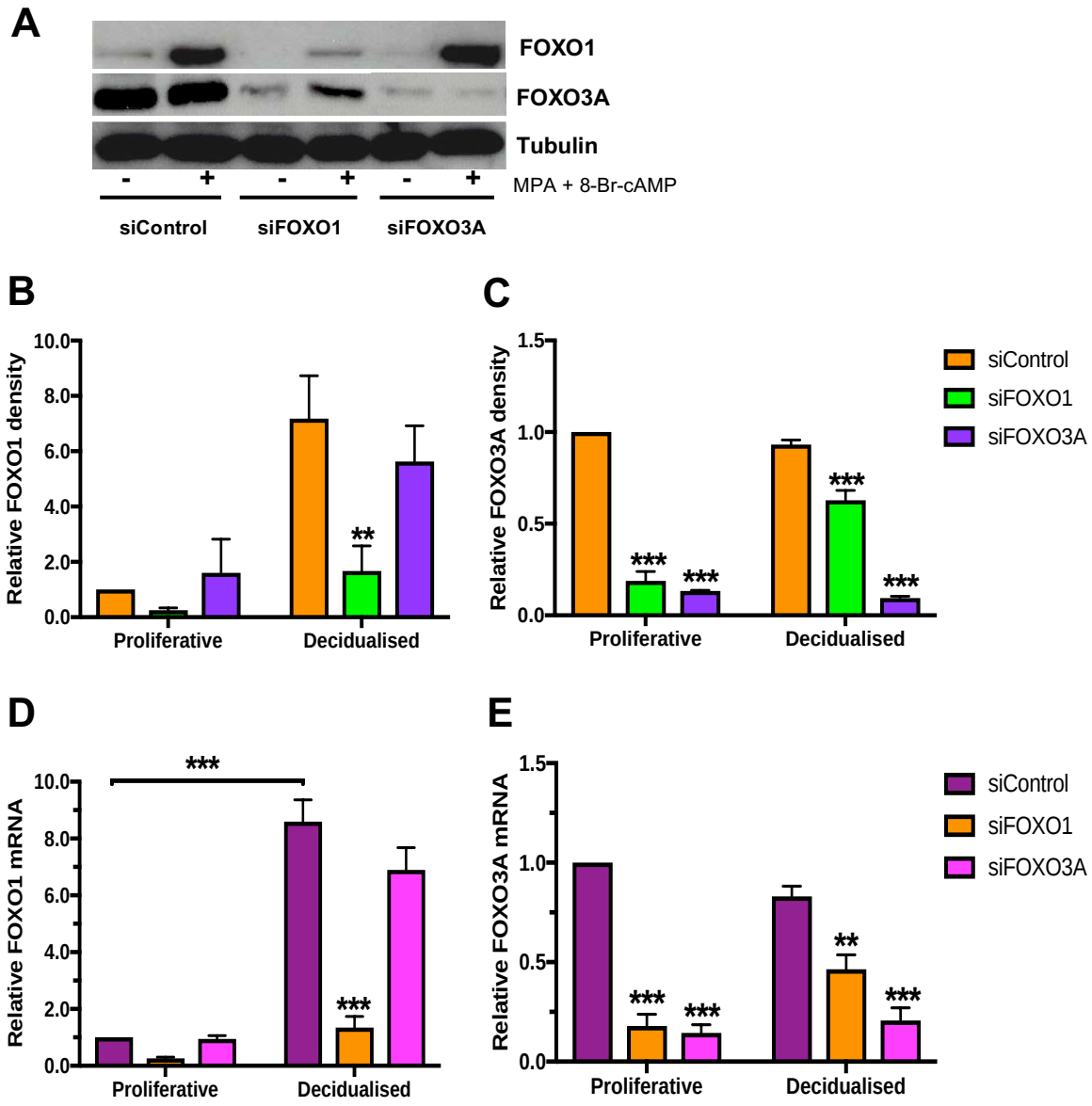

Figure 4.5: Knock-down of FOXO1 suppresses FOXO3A expression in St-T1b cells. St-T1b cells were transfected with siRNAs targeting FOXO1 (siFOXO1), FOXO3A (siFOXO3A) or control (siControl) overnight followed by E2 or MM1 medium for 24 h. **(A)** Representative Western blots showing FOXO1 and FOXO3A expression in whole-cell lysates with tubulin as a control. Graph of densitometry analysis of relative **(B)** FOXO1, and **(C)** FOXO3A protein levels normalised to the tubulin control. Real-time qPCR analysis of **(D)** FOXO1 and **(E)** FOXO3A mRNA expression normalised to β-actin. Results are the mean (+/- SEM) of 3 experiments and analysed using two-way ANOVA; *p<0.05; **p<0.01; ***p<0.001.

4.2.3.2 Over-expression of FOXO1 up-regulates FOXO3A expression in hESC

As the loss of FOXO1 suppressed FOXO3A expression in both primary hESC and St-T1b cells, the effect of FOXO1 over-expression on FOXO3A expression was investigated. St-T1b cells were transduced with recombinant adenovirus expressing HA-tagged murine FoxO1 (Ad-FoxO1) or empty control virus (Ad-CMV) for 24 h and incubated in E2 medium for another 24 h prior harvesting. Successful viral transduction was confirmed by real-time qPCR and Western blotting for HA-tagged FoxO1 expression (**Figure 4.6B**) which showed a large increase of mouse FoxO1 mRNA (**Figure 4.6A**) in cells treated with Ad-FoxO1. Both FOXO3A mRNA (**Figure 4.6C**) and protein levels (**Figure 4.6B**) were significantly increased in FOXO1 over-expressing cells compared to the control confirming the regulation of FOXO3A expression by FOXO1 in hESC.

4.2.3.3 Both FOXO1 and FOXO3A contribute to FOXO activity in hESC

FOXO transcriptional activity was also measured during decidualisation. The FHRE-Luc were co-transfected with siRNAs targeting FOXO1 (siFOXO1), or FOXO3A (siFOXO3A) or control (siControl) to try to estimate the relative contribution of FOXO1 and FOXO3A to overall FOXO activity when hESC are stimulated to decidualise. FOXO activity was significantly suppressed by either FOXO1 or FOXO3A knock-down in decidualised cells, while it did not significantly decrease in proliferative cells (**Figure 4.7**).

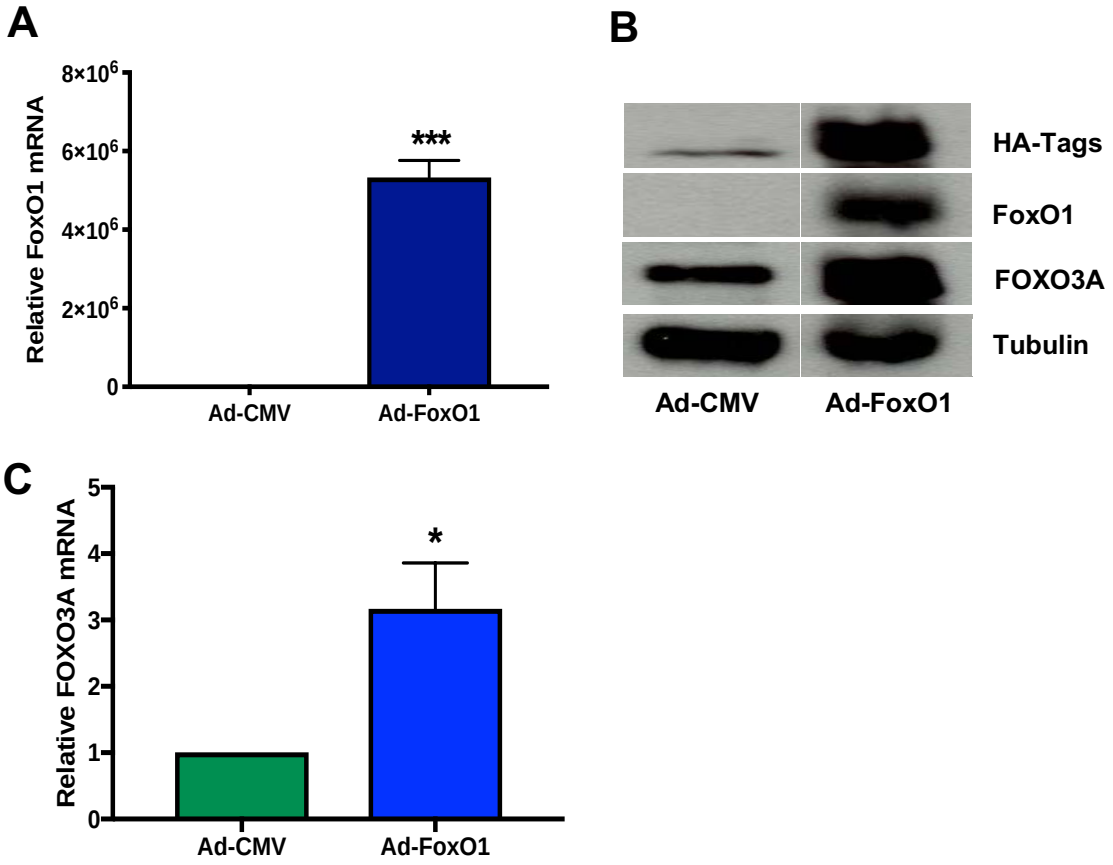

Figure 4.6: Over-expression of FOXO1 promotes FOXO3A expression in hESC. St-T1b cells were transduced with recombinant adenovirus expressing HA-tagged murine FoxO1 (Ad-FoxO1) or empty control virus (Ad-CMV) for 24 h and incubated in E2 medium for another 24 h prior harvesting. Viral transduction was confirmed by detection of **(A)** mouse FoxO1 mRNA and HA-tagged FoxO1 expression. **(B)** Representative Western blots showing the HA-tagged FoxO1 over-expression and FOXO3A expression with tubulin as loading control. **(C)** Real-time qPCR showing FOXO3A mRNA up-regulation. Results are the mean (+/- SEM) of 3 experiments and analysed using unpaired t-test; *p<0.05; **p<0.01; ***p<0.001.

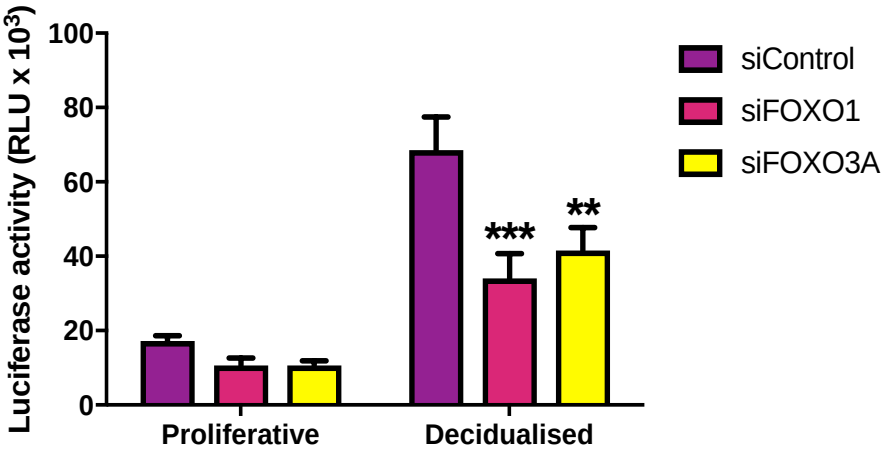

Figure 4.7: Silencing of FOXO1, or FOXO3A decreases overall FOXO activity in hESC. St-T1b cells were plated on 12-well plates overnight and co-transfected with FHRE-luc and siRNAs targeting FOXO1 (siFOXO1), FOXO3A (siFOXO3A) or control (siControl) overnight followed by incubation with E2 or MM1 medium for 24 h prior harvesting. The FHRE firefly luciferase activity was normalised to co-transfected pRL-CMV Renilla luciferase activity. Results are the mean (+/- SEM) of 3 experiments and analysed using two-way ANOVA; **p<0.01; ***p<0.001.

4.2.4 Effect of FOXO1/O3A knock-down on decidualisation related genes in hESC

FOXO1 regulates many genes involved in hESC decidualisation (Vasquez *et al.*, 2015). To confirm this relationship, FOXO1 or FOXO3A was knocked-down in St-T1b cells followed by stimulation with E2 or MM1 medium for 24 h. The knock-down efficiency was > 80% for both FOXO1 and FOXO3A at mRNA and protein level as shown in **Figure 4.5 D&E**. The expression of C/EBPβ (**Figure 4.8A**) and STAT3 (**Figure 4.8E**) was significantly decreased in decidualised St-T1b cells following FOXO1 knock-down. SOD2, a gene regulated by FOXO1 was also significantly decreased in decidualised cells following FOXO1, or FOXO3A knock-down (**Figure 4.8B**). FOXM1 mRNA expression was up-regulated in proliferative St-T1b cells following FOXO1 or FOXO3A knock-down, whilst it did not affect the cells treated for 24 h in MM1 medium (**Figure 4.8C**) suggesting that both FOXO1 and FOXO3A act as negative regulators of FOXM1 under proliferative

conditions. HOXA10 mRNA expression was found to significantly increased in both proliferative and decidualised St-T1b cell following FOXO1, or FOXO3A knock-down (**Figure 4.8D**).

4.2.5 Phosphorylation of FOXO1 by AKT kinase

FOXO transcription factors are downstream targets of the PI3K/Akt pathway (Brunet *et al.,* 1999). To gain an insight into the activity of Akt and its effects on FOXOs in hESC decidualisation, the presence and activity of Akt was examined through Western blotting. Both Akt and active phosphorylated Akt serine 473 ($pAkt^{S473}$) were detected in hESC. No changes were found in the total Akt levels in St-T1b cells cultured in E2 or MM1 medium from day 1 to day 6, whereas, there was a significant decrease of $pAkt^{S473}$ in cells cultured under decidual conditions for up to 6 days (**Figure 4.9**). The phosphorylation of FOXO1 of serine 256 ($pFOXO1^{S256}$) was also detected and decreased with decidualisation on day 6.

The knock-down of Akt-1, the predominant Akt isoform in hESC (Jiang *et al.*, 2005), led to an increase of FOXO1 protein and mRNA levels (**Figure 4.10 A&E**). As expected, total Akt activity was also reduced in St-T1b following the Akt-1 knock-down (**Figure 4.9B**). FOXO3A mRNA and protein levels were not affected by Akt-1 knock-down (**Figure 4.10 A&F**).

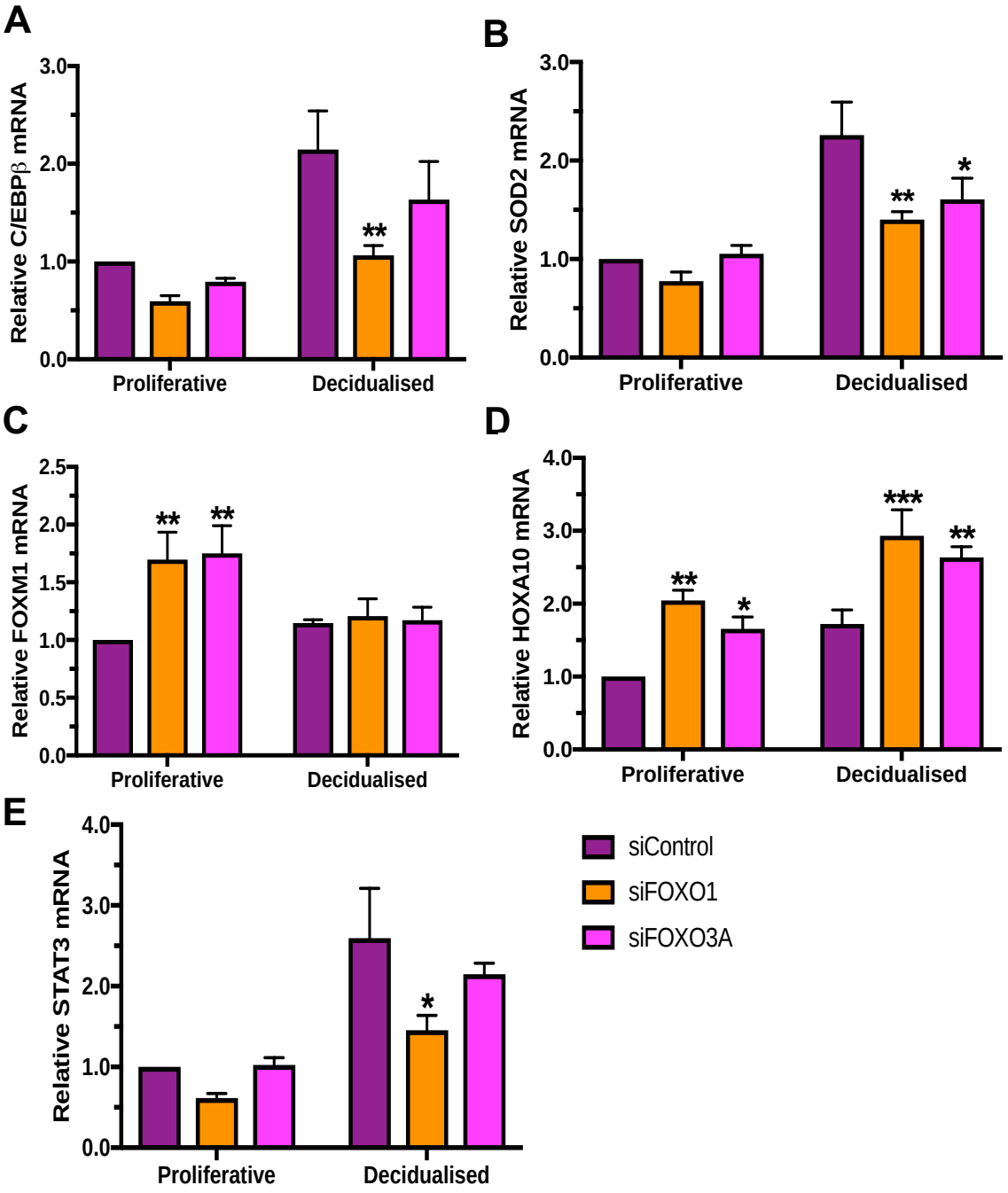

Figure 4.8: The effect of FOXO1 and FOXO3A knock-down on decidual gene expression in hESC. St-T1b cells plated on 6-well plates (2.2 x 10^5 cells/well) overnight and transfected with siRNAs targeting FOXO1 (siFOXO1), FOXO3A (siFOXO3A) or control (siControl) for 24 h followed by a further 24 h incubation in E2 or MM1 medium. Real-time qPCR analysis of **(A)** C/EBPβ; **(B)** SOD2; **(C)** FOXM1; **(D)** HOXA10; and **(E)** STAT3 mRNA expression normalised to β-actin. Results are the mean (+/- SEM) of 3 experiments and analysed using two-way ANOVA; *p<0.05; **p<0.01; ***p<0.001.

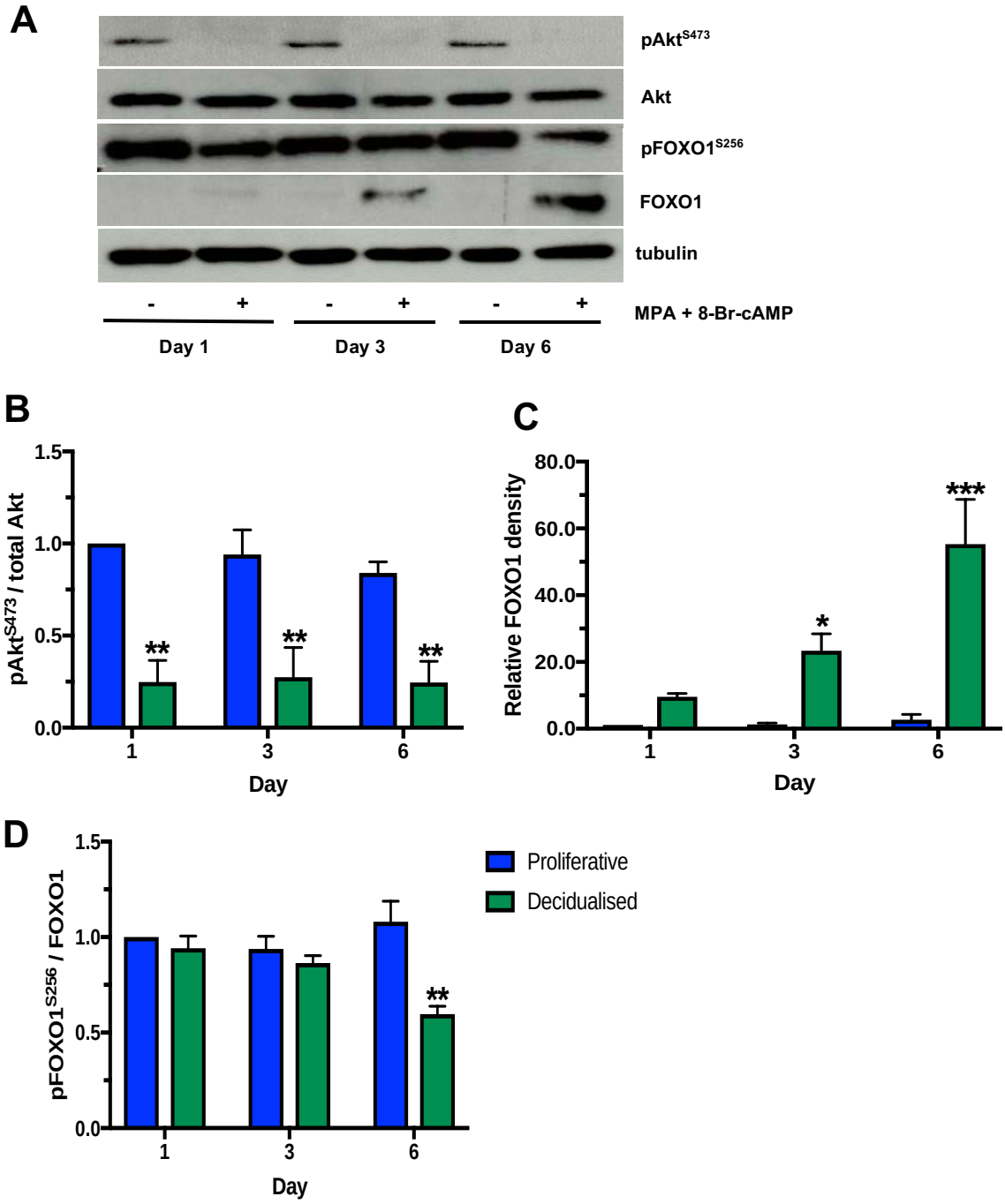

Figure 4.9: Akt activity decreases during hESC decidualisation. St-T1b cells were plated on 6-well plates (3.0 x 10^5 cells/well) overnight followed by 24 h stimulation with E2 or MM1 medium over 6 days and protein lysates were harvested in various time points. **(A)** Representative Western blots showing FOXO1, phospho-FOXO1 (pFOXO1^{S256}), total Akt, phospho-Akt at serine 473 (pAkt^{S473}) and tubulin as loading control. Graph of densitometry analysis of relative **(B)** FOXO1, **(C)** pAkt^{S473} / total Akt**, (D)** pFOXO1^{S256} /FOXO1 normalised to tubulin. Results are the mean (+/-SEM) of 3 experiments and analysed using unpaired t-test; **p<0.01; ***p<0.001.

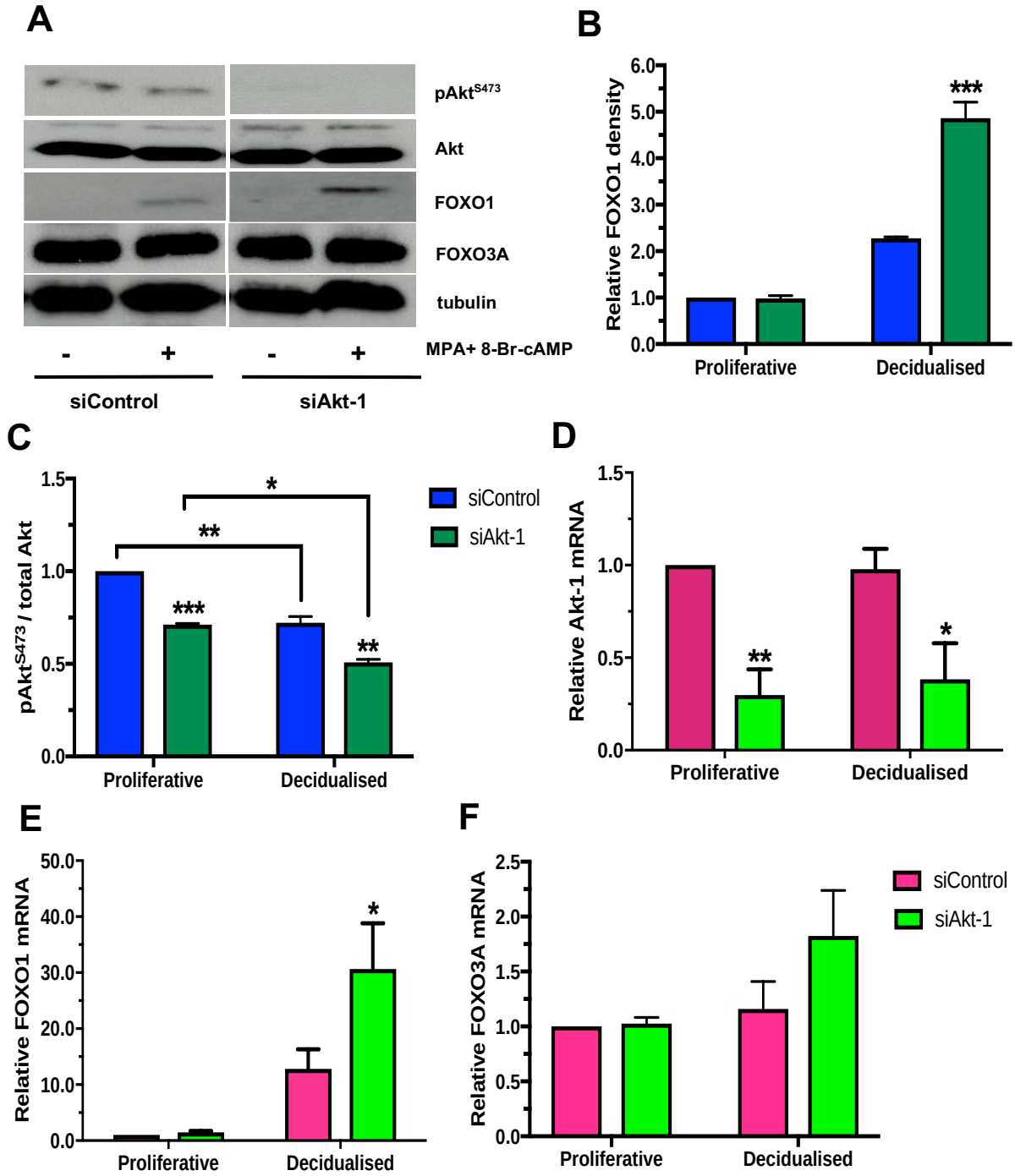

Figure 4.10: Effect of Akt-1 knock-down on FOXO1 expression during decidualisation. St-T1b cells (2.2 x 10^5 cells/well) were plated on 6-well plates overnight and transfected with siRNAs targeting Akt-1 (siAkt-1), or control (siControl), for 24 h followed by 24 h in E2 or MM1 medium. **(A)** Representative Western blots showing FOXO1, FOXO3A, total Akt, phospho-Akt ($pAkt^{S473}$) following Akt-1 knock-down with tubulin as a control. Graph of densitometric analysis of relative **(B)** FOXO1, **(C)** $pAkt^{S473}$ / total Akt, normalised to tubulin. Real-time qPCR analysis of **(D)** Akt-1, **(E)** FOXO1, and **(F)** FOXO3A mRNA expression normalised to β-actin mRNA. Results are the mean (+/- SEM) of 3 independent experiments and analysed using unpaired t-test; *p<0.05; **p<0.01.

4.2.6 Oxidative stress induces both FOXO1/O3A expression in hESC

FOXO3A was shown to be induced only in proliferative hESC (Kajihara *et al.,* 2006), the response to oxidative stress was examined in both proliferative and decidualised cells to further investigate the FOXO1 and FOXO3A expression in ESC. St-T1b cells were incubated with either E2 medium or MM1 medium for 24 h and then exposed to 200 µM H_2O_2 for a further 24 h. We found that exposure to H_2O_2 dramatically induced both FOXO1 and FOXO3A expression in decidualised cells (**Figure 4.11A&B**). In addition, the FOXO activity also increased with H_2O_2 (200 µM) treatment in St-T1b cells transfected with FHRE luciferase-reporter plasmids (**Figure 4.11C**).

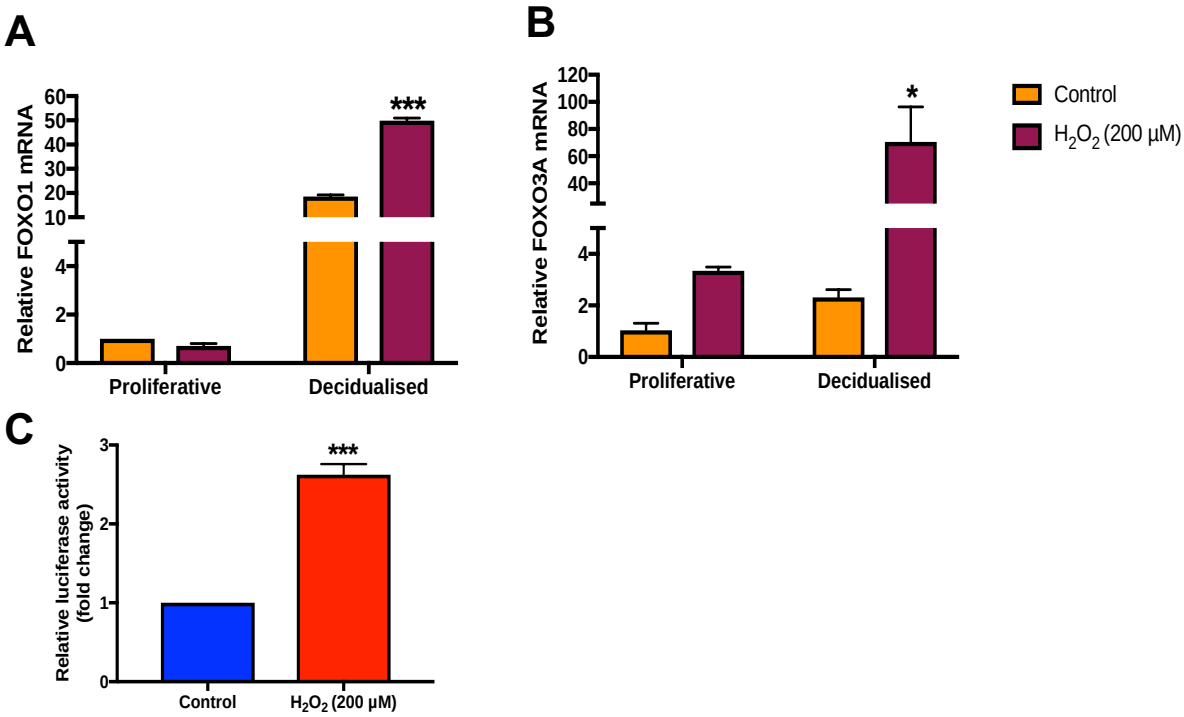

Figure 4.11: FOXO1 and FOXO3A expression are regulated by oxidative stress. St-T1b cells were pre-treated St-T1b cells with E2, or MM1, medium for 24 h and exposed to 200 µM H_2O_2 for 24 h, and the cells were lysed for the mRNA expression of **(A)** FOXO1 and **(B)** FOXO3A determined by real-time qPCR normalised to β-actin. **(C)** St-T1b cells were plated in a 12-well plate overnight and transfected with FHRE luciferase-reporter plasmids for 24 h followed by a further 24 h treatment with 200 µM H_2O_2. Firefly luciferase readings were normalised to Renilla activity. Results are the mean (+/- SEM) of 2 experiments and analysed using unpaired t-test; *p<0.05; ***p<0.001.

4.3 DISCUSSION

FOXO1 has been identified as a key transcriptional regulator of decidualisation (Christian *et al.,* 2011; Zhang *et al.,* 2013) and its loss leads to the impaired decidualisation in isolated mouse ESC and hESC, and recurrent implantation failure (Zhang *et al.,* 2014; Ujvari *et al.*, 2017). In agreement with previous studies, there was a large increase of FOXO1 expression in both primary hESC and St-T1b cells treated with 8-Br-cAMP (**Section 3.3.3.1**). In the present study showed that the treatment of cells with MPA alone did not induce FOXO1 activity and the combination of MPA and cAMP was not found to enhance FOXO1 expression consistent with Samalecos *et al.* (2009). These results are in contrast with the findings of Labied *et al.* (2006) which show greater FOXO expression with combined cAMP and MPA treatment in hESC. The activity of FOXO proteins is regulated by their subcellular localisation (Brunet *et al.,* 1999).

4.3.1 Dephosphorylation of FOXO1 by Akt in hESC decidualisation

The activation of the PI3K pathway leads to phosphorylation of Akt which in turn phosphorylates downstream target genes including FOXO1/O3A eliminating them from the nucleus (Tang *et al.*, 1999; Brosens and Gellersen, 2006). Studies have shown that progesterone activates the PI3K/Akt pathway leading to localisation of FOXO1 in the cytoplasm (*see* **Figure 1.8**). There are three Akt isoforms: Akt-1, Akt-2 and Akt-3. The double knock-out mice for Akt-1 and Akt-3 are embryonic lethal due to the failure of the placental vasculature (Yang *et al.*, 2005). In hESC, the total Akt, $pAkt^{S473}$ and Akt-1 mRNA levels were all reported to be decreased during *in vitro* hESC decidualisation, whilst Akt-2 and Akt-3 remain unchanged in decidualisation compared to control cells (Yoshino *et al.,* 2003, Fabi *et al.,* 2017). In the present study, the $pAkt^{S473}$ levels dramatically decreased with decidualisation over 6 days without a change in total Akt protein expression. There is limited

information on the role of Akt isoforms in hESC decidualisation; one recent study demonstrated that Akt-1 and Akt-2 negatively regulate decidualisation (Fabi *et al.,* 2017). Akt-1 is the predominant Akt isoform in hESC. Accordingly, knock-down of Akt-1 significantly decreased Akt activity ($pAkt^{S473}$) and promotes FOXO1 activity and subsequently increased the FOXO1 expression. FOXO1 has been shown to drive its own expression in decidualisation (Vasquez *et al.*, 2015). Collectively, these results are in line with the majority of literature indicating that progesterone is able to promote Akt activity which may reduce FOXO1 activity and expression, whilst cAMP increases PKA activity to up-regulate FOXO1 expression. Further investigation is needed to determine the effect of each Akt isoform on FOXO1 expression in hESC decidualisation.

4.3.2 Up-regulation of FOXO3A in hESC decidualisation

FOXO3A was reported to down-regulate in hESC decidualisation (Labied *et al.*, 2006; Kajihara *et al.*, 2006). Unlike FOXO1, FOXO3A is regulated by cAMP or MPA alone and suppressed in the combination of cAMP and MPA stimulation (Labied *et al.,* 2006). In contrast to this, the FOXO3A mRNA levels did not change in the cells induced with cAMP alone or a combination of cAMP and MPA (**Appendix I**). Furthermore, FOXO3A mRNA levels actually increase whilst protein levels remain similar or reduced in primary hESC and St-T1b cells during decidualisation induced with cAMP and MPA. This is consistent with a very recent study where FoxO3A mRNA and protein were found to be present in decidualisation of mouse ESC both *in vivo* and *in vitro* and maintain decidualisation and apoptosis-related factors (Long *et al.,* 2018). Furthermore, women with spontaneous abortion were found to have lower endometrial FOXO3A expression (Long *et al.,* 2018) indicating an important role for decidual FOXO3A-driven apoptosis during early pregnancy.

4.3.3 FOXO1 regulates FOXO3A in hESC decidualisation

Although FOXO1 and FOXO3A bind to similar FHRE DNA binding sequences, they regulate differently, but overlapping sets of genes. For example, in endothelial cells, PDGF and BMP4 are regulated by both FOXO1 and FOXO3A, whereas, the angiopoietin-2 expression is regulated by FOXO1, but not FOXO3A (Potente *et al.,* 2005). Here for the first time show that FOXO3A is regulated by FOXO1 in hESC. The knock-down of FOXO1 in primary hESC and St-T1b cells inhibits FOXO3A mRNA, as well as protein expression indicating that FOXO1 can promote FOXO3A expression in hESC (**Figure 4.2**). In addition, FOXO3A expression was up-regulated in the FoxO1 over-expressing in St-T1b cells. Overall, FOXO3A did not affect FOXO1 protein expression in primary hESC and St-T1b cells (*see* **Figure 4.3C**). However, in other cell types, FOXO3A has been reported for example to negatively regulate autophagy by inhibiting FOXO1 expression in prostate, colon, and breast cancers (Zhu *et al.,* 2014). In contrast, a study in human foreskin fibroblasts demonstrated that FOXO1 expression was stimulated by activated FOXO3A through direct binding to at least one FHRE consensus site in the *FOXO1* promoter (Essaghir *et al.*, 2009). In addition, FOXO1 has been reported to induce its expression in these cells (Essaghir *et al.*, 2009) in a similar manner to hESC under decidual conditions (Vasquez *et al.*, 2015). Taken together, FOXO1 regulates FOXO3A positively, but FOXO3A does not regulate FOXO1. Further studies are required to determine the interplay between FOXO1 and FOXO3A in hESC decidualisation.

4.3.4 Up-regulation of FOXO1 and FOXO3A in response to oxidative stress in hESC

FOXO3A plays a critical role in oxidative stress responses and the regulation of apoptosis (Kajihara *et al.,* 2006; Wang *et al.,* 2014). It has been reported that oxidative stress increases FOXO3A expression in proliferative hESC, but not in decidualised cells and that FOXO1

levels decrease significantly in response to oxidative stress in both proliferative and decidualised primary hESC (Kajihara *et al.,* 2006). It was proposed that the action of FOXO1 was to up-regulate SOD2 and repress FOXO3A during decidualisation protect and promote the survival of decidual hESC under oxidative stress conditions (Kajihara *et al.,* 2006). In contrast, the present study results show that FOXO1 and FOXO3A expression increases in decidualised cells after exposure to oxidative stress induced by hydrogen peroxide (**Figure 4.11**). From present results, it is likely that the up-regulation or maintenance of FOXO3A expression in hESC is due to the increasing FOXO1 expression/activity, and oxidative stress induces both FOXO3A and FOXO1 expression in hESC decidualisation. Further investigation is needed into the effect of oxidative stress on FOXO1 and FOXO3A expression during decidualisation. In the present study, hESC were treated with MM1 medium for only 24 h to initiate decidual changes prior to examining the effect of FOXO knock-down and oxidative stress. Therefore, the cells should be treated in MM1 medium for longer periods up to 6 days before being exposed to oxidative stress to determine whether their response changes with decidualisation.

4.3.5 SOD2 is regulated by FOXO1 in hESC

SOD2 is another marker for decidualisation which is up-regulated by FOXO transcription factors to scavenge superoxide radicals and protect cells from damage during decidualisation (Suzuki *et al.,* 1999; Kajihara *et al.*, 2006). The knock-down of FOXO1 in hESC was reported to reduce SOD2 expression during decidualisation, but not in control proliferative cells (Kajihara *et al.,* 2006) supporting my findings that SOD2 was dramatically up-regulated during decidualisation (**Figure 3.6B**), and significantly decreased following FOXO1 knock-down.

4.3.6 FOXO1 and FOXO3A negatively regulate HOXA10

HOXA10 is a member of the homeobox gene family known to be expressed in the uterus in response to oestrogen and progesterone, and its expression increases during the mid-secretory phase of the menstrual cycle when the progesterone levels peak (Taylor *et al.,* 1998). The loss of HOXA10 is associated with endometriosis, polycystic ovarian syndrome (PCOS) and infertility (Cermik *et al.,* 2003; Gui *et al.,* 1999). HOXA10 was also reported to reduce IGFBP-1 expression in hESC decidualisation (Kim *et al.,* 2007). In addition, a total of 494 genes were regulated by HOXA10 during hESC decidualisation by microarray analysis (Lu *et al.,* 2008) and its deletion can lead to defective implantation and decidualisation impairment in mice (Lim *et al.,* 1999). Interestingly, my results show that FOXO1 and FOXO3A knock-down up-regulates HOXA10 mRNA levels in hESC during decidualisation suggesting that HOXA10 may negatively regulated by FOXO1. This may explain the reduction of HOXA10 mRNA expression from day 3 to day 6 (**Figure 3.8B**) of stimulation due to increasing FOXO1 expression and activity in St-T1b cells (*see* **Section 3.2.3.1**). Whilst the FOXO3A mRNA goes up but its protein levels remain unchanged during decidualisation. We do not know its relative activity during decidualisation. These experiments were performed in the St-T1b cell line only due to time constraints. So, future studies should explore this relationship in primary hESC to confirm these findings.

Furthermore, FoxM1 has been reported to be directly regulated by HoxA10 during decidualisation in mice (Gao *et al.,* 2015). In my study, FOXM1 expression was increased following FOXO1 and FOXO3A knock-down in proliferative hESC which may be due to the increase of HOXA10 expression. However, FOXM1 expression did not change following FOXO1 and FOXO3A knock-down under decidual conditions which suggests that not only HOXA10, other factors like C/EBPβ and STAT3 may also regulate FOXM1 in hESC decidualisation.

4.3.7 Conclusion

In summary (**Figure 4.12**), here provide evidence that highlights maintenance of FOXO3A expression in hESC during decidualisation and shows FOXO1 was shown to positively regulate FOXO3A expression. In addition, FOXO1 and FOXO3A were found to regulate HOXA10 and FOXM1 negatively in hESC decidualisation.

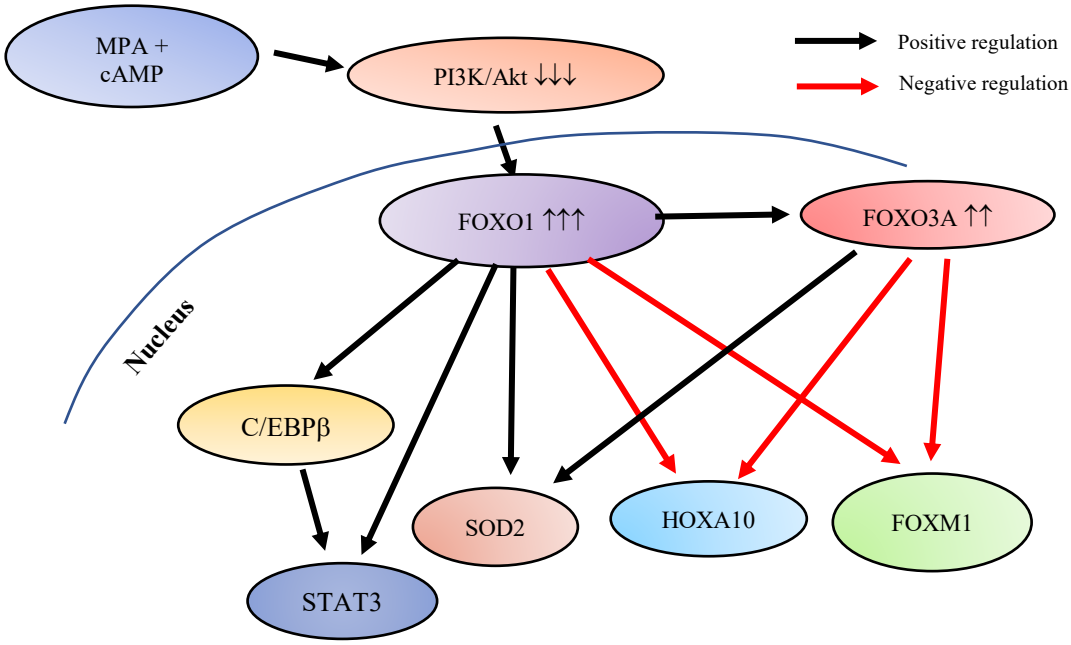

Figure 4.12: Summary findings of the gene regulated by FOXO1 in hESC during decidualisation.

CHAPTER 5:

REGULATION OF VEGF EXPRESSION BY FOXO1 AND FOXO3A IN HUMAN ENDOMETRIAL STROMAL CELL DECIDUALISATION

5.1 INTRODUCTION

VEGF plays a crucial role in the female reproductive system (Girling and Rogers, 2009) and the level of VEGF in the endometrium around the time of implantation is a marker of endometrial receptivity and correlates with reproductive success (Houzi *et al.*, 2009; El-Zenneni *et al.,* 2015; Jakovljev*ic et al.*, 2016; Bansal *et al.,* 2017). Lower levels of VEGF expression are detected in the decidual vasculature of women with recurrent miscarriage compared to those who have had healthy pregnancies (Vuorela *et al*., 2000) and the dysregulation of VEGF can also lead to pathological conditions such as preeclampsia and IUGR (Fan *et al.,* 2014).

The up-regulation of VEGF in endometrium induces angiogenesis which is important for cyclical endometrial regeneration, implantation, regulating trophoblast migration/function and maintenance of maternal-fetal blood supply (Plaisier, 2011). During decidualisation, the endometrium undergoes extensive angiogenesis and vascular remodelling in preparation for implantation (Dunn *et al.*, 2003). It is established that VEGF expression increases with *in vitro* decidualisation of primary hESC (Matsui *et al.*, 2004; Lockwood *et al.*, 2009) and decidual cells have been recognised as an important source of VEGF in the endometrium (Lin and Gu, 2005). However, the mechanisms underpinning VEGF up-regulation and the potential role of VEGFs on decidual hESC remained unclear. This is partly due to the fact that other cell types such as resident inflammatory cells also express VEGF.

The major physiological driver of VEGF expression is hypoxia (Ferrara, 2009). VEGF is up-regulated by HIF-1α which is induced by hypoxia during menstrual and proliferative phases, however, low HIF-1α levels are detected during the mid-secretory phase of the cycle (Maybin *et al.*, 2018). VEGF is reported to be up-regulated in response to E2 or progesterone treatment in hESC (Huang *et al.,* 1998; Classen-Linke *et al.,* 2000). However, others have

shown that VEGF expression in endometrial epithelial and hESC is not affected by E2 treatment (Lockwood *et al.,* 2002).

Preliminary findings from our laboratory demonstrated that adenoviral-mediated over-expression of wild-type or constitutively active FOXO1 in St-T1b cells results in a significant increase in VEGF production. Similarly, the over-expression of constitutively active FoxO1 in pancreatic islet cells in mice strongly up-regulated VEGF (Kikuchi *et al.*, 2012) and very recently, Jeon *et al.* (2018) reported that FOXO1 directly regulates VEGF expression in keratinocytes during wound healing.

In this chapter, the regulation of VEGF expression and secretion in hESC decidualisation was characterised in primary hESC and the St-T1b cell line. The role of FOXO1 in VEGF up-regulation in hESC during decidualisation and the potential interplay between FOXO1 and FOXO3A was also investigated.

5.2 RESULTS

5.2.1 VEGF expression in human ESCs during decidualisation

Endometrial VEGF mRNA levels increase during ESC decidualisation (Matsui *et al.,* 2004; Lockwood *et al.,* 2009). In order to characterise the up-regulation of VEGF in hESC during decidualisation, primary hESC and St-T1b cells were grown to confluence and then incubated with E2 or MM1 medium over 6 days. Fresh medium was added to the cells 24 h prior to harvesting cell lysates and supernatants at 3 and 6 days. VEGF mRNA and protein levels were assessed by real-time qPCR and ELISA respectively. There was a significant increase in VEGF mRNA expression in primary hESC during decidualisation (**Figure 5.1A**). Surprisingly, although VEGF mRNA expression increased in St-T1b cells at 3 and 6 days of stimulation, it did not reach significance (**Figure 5.2A**). VEGF protein secretion was significantly increased with decidualisation in both primary hESC (**Figure 5.1B**) and St-T1b

cells (**Figure 5.2B**) which is consistent with the protein array data shown in Chapter 3 (**Section 3.2.4**). Shorter-term stimulation with E2 or MM1 medium was also examined in St-T1b cells. Rapid induction of VEGF secretion was observed following stimulation with MM1 medium which was detected as early as 5 h onwards whereas, the level of VEGF released from the proliferative cells remained low over 24 h (**Figure 5.2B**).

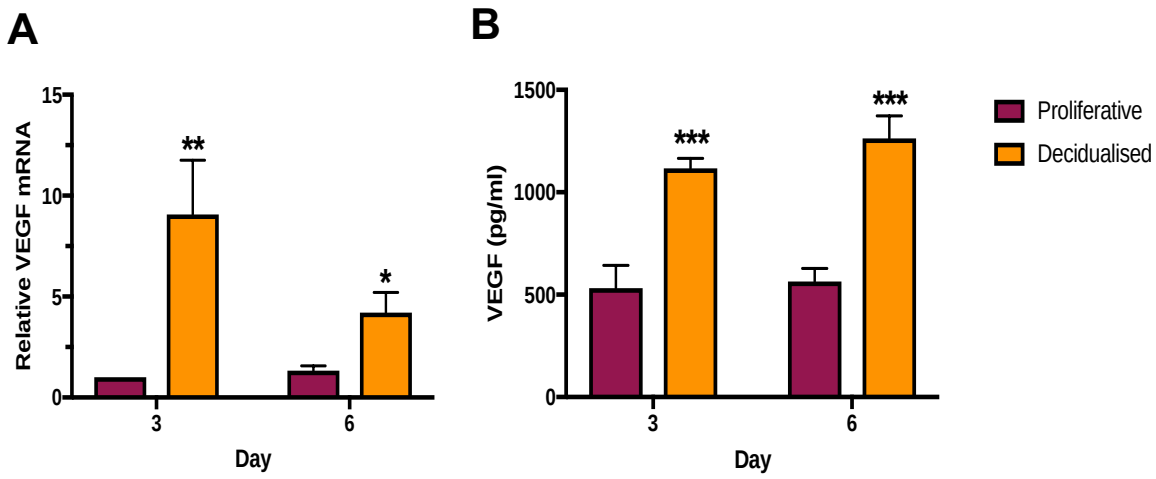

Figure 5.1: Up-regulation of VEGF expression and secretion in primary hESC during decidualisation. Primary hESC isolated from 5 individuals were incubated in E2 or MM1 medium, and RNA and cell supernatants were harvested after 3 and 6 days. **(A)** Real-time qPCR analysis of VEGF mRNA expression normalised to β-actin. **(B)** VEGF protein secretion determined by ELISA. Results are the mean (+/- SEM) of 5 independent experiments and analysed using unpaired t-test; *p<0.05; **p<0.01; ***p<0.001.

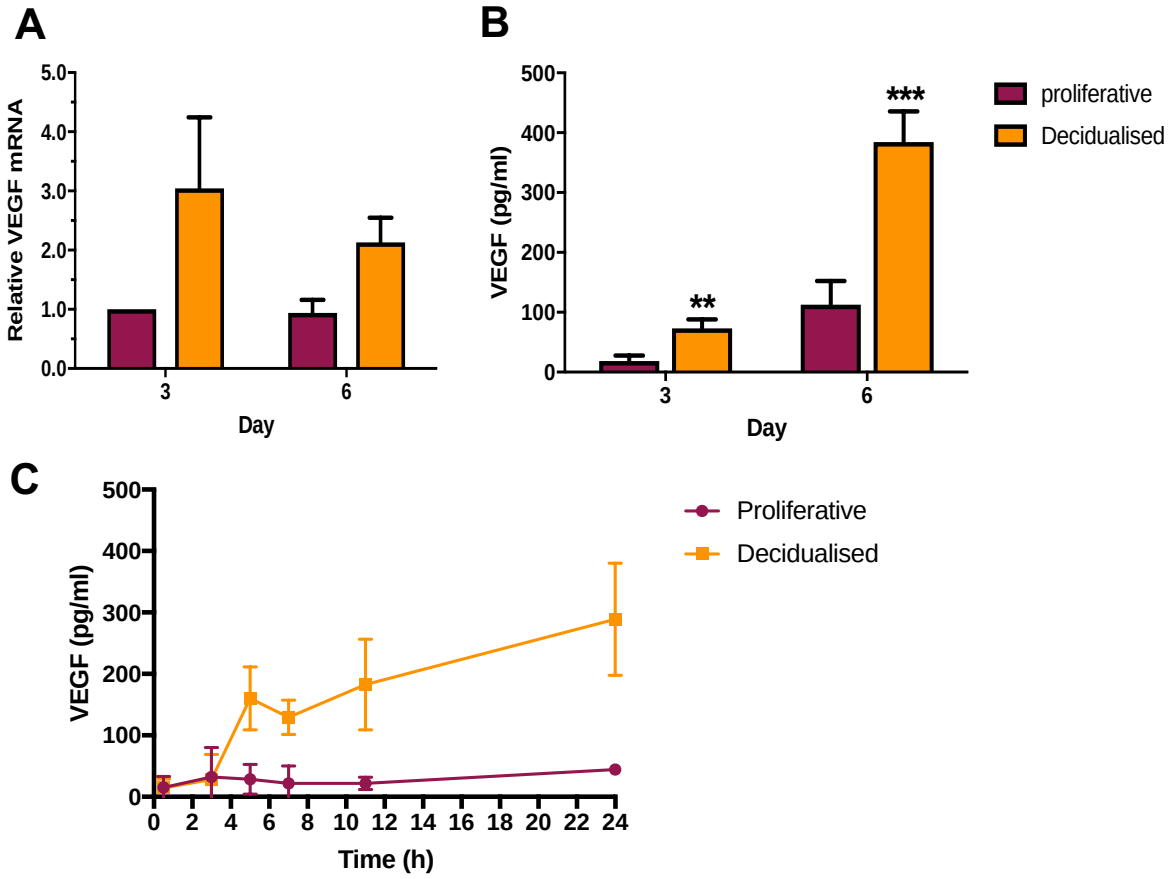

Figure 5.2: Up-regulation of VEGF expression in St-T1b cells during decidualisation. St-T1b cells were incubated in E2 or MM1 medium, RNA and cell supernatants were harvested after 3 and 6 days. **(A)** Real-time qPCR analysis of VEGF expression normalised to β-actin. The VEGF protein secretion was determined by ELISA **(B)** over 6 days and **(C)** 24 h time course (30 min, 3, 5, 7, 11 and 24 h). Results are the mean (+/- SEM) of 4 independent experiments and analysed using an unpaired t-test; *p<0.05; **p<0.01; ***p<0.001.

5.2.2 The effect of progesterone on VEGF expression in hESC

Progesterone has been reported to either increase (Shifren *et al.,* 1996), or have no effect on VEGF expression (Okada *et al.,* 2011) in primary hESC. In order to determine the effect of progesterone on VEGF expression in hESC, St-T1b cells were grown to confluence in 24-well plates and then incubated with different concentrations of MPA (0.1, 1, and 100 μM) over 6 days and VEGF levels assessed by ELISA. VEGF production was unaffected at lower

concentrations of MPA and significantly reduced at high MPA concentrations (100 μM) in hESC (**Figure 5.3)**.

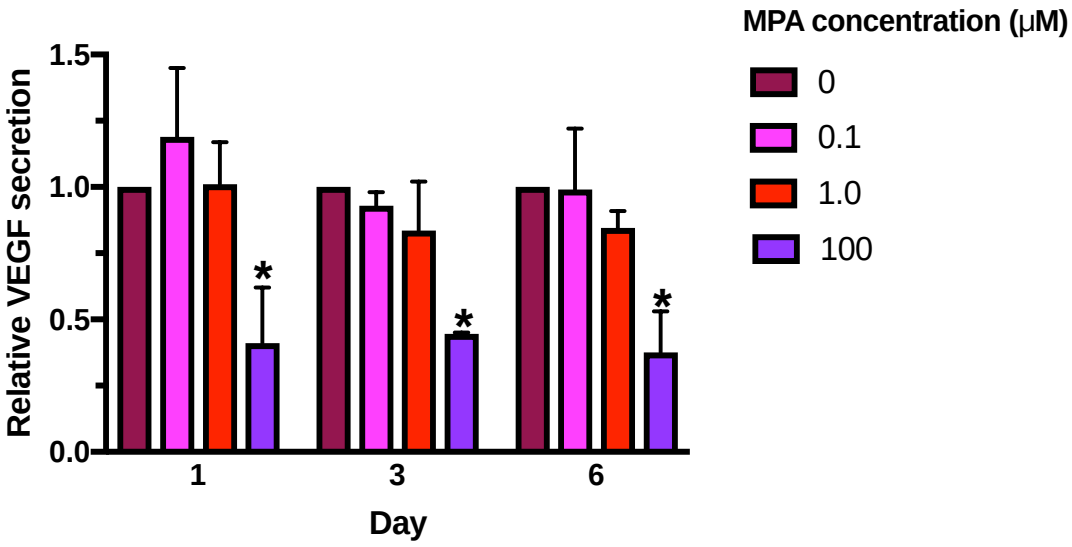

Figure 5.3: Effect of progesterone on VEGF secretion in hESC. St-T1b cells were plated in 24-well plates (1.2 x 10^5 cells/well) overnight and incubated with various concentrations of MPA in duplicates for 24 h on various days. The supernatants were collected at different time points and VEGF secretion assessed by ELISA. Results are the mean (+/- SEM) of 3 experiments and analysed using two-way ANOVA with Dunnett test; **p<0.01.

5.2.3 The effect of oestrogen on VEGF expression in hESC

17β-Oestradiol (E2) has been reported to either stimulate VEGF production in hESC (Classen-Linke *et al.,* 2000; Okada *et al.*, 2010) or have no effect (Lockwood *et al.,* 2002). To determine the effect of E2 on VEGF expression in St-T1b cells, confluent monolayers grown on 24-well plates were incubated with different concentrations of E2 (1, 100 and 10,000 nM) over 6 days. The 24 h supernatants were collected, and VEGF levels were assessed by ELISA. E2 was not found to affect VEGF secretion levels in St-T1b cells **(Figure 5.4).**

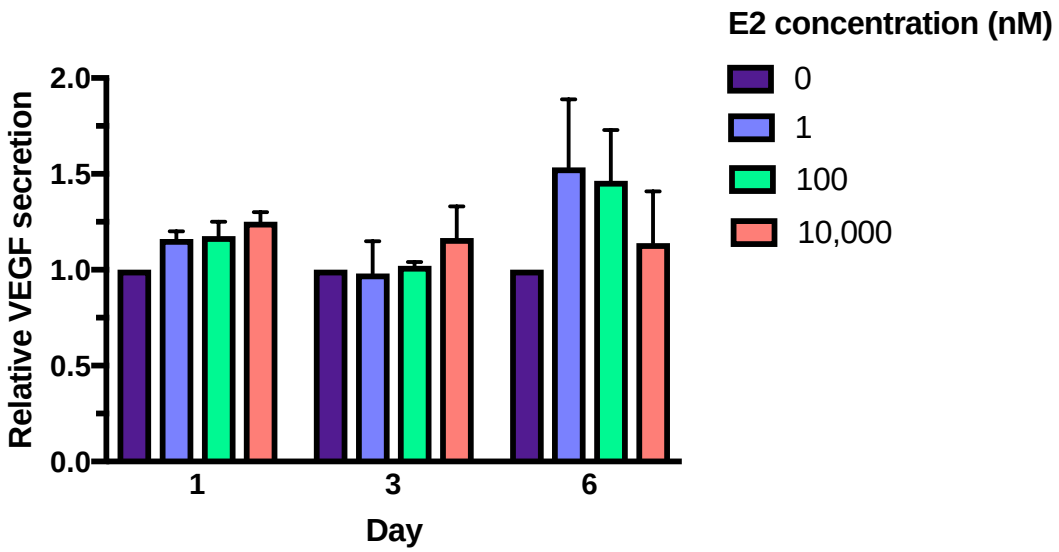

Figure 5.4: 17β-Oestradiol (E2) does not affect VEGF secretion in hESC. St-T1b cells were plated on 24-well plates (1.2 x 10^5 cells/well) overnight and incubated in various concentrations of E2 in duplicates. The 24 h supernatants were collected at different time points and VEGF secretion assessed by ELISA and expressed relative to the control. Results are the mean (+/- SEM) of 3 experiments and analysed using two-way ANOVA with Dunnett test.

5.2.4 The effect of MPA and cAMP on VEGF expression

As shown in Figure 5.3, high concentrations of MPA suppressed VEGF expression in hESC. In order to determine whether the MPA present in the MM1 decidualising medium affects VEGF expression in hESC, St-T1b cells were plated in 24-well plates overnight and incubated in DMEM/F12 with 2% FBS (control) containing 0.5 mM 8-Br-cAMP and/or 1 μM MPA over 3 days. Cell culture supernatants were collected every 24 h and VEGF levels assessed by ELISA. VEGF secretion increased in the cells treated with 8-Br-cAMP, or the combination of 8-Br-cAMP and MPA. Cells treated with both 8-Br-cAMP and MPA produced less VEGF than the cells treated with 8-Br-cAMP alone (**Figure 5.5**). MPA alone did not affect VEGF expression which is consistent with the earlier findings in this study (**Section 5.2.2**).

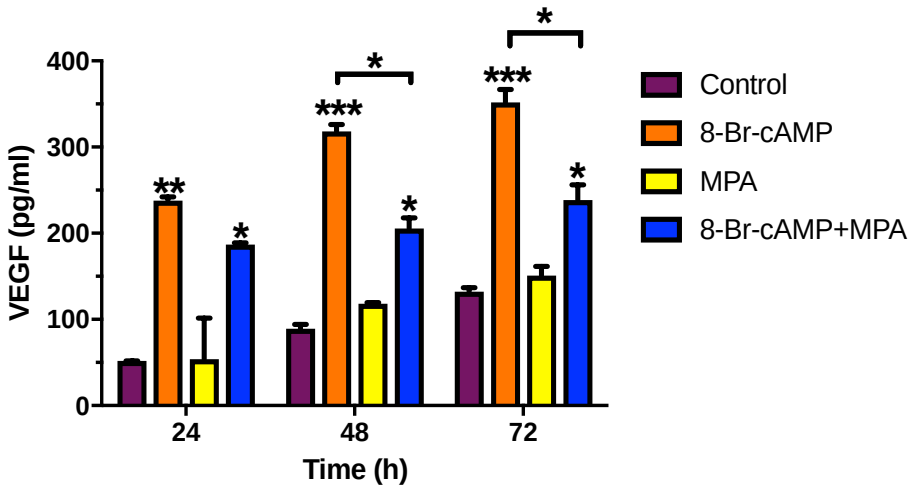

Figure 5.5: Effect of MPA and cAMP on hESC VEGF secretion. St-T1b cells were plated in 24-well plates (1.2 x 10^5 cells/well) overnight and incubated with DMEM/F12 supplemented with 2% FBS (control) containing 0.5 mM 8-Br-cAMP and/or 1 μM MPA over 3 days. The supernatants were collected every 24 h and VEGF secretion assessed by ELISA. Results are the mean (+/- SEM) of 3 experiments and analysed using two-way ANOVA with Dunnett test; *p<0.05; **p<0.01; ***p<0.001.

5.2.5 FOXO1 and FOXO3A regulate VEGF expression and release in hESC

5.2.5.1 Effect of FOXO1 or FOXO3A knock-down on VEGF expression and secretion in hESC

To determine whether FOXO1 is driving VEGF expression and release during hESC decidualisation, FOXO1 was knocked-down in hESC using siRNA to determine the effect on VEGF mRNA and protein levels. Primary hESC and St-T1b cells were transfected with siRNAs targeting FOXO1 (siFOXO1), FOXO3A (siFOXO3A), or control (siControl) using Viromer Blue for 24 h followed by 24 h stimulation with E2 or MM1 medium. Real-time qPCR and Western blotting were used to confirm FOXO1 and FOXO3A knock-down (refer to **Chapter 4**). VEGF mRNA expression was significantly suppressed when FOXO1 was knocked-down in both primary hESC (**Figure 5.6A**) and St-T1b cells (**Figure 5.7A**) during decidualisation. Consistent with these findings, VEGF protein secretion was also suppressed

by FOXO1 knock-down (**Figure 5.6**). Conversely, VEGF expression and protein secretion were significantly increased with FOXO3A knock-down in primary hESC following decidualisation **(Figure 5.6A&B)**. VEGF protein secretion was also determined in 24 h supernatants by ELISA. In contrast, FOXO3A knock-down in St-T1b cells did not affect VEGF mRNA and protein secretion levels in decidualised St-T1b cells (**Figure 5.7**).

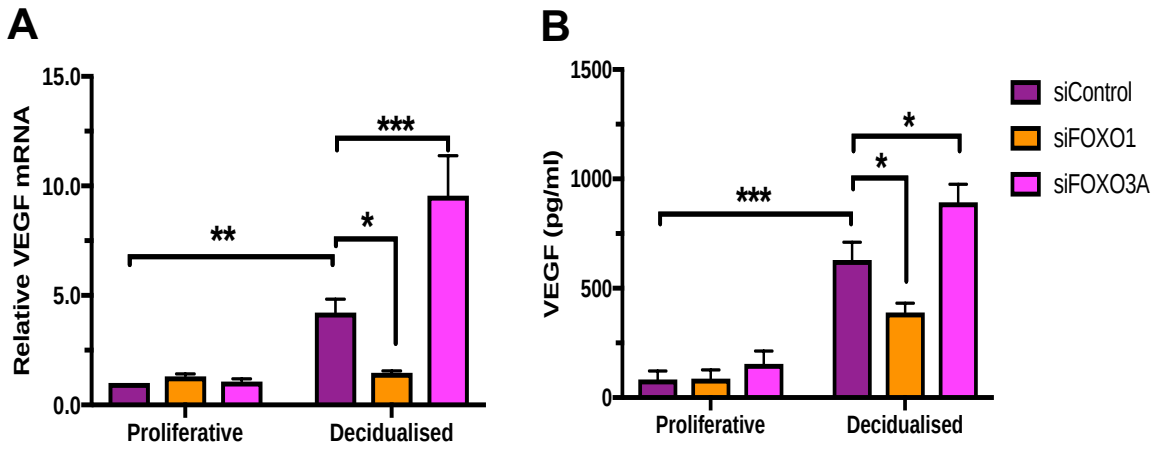

Figure 5.6: VEGF expression and secretion following FOXO1 and FOXO3A knock-down in proliferative and decidualised primary hESC. Primary hESC were plated on 6-well plates overnight and transfected with siRNAs targeting FOXO1 (siFOXO1), FOXO3A (siFOXO3A), or control (siControl) overnight followed by stimulation with E2 or MM1 medium for 24 h prior to harvesting. **(A)** Real-time qPCR analysis of VEGF mRNA expression normalised to β-actin levels. **(B)** VEGF protein secretion in 24 h culture supernatants measured by ELISA. Results are the mean (+/- SEM) of 3 experiments and analysed using two-way ANOVA with Dunnett test; *p<0.05; **p<0.01; ***p<0.001.

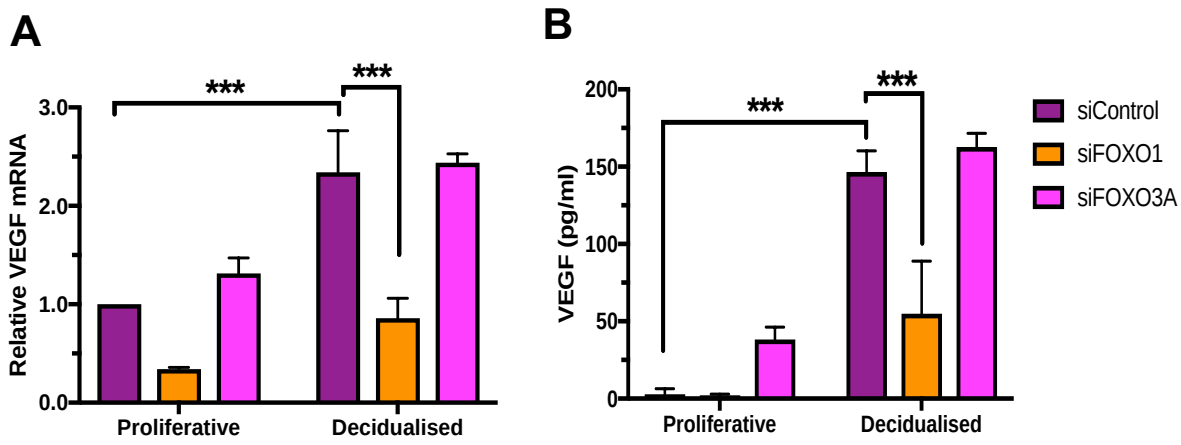

Figure 5.7: VEGF expression and secretion following FOXO1 and FOXO3A knock-down in proliferative and decidualised St-T1b cells. St-T1b cells were plated on 6-well plates and transfected with siRNAs targeting FOXO1 (siFOXO1), FOXO3A (siFOXO3A), or control (siControl) overnight followed by stimulation with E2 or MM1 medium for 24 h prior to harvesting. **(A)** Real-time qPCR analysis of VEGF mRNA expression normalised to β-actin levels. **(B)** VEGF protein secretion in 24 h culture supernatants measured by ELISA. Results are the mean (+/- SEM) of 3 experiments and analysed with two-way ANOVA; *p<0.05; **p<0.01; ***p<0.001.

5.2.5.2 FOXO1 over-expression increases VEGF expression in hESC

St-T1b cells were plated at a density of 2.5 x 10^5 cells/well on 6-well plates, incubated overnight, transduced with adenovirus encoding HA-tagged murine FoxO1 (Ad-FoxO1) or empty control virus (Ad-CMV) for 24 h and incubated in E2 medium for 24 h prior to harvesting. Successful viral infection was confirmed by qPCR and Western blotting for HA-tagged FoxO1. A large increase of both FoxO1 mRNA and protein was detected in cells treated with Ad-FoxO1 (*see* **Section 4.3.3.2)**. VEGF mRNA expression was up-regulated with FOXO1 over-expression (**Figure 5.8A**). VEGF protein levels were also increased in Ad-FoxO1 treated St-T1b cells (**Figure 5.8B**). Collectively, these results show that FOXO1 promotes VEGF mRNA expression and protein secretion during hESC decidualisation. In

addition, FOXO3A appears to suppress FOXO1 activity suggesting that it is able to compete with FOXO1 to regulate *VEGF* gene expression.

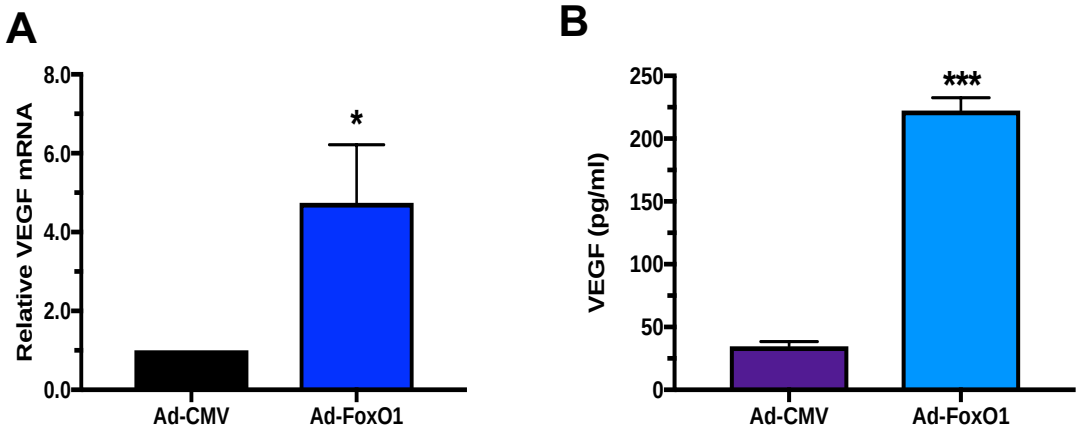

Figure 5.8: FoxO1 over-expression in hESC promotes VEGF production. St-T1b cells were transduced with an adenovirus encoding HA-tagged murine FoxO1 (Ad-FoxO1) or empty control virus (Ad-CMV) overnight and incubated in fresh E2 medium for another 24 h prior to harvesting. **(A)** Real-time qPCR analysis of VEGF mRNA normalised to β-actin. **(B)** VEGF protein secretion assessed in cell supernatants by ELISA. Results are the mean (+/- SEM) of 3 experiments and analysed using unpaired t-test; *p<0.05; ***p<0.001.

5.2.6 *VEGF* promoter activity increases during hESC decidualisation

VEGF protein secretion was found to increase at 5 h following stimulation with MM1 medium (**Section 5.2.1**) suggesting *de novo* synthesis. Various transcription factors have been reported to regulate the *VEGF* promoter (Pages and Pouyssegur, 2004) as shown in **Figure 1.11**. Therefore, *VEGF* promoter activity was examined using *VEGF* promoter-firefly luciferase reporter constructs (pGL-VEGF-Luc). St-T1b cells were co-transfected with *VEGF* promoter (pGL-*VEGF*-Luc-1.8, -2.9, -4.7 kb) and pRL-CMV, a Renilla luciferase control plasmid (*see* **Section 2.14.1**). The cells were stimulated with E2 or MM1 medium for 24 h and the readings normalised to pRL-CMV Renilla activity to determine relative firefly luciferase activity. Incubation of St-T1b cells in MM1 medium increased the activity of all three *VEGF* promoter constructs. Interestingly, St-T1b cells transfected with

the pGL-*VEGF* 2.9 kb construct showed the greatest activity change between proliferative and decidual conditions, its activity increased by 50% in the decidualised cells. Whereas, cells transfected with the 4.7 kb construct had the lowest luciferase activity compared to cells transfected with 1.8 kb and 2.9 kb constructs **(Figure 5.9)**.

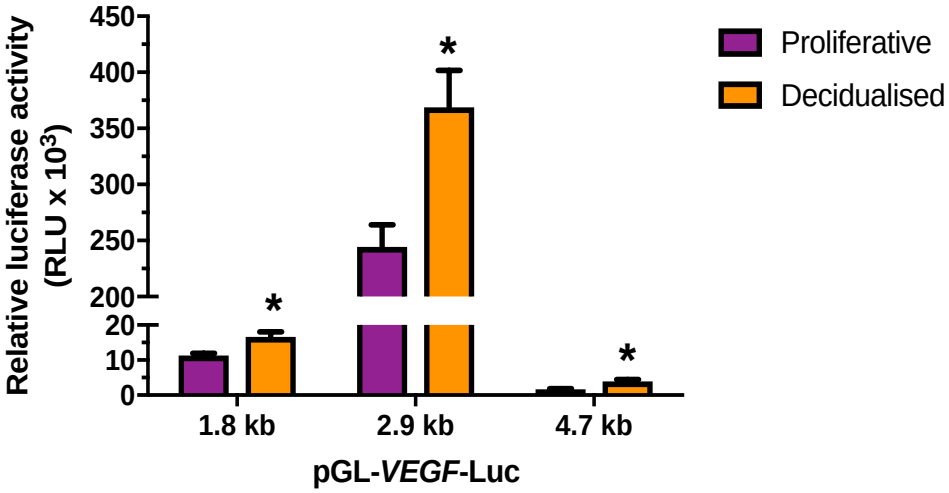

Figure 5.9: *VEGF* promoter activity increases hESC decidualisation. St-T1b cells were co-transfected with pGL-*VEGF*-Luc-1.8, -2.9 and -4.7 kb and pRL-CMV control plasmids overnight followed by stimulation with E2 or MM1 medium for 24 h. Firefly luciferase readings were normalised to Renilla luciferase activity. Results are the mean (+/- SEM) of 3 experiments and analysed using unpaired t-test; *p<0.05.

5.2.7 VEGF expression is regulated by FOXO transcription factors

Due to the strong up-regulation of both FOXO1 and *VEGF* expression in decidualisation and previous preliminary findings in our laboratory and others (Vasquez *et al.*, 2015), we hypothesised that *VEGF* transcription was being driven directly by FOXO1 in hESC decidualisation. In addition, a number of FHRE sites were identified within 2.5 kb of 5 kb human *VEGF* promoter sequences. In order to determine the effect of FOXO1 on *VEGF* expression, St-T1b cells were co-transfected with pGL-*VEGF*-Luc-1.8 kb or -2.9 kb constructs with constitutively active FOXO1 (caFOXO1) or FOXO3A (caFOXO3A) mutant plasmids (Ramaswamy *et al.*, 2002), or the pcDNA3.1 parent plasmid as a control with pRL-

CMV. Firefly luciferase readings were normalised to pRL-CMV Renilla activity. The activity of both the pGL-*VEGF*-Luc-1.8 kb and -2.9 kb constructs increased with the over-expression of caFOXO1 (**Figure 5.10**). Although the activity of the pGL-*VEGF*-Luc-1.8 kb construct was lower than that of cells transfected with pGL-*VEGF*-Luc-2.9 kb, both increased by a similar amount with caFOXO1 over-expression. In contrast, caFOXO3A over-expression strongly suppressed activity in cells transfected with both *VEGF* promoter constructs.

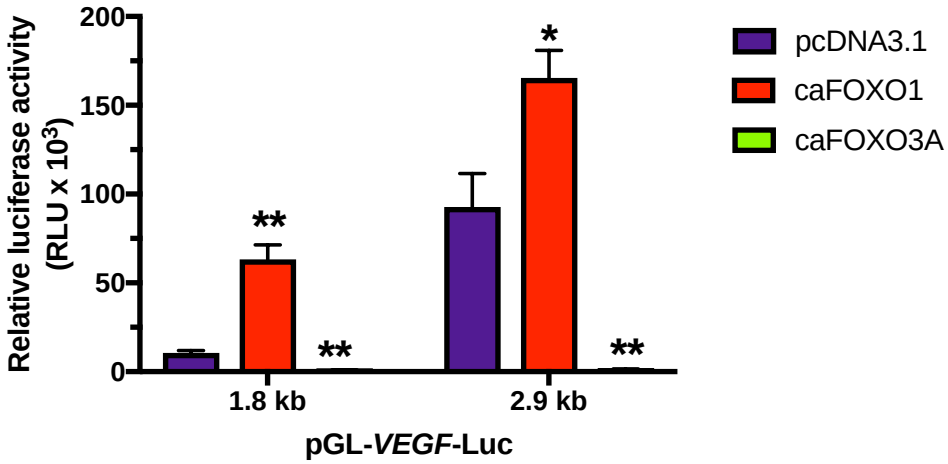

Figure 5.10: Over-expression of FOXO transcription factors regulates *VEGF* promoter activity in hESC. St-T1b cells were plated on 12-well plates overnight and co-transfected with pGL-VEGF-Luc-1.8 kb or -2.9 kb and constitutively active mutant FOXO1 (caFOXO1) or FOXO3A (caFOXO3A) mutant plasmids or pcDNA3.1 as a control for 24 h. The firefly luciferase readings were normalised to Renilla activity. Results are the mean (+/- SEM) of 3 experiments and analysed using two-way ANOVA; *p<0.05; **p<0.01; ***p<0.001.

To determine the effect of loss of endogenous FOXO1 or FOXO3A activity on *VEGF* promoter activity, St-T1b cells were co-transfected with either pGL-*VEGF*-Luc-1.8 kb or -2.9 kb and FOXO1, FOXO3A or control siRNAs overnight and subsequently stimulated for 24 h with E2 or MM1 medium. *VEGF* promoter activity in cells transfected with pGL-*VEGF*-Luc-1.8 kb and -2.9 kb constructs was significantly reduced following FOXO1 knock-down in both E2 medium and MM1 medium conditions (**Figure 5.11A**). Whereas,

VEGF promoter activity increased upon FOXO3A knock-down under both proliferative and decidualised conditions **(Figure 5.11B)**.

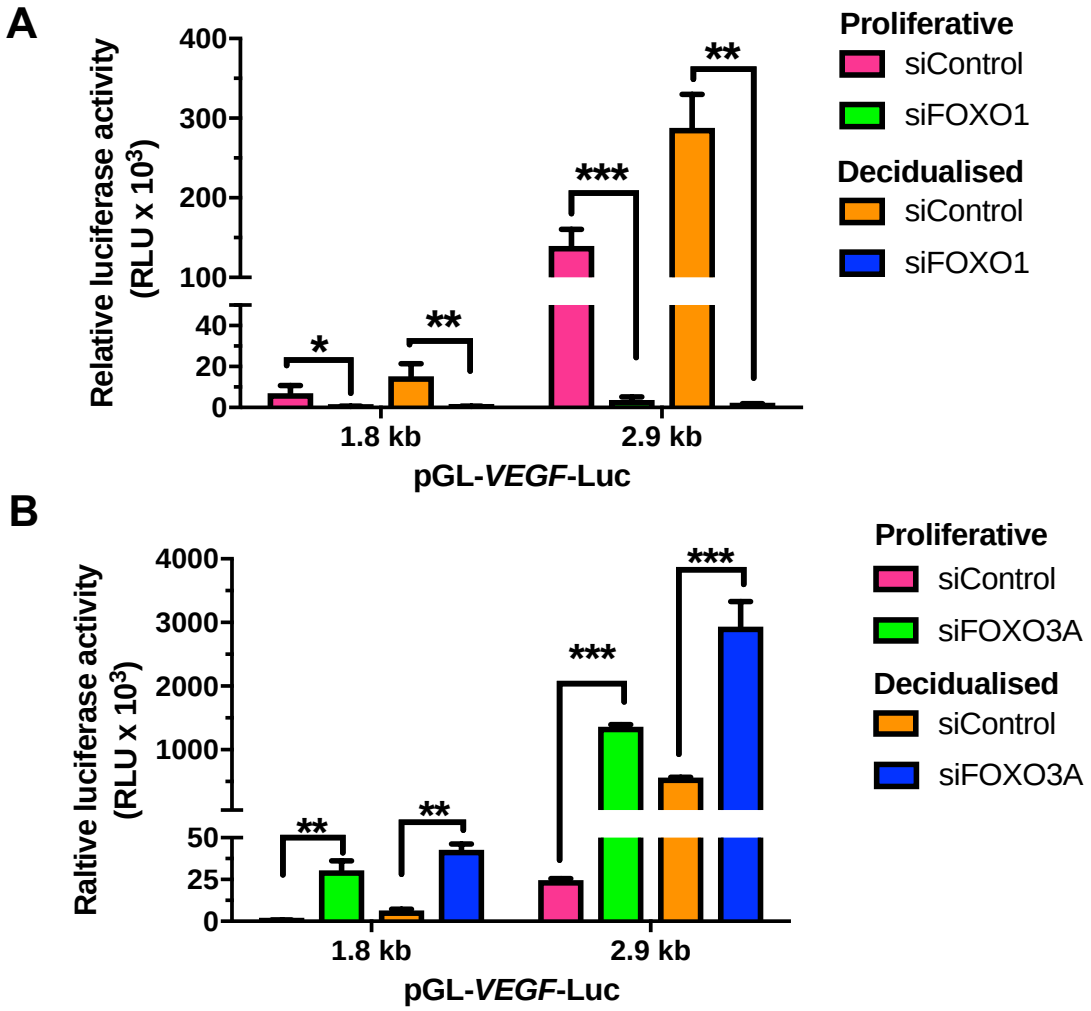

Figure 5.11: FOXO1 and FOXO3A regulate *VEGF* promoter activity in hESC. St-T1b cells were plated on 12-well plates overnight and co-transfected with pGL-*VEGF*-Luc-1.8 kb or -2.9 kb and siRNAs targeting **(A)** FOXO1 (siFOXO1), **(B)** FOXO3A (siFOXO3A), or control (siControl) for 24 h followed by 24 h treatment with E2 or MM1 medium. The firefly luciferase readings were normalised to Renilla activity. Results are the mean (+/- SEM) of 3 experiments and analysed using two-way ANOVA; *p<0.05; **p<0.01; ***p<0.001.

5.2.8 FoxO1 drives Vegf expression in MEFs

In order to extend our findings and confirm FoxO regulation of VEGF more broadly in fibroblasts, MEFs isolated from floxed FoxO mice (Paik *et al.*, 2007) were transduced with

a recombinant adenovirus encoding Cre recombinase (Ad-Cre) to induce Cre-mediated knock-out of FoxO in the cells. MEFs were grown to confluence and infected with MOI 50 Ad-Cre, or Ad-CMV empty vector (control) for 24 h prior to being seeded onto 6-well-plates. The expression of Cre-recombinase in the Ad-Cre transduced cells was confirmed by RT-PCR (**Figure 5.12A**) and the loss of FoxO1 and FoxO3a protein by Western blotting (**Figure 5.12B**). A significant increase in FoxO1 expression was observed in the Ad-CMV treated MEFs following 24 h stimulation with 0.25 mM 8-Br-cAMP compared to the control. Vegf expression was increased by more than 2-fold at 24 h following treatment with 8-Br-cAMP (**Figure 5.12D**). Whereas, in MEFs pre-treated with Ad-Cre for 24 h, FoxO1 mRNA expression was dramatically reduced indicating that FoxO1 had been deleted from the majority of the Ad-Cre transduced MEFs (**Figure 5.12B**). There was no cAMP-mediated increase in Vegf mRNA expression following FoxO1 knock-out indicating that FoxO1 regulates *Vegf* expression in these cells (**Figure 5.12D**).

Floxed FoxO MEFs were co-transfected with pGL-*VEGF*-Luc-2.9 kb and either caFOXO1 or caFOXO3A plasmids, or the pcDNA3.1 were used as a control plasmid. The MEFs behaved like the St-T1b cells and the *VEGF* promoter activity was increased with FOXO1 over-expression and suppressed by FOXO3A (**Figure 5.13A**).

In addition, the Ad-Cre and Ad-CMV transduced MEFs were plated on 12-well plates overnight and transfected with pGL-*VEGF*-Luc-2.9 kb followed by stimulation with or without 0.25 mM 8-Br-cAMP for 24 h. *VEGF* promoter activity was increased in 8-Br-cAMP treated control cells which is consistent with the earlier Vegf mRNA expression results following cAMP stimulation. *VEGF* promoter activity was suppressed in the Ad-Cre pre-treated FoxO knock-out MEFs stimulated with cAMP (**Figure 5.13B**).

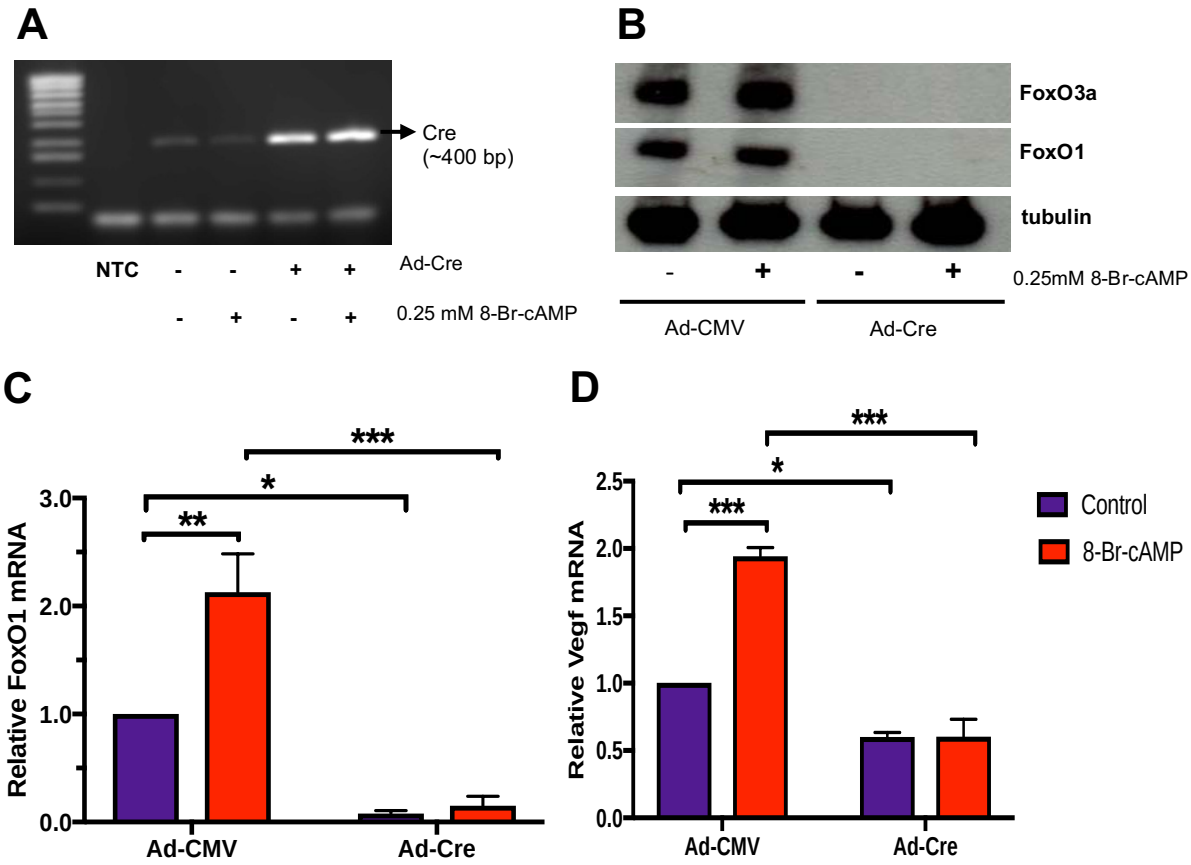

Figure 5.12: FoxO1 drives cAMP-stimulated Vegf expression in MEFs. MEFs isolated from 3 different mice were plated on 6-well plates overnight and infected with adenovirus encoding Cre recombinase (Ad-Cre), or empty adenovirus (Ad-CMV, control) for 24 h followed by stimulation with, or without, 0.5 mM 8-Br-cAMP. Cell lysates were harvested after 24 h. **(A)** Detection of Cre-recombinase in Ad-Cre transduced MEFs by RT-PCR. **(B)** Representative Western blot of FoxO1 and FoxO3a in MEF whole-cell lysates. Tubulin was used as loading control. Real-time qPCR was used to determine the expression of **(C)** FoxO1, and **(D)** VEGF mRNA normalised to β-actin mRNA levels. Results are the mean (+/- SEM) of 3 experiments and analysed using unpaired t-test; *p<0.05; **p<0.01; ***p<0.001.

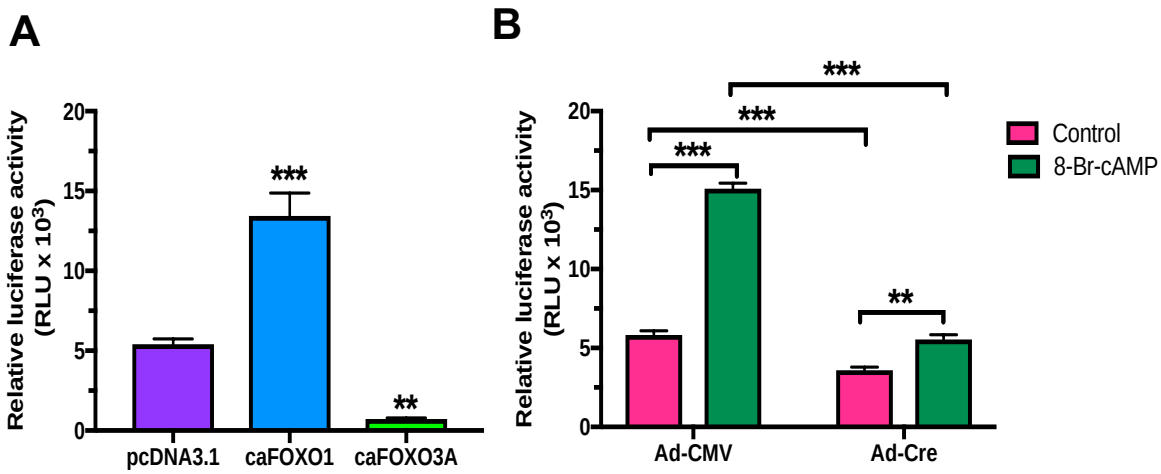

Figure 5.13: FOXO1 is required for cAMP-stimulated *VEGF* promoter activity in MEFs. (A) MEFs isolated from 3 different mice were plated on 12-well plates overnight and co-transfected with pGL-*VEGF*-Luc-2.9 kb and constitutively active FOXO1 (caFOXO1), FOXO3A (caFOXO3A) or pcDNA3.1 plasmids as a control for 24 h. **(B)** Floxed FoxO MEFs were transduced with adenovirus encoding Cre recombinase (Ad-Cre), or Ad-CMV (control), overnight and transfected with pGL-*VEGF*-Luc-2.9 kb for 24 h followed by incubation in DMEM medium supplemented with 2% FBS (control), and 0.25 mM 8-Br-cAMP for a further 24 h. *VEGF* promoter activity was determined using the dual luciferase assay. Results are the mean (+/- SEM) of 3 experiments and analysed using one-way ANOVA and unpaired t-test; **p<0.01; ***p<0.001.

5.3.9 FOXM1 regulates FOXO3A and VEGF expression in hESC

FOXM1 transcription factor plays important roles in cell proliferation and differentiation (Zhang *et al.,* 2013) and was reported to up-regulate VEGF in breast carcinoma cells (Karadedou *et al.*, 2012). FOXM1 transcription factor is up-regulated in hESC following decidualisation (**Figure 3.6E**) and its deletion is reported to impair the differentiation of hESC through a loss of STAT3 activity (Jiang *et al.,* 2015). In order to determine the consequences of FOXM1 inhibition on VEGF expression in hESC, sub-confluent St-T1b cells were incubated with E2 or MM1 medium for 3 days and then treated with thiostrepton (3 μM), which inhibits FOXM1 expression, overnight prior to harvesting. FOXM1 mRNA expression was significantly decreased in decidualised cells as was STAT3 mRNA

expression (**Figure 5.14A&B**). There was an increase of FOXO3A mRNA (**Figure 5.14C**) and protein expression (**Figure 5.14G**) following the inhibition of FOXM1 in hESC whereas there were no changes in FOXO1 mRNA (**Figure 5.14D**) and protein levels (**Figure 5.14F**). VEGF mRNA expression was significantly decreased in decidualised cells (**Figure 5.14E**).

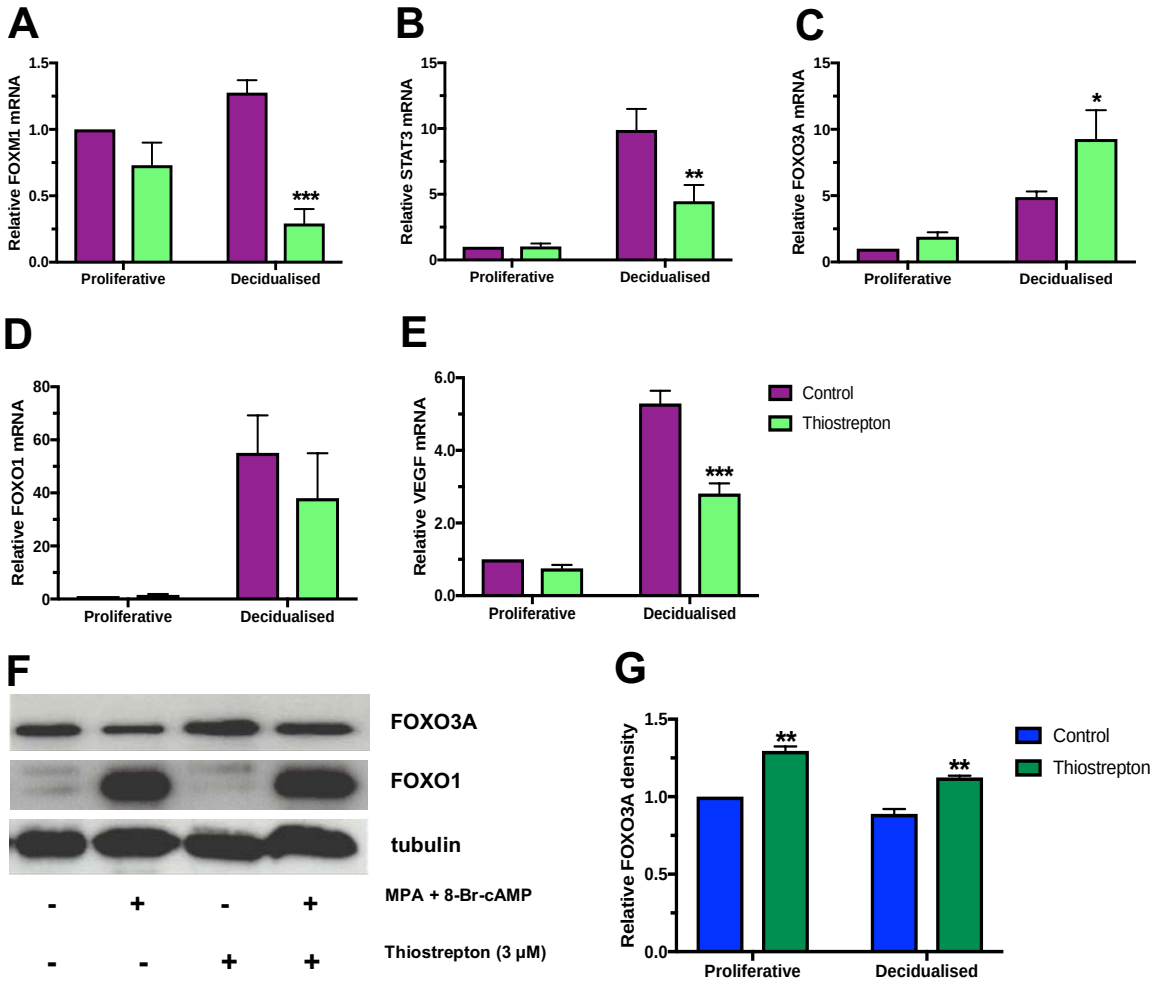

Figure 5.14: Inhibition of FOXM1 increases FOXO3A and suppresses VEGF expression in decidualised hESC St-T1b cells were treated with E2 or MM1 medium for 3 days and followed by thiostrepton (3 µM) treatment overnight prior harvesting cell lysates and supernatants Real-time qPCR analysis of **(A)** FOXM1, **(B)** STAT3, **(C)** FOXO3A, **(D)** FOXO1, and **(E)** VEGF mRNA expression normalised to β-actin following FOXM1 inhibition. **(F)** Representative Western blots showing FOXO1 and FOXO3A expression with tubulin as a loading control. **(G)** Densitometry analysis of relative FOXO3A protein levels normalised to tubulin. Results are the mean (+/- SEM) of 3 experiments and analysed using unpaired t-test; *p<0.05; **p<0.01; ***p<0.001.

5.2.10 FOXO1 directly regulates *VEGF* promoter activity in hESC

We have shown that FOXO1 stimulates *VEGF* promoter activity. However, it is not known whether FOXO1 can bind directly to the *VEGF* promoter to regulate its expression in hESC. In order to address this question, ChIP assays were performed on proliferative and decidualised St-T1b cells. The cells were treated with E2 or MM1 medium for 6 days and then harvested. The cross-linked protein-chromatin material was then sonicated to obtain 200-500 bp DNA fragments for each cell type which were then immunoprecipitated with specific antibodies to obtain protein-DNA complexes of interest. Immunoprecipitation with anti-FOXO1 (H-128, Santa Cruz) antibodies was used to determine the FOXO1 binding to the FHRE sequences identified in the *VEGF* promoter in St-T1b incubated with E2 or MM1 medium with rabbit IgG (sc2027) as a negative control and anti-Pol II (RNA polymerase II) antibody was also used as a positive control to optimise the ChIP conditions.

The *VEGF* promoter sequence was analysed using UCSC gene browser, Genomatix MatInspector and rVISTA to look for putative FOXO binding-sites (**Figure 5.15**). As we had evidence from the *VEGF* promoter reporter assay that the 2.9 kb region upstream from the transcriptional start site was regulated by FOXO1, we focused our efforts on this sequence. Both FOXO1 and FOXO3A have very similar DNA binding sites as shown in **Figure 5.16**. Various sets of the primers were designed from the human *VEGF* promoter DNA sequence using Primer3 and Primer-BLAST (Koressaar and Remm, 2007) (**Figure 5.17**). Each primer set amplifies a DNA fragment of 150 to 170 bp nucleotides in length. In addition, a set of primers amplifying a non-transcribed intergenic region (NegC) was used as an internal background control. All the primers were tested on human genomic DNA to ensure efficient amplification of the target sequence before running on the ChIP material. The results were expressed as a percentage of the 'input' DNA to normalise them according

to the amount of chromatin input used (*see* **Section 2.16**) and the relative fold enrichment to NegC was calculated.

In order to ensure that the conditions for ChIP were optimal, ChIP assays were run using an anti-Pol II antibody. This showed strong enrichment of Pol II binding near to the *VEGF* transcriptional start site confirming that the *VEGF* gene was actively transcribed in these cells (**Figure 5.20**). An anti-isotype matched IgG antibody was used as a negative control. Three different ChIP grade anti-FOXO1 antibodies were trialled, but only one (Santa Cruz, H128) successfully precipitated chromatin-associated FOXO1. Initially the endothelial cell line, HMEC-1, which constitutively expresses higher levels of FOXO1 than ESC was used to examine FOXO1 binding sites in the *VEGF* promoter (**Appendix B1**) prior to using proliferative and decidualised St-T1b cells.

To confirm that the ChIP had been successful in the St-T1b cells, a well characterised FOXO1 binding site in *IGFBP-1* promoter was used as a positive control. There was significant enrichment of FOXO1 binding at this site (**Appendix B2**) in decidualised hESC which is consistent with previous reports (Vasquez *et al.,* 2015). Enrichment of FOXO1 binding was also detected at VEGF ChIP-1-to-3. Notably, the level of enrichment increased significantly with decidualisation corresponding to the rise in FOXO1 expression in hESC and was negligible under proliferative conditions (**Figure 5.18 A-D**). Collectively, these results indicate that FOXO1 binds directly to the *VEGF* promoter.

aatttggtgacaatgtgggcactggctgagtccttaagagtacattgttgtaaatgccggtgacaacacactggg
gcatgggatccagagttaacccctccaggtcacagccaggttatatctccacaatgaaggggggaggtgggccat
actttctcgccctaatgaaggtagctcaaaaaccctaggccaggttgtaatcctagccttatataaaaggaatt
ctgtgccctcactcccctggatccctgggcaaagccccagagggaaacacaaacaggttgttgtaacacaccttg
ctgggtaccaccatggaggacagttggcttatgggggtgggggtgcctggggccacggagtgactggtgatggc
tatccctccttggaacccctccagcctcctcttagcttcagatttgtttatttgttttttactaagacctgctct
ttcaggtctgttggctcttttaggggctgaagaaggccgagttgagaagggatgcaagggaggggccagaatga
gcccttagggctcagagcctccatcctgccccaagatgtctacagcttgtgctcctggggtgctagaggcgcaca
aggaggaaagttagtggcttcccttccatatcccgttcatcagcctagagcatggagcccaggtgaggaggcctg
cctgggaggggccctgagccaggaaataaacatttactaactgtacaaagaccttgtccctgctgctggggagc
ctgccaagtggtggagacaggactagtgcacgaatgatggaaagggagggtggggtgggtgggagccagcccctt
ttcctcataagggccttaggacaccataccgatggaactgggggtactggggaggtaacctagcacctccaccaa
accacagcaacatgtgctgaggatggggctgactaggtaagctccctggagcgttttggttaaattgagggaaat
tgctgcattcccattctcagtccatgcctccacagaggctatgccagctgtaggccagaccctggcaagatctgg
gtggataatcagactgactggtcccactcttcccacaggcctcagagccccaactttgttccctggggcagcctg
gaaatagccaggtcagaaaccagctaggaatttttccaagctgcttcctatatgcaagaatgggatggggccttt
gggagcacttagggaagatgtggagagttggaggaaaaggggggcttggaggtaagggagggggactgggggaagga
taggggagaagctgtgagcctggagaagtagccaagggatcctgagggaatgggggagctgagacgaaacccccca
tttctattcagaagatgagctatgagtctgggcttgggctgatagaagccttggcccctggcctggtgggagctc
tgggcagctggcctacagacgttccttagtgctggcgggtaggtttgaatcatcacgcaggccctggcctccacc
cgcccccaccagcccccctggcctcagttccctggcaacatctggggttgggggggcagcaggaacaagggcctct
gtctgcccagctgcctcccccctttgggttttgccagactccacagtgcatacgtgggctccaacaggtcctcttc
cctcccagtcactgactaaccccggaaccacacagcttcccgttctcagctccacaaacttggtgccaaattctt
ctcccctgggaagcatccctggacacttcccaaaggaccccagtcactccagcctgttggctgccgctcactttg
atgtctgcaggccagatgagggctccagatggcacattgtcagagggacacactgtggcccctgtgcccagccct
gggctctctgtacatgaagcaactccagtcccaaatatgtagctgtttgggaggtcagaaataggggtccagga
gcaaactcccccacccccttccaaagcccattccctctttagccagagccggggtgtgcagacggcagtcact
agggggcgctcggccaccacagggaagctgggtgaatggagcgagcagcgtcttcgagagtgaggacgtgtgtgt
ctgtgtgggtgagtgagtgtgtgcgtgtggggttgagggcgttggagcggggagaaggccaggggtcactccagg
attccaatagatctgtgtgtccctctccccacccgtccctgtccggctctccgccttcccctgccccttcaata
ttcctagcaaagagggaacggctctcaggccctgtccgcacgtaacctcactttcctgctccctcctcgccaatg
ccccgcgggcgcgtgtctctggacagagtttccgggggcggatgggtaattttcaggctgtgaaccttggtgggg
gtcgagcttccccttcattgcggcgggctgcgggccaggcttcactgagcgtccgcagagcccgggcccgagccg
cgtgtggaagggctgaggctcgcctgtccccgccccccggggcgggccgggggcggggtcccggcggggcggagc
catgcgccccccccttttttttttaaaagtcggctggtagcggggaggaTCGCGGAGGCTTGGGGCAGCCGGGTA
GCTCGGAGGTCGTGGCGCTGGGGGCTAGCACCAGCGCTCTGTCGGGAGGCGCAGCGGTTAGGTGGACCGGTCAGC
GGACTCACCGGCCAGGGCGCTCGGTGCTGGAATTTGATATTCATTGATCCGGGTTTTATCCCTCTTCTTTTTTCT
TAAACATTTTTTTTTAAAACTGTATTGTTTCTCGTTTTAATTTATTTTTGCTTGCCATTCCCCACTTGAATCGGG
GAAACCAGCAGAAAGAGGAAAGAGGTAGCAAGAGCTCCAGAGAGAAGTCGAGGAAGAGAGAGACGGGGTCAGAGA
GAGCGCGCGGGCGTGCGAGCAGCGAAAGCGACAGGGGCAAAGTGAGTGACCTGCTTTTGGGGGTGACCGCCGGAG
CGCGGCGTGAGCCCTCCCCCTTGGGATCCCGCAGCTGACCAGTCGCG……**ATG AAC TTT CTG CTG**
+ 1039 bp

Figure 5.15: Human *VEGF* promoter and 5' UTR sequences showing potential FOXO consensus binding sites. The human VEGF-A reference gene sequence (NM_001025366) was analysed using UCSC genome browser, Genomatix MatInspector and rVISTA for the presence of FHRE consensus sequences highlighted (yellow) with potential FOXO core binding sites underlined. The sequence of the previously identified FOXM1 (M1) binding site is highlighted in green (Karadedou *et al.*, 2012). The primer binding sites designed to amplify regions containing the FHRE sites are underlined and in italics. The transcription start site is highlighted in red and 5' UTR sequences are in capitals. The relative position of the start codon and translated sequence is indicated in emboldened capitals.

FOXO1	FOXO3A	FOXO4
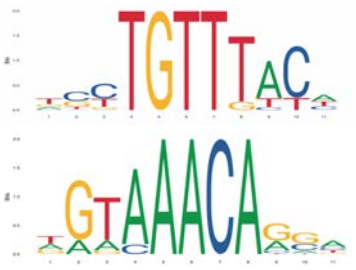	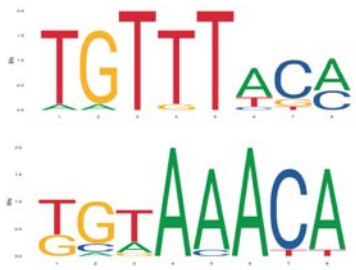	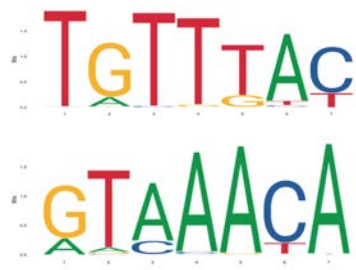

Figure 5.16: Weblogo representation of the preferred FOXO1, FOXO3A and FOXO4 motifs (from JASPER http://jasper.binf.ku.dk).

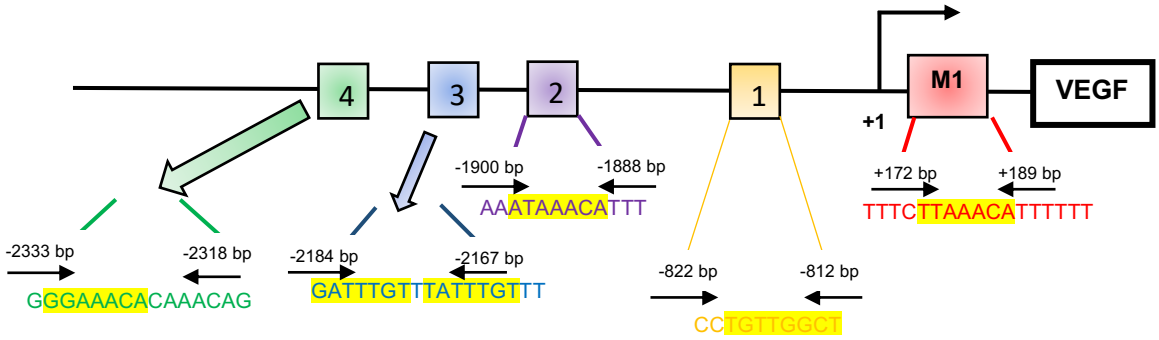

Figure 5.17: Schematic representation of the human *VEGF* promoter indicating the relative positions of the four candidate FHRE sequences. The position and sequence of the previously identified FOXM1 (M1) binding site is shown in red (Karadedou et al., 2012).

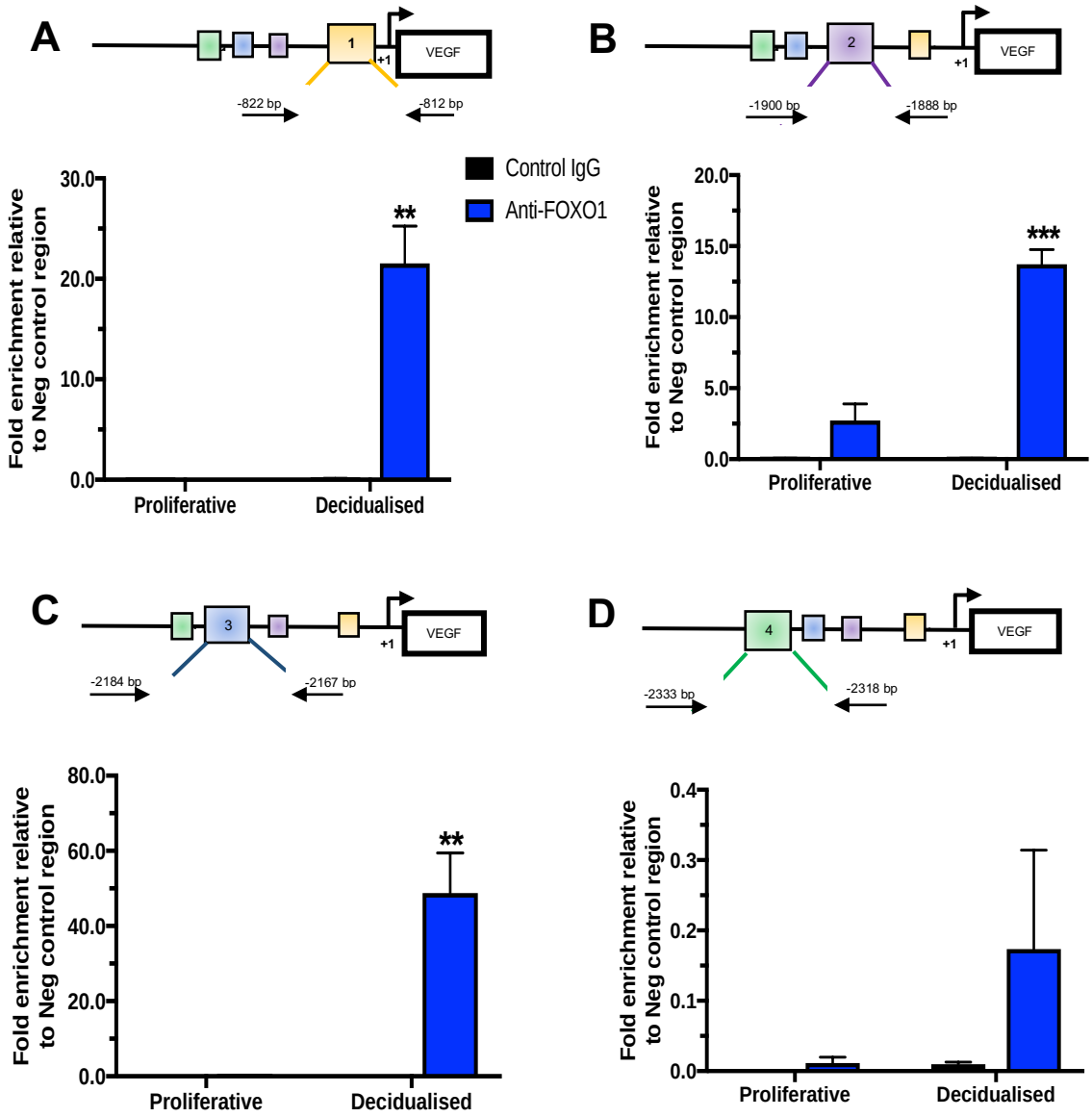

Figure 5.18: FOXO1 binds directly to *VEGF* promoter in decidualised hESC. ChIP assays were performed in proliferative and decidualised St-T1b cells and immunoprecipitated with anti-FOXO1, or control IgG antibodies. The % Input was used to determine the enrichment of VEGF binding. The fold enrichment of FOXO1 binding to the VEGF **(A)** ChIP-1, **(B)** ChIP-2, **(C)** ChIP-3, and **(D)** ChIP-4 sites to the NegC regions determined by real-time qPCR. Results are mean (+/- SEM) of 2 ChIP experiments and analysed using unpaired t-test; *p<0.05; **p<0.01.

5.3.11 FOXO3A binds directly to FHRE in the human *VEGF* promoter in hESC

To determine whether FOXO3A binds at the same FHREs as FOXO1 in the *VEGF* promoter, we performed ChIP assays in St-T1b proliferative and decidualised cells. The cells were treated with E2 or MM1 medium for 6 days and the cells were harvested for ChIP. Immunoprecipitation with ChIP-grade anti-FOXO3A (ab12162, Abcam) antibody was used to determine the FOXO3A binding sites in the *VEGF* promoter. The results were calculated as a percentage of the 'input' DNA to normalise them according to the amount of chromatin input that was used in the experiment and the fold enrichment at the individual putative FHRE compared to the NegC regions was subsequently calculated (*see* **Section 2.16**). The fold enrichment of VEGF ChIP-1-to-3 were significantly increased compared to the IgG control antibody indicating FOXO3A enrichment at these sites mainly in proliferative cells (**Figure 5.19**). This is consistent with greater FOXO3A activity and very low FOXO1 activity in the proliferative hESC whilst, only the VEGF ChIP-1 and -3 sites bound FOXO3A in the decidualised St-T1b cells (**Figure 5.19C**). Similar to the FOXO1 results, no enrichment was detected at VEGF ChIP-4 confirming that this is not a binding site for FOXO transcription factors (**Figure 5.19D**). Collectively the data show that FOXO3A binds to the same binding sites as FOXO1 in this 2.9 kb region of the *VEGF* gene promoter.

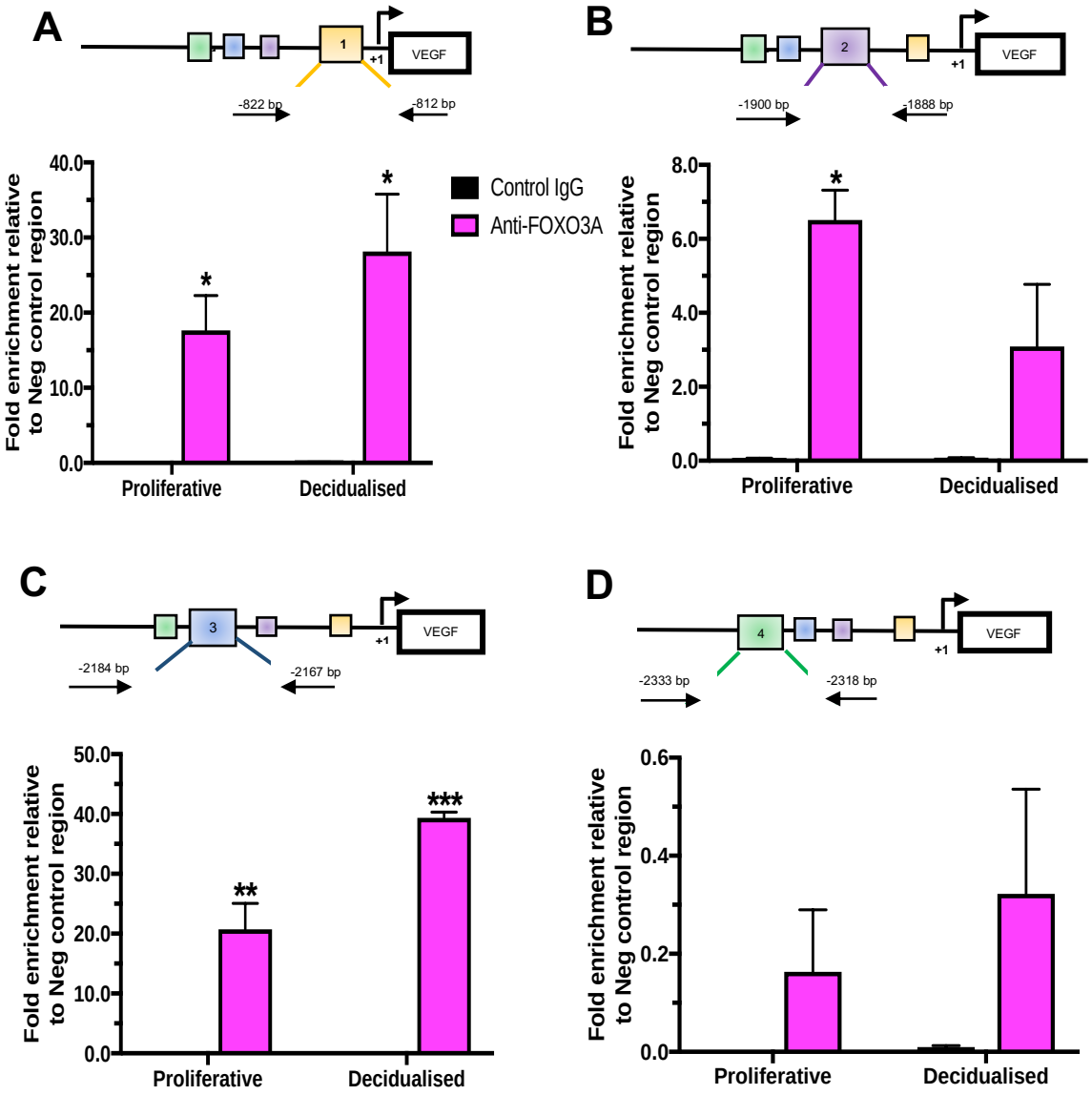

Figure 5.19: FOXO3A binds directly to FHRE in the *VEGF* promoter in hESC. ChIP assays were performed in St-T1b proliferative and decidualised St-T1b cells immunoprecipitated with anti-FOXO3A, or isotype specific IgG control antibodies to determine the enrichment of binding to the VEGF promoter region. The % Input was used to determine the enrichment of VEGF binding. The fold enrichment of FOXO3A binding to VEGF **(A)** ChIP-1, **(B)** ChIP-2, **(C)** ChIP-3, and **(D)** ChIP-4 compared to NegC regions by real-time qPCR. Results are mean (+/- SEM) of 2 ChIP independent experiments and analysed using unpaired t-test; *p<0.05; **p<0.01.

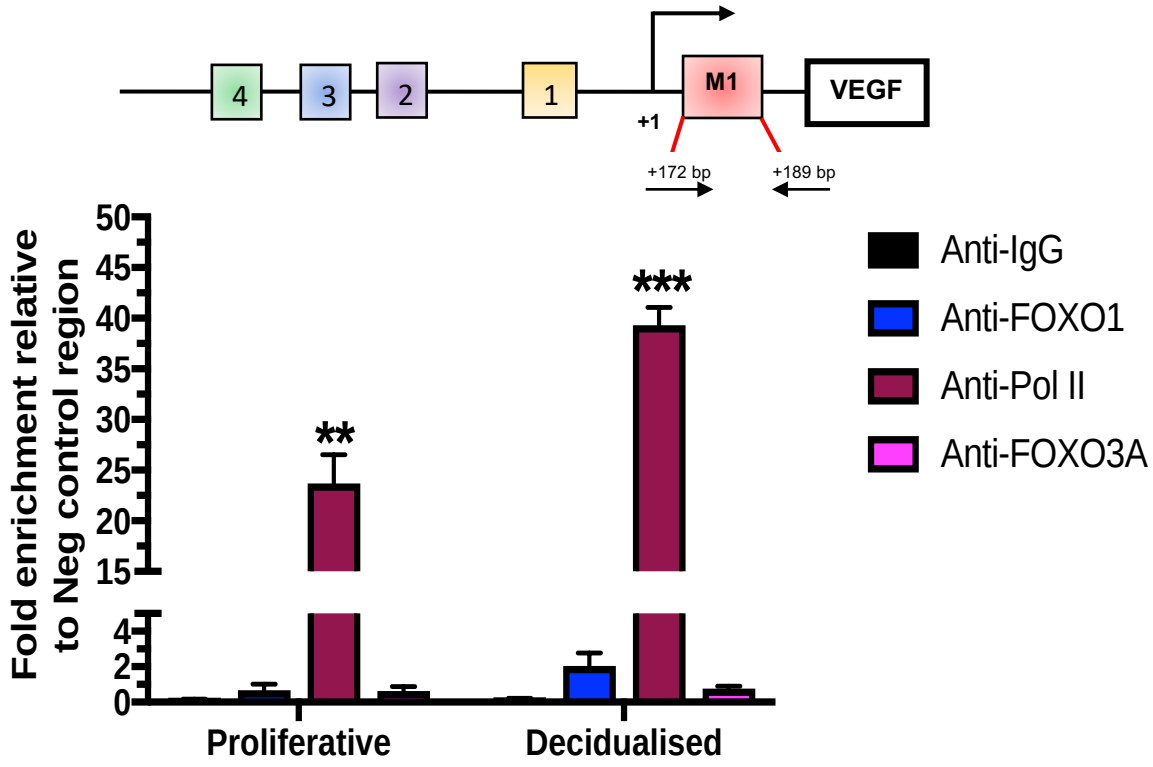

Figure 5.20: FOXO1 and FOXO3A do not bind to VEGF-FOXM1 site in decidualised hESC. ChIP assays were performed in proliferative and decidualised St-T1b cells and immunoprecipitated with anti-FOXO1, anti-FOXO3A antibodies or control IgG antibodies and Pol II antibodies as a positive control to determine the enrichment of binding to the *VEGF* promoter region. The % Input was used to determine the enrichment of *VEGF* binding. The fold enrichment of VEGF-FOXM1 binding normalised to NegC regions by real-time qPCR. Results are mean (+/- SEM) of 2 ChIP experiments and analysed using two-way ANOVA; **p<0.01; ***p<0.001.

5.3 DISCUSSION

5.3.1 Up-regulation of VEGF expression and secretion in hESC decidualisation.

VEGF expression and secretion were found to be up-regulated during hESC decidualisation in both primary hESC and St-T1b cells which is consistent with earlier findings (Matsui *et al.,* 2004, Lockwood *et al.,* 2009). VEGF expression was induced rapidly, and increased VEGF secretion detected after 5 h stimulation in MM1 medium-treated cells. This indicates VEGF is being produced *de novo* and not being released from intracellular stores. Indeed, my results show that MM1 stimulation activates the *VEGF* promoter and up-regulates VEGF

mRNA. This is consistent with the majority of studies which show that VEGF is not stored significantly in most cell types (Ferrara, 2010).

5.3.2 VEGF secretion in hESC decidualisation is regulated by a cAMP-stimulated pathway

VEGF secretion in hESC has been reported to be regulated by E2 (Classen-Linke *et al.,* 2000) and progesterone (Shifren *et al.,* 1996), but their effects are still controversial as other studies have reported that E2 and progesterone do not affect VEGF expression in hESC (Lockwood *et al.,* 2002; Okada *et al.,* 2011). In the present study, VEGF secretion was not stimulated by E2 even at high concentrations and progesterone reduced VEGF secretion at high concentrations in hESC. These findings also indicated that the concentration of E2 (1 nM) in the E2 growth medium does not significantly affect VEGF levels in the present experiments. VEGF secretion is mediated by the cAMP-PKA pathway during hESC decidualisation and cAMP treatment alone was found to increase VEGF secretion. Progesterone (MPA; 1 μM) reduced the level of VEGF secretion stimulated by cAMP. This is likely to be due to the increased PI3K/Akt signalling stimulated by progesterone (Yoshino *et al.*, 2003; Fabi *et al.*, 2017), which promotes FOXO phosphorylation and translocation from nucleus to cytoplasm decreasing FOXO activity.

5.3.3 FOXO1 and FOXO3A positively and negatively regulate *VEGF* transcription in hESC during decidualisation

In the present findings demonstrated that over-expression of FOXO1 stimulates VEGF expression and secretion, while, FOXO1 knock-down reduces VEGF expression and secretion in hESC under decidual conditions. Furthermore, the present results have identified that FOXO3A antagonises VEGF expression. Three fragments of the human *VEGF* promoter (pGL-*VEGF*-Luc-1.8 kb, -2.9 kb and -4.7 kb) were used to define the role of

FOXO1 in *VEGF* transcription. The activity of all three *VEGF* promoter reporter constructs was significantly increased during hESC decidualisation. The 4.7 kb fragment was found to have the lowest relative activity which may indicate the presence of negative regulator regions. Although the -1.8 kb construct had lower overall activity than 2.9 kb fragment, caFOXO1 increased the activity of both constructs which indicates that there are FOXO1 binding sites within the 1.8 kb region. Consistent with VEGF expression and protein data, over-expression of caFOXO1 increased *VEGF* promoter activity, whereas caFOXO3A suppressed it. FOXO1 knock-down also reduced *VEGF* promoter activity whilst FOXO3A knock-down increased its activity. The role of FOXO1 in up-regulating VEGF expression was also confirmed in MEFs isolated from the floxed FoxO mice. The $FoxO^{F/F}$ mutant mice possess loxP sites flanking exon 2 of the FoxO genes which are inactivated by Cre recombinase treatment (Paik *et al.,* 2007). VEGF secretion increased with the 8-Br-cAMP stimulation in floxed FoxO MEFs which again shows that VEGF is expressed through activation of the PKA pathway leading to increased FOXO activity in fibroblasts. Following Cre recombinase-mediated FoxO deletion, Vegf expression decreased. FOXO3A was reported to reduce VEGF expression in breast carcinoma cells (Karadedou *et al.*, 2012).

5.3.4 FOXO1 and FOXO3A directly regulate VEGF in hESC

We demonstrated that FOXO1 is important in the transcriptional regulation of *VEGF* gene expression. It was therefore, necessary to determine whether FOXO1 binding elements exist within the promoter and, if so, which putative FHRE is critical for promoter activity during hESC decidualisation. ChIP was used to determine whether FOXO1 and FOXO3A bind directly to FHRE identified *VEGF* gene promoter in hESC. The decidual markers, IGFBP-1 which were reported to be direct targets of FOXO1 in hESC decidualisation (Vasquez *et*

al., 2015), were used as positive control sites to confirm the validity of the ChIP assays (*see* **Appendix B2**).

Four potential FHRE binding sites were identified in a 2.9 kb region upstream of the *VEGF* start codon using various programs. All FOXO proteins recognise two FHRE consensus sequences: 5′-GTAAA(T/C)AA-3′ known as Daf-16 family member-binding element (DBE) and 5'-(C/A)(A/C)AAA(C/T)AA-3' which is the insulin-responsive element (IRE) (Obsil *et al.*, 2011). There are also several alternative binding sites (Weigelt *et al.*, 2001) which make FOXO binding sites harder to predict. Four sites containing FOXO consensus binding sequences were examined by ChIP assays. There was an enrichment of FOXO1 binding at three of the sites – VEGF ChIP-1-to-3. Importantly, the enrichment of FOXO1 binding to the *VEGF* promoter was only significantly detected in decidualised St-T1b cells corresponding to the up-regulation of FOXO1 expression and activity. The VEGF ChIP-1 site is located ~ 700 bp up-stream of the *VEGF* transcription start site and was reported in a very recent study to bind to FOXO1 during wound healing to promote *VEGF* expression in keratinocytes (Joen *et al.,* 2018). As shown in **Figure 5.21**, VEGF ChIP-3 site showed the greatest enrichment for FOXO1 in decidualised hESC. These results are consistent with ChIPseq data deposited by Vasquez *et al.* (2015), which are available through the Cistrome Project (http://www.cistrome.org/), and when interrogated in UCSC gene browser and indicate a peak of FOXO1 binding to *VEGF* approximately around ~2.0 kb upstream of the transcriptional start site in decidual hESC. The VEGF ChIP-4 site which is a 100 % sequence match with the IRE-binding site showed no enrichment of FOXO1. Water-mediated interactions are one of the important factors for DNA recognition by FOXO proteins, the imbalance in the network of the hydrogen-bonds and water-mediated interactions may lead to the low binding affinity for the IRE sequence (Brent *et al.,* 2008).

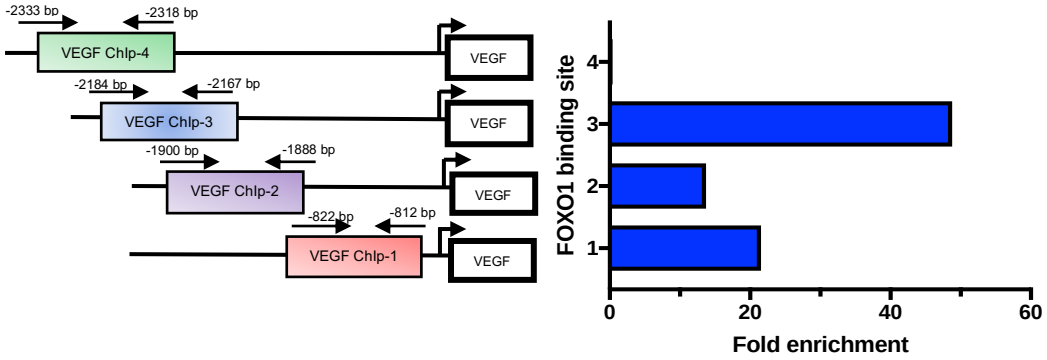

Figure 5.21: FOXO1 binding sites identified by ChIP analysis in human *VEGF* promoter in hESC. Graph showing the degree of enrichment of FOXO1 binding normalised to input DNA and NegC regions in decidualised hESC.

There is no evidence in the literature of the competitive binding of FOXO3A to regulate FOXO1 transcriptional activity. Consistent with our expression data, we found enrichment in FOXO3A binding at three (ChIP-1-3) of the FHRE sites in *VEGF* promoter sequences. The degree of enrichment at these sites was greater in proliferative St-T1b cells, with the exception of VEGF ChIP-3. By *in silico* sequence analysis, the ChIP-3 site was predicted to be a FOXO1/3/4 site. The VEGF ChIP-3 site was found to have higher FOXO3A enrichment compared to the other three sites. In contrast, the enrichment of FOXO3A at the ChIP-2 site was low compared to ChIP-1 and ChIP-3 sites (**Figure 5.22**). Collectively, the expression and ChIP data indicate that VEGF is directly regulated positively and negatively by FOXO1 and FOXO3A respectively in hESC as summarised in **Figure 5.23**.

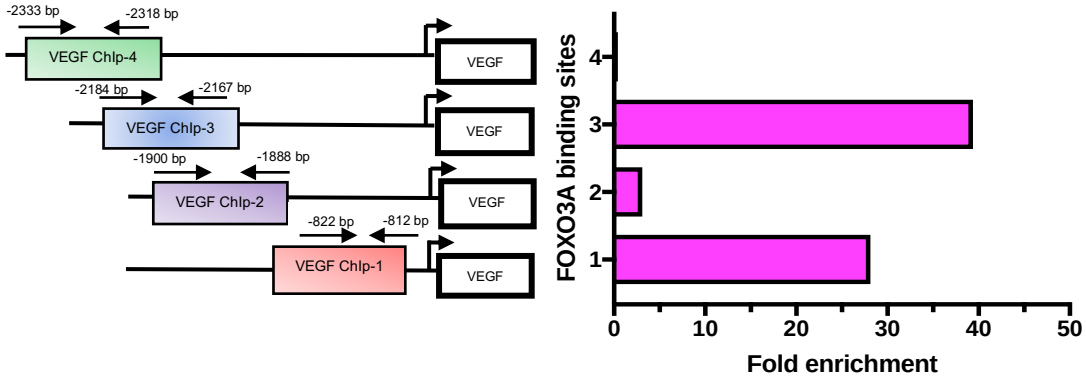

Figure 5.22: FOXO3A binding sites identified by ChIP analysis in the human *VEGF* promoter. Graph shows the degree of enrichment of FOXO3A binding normalised to input DNA and NegC regions in decidualised hESC.

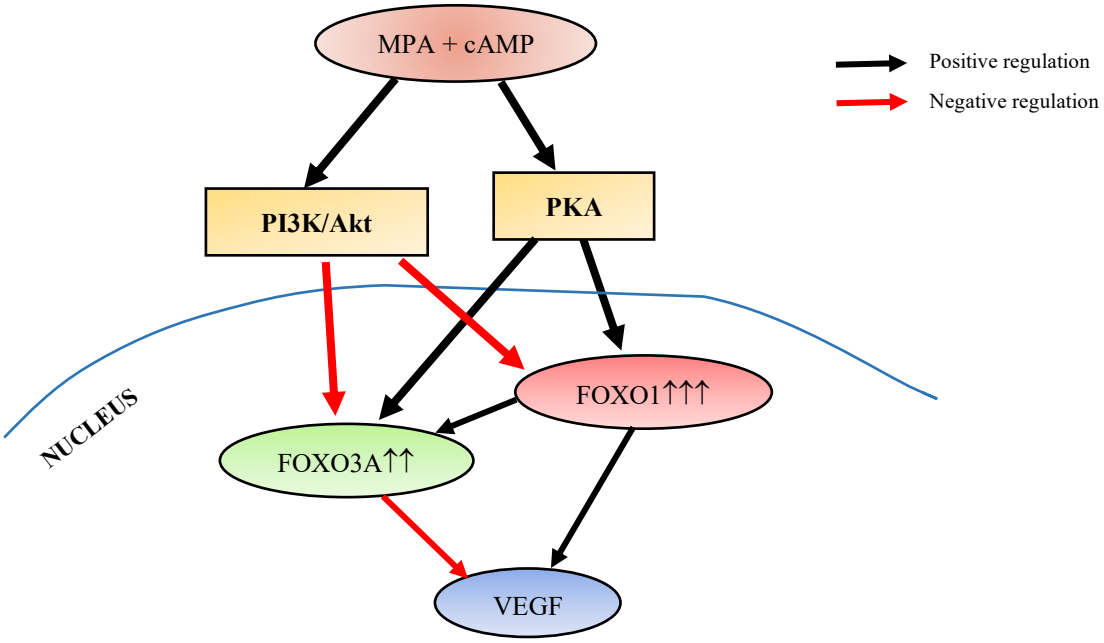

Figure 5.23: Summary of the regulation of VEGF by FOXO transcription factors in hESC.

5.3.5 FOXM1 and FOXO3A compete to regulate VEGF expression in hESC

FOXM1 plays a critical role in hESC decidualisation (Jiang *et al.,* 2015) and is regulated by E2 and progesterone (Xie *et al.,* 2014). It was shown in breast carcinoma cells that FOXM1 positively regulates VEGF expression through binding to the ChIP-M1 site (**Figure 5.17**) and this was inhibited by competitive FOXO3A binding at the same site (Karadedou *et al.*, 2012). However, both FOXO1 and FOXO3A were found to negatively regulate FOXM1

expression in hESC (*see* **Figure 4.8C**). In agreement with Karadedou *et al.* (2012), the present findings have shown increased FOXO3A and reduced STAT3 and VEGF mRNA expression following FOXM1 inhibition with thiostrepton in hESC. The observed reduction in VEGF may be due to the up-regulation of FOXO3A leading to increased FOXO3A binding to the *VEGF* promoter. However, the present results did not detect FOXO3A or FOXO1 enrichment at this site in hESC. Further research would be required to determine whether FOXM1 is binding directly to the *VEGF* promoter in hESC, or simply acting indirectly via up-regulation of FOXO3A and STAT3. This could be determined by performing knock-down of FOXM1 to confirm the results obtained with thiostrepton and over-expression of FOXM1 in combination with FOXO3A knock-down as well as the appropriate ChIP experiments.

5.3.6 Conclusion

In conclusion, the present study shows that the *VEGF* gene is directly regulated by FOXO1 and FOXO3A in hESC in a positive and negative manner. Furthermore, these results were confirmed in MEFs which indicate that this may be a more general mechanism regulating the angiogenesis promoting response in stromal cells. Moreover, both FOXO1 and FOXO3A bind to the *VEGF* promoter at the same FHRE sites, which leads us to propose that FOXO1 and FOXO3A directly compete to regulate *VEGF* in hESC. Thus, the up-regulation of VEGF in hESC during decidualisation may be due to an overall shift in the balance from FOXO3A to FOXO1 activity.

CHAPTER 6:

THE REGULATION OF Flt-1/sFlt-1 EXPRESSION IN HUMAN ENDOMETRIAL STROMAL CELL DECIDUALISATION

6.1 INTRODUCTION

Multiple soluble splice variants of Flt-1 have been reported (Thomas *et al.,* 2009; Heydarian *et al.,* 2009; He *et al.*, 1999). sFlt-1-i13 is the predominant splice variant in endothelial cells and is expressed in most human tissues, whereas sFlt-1-e15a is thought to be a primate-specific isoform mainly expressed in placenta, with much lower concentrations in other tissues (Jebbink *et al.,* 2011). Interestingly, sFlt-1-i13 is the predominant isoform in the rhesus monkey placenta (Rajakumar *et al*., 2009).

Up-regulation of Flt-1 (Andraweera *et al.*, 2012; Nishizawa *et al.*, 2011; Chung *et al.*, 2004) and sFlt-1 (Muy-Rivera *et al.*, 2005; Maynard *et al.*, 2003) are associated with preeclampsia and unexplained fetal growth restriction (Nikuei *et al.,* 2015). sFlt-1 is over-expressed in the placentas of preeclamptic patients, and leads to the maternal syndrome, for example, hypertension and renal dysfunction, by hindering the physiological activity of VEGF in the maternal circulation (Kendall and Thomas, 1993; Maynard *et al.,* 2003; Shibuya *et al.,* 2011; Pang *et al.,* 2013; Hod *et al.,* 2015).

There are only a few studies that report sFlt-1/Flt-1 in the context of the endometrium. Higher expression of sFlt-1 was detected in the mid to late proliferative phase compared to secretory phase in hESC isolated during different phases of the menstrual cycle (Krussel *et al.*, 1999). It was also reported that the Flt-1 receptor exhibited strong expression throughout the secretory phase but decreased in the late secretory phase in hESC (Krussel *et al.,* 1999; Jee *et al.,* 2009). Very recent studies show that sFlt-1 expression is down-regulated during decidualisation at both the protein and mRNA level in hESC and is negatively correlated with PRL and VEGF expression (Cottrell *et al.,* 2017). However, the mechanisms regulating Flt-1 expression and production of its soluble isoforms during hESC decidualisation is still unknown.

In this chapter, changes in the expression of Flt-1 receptor and sFlt-1 production during *in vitro* decidualisation of hESC are investigated. The Flt-1 receptor was previously reported to be regulated by FOXO1 in endothelial cells (Potente *et al*., 2005; Furuyama *et al.,* 2004). Therefore, we also determined whether FOXO1 regulates *Flt-1* gene activity during hESC decidualisation. These findings may have important implications in pregnancy complications, such as preeclampsia that involve abnormal decidualisation, implantation and angiogenesis at the maternal-fetal interface.

6.2 RESULTS

6.2.1 Changes in sFlt-I expression in hESC during decidualisation

In order to characterise the expression of sFlt-1 in hESC during decidualisation, primary hESC and St-T1b cells were grown to confluence and then incubated with E2 or MM1 medium at different time points over 6 days. Fresh medium was added to the cells 24 h prior to harvesting of RNA lysates and collection of cell supernatants at 3 and 6 days. sFlt-1 mRNA and protein levels were assessed by real-time qPCR and ELISA respectively. Relatively high levels of total sFlt-1 were detected in proliferative cells incubated in E2 medium and there was significant ($p<0.01$) down-regulation of sFlt-1 secreted levels during decidualisation in both primary hESC, isolated from five individuals at passage 3, (**Figure 6.1A)** and St-T1b cells **(Figure 6.2A**). Consistent with these results, the sFlt-1 protein levels in the cells also decreased with decidualisation from day 3 to day 6 of stimulation by Western blotting in primary hESC (**Figure 6.1B**) and St-T1b cells (**Figure 6.2B**) and were nearly undetectable on day 6 of stimulation with MM1 medium. Total sFlt-1 secretion in proliferative cells also found to increase as early as 11 h, while the sFlt-1 levels in decidualised cells remained unchanged (**Figure 6.2C**).

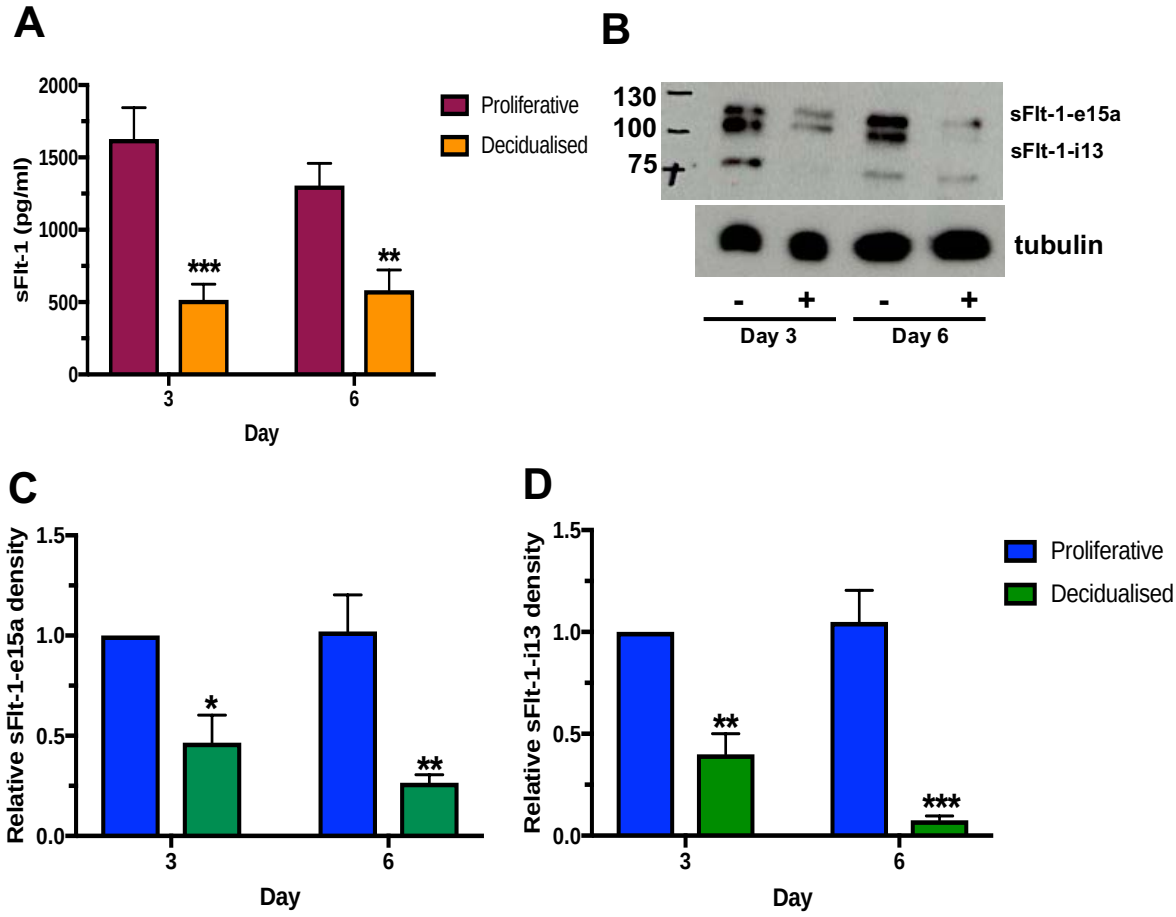

Figure 6.1: Decidualisation leads to a decrease in sFlt-1 release in primary hESC. Primary hESC were incubated in E2 or MM1 medium and protein lysates and supernatants were harvested after 3 and 6 days. **(A)** The sFlt-1 secretion in supernatants was determined by ELISA in primary hESC. **(B)** Representative Western blotting analysis of sFlt-1 protein with tubulin as loading control. Densitometric analysis of relative **(C)** sFlt-1-e15a and **(D)** sFlt-1-i13 protein levels normalised to tubulin. Results are the mean (+/- SEM) of 5 experiments and analysed using an unpaired t-test; **p<0.01; ***p<0.001.

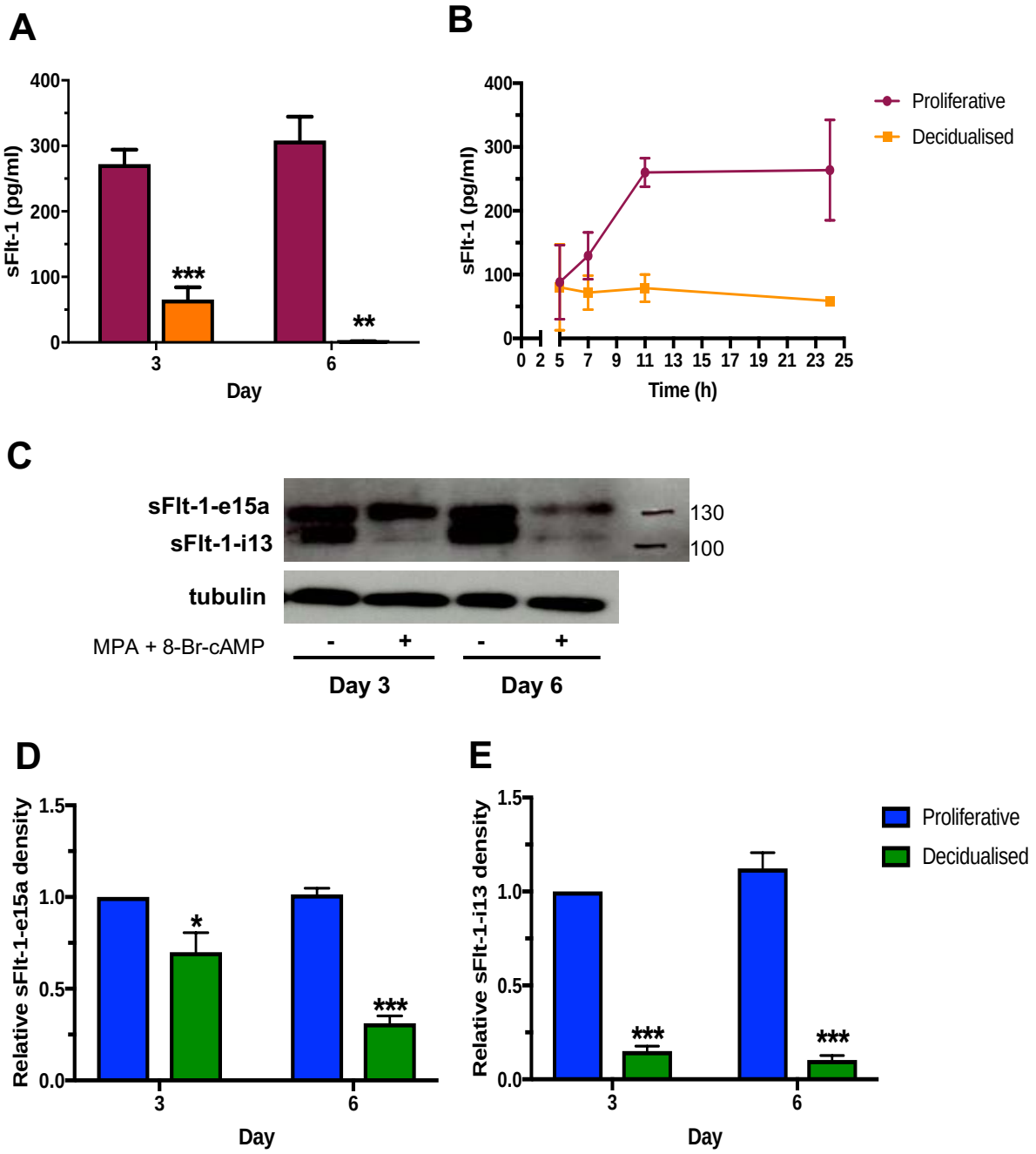

Figure 6.2: Decidualisation leads to a decrease in sFlt-1 release in St-T1b cells. St-T1b cells were incubated in E2 or MM1 medium and protein lysates and supernatants were harvested over 6 days. The sFlt-1 secretion in supernatants was determined by ELISA in St-T1b cells treated **(A)** over 6 days and **(B)** 24 h. **(C)** Representative Western blotting analysis of sFlt-1 protein with tubulin as loading control. **(D)** Densitometric analysis of relative **(D)** sFlt-1-e15a and **(E)** sFlt-i13 protein levels normalised to tubulin. Results are the mean (+/- SEM) of 3 experiments and analysed using an unpaired t-test; *p<0.05; **p<0.01; ***p<0.001.

The mRNA expression of the two major isoforms, sFlt-1-i13 and sFlt-1-e15a mRNA was also determined. sFlt-1-e15a mRNA was also significantly suppressed in decidualised primary hESC consistent with the ELISA results in primary hESC (**Figure 6.3A**). However, the sFlt-i13 isoform mRNA was surprisingly found to increase in decidualisation in primary hESC on day 3 but was found to be similar to the proliferative controls at day 6 of stimulation (**Figure 6.3B**). Similarly, sFlt-1-e15a mRNA expression in St-T1b cells was found to be significantly decreased from 24 h of stimulation with MM1 medium (**Figure 6.4A**) and at 3 and 6 days compared to control (**Figure 6.4B**), whereas, the sFlt-1-i13 mRNA expression significantly increased ($p<0.01$) at day 3 and day 6 of *in vitro* decidualisation in St-T1b cells (**Figure 6.4 C&D**). Collectively, these results indicate that sFlt-1 secretion is significantly down-regulated with hESC decidualisation.

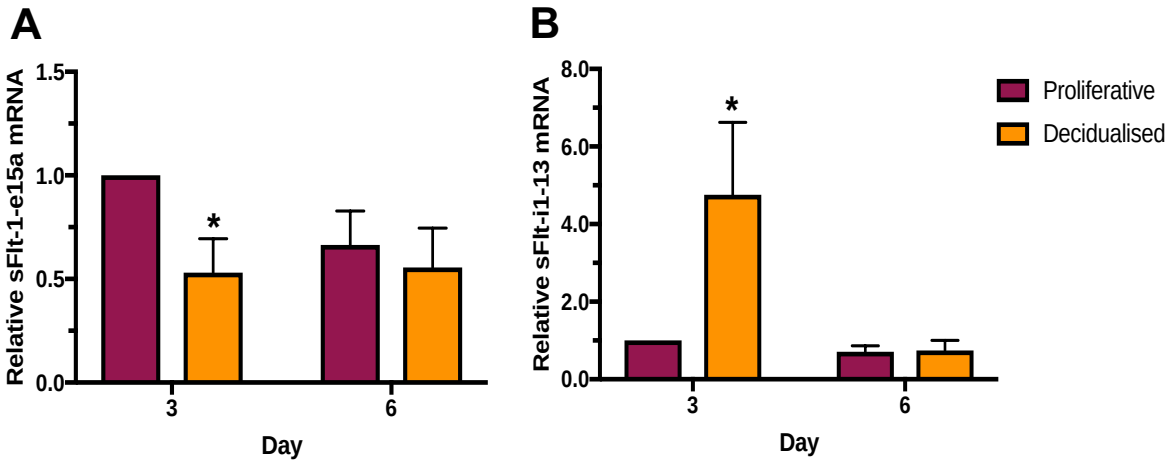

Figure 6.3: Changes in sFlt-1 mRNA isoform expression in primary hESC during decidualisation. Primary hESC were incubated in E2 or MM1 medium, over 6 days and RNA lysates were harvested after 3 and 6 days. Real-time qPCR analysis showing relative **(A)** sFlt-1-e15a and **(B)** sFlt-1-i13 mRNA expression normalised to β-actin. Results are the mean (+/- SEM) of 5 experiments and analysed using an unpaired t-test; *$p<0.05$; **$p<0.01$; ***$p<0.001$.

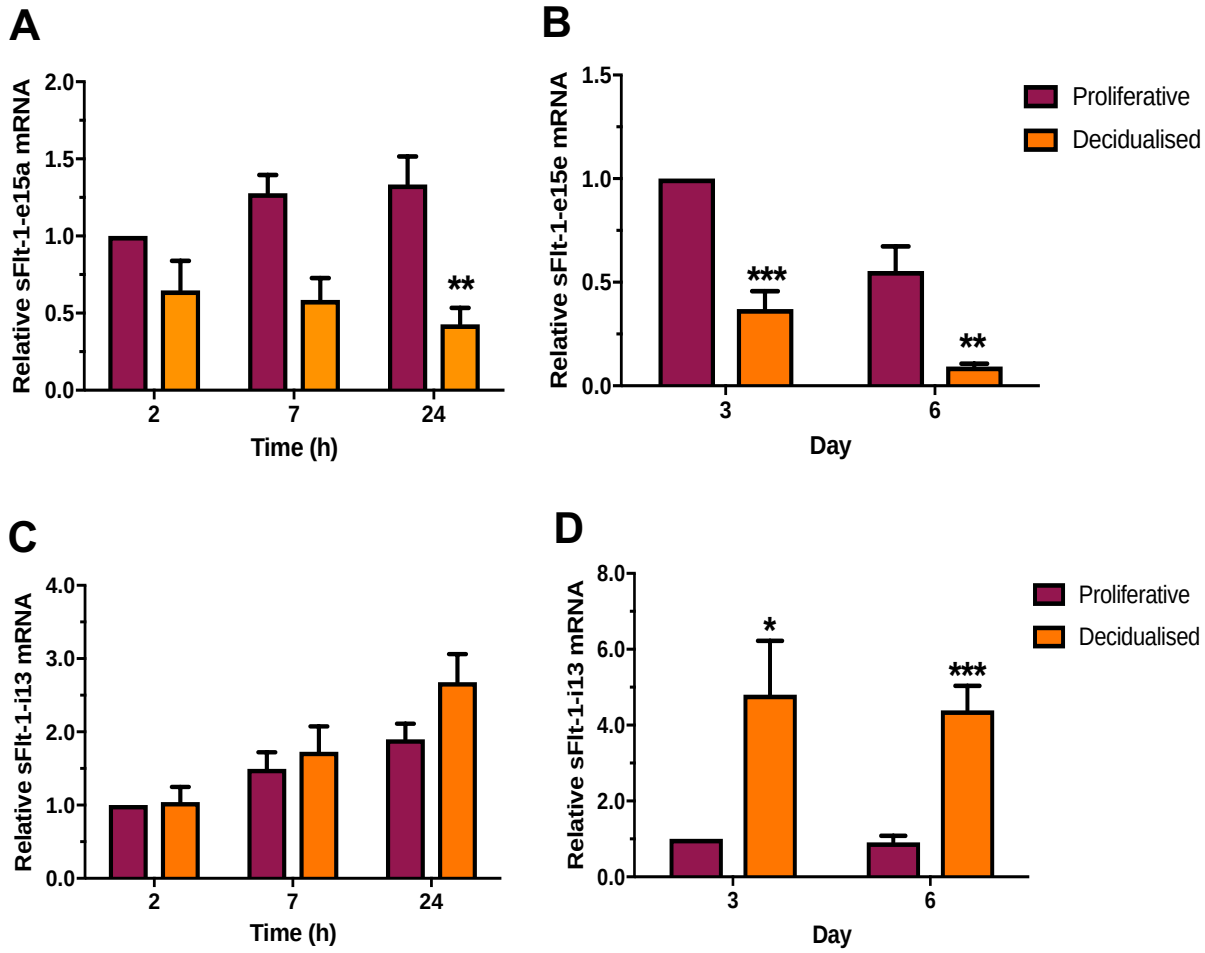

Figure 6.4: Changes in sFlt-1 mRNA isoform expression in St-T1b cells during decidualisation. St-T1b cells were incubated in E2 or MM1 medium, over 6 days and RNA lysates were harvested within 24 h and longer term (3 and 6 days). Real-time qPCR analysis showing relative **(A, B)** sFlt-1-e15a and **(C, D)** sFlt-1-i13 mRNA expression normalised to β-actin. Results are the mean (+/- SEM) of 3 experiments and analysed using an unpaired t-test; *p<0.05; **p<0.01; ***p<0.001.

6.2.2 Does FOXO1 regulate sFlt-1 expression and release in hESC?

6.2.2.1 Effect of FOXO1 knock-down on sFlt-1 expression and secretion in hESC

FOXO1 is known to regulate Flt-1 in endothelial cells (Potente *et al.*, 2005). To determine whether FOXO1 or FOXO3A regulate sFlt-1 expression and release during hESC decidualisation, primary hESC and St-T1b cells were transfected with FOXO1, FOXO3A or control siRNAs using Viromer Blue reagent overnight followed by 24 h stimulation with E2

or MM1 medium. sFlt-1-e15a mRNA expression was significantly suppressed following FOXO1 knock-down in both primary hESC (**Figure 6.5A**) and St-T1b cells (**Figure 6.6A**) following 24 h stimulation with MM1 medium. Surprisingly, there were no significant changes in sFlt-1-i13 isoform mRNA in either primary hESC (**Figure 6.5B**) or St-T1b cells (**Figure 6.6B**) following FOXO1 knock-down. In primary hESC following FOXO3A knock-down, sFlt-1-e15a mRNA expression increased (**Figure 6.5A**) in the proliferative cells. In contrast, sFlt-1-e15a and sFlt-1-13 mRNA expression did not change in St-T1b cells following FOXO3A knock-down (**Figure 6.6 A&B**). Furthermore, levels of total sFlt-1 secretion, assayed by ELISA, were also suppressed in the primary hESC (**Figure 6.5C**) and St-T1b cells (**Figure 6.6C**) following FOXO1 knock-down. Consistent with these findings, sFlt-1-e15a protein expression was also significantly decreased in primary hESC (**Figure 6.5E**) and St-T1b cells (**Figure 6.6E**) following FOXO1 knock-down, whereas, FOXO3A knock-down did not affect the sFlt-1 protein levels.

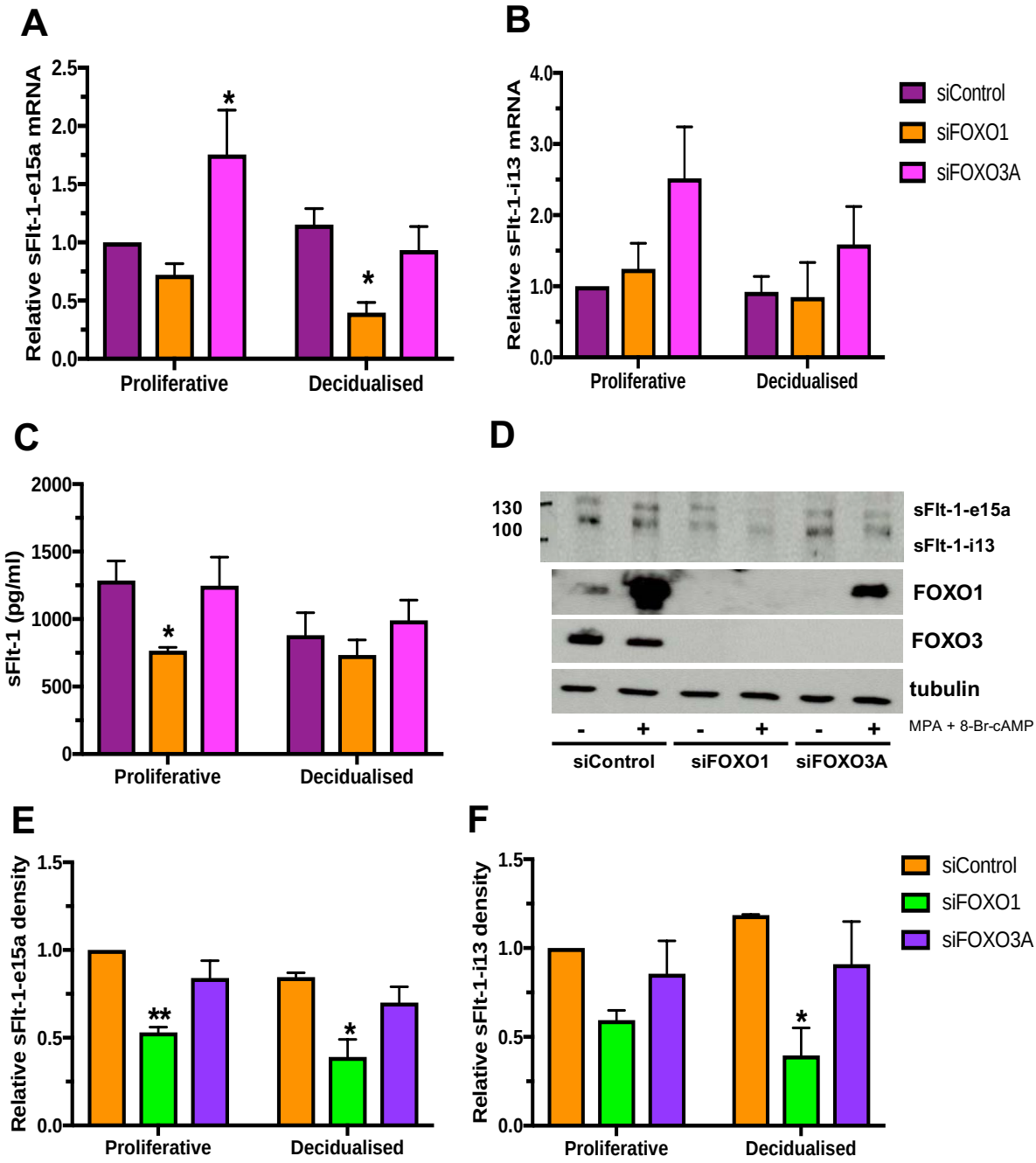

Figure 6.5: Effect of FOXO1 knock-down on sFlt-1 expression in primary hESC decidualisation. Primary hESC were plated on 6-well plates overnight and transfected with siRNAs targeting FOXO1 (siFOXO1), or FOXO3A (siFOXO3A), or control (siControl) overnight followed by stimulation with E2 or MM1 medium for 24 h. Real-time qPCR analysis of **(A)** sFlt-1-e15a and **(B)** sFlt-1-i13 mRNA normalised to β-actin. **(C)** Total sFlt-1 protein secretion in hESC supernatants by ELISA. (**D**) Representative Western blots showing sFlt-1 protein with tubulin as a loading control. Densitometric analysis of relative **(E)** sFlt-1-e15a and **(F)** sFlt-i13 protein levels normalised to tubulin. Results are the mean (+/- SEM) of 3 experiments and analysed using two-way ANOVA; *p<0.05; **p<0.01; ***p<0.001.

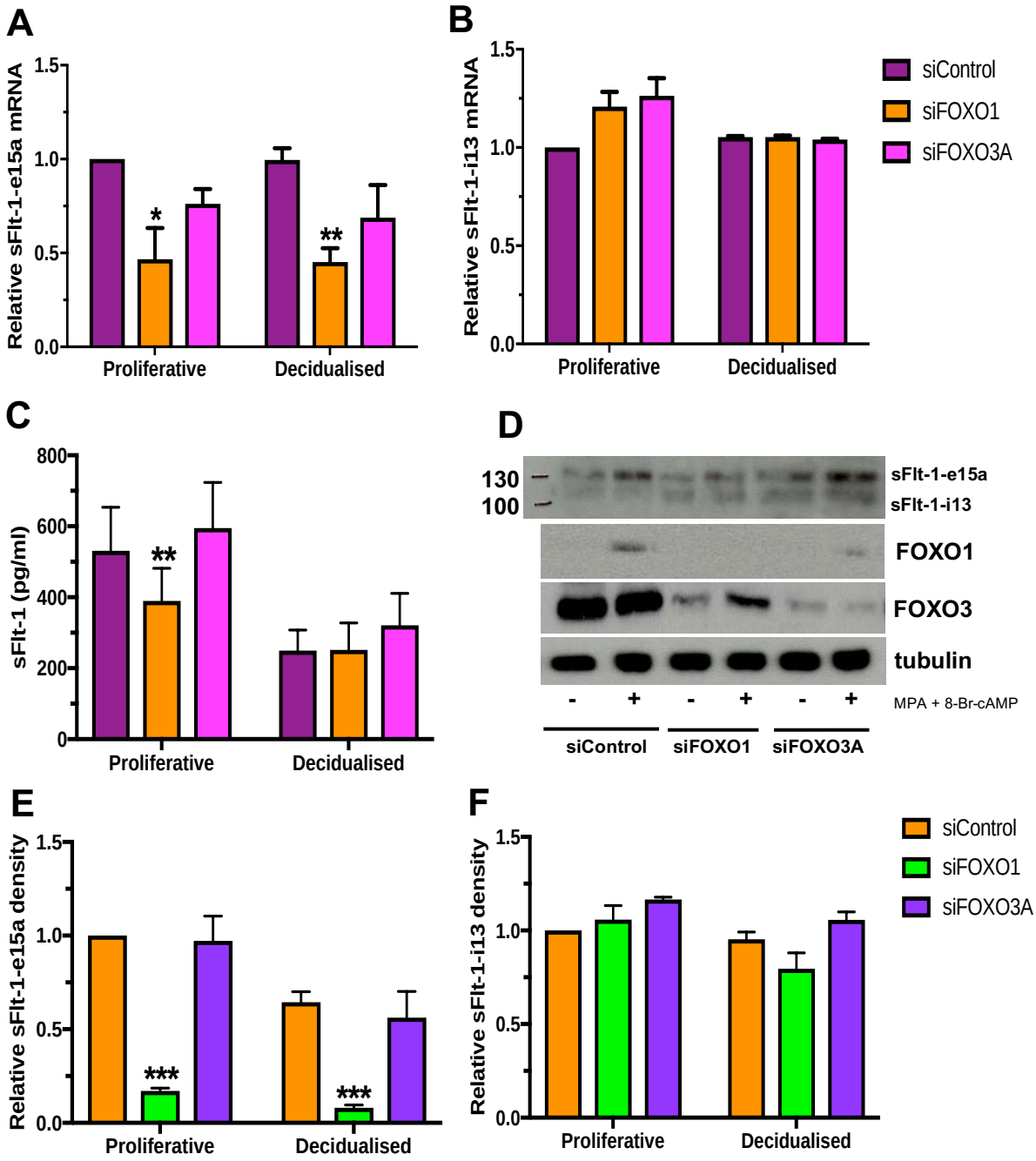

Figure 6.6: Effect of FOXO1 knock-down on sFlt-1 expression in St-T1b cell decidualisation. St-T1b cells were plated on 6-well plates overnight and transfected with siRNAs targeting FOXO1 (siFOXO1), FOXO3A (siFOXO3A), or control (siControl) overnight followed by stimulation with either E2 or MM1 medium for 24 h. Real-time qPCR analysis of **(A)** sFlt-1-e15a and **(B)** sFlt-1-i13 mRNA normalised to β-actin. **(C)** Total sFlt-1 protein secretion in St-T1b cell supernatants by ELISA. (**D**) Representative Western blots of FOXO1, FOXO3A and sFlt-1 protein with Tubulin as control. Densitometric analysis of relative **(E)** sFlt-1-e15a and **(F)** sFlt-1-i13 protein levels normalised to tubulin. Results are the mean (+/- SEM) of 3 experiments and analysed using two-way ANOVA; *p<0.05; **p<0.01; ***p<0.001.

6.2.2.2 FOXO1 over-expression increases sFlt-1 expression

St-T1b cells were plated at a density of 2.5 x 10^5 cells per well on a 6-well plate overnight. The cells were then transduced with recombinant adenovirus expressing HA-tagged murine FoxO1 (Ad-FoxO1) or empty control virus (Ad-CMV) for 24 h and incubated in E2 medium for another 24 h prior to harvesting. The cell lysates were harvested for real-time qPCR and Western blotting. Successful viral transduction was confirmed by real-time qPCR and Western blotting as described previously for the HA-tagged FoxO1 (*see* **Figure 4.6B**) which showed a large increase of mouse FoxO1 mRNA and protein expression in cells treated with Ad-FoxO1 (*see* **Section 4.2.3.2)**. We found that sFlt-1-e15a mRNA was significantly increased following FoxO1 over-expression (**Figure 6.7A**). Interestingly, no significant change of sFlt-1-i13 isoform mRNA expression was observed in FoxO1 over-expressing cells (**Figure 6.7B**). Total sFlt-1 protein secretion was also measured by ELISA in the cell supernatants. Consistent with the sFlt-1-e15a mRNA results, total sFlt-1 protein secretion was increased with Ad-FoxO1 transduction of hESC (**Figure 6.7C**).

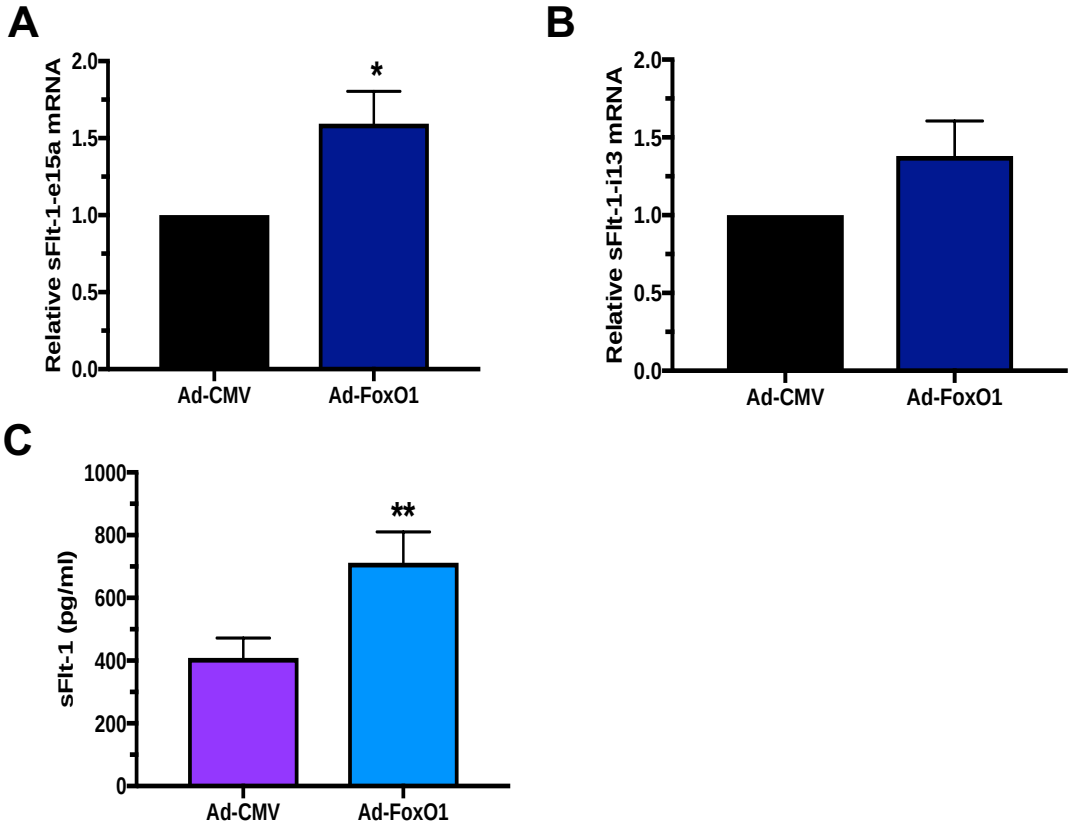

Figure 6.7: FOXO1 over-expression in hESC promotes sFlt-1 expression and secretion. St-T1b cells were transduced with recombinant adenoviruses encoding FoxO1 (Ad-FoxO1), or empty virus control (Ad-CMV) overnight and incubated in fresh E2 medium for another 24 h prior harvesting. Real-time qPCR was used to measure the mRNA expression of **(A)** sFlt-1-e15a, and **(B)** sFlt-1-i13 normalised to β-actin. **(C)** The sFlt-1 protein secretion on FoxO1 over-expression was assessed by sFlt-1 ELISA in cell supernatants. Results are the mean (+/- SEM) of 3 experiments and analysed using an unpaired t-test; *p<0.05; **p<0.01; ***p<0.001.

6.2.3 Changes in Flt-1 expression in hESC during decidualisation

To determine whether full-length Flt-1 was expressed in hESC, qPCR was used to determine the presence of Flt-1 mRNA during hESC decidualisation. Primary hESC and St-T1b cells were stimulated with E2 or MM1 medium over 6 days and RNA was purified. Levels of Flt-1 mRNA were significantly increased in both primary hESC **(Figure 6.8A)** and St-T1b cells **(Figure 6.8B)** after 6 days decidualisation.

Indirect flow cytometry was used to determine the presence of Flt-1 receptor on the surface of hESC; St-T1b cells were grown to confluence and treated with E2 or MM1 medium for 6 days. The cells were fixed without permeabilisation followed by staining with anti-Flt-1 antibody, or an irrelevant IgG control antibody staining. Propidium iodide was used to counterstain the DNA. Surface Flt-1 receptor was detected in both proliferative and decidualised cells (**Figure 6.9 A&B**). There was a slight shift of the peaks indicating the presence of more surface Flt-1 receptor on proliferative cells (**Figure 6.9C**).

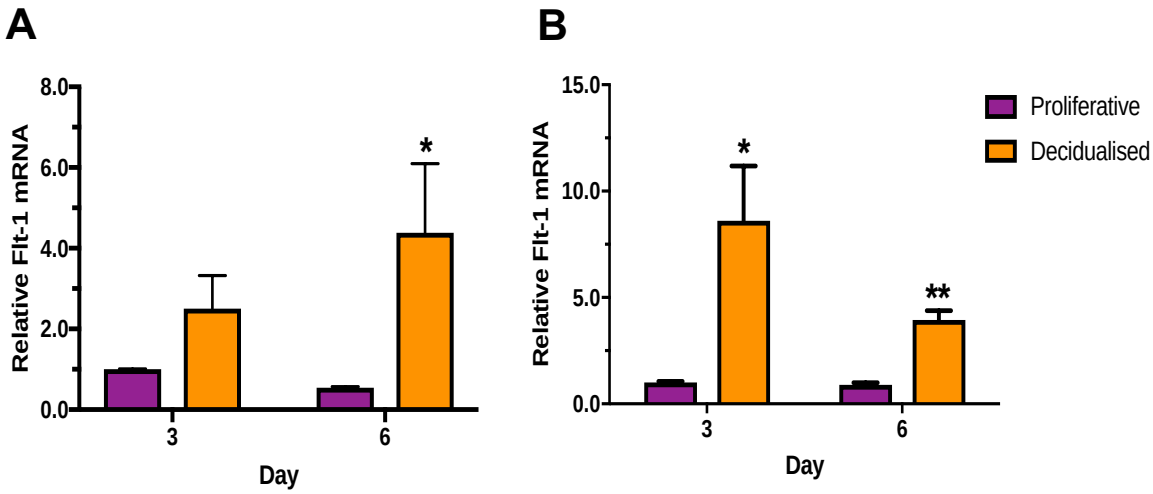

Figure 6.8: Flt-1 expression increases in decidualised hESC. Primary hESC and St-T1b cells were incubated in E2 or MM1 medium and RNA lysates harvested after 3 and 6 days. Real-time qPCR was used to determine the Flt-1 mRNA expression normalised to β-actin in **(A)** primary hESC and **(B)** St-T1b cells, respectively. Results are the mean (+/- SEM) of 3 experiments and analysed using an unpaired t-test; *p<0.05; **p<0.01; ***p<0.001.

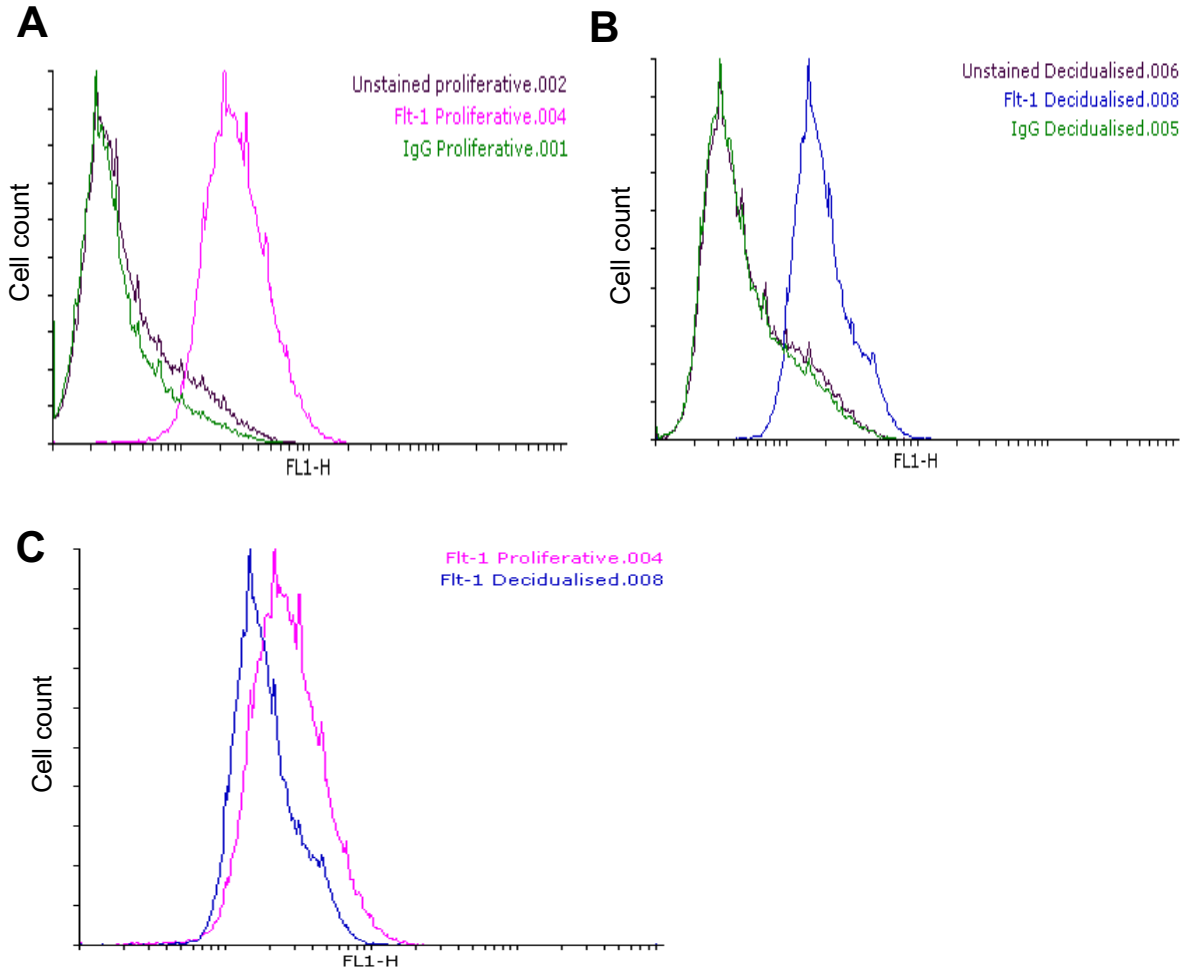

Figure 6.9: Expression of Flt-1 on hESC by FACS. St-T1b cells were grown to confluence and stimulated with E2 or MM1 medium, for 6 days. The cells were fixed and stained with anti-Flt-1 or control IgG antibodies and then incubated with either Alexa Fluor 488 (Flt-1) antibody or Alexa Fluor 594 (control antibody). Representative scans of surface Flt-1 expression on **(A)** proliferative, and **(B)** decidualised St-T1b cells as indicated. **(C)** Representative overlay scans of proliferative and decidualised cells.

6.2.4 *Flt-1* promoter activity during hESC decidualisation

In order to determine whether the *Flt-1* gene transcription is activated by decidualisation, *Flt-1* promoter activity was examined by dual luciferase assays. St-T1b cells were co-transfected with a 1.8 kb *Flt-1* promoter luciferase-reporter construct (p*Flt-1*-Luc) and the pRL-CMV control plasmid. The cells were stimulated with E2 or MM1 medium for 24 h and the firefly luciferase activity normalised to pRL-CMV Renilla activity to determine the

relative *Flt-1* promoter activity. Incubation of St-T1b cells in MM1 medium containing 8-Br-cAMP was found to increase the activity of Flt-1-Luc by 2-fold which is consistent with the Flt-1 mRNA results (**Figure 6.10**).

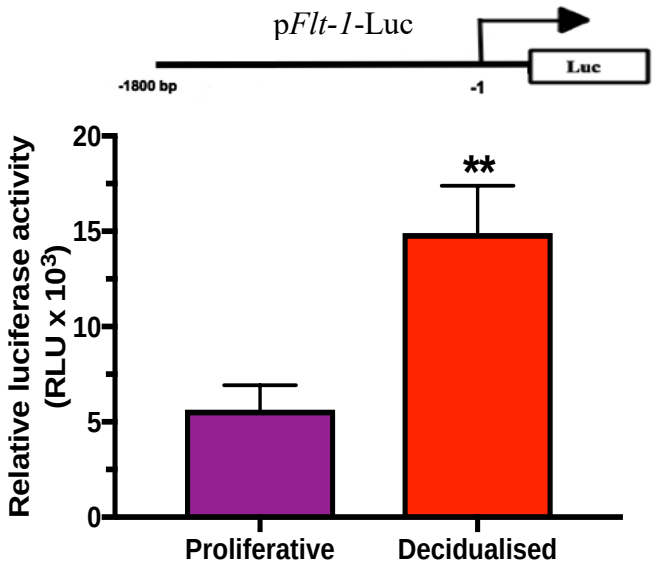

Figure 6.10: Activity of *Flt-1* promoter increases in hESC during decidualisation. Relative *Flt-1* promoter activity determined by using a 1.8 kb *Flt-1* promoter luciferase-reporter construct (p*Flt-1*-Luc). Following transfection cells were stimulated with E2 or MM1 medium for 24 h and the firefly luciferase readings normalised to Renilla activity. Results are the mean (+/- SEM) of 3 experiments and analysed using unpaired t-test; *p<0.05, **p<0.01, *** p<0.001.

6.2.5 Flt-1 expression is regulated by FOXO1 transcription factors

FOXO1 has been shown to regulate the *Flt-1* promoter in endothelial cells (Roupé *et al.*, 2014; Potente *et al.*, 2005). Therefore, the binding of FOXO1 to the *Flt-1* promoter in hESC was examined. St-T1b cells were co-transfected with p*Flt-1*-Luc with constitutively active FOXO1 plasmids (caFOXO1) or FOXO3A (caFOXO3A) (Ramaswamy *et al.*, 2002) or the pcDNA3.1 parent plasmid as a control. The p*Flt-1*-Luc readings were normalised to the pRL-CMV Renilla activity to determine the relative *Flt-1* promoter activity. *Flt-1* promoter

activity increased in cells over-expressing caFOXO1 whilst, there was no significant change in cells co-transfected with caFOXO3A (**Figure 6.11A**).

To further explore the effect of FOXO1 and FOXO3A transcription factors on *Flt-1* expression, St-T1b cells were co-transfected with p*Flt-1*-Luc with either FOXO1 or FOXO3A siRNAs. FOXO1 knock-down significantly decreased the *Flt-1* promoter activity in both proliferative and decidualised cells, however, loss of FOXO3A did not affect the pFlt-1-Luc promoter activity (**Figure 6.11B**).

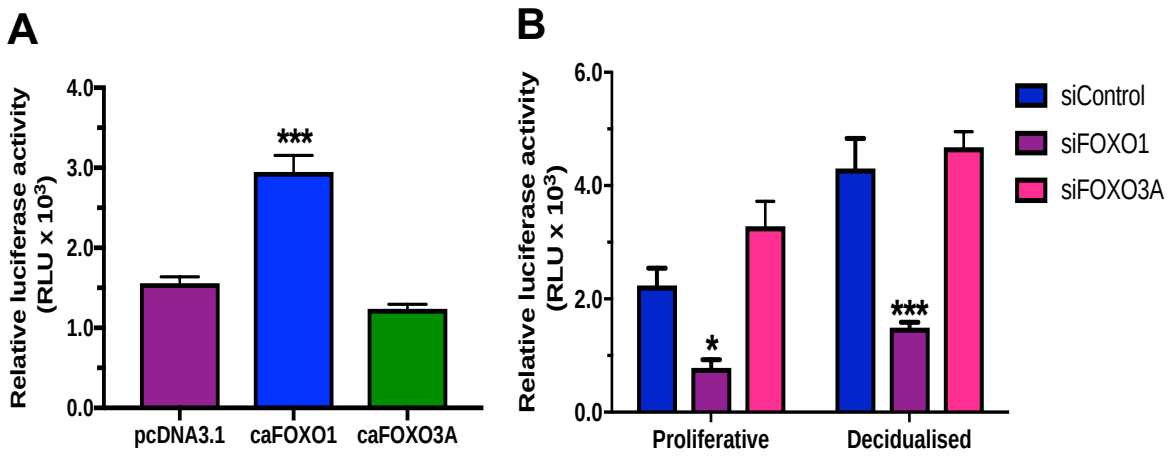

Figure 6.11: FOXO1 transcription factor regulates *Flt-1* promoter activity in hESC. (A) St-T1b cells were plated on 12-well plates overnight and co-transfected with a 1.8 kb *Flt-1* promoter luciferase-reporter construct (p*Flt-1*-Luc) and constitutively active FOXO1 (caFOXO1), FOXO3A (caFOXO3A) plasmids or pcDNA3.1 as a control for 24 h. **(B)** The St-T1b cells were co-transfected with pFlt-1-Luc and siRNAs targeting FOXO1 (siFOXO1), or FOXO3A (siFOXO3A), or control (siControl) for 24 h followed by 24 h treatment with E2, or MM1 medium. The firefly luciferase readings were normalised to Renilla activity. Results are the mean (+/- SEM) of 3 experiments and analysed using one-way and two-way ANOVA; *p<0.05; **p<0.01; ***p<0.001.

6.2.6 FoxO1 drives Flt-1 expression in MEFs

In order to extend our findings and confirm FoxO1 regulation of *Flt-1* in fibroblasts, MEFs isolated from the floxed FoxO transgenic mice were transduced with a recombinant

adenovirus encoding Cre recombinase (Ad-Cre) to induce Cre-mediated knock-out of FoxOs in the cells. MEFs were grown to confluence and infected with Ad-Cre, or Ad-CMV (control) at MOI of 50 for 24 h prior to being seeded onto 6-well-plates. The expression of Cre-recombinase in the Ad-Cre treated cells were confirmed by RT-PCR and the deletion of FoxO1 and FoxO3a were confirmed by PCR and Western blotting as shown previously in **Figure 5.10**. *Flt-1* expression increased by more than 2-fold at 24 h following treatment with 8-Br-cAMP (**Figure 6.12A**). However, the cAMP-mediated increase in Flt-1 mRNA was blunted following FoxO1 knock-out indicating that FoxO1 regulates *Flt-1* expression in these cells (**Figure 6.12A**).

In addition, MEFs were co-transfected with p*Flt-1*-Luc and caFOXO1, caFOXO3a plasmids, or the pcDNA3.1 as a control. The MEFs were found to behave like the St-T1b cells, as the *Flt-1* activity was increased with caFOXO1 over-expression, while no effect was observed with caFOXO3a (**Figure 6.12B**).

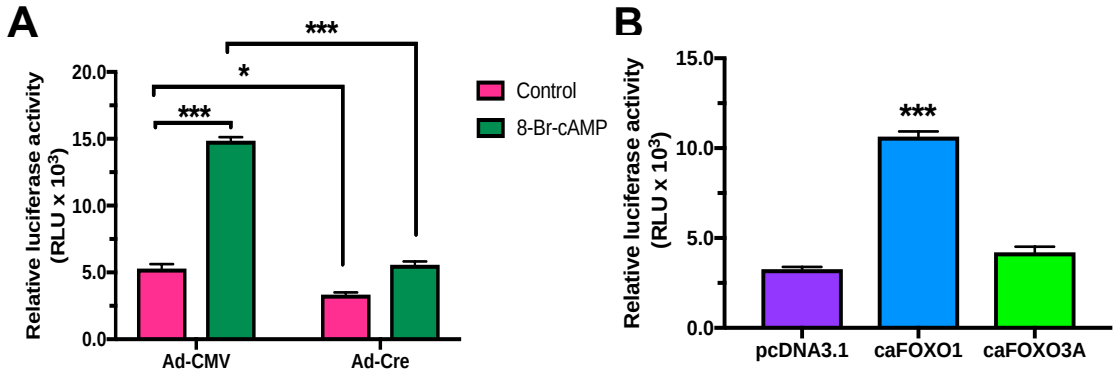

Figure 6.12: FoxO1 increases *Flt-1* promoter activity in MEFs. (A) MEFs were transduced with adenovirus encoding Cre recombinase (Ad-Cre) or empty control virus (Ad-CMV) overnight and then transfected with a 1.8 Kb *Flt-1* promoter luciferase-reporter construct (p*Flt-1*-Luc) overnight followed by stimulation with DMEM medium supplemented with 2% FBS (control), or 0.25 mM 8-Br-cAMP for 24 h. **(B)** MEFs were plated on 12-well plates overnight and co-transfected with p*Flt-1*-Luc and with constitutively active mutant FOXO1 (caFOXO1) or FOXO3A (caFOXO3A) plasmids or pcDNA3.1 as a control for 24 h. The firefly luciferase readings were normalised to Renilla activity. Results are the mean (+/- SEM) of 3 experiments and analysed using one-way ANOVA; *p<0.05, ** p<0.01, ***p<0.001.

6.2.7 FOXO1 directly regulates *sFlt-1/Flt-1* promoter activity in hESC

We have shown that FOXO1 can activate *Flt-1* promoter reporter activity; however, it is not known whether FOXO1 can bind directly to *Flt-1* promoter to regulate its expression in hESC. In order to address this question, ChIP assays were performed in decidualised St-T1b cells. The cells were treated with MM1 medium for 6 days and then harvested for ChIP. The chromatin was fragmented by sonication and immunoprecipitated with anti-FOXO1 (H-128, Santa Cruz) and anti-FOXO3A (ab12126, Abcam) antibodies or an irrelevant rabbit IgG control antibody to determine the FOXO1 and FOXO3A binding to potential FHRE sequences in the *Flt-1* promoter in St-T1b incubated with E2 or MM1 medium.

The *Flt-1* promoter sequence was analysed using the UCSC genome browser, Genomatix MatInspector and rVISTA to look for putative FHRE binding-sites (**Figure 6.13**). The

degree of conservation of the identified sites was analysed following alignment of a ~3 kb of the *Flt-1* gene sequence upstream of the start codon of several species using CLUSTAL Omega (Sievers *et al.*, 2011) (**Figure 6.14**). Various sets of primers were designed from the human *Flt-1* promoter sequence using Primer3 and Primer-BLAST (**Figure 6.13**). Each primer set amplifies a PCR fragment approximately 120 bp nucleotides in length flanking the FHRE site (**Figure 6.14**). In addition, a set of primers amplifying a non-transcribed intergenic region (NegC) was used as an internal background control. All the primers were tested on the genomic DNA to ensure efficient amplification of the target sequence before use on the ChIP material. The results of the ChIP were expressed as a percentage of the 'input' DNA to normalise them according to the amount of chromatin input used in each experiment and the fold enrichment was calculated by normalising it to the NegC result. We found that all the three sequences containing the potential FOXO sites were enriched relative to the input chromatin (**Figure 6.15**), indicating FOXO1 binds directly to the *Flt-1* promoter at all three sites. Whereas, there was no enrichment of FOXO3A binding to these regions supporting our results showing that unlike VEGF, *Flt-1* is not regulated by FOXO3A **(Figure 6.15).**

aatatcattgattagcatcttagattataaagattgtttcagctgtccatcaaatacctgttctggctttacaga
cacaatgtagattcattgctggcagcaggtttggaaagtgttgtctctttatgagttaaaaatatcaaaatggca
tttgaaaaaatgtattagcaaattaaacctttgtacatggtactatggaccactttcccccagagtcaaatgtgt
gtc*tctcctgagaagccctcctt*gggttttccctgccaataaatgtgcctttacttctctgagctgatggagga**c**
taaacacccctccagcactggaatgccgg*tcctgcagccacttcaagt*gtccaccttcttatcacagtccaagcc
ctttagaaggcaaagatgatggctctccatcagtgttttcagccctaacccaatgcctggcccctgttgaatgct
gcagaaggacaatgctgacagcttctccttgaaagagggtgtgggagtgacaagcagctctcaggtgagaccaac
agacactgtggctccgcacgtatgtcccaggctgtgttctgggctgggggaccagcaaggagaaggatcagctgt
ccgcttccagctgttctgagggatgatgctgtgggttttagaggaggcaggggtgcgggaggcagagaaaggcgc
caggaagagtggtgaggagaactggaaaaacagaaagcgctggtgaagccagcaggcaagcaatgactccggcag
tcttccttgcctctgaagcagaagggatccagggacagttagtggctcaggtcctgcggctccaggtgcccagac
gtgcatttcctgtgtggagtggccggggcctctccttggtgtgcagcccagaaatgtggcaactttgggttaccc
aaccttcctaggcggggaggtagtccagtccttcaggaagagtctctggctccgttcaa*gagccatcacagtccc*
*ttgt*attacatccctctgacgggttccaatagga**ctatttttca**aatctgcggtatttaca*gagacaagactggg*
*ctgctc*cgtgcagccaggacgacttcagcctttgaggtaatggagacataattg**aggaacaacgtggaatt**agtg
tcatagcaaatgatctagggcctcaagttaatttcagccggttgtggtcagagtcactcatcttgagtagcaagc
tgccaccagaaagatttctttttcgagcatttagg*gaataaag*ttcaagtgccctgcgctt*ccaagttgcaggag*
*cagttt*cacgcctcagcttttaaaggtatcataatgttattcc**ttgttttgcttct**aggaagcagaag*actgag*
*gaaatgacttgggc*gggtgcatcaatgcggccgaaaaagacacggacacgctcccctgggacctgagctggttcg
cagtcttcccaaaggtgccaagcaagcgtcagttcccctcaggcgctccaggttcagtgccttgtgccgagggtc
tccggtgccttcctagacttctcgggacagtctgaaggggtcaggagcggcgggacagcgcgggaagagcaggca
aggggagacagccggactgcgcctcagtcctccgtgccaagaacaccgtcgcggaggcgcggccagcttcccttg
gatcggactttccgcccctagggccaggcggcggagcttcagccttgtcccttccccagtttcgggcggccccca
gagctgagtaagccgggtggagggagtctgcaaggatttcctgagcgcgatgggcaggaggaggggcaagggcaa
gagggcgcggagcaaagaccctgaacctgccggggccgcgctcccgggcccgcgtcgccagcacctccccacgcg
cgctcggccccgggccacccgccctcgtcggcccccgcccctctccgtagccgcagggaagcgagcctgggagga
agaagagggtaggtggggaggcggatgaggggtgggggacccccttgacgtcaccagaaggaggtgccggggtagg
aagtgggctggggaaaggttataaatcgcccccgccctcggctgctcttc**A**TCGAGGTCCGCGGGAGGCTCGGAG
CGCGCCAGGCGGACACTCCTCTCGGCTCCTCCCCGGCAGCGGCGGCGGCTCGGAGCGGGCTCCGGGGCTCGGGTG
CAGCGGCCAGCGGGCGCCTGGCGGCGAGGATTACCCGGGGAAGTGGTTGTCTCCTGGCTGGAGCCGCGAGACGGG
CGCTCAGGGCGCGGGGCCGGCGGCGGCGAACGAGAGGACGGACTCTGGCGGCCGGGTCGTTGGCCGCGGGGAGCG
CGGGCACCGGGCGAGCAGGCCGCGTCGCGCTCACC **ATG GTC AGC TAC TGG**

+1

Figure 6.13: Human *Flt-1* promoter and 5' UTR sequences showing potential FOXO consensus binding sites. Human *Flt-1* reference sequence (NM_002019) was analysed using the UCSC genome browser, Genomatix MatInspector and rVISTA for the presence of FHRE consensus sequences and the potential FOXO binding sites are highlighted (yellow) and HIF-1α binding site (blue). The transcription start codon (ATG) and coding region is in bold and the 5' UTR untranslated sequences from the transcription start site (red) are in capitals. The position of the primers designed to amplify regions containing the FHRE sites are underlined and in italics.

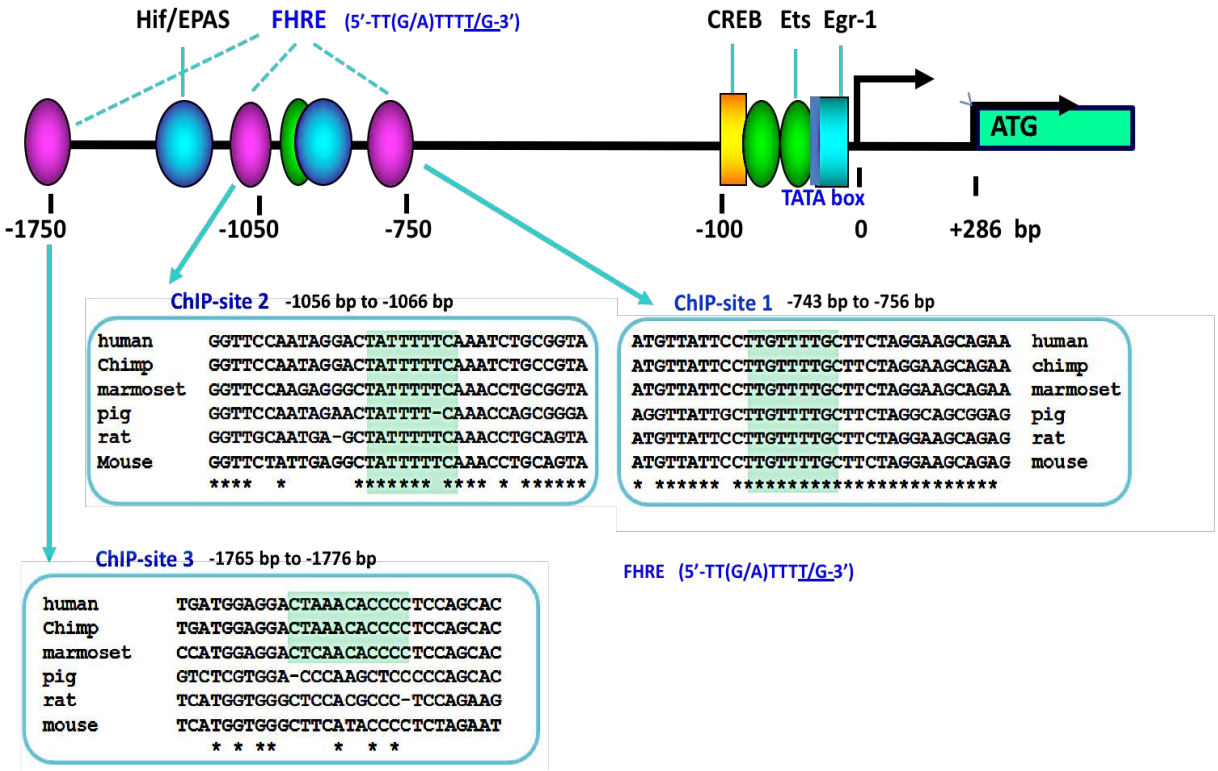

Figure 6.14: FHRE consensus sites in the *Flt-1* gene promoter. Schematic representation of the human *Flt-1* promoter showing the candidate putative FHRE consensus sequences and other characterised transcription factor binding sites identified previously (Takeda *et al.*, 2004; Jin *et al.*, 2009). The boxes show the degree of conservation of the FHRE sites determined using multiple sequence alignment with CLUSTAL-Omega.

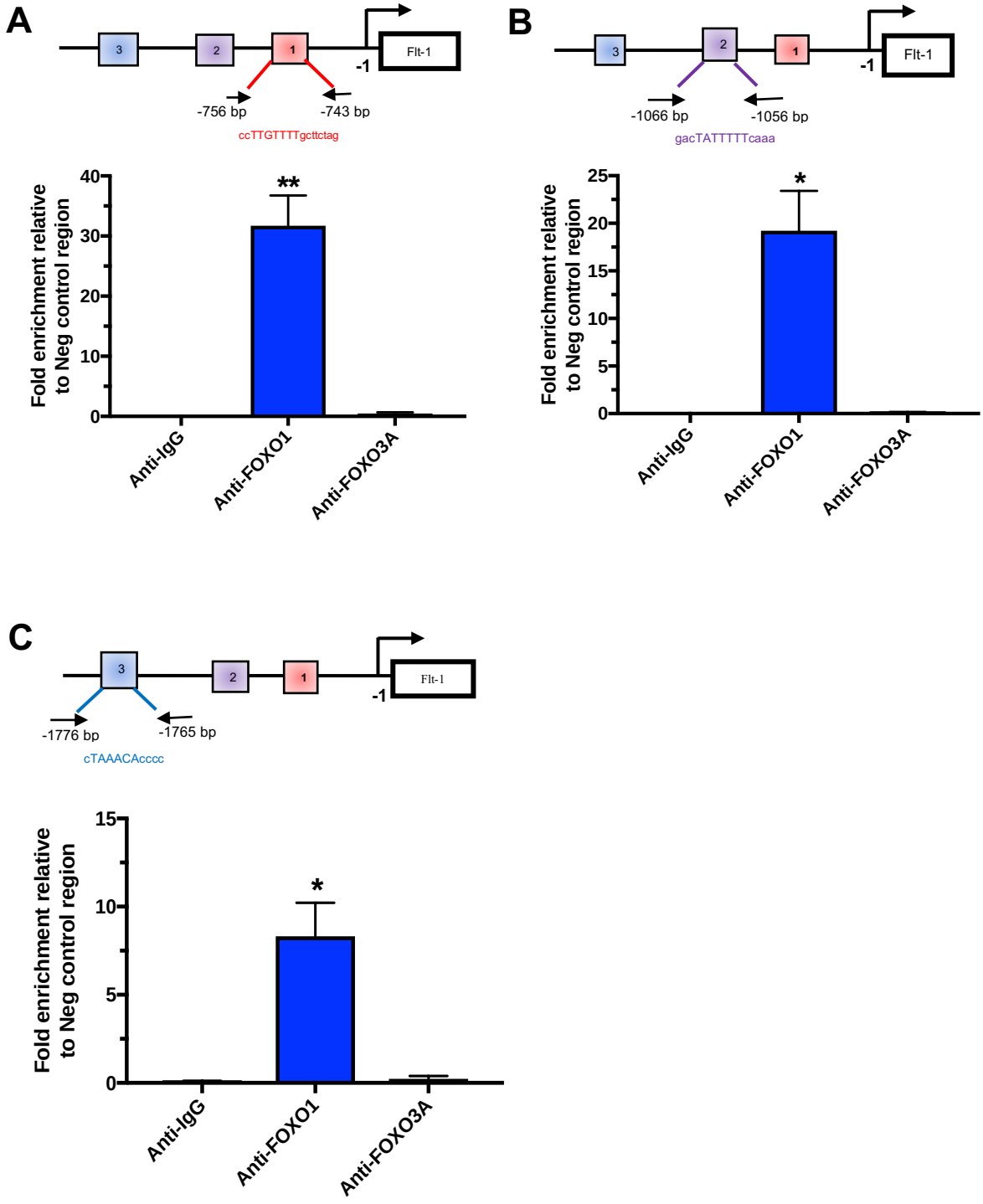

Figure 6.15: FOXO1 binds directly to *Flt-1* promoter in decidualised hESC. ChIP assays were performed in St-T1b cells decidualised for 6 days and immunoprecipitated with rabbit anti-FOXO1 antibody, FOXO3A antibody or, control IgG and the % Input was used to determine the enrichment of *Flt-1* binding at **(A)** ChIP-1, **(B)** ChIP-2, and **(C)** ChIP-3 binding regions normalised to NegC region by real-time qPCR. Results are mean (+/- SEM) of 2 independent of ChIP experiments and analysed using one-way ANOVA; *p<0.05; **p<0.01.

6.3 DISCUSSION

The level of sFlt-1 expression in ESC may potentially influence fertility, embryo implantation, placentation and early pregnancy. sFlt-1 acts to block VEGF activity and so may affect angiogenesis and other functions such as trophoblast and leukocyte migration (Li *et al.*, 2015) into the endometrium that are required for establishing a normal pregnancy. Little is known of the expression and regulation of Flt-1/sFlt-1 in the hESC. Krussel *et al.* (1999) found peak sFlt-1 mRNA expression was detected in endometrial epithelial and stromal cells isolated from the mid- to late- proliferative phase of the menstrual cycle. sFlt-1 production was reported to be inhibited by E2 in proliferative hESC (Okada *et al.,* 2010) and thrombin has been shown to induce sFlt-1 expression during stromal cell decidualisation (Lockwood *et al.,* 2007).

6.3.1 Down-regulation of sFlt-1 in hESC decidualisation

In the present study, proliferative hESC are capable of producing relatively high levels of sFlt-1 and that total sFlt-1 production was markedly reduced in decidualised hESC compared to proliferative cells supporting the earlier studies in hESC isolated from an endometrial tissues from healthy women in different phases of the menstrual cycle showing that sFlt-1 mRNA expression peaks during mid-proliferative phase and decreases in secretory phase (Krussel *et al.*, 1999). While the present studies were being performed, a study was published showing sFlt-1 is produced by hESC and reduced by decidualisation (Cottrell *et al.,* 2017). Cottrell *et al.* (2017) showed that total sFlt-1 expression both at the RNA and protein level is down-regulated with hESC decidualisation. However, Cottrell *et al.* (2017) did not look into the regulation and expression of sFlt-1 mRNA splice variants. The two predominant sFlt-1 isoforms, sFlt-1-i13 and sFlt-1-e15a, were investigated in the present study. sFlt-1-e15a is a primate-specific sFlt-1 isoform, mainly produced by non-endothelial cells types,

for example, smooth muscle cells, dendritic cells and epithelial cells (Thomas *et al.*, 2009; Sela *et al.*, 2009; Jebbink *et al.,* 2011). Sela *et al.* (2009) showed that endothelial cells produce mainly sFlt-1-i13. Furthermore, Jebbink *et al.* (2011) investigated sFlt-1 mRNA splice variant expression in 21 different human tissues, including HUVEC and human brain microvascular endothelial cells, and showed that the sFlt-1-e15a isoform is the predominant isoform expressed in placenta. Both sFlt-1-e15a and sFlt-1-i13 were found to be produced in both primary hESC and St-T1b cells. Consistent with the sFlt-1 ELISA results, Western blotting showed that sFlt-1-i13 and sFlt-1-e15a decreased with decidualisation in hESC. However, sFlt-1-i13 mRNA expression was found to increase during decidualisation in primary hESC and St-T1b cells. Furthermore, sFlt-1-i13 mRNA expression also increased in primary hESC stimulated with MM1 medium for 3 days but remained at similar levels as proliferative hESC on day 6 of stimulation. This difference in the sFlt-1-i13 mRNA and protein expression results may be due to the action of miRNAs which have been shown to be up-regulated during decidualisation (Aoyagi *et al.*, 2017, Tochigi *et al.*, 2017).

Fan *et al.* (2014) demonstrated that endometrium-specific over-expression of VEGF in mouse ESC, using viral vectors, triggers excess production of sFlt-1 (Fan *et al.,* 2014). Furthermore, Xiao *et al.* (2018) also showed that VEGF regulates sFlt-1 and sFlt-1-e15a mRNA and protein expression in human choriocarcinoma (JEG3) and human trophoblast (HTR-8/SVneo) cell lines. According to these findings, it is also a possibility that up-regulation of the sFlt-1-i13 isoform mRNA is driven in an autocrine manner by increased VEGF expression during hESC decidualisation. The preliminary results showed that both sFlt-1-e15a and sFlt-1-i13 mRNA were decreased following VEGF knock-down St-T1b cells (**Appendix F**) which would be consistent with the previous studies (Fan *et al.*, 2014; Xiao *et al.*, 2018). We also do not know the effect of exogenous VEGF or PIGF on sFlt-1-

i13 isoform expression in hESC during decidualisation, therefore, further investigation of the effect of VEGF on sFlt-1-i13 expression in hESC decidualisation is needed.

6.3.2 Regulation of sFlt-1/Flt-1 during hESC decidualisation

sFlt-1-e15a and sFlt-1-i13 protein levels were consistent with the total secreted sFlt-1 and found to decrease in hESC decidualisation. Whereas, sFlt-1-i13 isoform mRNA expression was more variable but increased at day 3 of decidualisation in both primary hESC and St-T1b cells. The oxygen-sensing jumonji domain containing protein 6 (JMJD6) is known to directly affect the splicing pattern of Flt-1 to produce sFlt-1 in endothelial cells (Palmer *et al.,* 2016; Boeckel *et al.,* 2011). JMJD6 hydroxylates U2AF65, a component of the splicing machinery, under normal conditions to produce the full-length membrane bound Flt-1 transcript (Boeckel *et al.,* 2011). However, hypoxia was found to decrease JMJD6 activity reducing its ability to hydroxylate U2AF65 splicing factor directing the transcription of sFlt-1 mRNA (Palmer *et al.*, 2016). Interestingly, there are different regulation patterns in sFlt-1 production by JMJD6 between endothelial and trophoblast cells. JMJD6 knock-down in endothelial cells increased both sFlt-1-i13 and sFlt-1-e15a isoforms, in contrast with sFlt-1-e15a is the only isoform significantly produced from trophoblast cells that are affected by JMJD6 knock-down (Palmer *et al.*, 2016). Also, decidualisation is a complex event with various biochemical changes and regulated by various hormones, growth factors and cytokines which may potentially affect the JMJD6 factor subsequently influencing the splicing conditions. There are no studies on the activity of JMJD6 in hESC decidualisation, therefore, further studies are needed to examine the role of JMJD6 on sFlt-1 isoforms expression in hESC.

Apart from differential JMJD6 expression affecting Flt-1 mRNA splicing, post-transcriptional regulation, or microRNAs (miRNA) might also be a factor leading to sFlt-

1/Flt-1 splicing and expression in hESC during decidualisation. miRNA are small, endogenous, and non-coding RNAs that are key regulators of gene expression, either mediating translational repression, or direct mRNA degradation (Pillai, 2005). The gain or loss of miR-221/222 function in human endothelial cells leads to changes VEGF, Flt-1 and VEGFR-2 expression (Poliseno *et al.*, 2006). A number of studies have identified the expression of miRNAs in the reproductive tract tissues including endometrial tissue in both healthy and diseased states (Chegini, 2010; Filigheddu *et al.*, 2010; Myatt *et al.*, 2010; Qian *et al.*, 2009). In addition, a number of studies have reported the expression of miRNAs in hESC during *in vitro* decidualisation (Wang *et al.*, 2016; Aoyagi *et al.*, 2017; Tochigi *et al.*, 2017). These findings raise the possibility that sFlt-1/Flt-1 mRNA expression might be differentially affected by miRNAs in hESC decidualisation. As mature miRNAs bind to their target mRNAs typically in the 3'-untranslated region (3'UTR) miRNA (Felekkis *et al.*, 2010), the alternative 3'UTRs of the Flt-1/sFlt-1 mRNAs may, therefore, represent selective targets for miRNAs. Therefore, the effect of decidual-related miRNAs on the sFlt-1 isoform expression should be investigated.

6.3.3 FOXO1 regulates sFlt-1-e15a in hESC decidualisation

The present findings found that sFlt-1-e15a isoform expression in hESC is regulated by FOXO1. The reduction of FOXO1 suppressed total sFlt-1 protein secretion and the expression of sFlt-e15a mRNA and protein. As discussed earlier, the sFlt-1 production was decreased and FOXO1 expression was increased in decidualisation. However, FOXO1 knock-down only affected sFlt-1 expression in proliferative hESC. FOXO1 activity is strongly up-regulated during decidualisation whilst sFlt-1 secretion and sFlt-1-e15a mRNA expression decreases suggesting other mechanisms are clearly responsible for the suppression of sFlt-1 during decidualisation.

6.3.4 Flt-1 receptor expression in hESC

In the present study, the Flt-1 receptor was detected on the cell surface in both proliferative and decidualised hESC. Flt-1 mRNA expression and promoter activity was found to increase initially with hESC decidualisation, but the expression level then decreased from day 3 to day 6 of stimulation supporting an earlier study in human epithelial and stromal cells isolated from a endometrial tissues from healthy women in different phases of the menstrual cycle showing that Flt-1 mRNA expression peaks during the secretory phase and then decreases to the late secretory phase (Krussel *et al.*, 1999; Jee *et al.*, 2009). Overall the fact that the Flt-1 receptor is maintained at the cell surface and sFlt-1 levels dramatically decrease suggests that decidual hESC may be more responsive to VEGF and PIGF. Although little is known about the expression of Flt-1 receptor during hESC decidualisation, there are many studies reporting the up-regulation of Flt-1 expression in the placenta leading to preeclampsia in pregnancy (Nikuei *et al.*, 2015; Andraweera *et al.,* 2012; Nishizawa *et al.*, 2011; Chung *et al.*, 2004). Therefore, it will be important to understand how changes of Flt-1 expression in hESC during decidualisation may be associated with the onset of pregnancy complications like preeclampsia.

6.3.5 FOXO1 regulates *Flt-1* in hESC

The knock-down of FOXO1 by siRNA suppressed the *Flt-1* promoter activity in hESC, whereas, no effect was observed in hESC following FOXO3A knock-down which supports previous studies in endothelial cells showing FOXO1, but not FOXO3A, regulates *Flt-1* gene expression (Potente *et al.*, 2005). Furthermore, MEFs were also used in this study to determine the effect of FOXO1 on *Flt-1* expression and we found that *Flt-1* promoter activity increased in MEFs over-expressing caFOXO1, while over-expression of caFOXO3A had no effect. Consistent with these results, the *Flt-1* promoter activity decreased following global

FoxO knock-out in MEFs. These results are also in agreement with previous studies in FoxO-deficient mice which show that FoxO deletion reduced the Flt-1 expression in endothelial cells and led to the failure of angiogenesis (Furuyama *et al.*, 2004).

FOXO1 activity also affected sFlt-1 levels. Knock-down of FOXO1 reduced sFlt-1-e15a mRNA expression, whereas over-expression of FOXO1 increased sFlt-1-e15a mRNA expression consistent with the *Flt-1* promoter activity in hESC. FOXO3A had no effect on *Flt-1* promoter activity or full-length Flt-1 and sFlt-1 expression.

6.3.6 FOXO1 directly binds to *Flt-1* promoter

Overall, FOXO1 knock-down decreased the *Flt-1* promoter activity and over-expression of FOXO1 increased *Flt-1* promoter activity in St-T1b cells. Therefore, ChIP was used to determine whether FOXO1 directly bound to the *Flt-1* promoter. There was FOXO1 enrichment at three potential FHRE binding sites identified in the *Flt-1* promoter sequence with the greatest binding at the Flt-1 ChIP-1 site in decidualised hESC (**Figure 6.16**). These sites appear with marks in the FOXO1 ChIP-seq data in hESC decidualisation (Vasquez *et al.*, 2015). Interestingly, when ChIP was performed in human microvessel endothelial cell (HMEC-1) there was no FOXO enrichment at ChIP site 1 and the greatest binding was found at the ChIP-3 site which may reflect cell-specific differences in *Flt-1* gene regulation (**Appendix B4**). Combined with the mRNA and protein expression data these results suggest that FOXO1 promotes *Flt-1* gene expression in decidualised hESC, but that is also subject to regulation by other decidual factors that negatively impact on its expression.

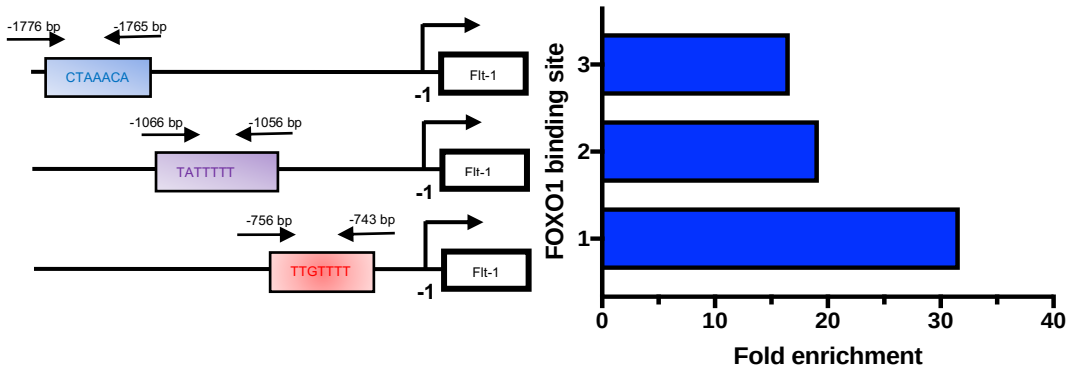

Figure 6.16: FOXO1 binding sites identified by ChIP analysis in the *Flt-1* promoter. Graph shows the degree of enrichment of FOXO1 binding normalised to input DNA and negative control region.

6.3.7 Conclusion

First, the predominant sFlt-1 isoform, sFlt-1-e15a mRNA and protein expression are down-regulated with hESC decidualisation. Despite increases in sFlt-i13 mRNA, the protein levels of this isoform also declined dramatically with hESC decidualisation reflecting the decline in the overall level of sFlt-1 secreted by the cells. Second, the *Flt-1* gene promoter activity and relative full-length Flt-1 receptor mRNA expression were also increased, and the receptor maintained on the cell surface with hESC decidualisation (**Figure 6.17**). This suggests that the hESC may themselves become more responsive to VEGF and PIGF following decidualisation.

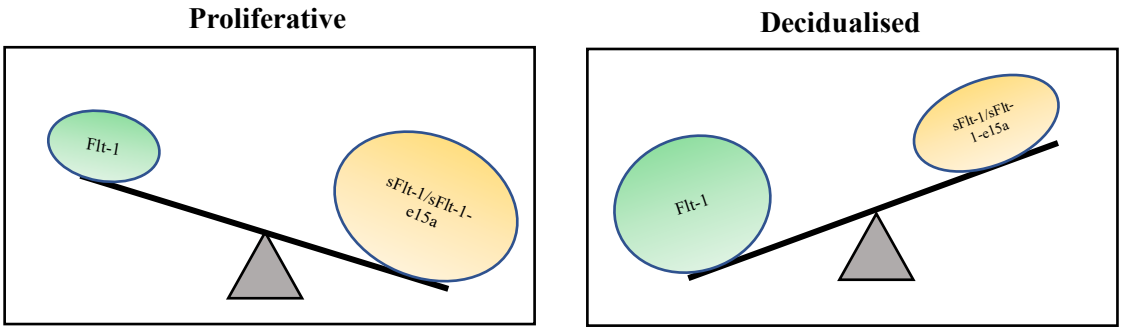

Figure 6.17: Summary of Flt-1/sFlt-1 expression in hESC during decidualisation.

CHAPTER 7:

PRO-ANGIOGENIC ACTIVITY OF HUMAN ENDOMETRIAL STROMAL CELLS AND THEIR FUNCTIONAL RESPONSE TO VEGF

7.1 INTRODUCTION

The human endometrium is a dynamic organ that undergoes cyclic changes of periodic growth, breakdown, regeneration and remodelling. Endometrial tissue remodelling is regulated by ovarian hormones as well as various cytokines and growth factors that are produced locally and act in an autocrine and paracrine manner (Okada *et al.*, 2017). Angiogenesis is crucial for human endometrial development and differentiation in preparation for implantation and maintenance of any subsequent pregnancies (Gordon *et al.*, 1995).

VEGF has pleiotropic activities on endothelial cells playing a crucial role in physiological neo-vascularisation via VEGFR-2/KDR (Terman *et al.*, 1991) and VEGFR-1/Flt-1 (Shibuya *et al.,* 1990) and co-receptors such as NRP-1 (*see* **Figure 1.11**). In addition, it also has many effects on non-endothelial cell types, such as inflammatory and neuronal cells in many cases acting through VEGFR-1/Flt-1 (Dewerchin and Carmeliet, 2012). VEGF activates key cell signalling pathways such as MAPK and Akt (Claesson-Welsh, 2016). Although the pro-angiogenic properties of VEGF are well characterised, the effect of VEGF on hESC function has yet to be investigated.

In this chapter, the pro-angiogenic activity of decidual hESC is examined to determine the relative contributions of VEGF activity and sFlt-1. In addition, as the Flt-1 receptor identified on the surface of hESC and maintained in decidual cells, the action of VEGF on hESC signalling and function was examined.

7.2 RESULTS

7.2.1 Angiogenic activity of decidual hESC conditioned medium

In order to determine the relative angiogenic activity in decidualised and proliferative hESC CM, cell supernatants were collected, and their activity assessed in scratch-wound, tube formation, and spheroid sprouting assays. St-T1b cells were seeded on 10 cm Ø culture dishes. Cells were grown to confluence and incubated with E2 or MM1 medium for 6 days. The cells were re-stimulated with fresh medium 24 h prior to harvesting the CM. The cell supernatants were collected, aliquoted and stored at -20^{o}C for use in functional assays.

7.2.1.1 Decidual hESC conditioned medium promotes HUVEC migration

Wound healing assays were performed with HUVEC grown to confluence on the 12-well plates. A scratch-wound was created using the end of a 200 µl tip after starving the cells for 4 h in DMEM/F12 medium. The cells were then incubated with DMEM/F12 supplemented with 1% FBS (control), proliferative hESC CM, decidual CM or VEGF (50 ng/ml) as a positive control. Images of eight fields for each condition were captured at 0 h and 24 h with an EVOS inverted phase microscope under the 10 X objective as shown in **Section 2.17.1**. Cells incubated in decidual CM migrated significantly faster than those in the proliferative CM and controls **(Figure 7.1B)**. Assays were also performed with CM diluted with DMEM/F12 medium in ratio 1:4 and 2:3 (DMEM/F12 medium: hESC CM). Similarly, HUVEC incubated in 60% or 80% decidual CM migrated faster than those in the same concentration of proliferative cell CM (**Figure 7.2B**).

7.2.1.2 Effect of decidual hESC conditioned medium on *in vitro* endothelial tube formation

Matrigel tube formation assays were performed in 12-well plates. HUVEC were resuspended in control medium, proliferative CM or decidual hESC CM, or VEGF (50 ng/ml) as a positive control and added on top of a layer of growth factor-reduced Matrigel as described in **Section 2.17.2**. Images of capillary-like endothelial tubes were taken every 6 h up to 24 h using an IncuCyte ZOOM® (Essen Bioscience) with 4 X objective. The number of meshes and branches were analysed with the Angiogenesis Analyser, ImageJ plugin software. VEGF promoted tube formation at all time points relative to the control medium. The meshes started to break up and number of branch points reduced from 12 h under all conditions **(Figure 7.3B)** therefore tube formation was measured at 6 h. Decidual hESC CM induced significantly greater mesh formation than proliferative CM (**Figure 7.3 B&C**). However, the proliferative CM showed reduce tube formation compared with the control medium (**Figure 7.3 B&C**). Overall, the decidual CM was more angiogenic compared to the proliferative CM measured either by mesh or branch formation (**Figure 7.3 B&C**).

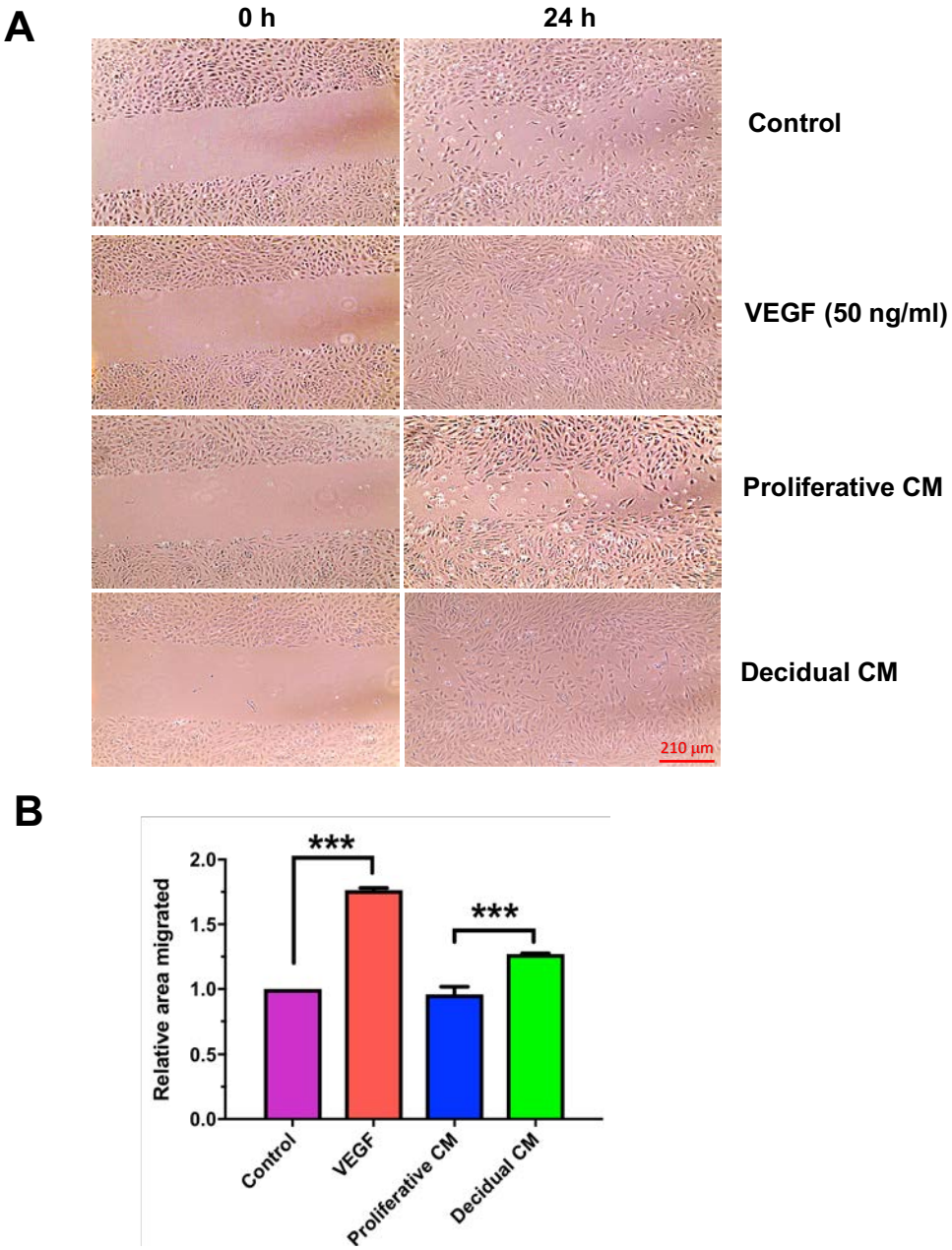

Figure 7.1: Decidual cell conditioned medium (CM) promotes endothelial cell migration. Confluent HUVEC monolayers were scratch-wounded and with various VEGF or hESC CM. **(A)** Representative images taken at time 0 and 24 h of HUVEC treated with VEGF (50 ng/ml), proliferative CM, decidual CM or DMEM/F12 containing 1% FBS (control). **(B)** Graph showing the mean relative migrated area normalised to the control. Images were taken at time 0 and 24 h of 8-fields using an EVOS phase-contrast microscope under the 10 X objective and the mean area of wound closure measured using ImageJ software and normalised to control. Results are the mean (+/- SEM) of 3 experiments performed in duplicate and analysed using one-way ANOVA; ***$p<0.001$.

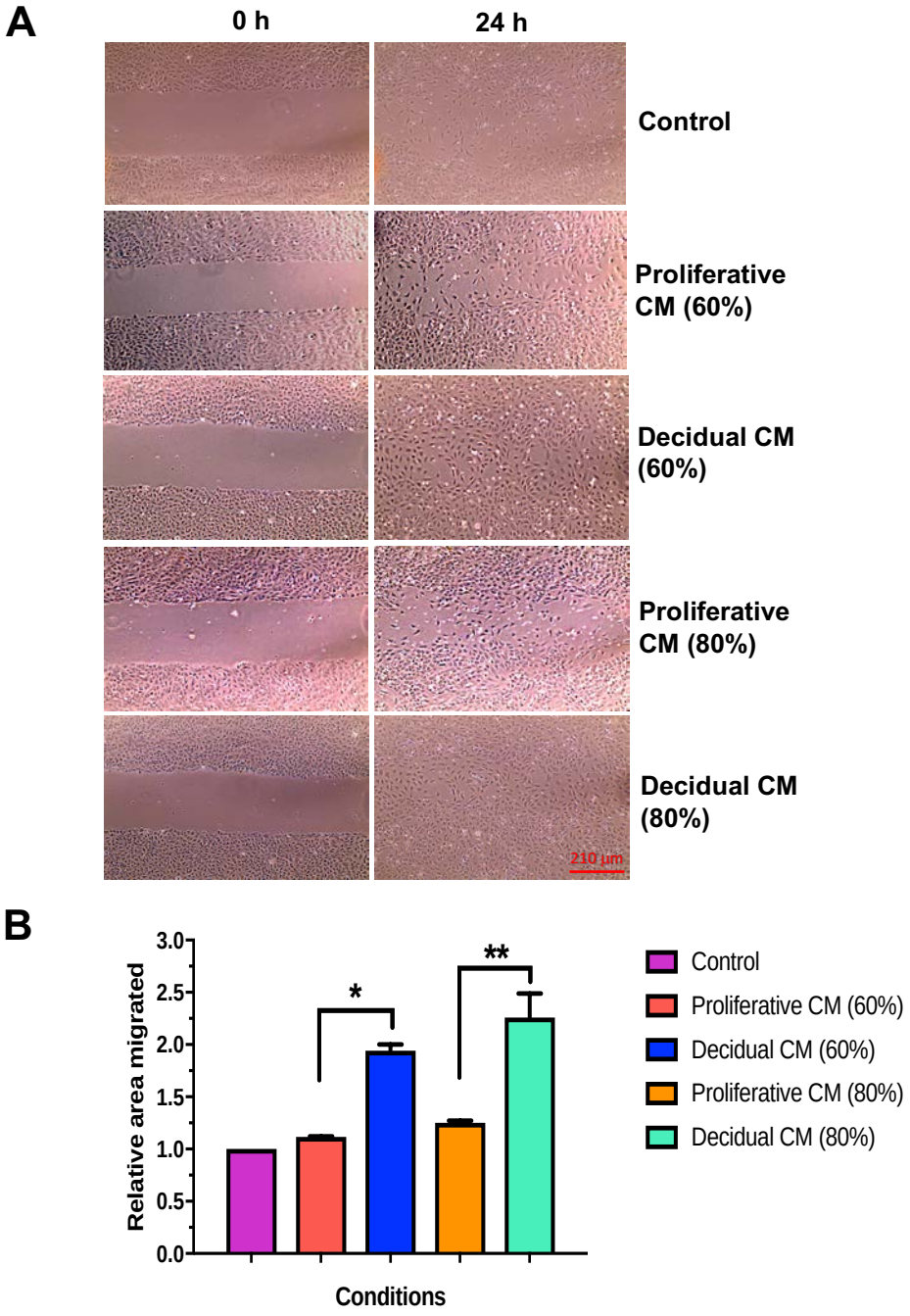

Figure 7.2: Diluted decidual cell conditioned medium (CM) promotes endothelial cell migration. Confluent HUVEC monolayers were scratch-wounded and treated with 60% or 80% of decidual or proliferative hESC CM. **(A)** Representative images taken at time 0 and 24 h. **(B)** Analysis of the relative mean migrated area normalised to the control. Images were taken at time 0 and 24 h of 8-fields using an EVOS phase-contrast microscope under the 10 X objective and the mean area of wound closure measured using ImageJ software and normalised to control. Results are the mean (+/- SEM) of 3 experiments performed in duplicate and analysed using one-way ANOVA; *p<0.05; **p<0.01.

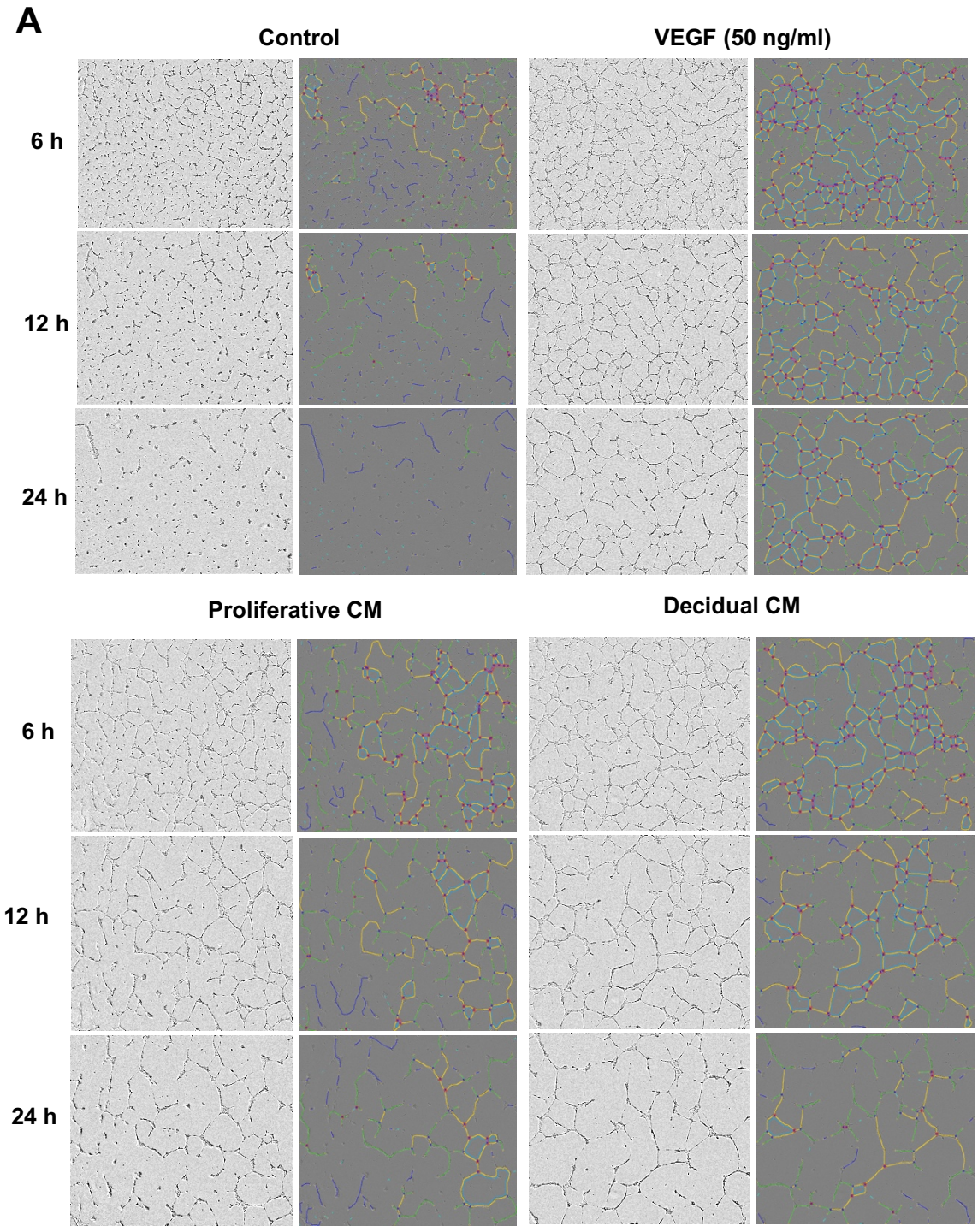
A
Control
VEGF (50 ng/ml)
6 h
12 h
24 h
Proliferative CM
Decidual CM
6 h
12 h
24 h

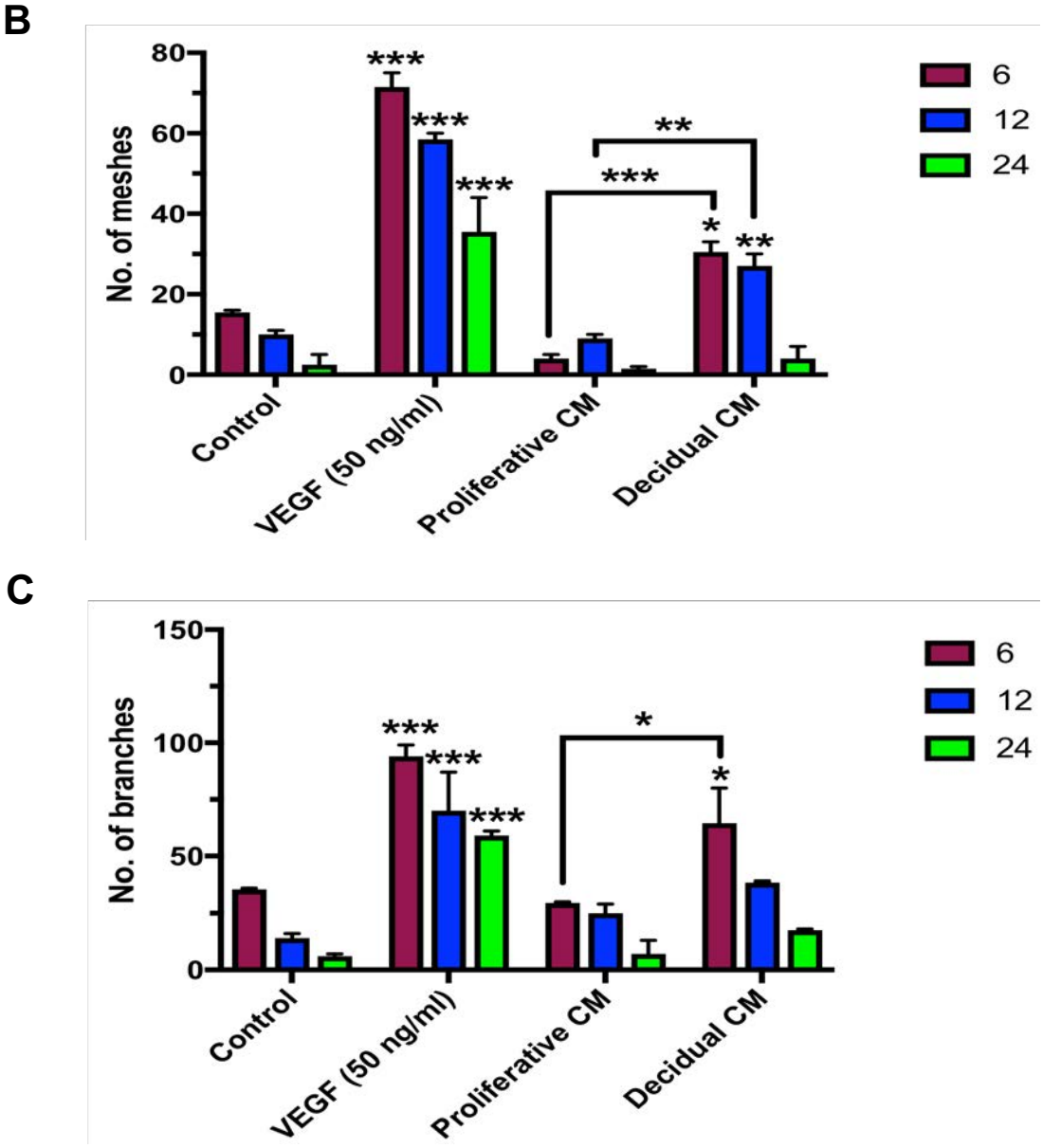

Figure 7.3: Decidual hESC conditioned medium (CM) stimulates in vitro endothelial tube formation. HUVEC (180,000 cells/well) were seeded on growth factor-reduced Matrigel in a 12-well plate. **(A)** Representative images taken at 6, 12 and 24 h following treatment with VEGF (50 ng/ml), proliferative and decidual hESC CM, or control (DMEM/F12 containing 1% FBS). Graphs showing the mean number of **(B)** meshes and **(C)** branches formed at the indicated time points. Images were taken using an IncuCyte ZOOM® system under 4 X objective. Results are the mean (+/-SEM) of 3 independent experiments performed in duplicate and analysed using two-way ANOVA; *p<0.05; **p<0.01; ***p<0.001.

7.2.1.3 Decidual hESC conditioned medium stimulates multicellular spheroid sprouting

In order to further characterise the effect of decidual CM on angiogenesis, multicellular (HUVEC and St-T1b) spheroid sprouting assays were performed. Mixed spheroids formed from HUVEC and St-T1b cells were embedded into the growth factor-reduced Matrigel on 24-well plates as described in **Section 2.17.3** and incubated with proliferative or decidual hESC CM, VEGF (50 ng/ml) or DMEM/F12 supplemented with 1% FBS as a control. Images of the spheroids were taken after 24 h with an EVOS microscope under the 10 X objective. VEGF induced a significant increase in spheroid sprouting compared with control medium. Spheroids treated with decidual CM sprouted significantly more than those with proliferative CM, which were found to be similar to the control **(Figure 7.4).**

7.2.2 FOXO1 knock-down in hESC reduces pro-angiogenic activity

In Chapter 5, I demonstrated that FOXO1 directly regulates VEGF in hESC (**Figure 5.7B**). To further investigate this, we conducted wound healing and tube formation assays using CM harvested from hESC following FOXO1 or FOXO3A knock-down. Scratch-wounds were created in confluent HUVEC monolayers and the cells treated with CM harvested from proliferative St-T1b, or St-T1b cells stimulated to decidualise for 24 h following FOXO1, FOXO3A, or control knock-down. CM collected from FOXO1, or FOXO3A knock-down ESC did not significantly affect HUVEC migration compared to the cells treated with control CM (**Figure 7.5 A-B**).

Matrigel tube formation assays were performed with HUVEC resuspended in proliferative CM or decidual hESC CM, control medium or VEGF (50 ng/ml) and added on top of a layer of growth factor-reduced Matrigel as described in **Section 2.17.2**. Images of capillary-like endothelial tube formation were taken every 6 h up to 24 h. CM collected following FOXO1

knock-down in hESC significantly reduced the number of meshes and branches formed (**Figure 7.6**) whereas FOXO3A knock-down in hESC had no significant effect on mesh and branch formation induced by CM (**Figure 7.6**).

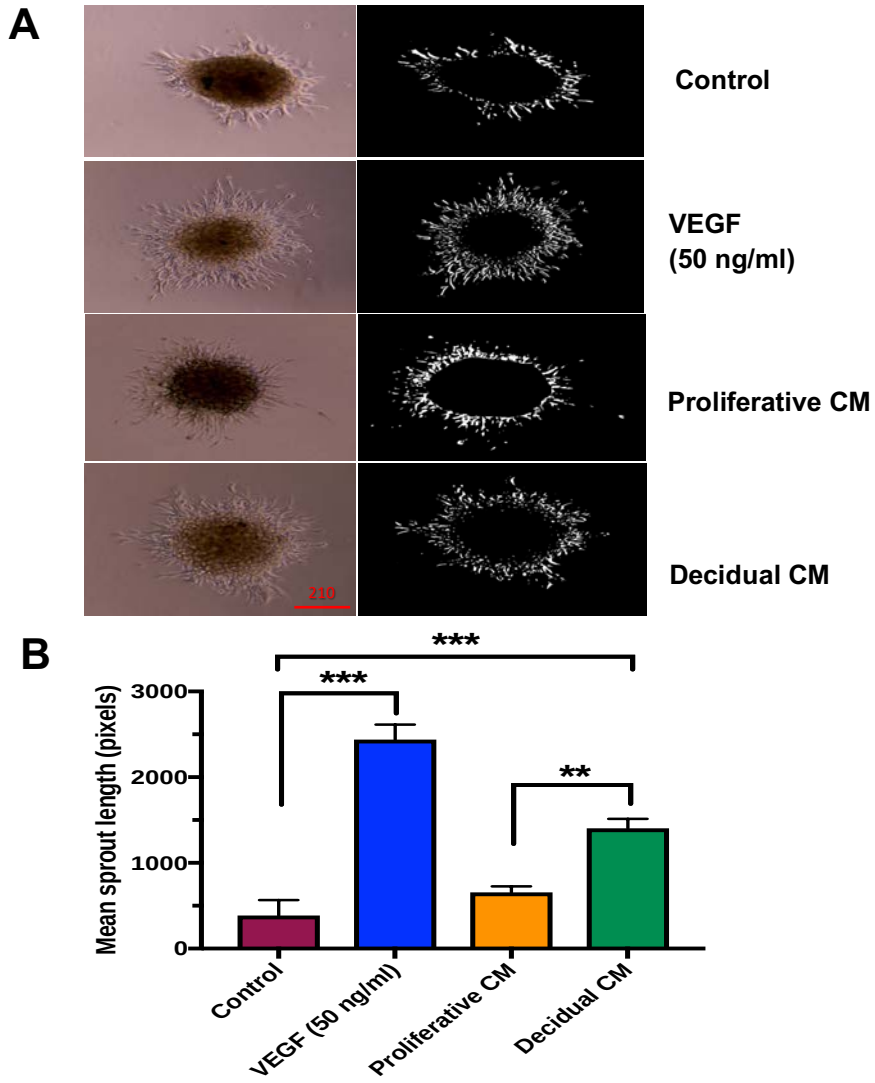

Figure 7.4: Decidual hESC conditioned medium (CM) promotes mixed endothelial/St-T1b cell spheroid sprouting. HUVEC and St-T1b cells were mixed in a 1:1 ratio and seeded in 96-well rounded bottom plates in 0.25% methylcellulose overnight. The spheroids were embedded in growth factor-reduced Matrigel and incubated in DMEM/F12 supplemented with 1% FBS (control), VEGF (50 ng/ml), proliferative CM, or decidual hESC CM. **(A)** Representative images taken after 24 h incubation under 10 X objective. **(B)** Graph showing mean of sprout lengths relative to control analysed using ImageJ. Results are mean (+/- SEM) of 2 independent experiments performed in duplicate (12 replicates per well) and analysed using two-way ANOVA. **p<0.01; ***p<0.001.

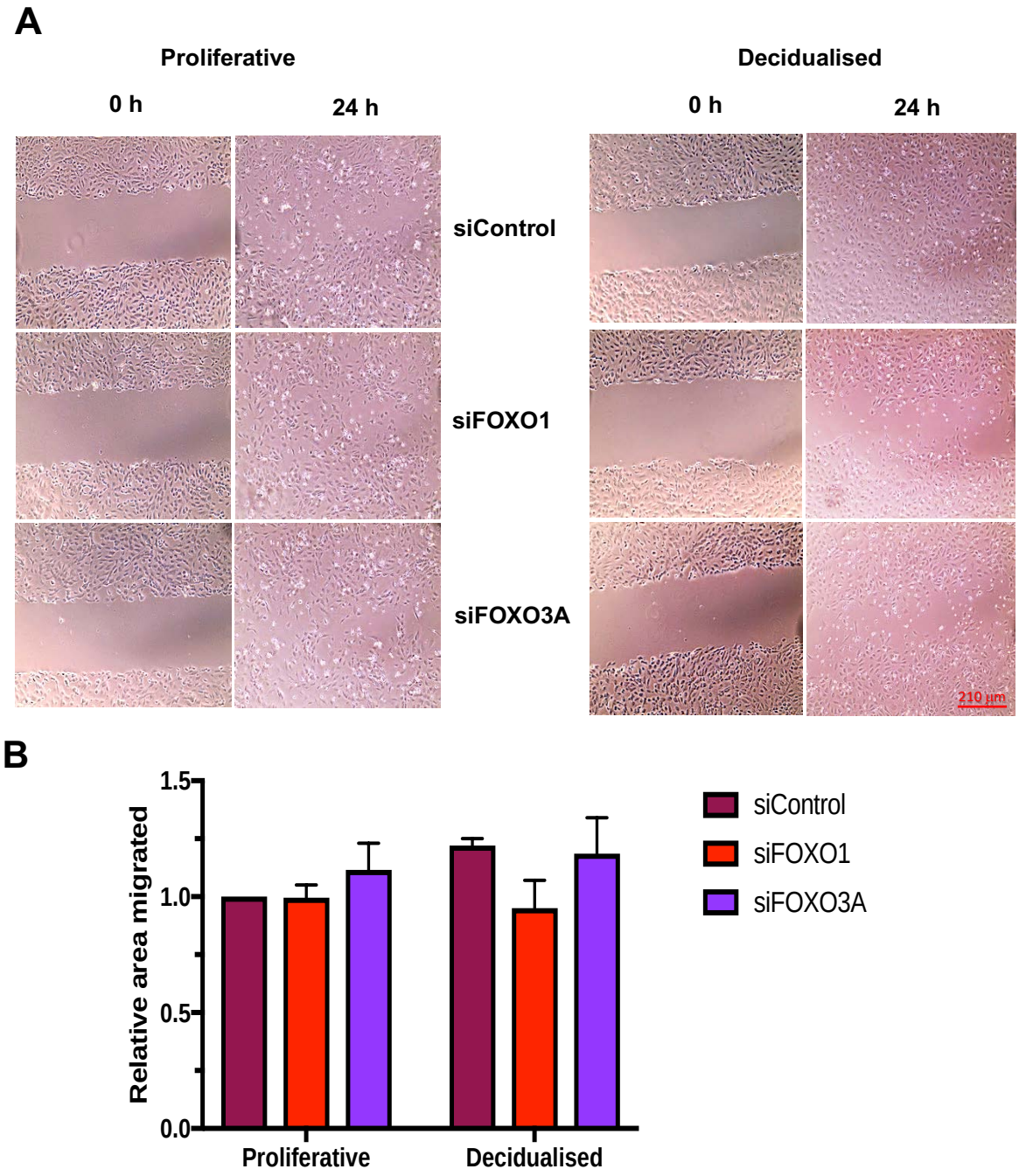

Figure 7.5: FOXO1 knock-down in hESC does not affect CM-driven endothelial cell migration. St-T1b cells were transfected with siRNAs targeting FOXO1 (siFOXO1), FOXO3A (siFOXO3A), control (siControl) overnight and incubated with E2 or MM1 medium for 24 h. The CM was collected and used in endothelial wound healing assays. **(A)** Representative images taken at time 0 h and 24 h following addition of CM. **(B)** Graph showing relative mean migrated area normalised to the control. Results are the mean (+/-SEM) of 2 independent experiments performed in duplicate and analysed using one-way ANOVA.

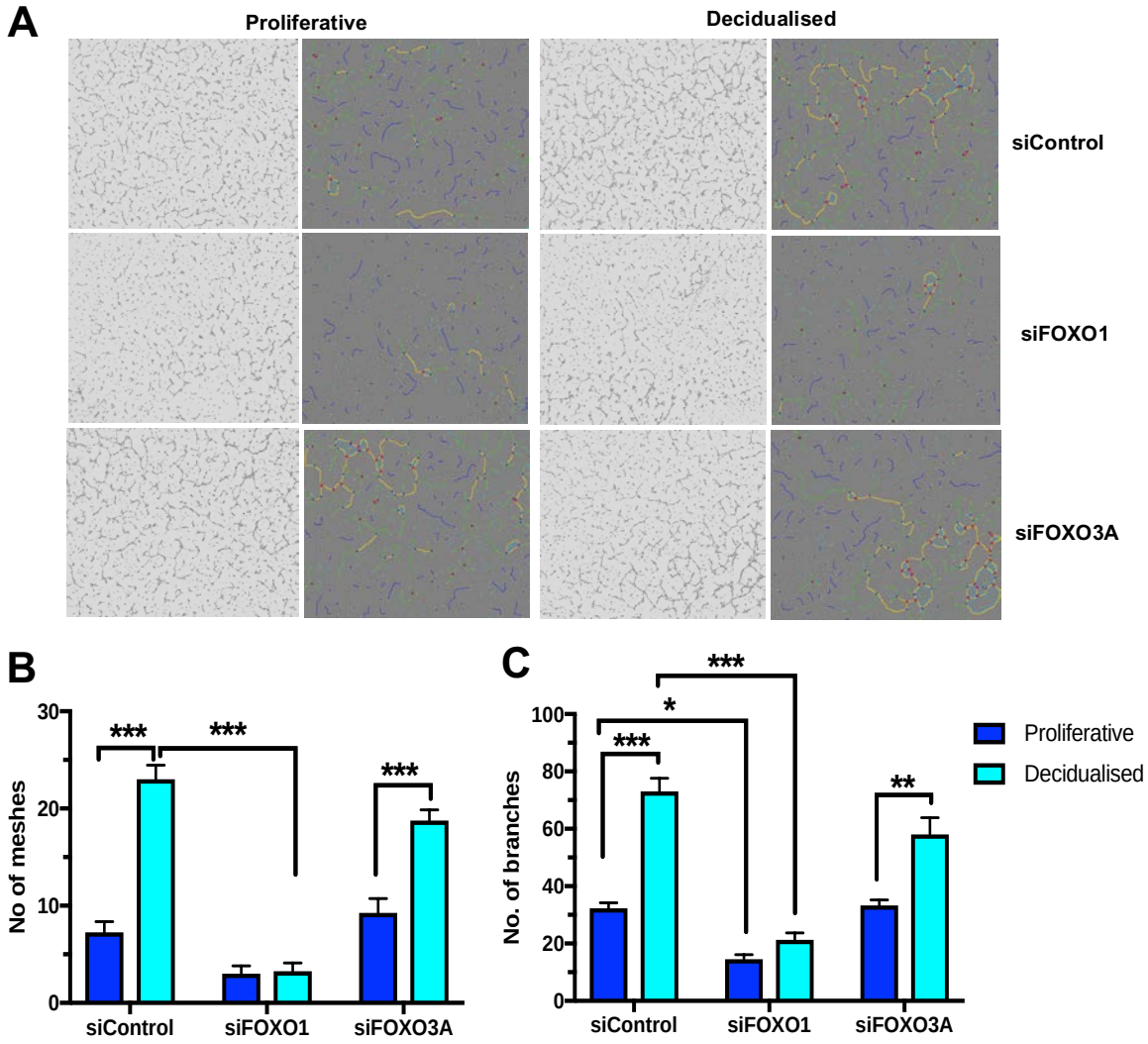

Figure 7.6: FOXO1 activity in hESC is critical for their pro-angiogenic effect during decidualisation. St-T1b cells were transfected with siRNAs targeting FOXO1 (siFOXO1), FOXO3A (siFOXO3A), or control (siControl) overnight and incubated with E2 or MM1 medium for 24 h. The CM was collected and used in endothelial tube formation assays. **(A)** Representative images taken at 6 h following addition of CM using the IncuCyte ZOOM® system under 4 X objective. Graph showing the mean number of **(B)** meshes and **(C)** branches quantified using Angiogenesis Analyser in ImageJ. Results are the mean (+/-SEM) of two independent experiments performed in duplicate and analysed using one-way ANOVA; *p<0.05; **p<0.001; and ***p<0.001.

7.2.3 VEGF activity in decidual hESC CM

In order to determine the relative activity of VEGF in decidual hESC supernatants, functional assays were performed following the blockade of VEGF activity with recombinant sFlt-1 in hESC CM. Decidual CM was incubated with 0.5, 1.5 or 3.0 ng/ml of recombinant sFlt-1 for an hour at room temperature. Scratch-wounds were created (as described in **Section 2.17.1)** in confluent HUVEC monolayers. The migration in HUVEC was found to be significantly slower with hESC CM pre-treated 1.5 ng/ml and 3.0 ng/ml of sFlt-1 (**Figure 7.7 B-C**). Subsequently, 1.5 ng/ml of recombinant sFlt-1 was used for tube formation assays due to the limited amount of CM that could be readily collected. Consistent with the wound healing assay results, sFlt-1 blocked the pro-angiogenic effect of decidual CM in tube formation assays (**Figure 7.8**). These results confirm that VEGF contributes the majority of the angiogenic secreted by decidual hESC.

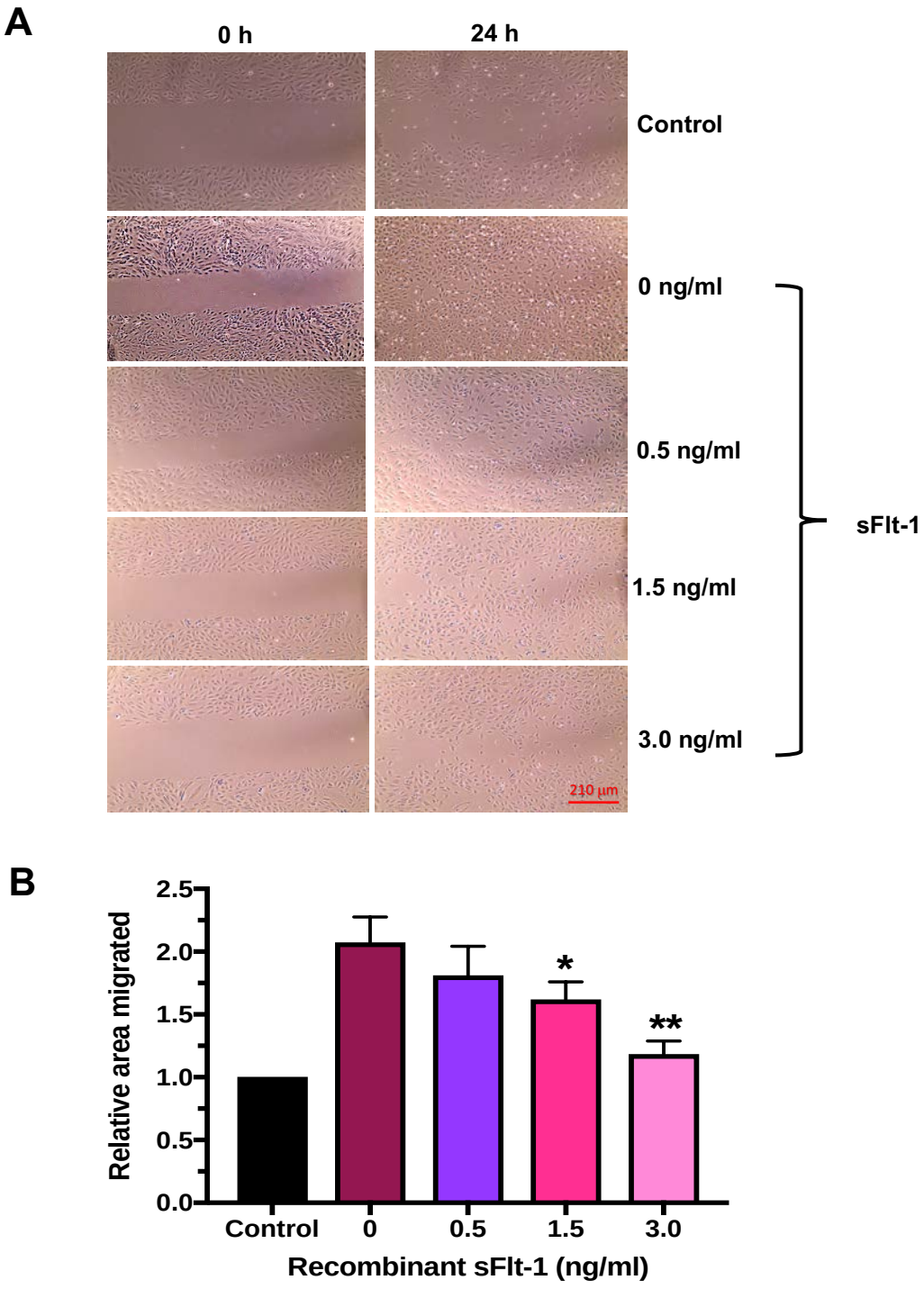

Figure 7.7: VEGF activity in decidual hESC conditioned medium (CM) drives endothelial cell migration. HUVEC were grown on 12 well-plates until they reached confluence and then scratch-wounded and treated with various CM. **(A)** Representative images taken at time 0 and 24 h of HUVEC treated with decidual hESC CM in the absence, or presence, of recombinant sFlt-1. **(B)** Graph showing relative mean migrated area normalised to the control. Results are the mean (+/-SEM) of 3 experiments performed in duplicate and analysed using two-way ANOVA; * $p<0.05$, ** $p<0.01$.

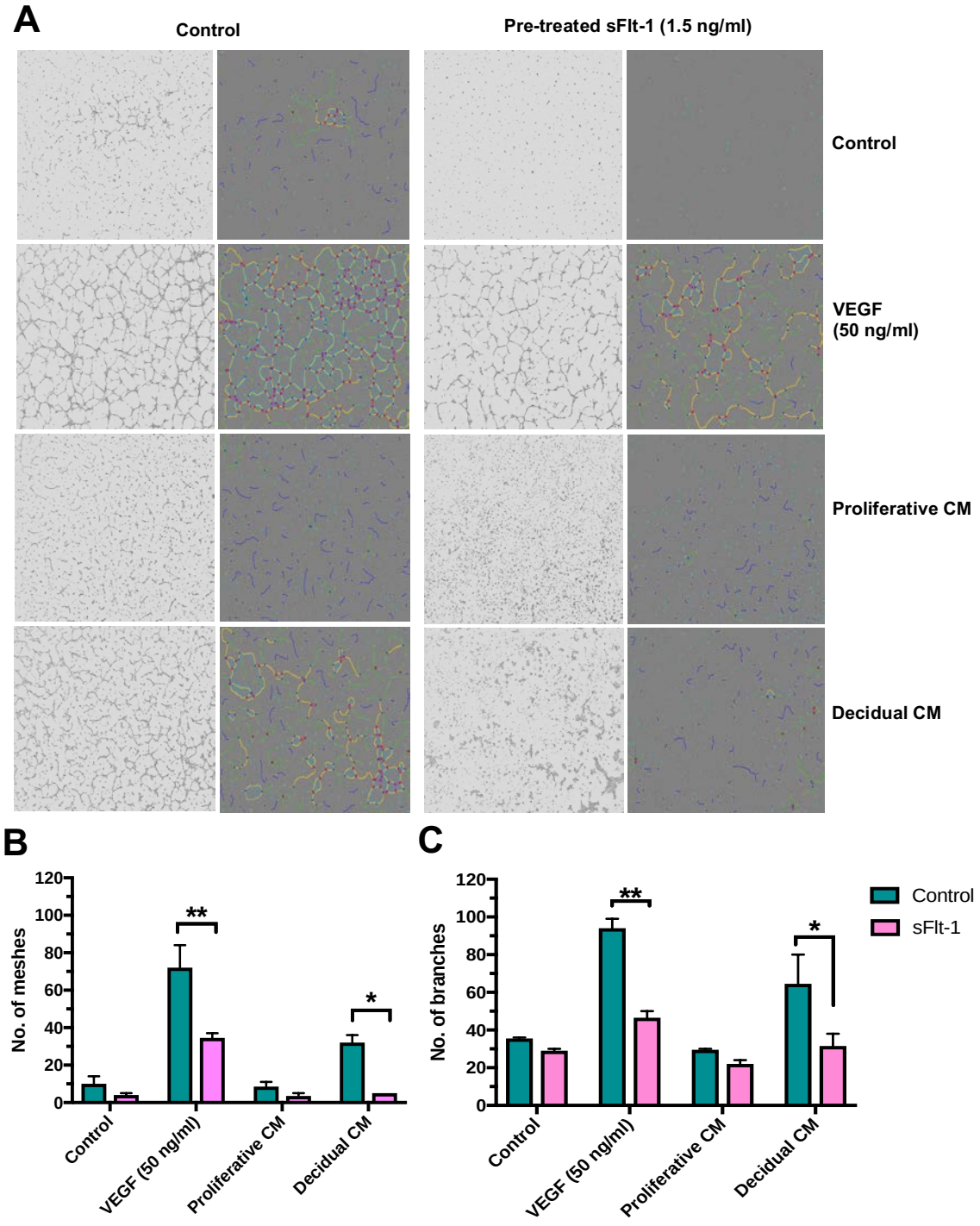

Figure 7.8: VEGF activity in decidual hESC conditioned medium (CM) drives in vitro endothelial tube formation. HUVEC (180,000 cells/well) were seeded on growth factor-reduced Matrigel and treated with CM or VEGF. **(A)** Representative images taken at 6 h using the IncuCyte ZOOM® system under 4 X objective. Analysis of the mean number of **(B)** meshes, and **(C)** branches using the ImageJ Angiogenesis Analyser plug-in. Results are the mean (+/- SEM) of 2 experiments performed in duplicate and analysed using two-way ANOVA; *p<0.05, **p<0.01.

7.2.4 Immunoprecipitation of sFlt-1/Flt-1 from decidual-derived CM reveals the presence of shed micro-vesicles but does not promote VEGF activity in CM

To further investigate, the significance of VEGF in both proliferative and decidual CM, VEGF was immunoprecipitated with anti-Flt-1 antibody, or an irrelevant control antibody and protein A/G beads overnight on a rotary stirrer at 4ºC. The supernatant was collected in new tubes after magnetic separation and stored at -20ºC for wound healing assays. The beads were then washed few times with serum-free medium and resuspended in SDS lysis buffer separated by SDS-PAGE and Western blotted as described in **Section 2.15**. Western blotting confirmed the precipitation of sFlt-1 (**Figure 7.9A**). Surprisingly, full-length Flt-1 receptor was also strongly detected in the medium, suggesting the presence of membrane bound vesicles shed into the CM. More sFlt-1/Flt-1 was detected in proliferative CM than decidual CM. In addition, an ELISA was run to confirm the reduction of sFlt-1 levels in IP CM before angiogenesis assays were performed. The level of sFlt-1/Flt-1 in proliferative CM was significantly decreased (**Figure 7.9B**). The supernatants were used in scratch-wound assays and the anti-Flt-1 IP CM significantly reduced the migration in HUVEC (**Figure 7.9 C&D**). As the removal of sFlt-1 from CM did not show the expected increase in endothelial migration, VEGF levels were examined on CM following IP by ELISA. Surprisingly, the VEGF levels in CM decreased following Flt-1 IP in the decidual CM (**Figure 7.10)** indicating that the decrease in endothelial migration was potentially due to a reduction of VEGF in CM.

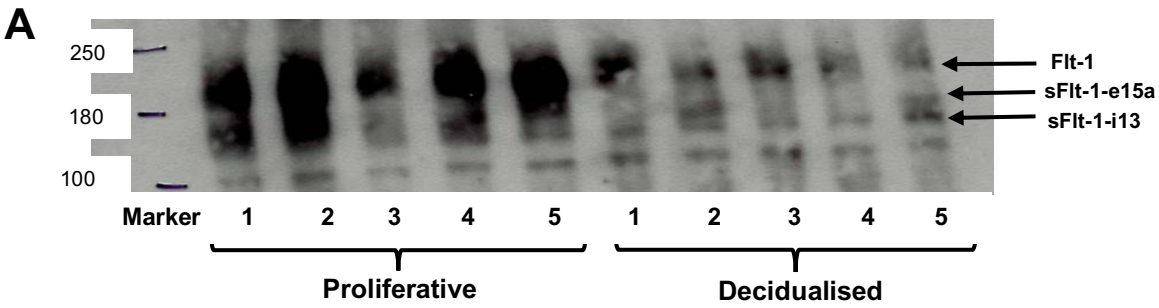
A
250
180
100
Flt-1
sFlt-1-e15a
sFlt-1-i13
Marker
1
2
3
4
5
1
2
3
4
5
Proliferative
Decidualised

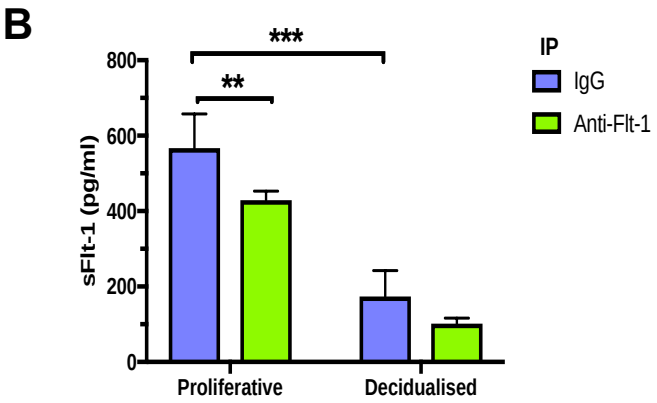
B
***
**
800
600
400
200
0
sFlt-1 (pg/ml)
IP
IgG
Anti-Flt-1
Proliferative
Decidualised

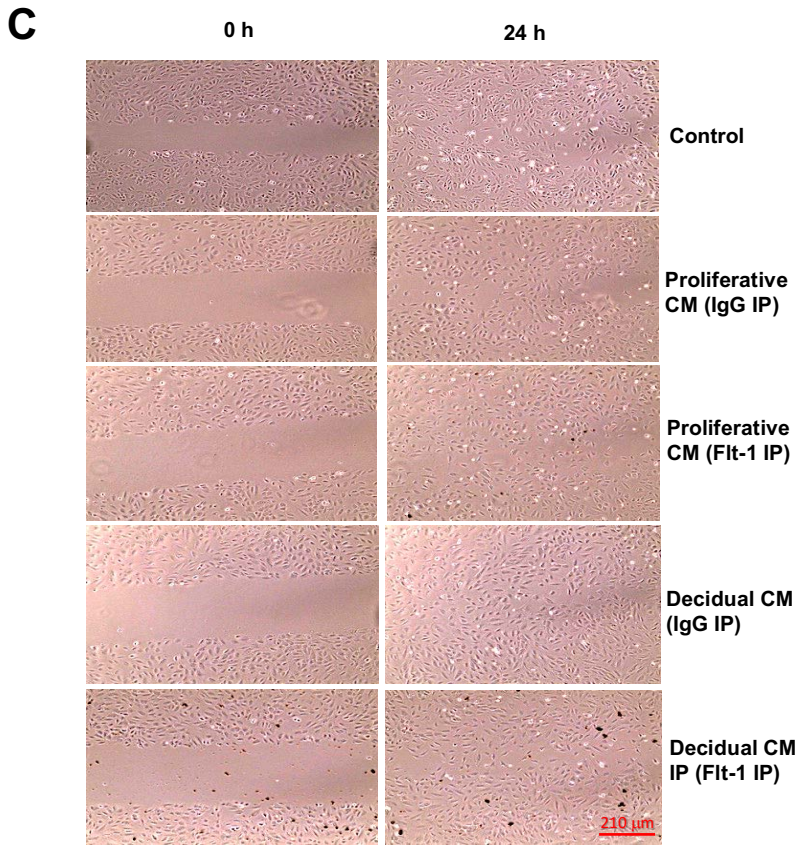
C
0 h
24 h
Control
Proliferative CM (IgG IP)
Proliferative CM (Flt-1 IP)
Decidual CM (IgG IP)
Decidual CM IP (Flt-1 IP)
210 µm

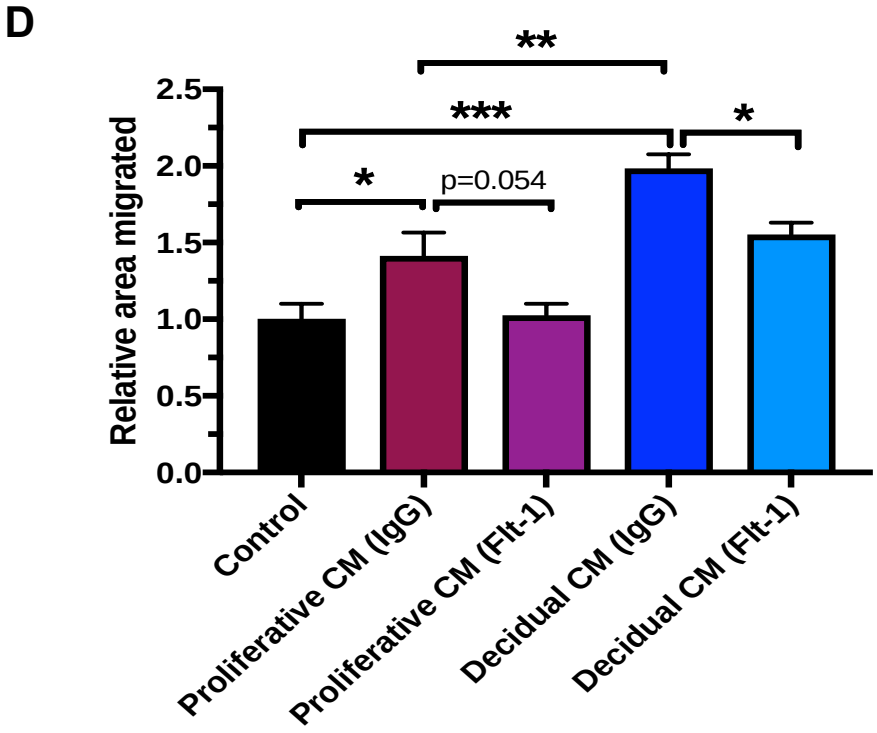

Figure 7.9: Presence and activity of sFlt-1/Flt-1 in decidual cell-derived hESC conditioned medium (CM). St-T1b cells were stimulated with E2 or MM1 medium for 6 days and 24 h CM was collected. The CM were incubated with anti-Flt-1, or control (IgG) antibodies and protein A/G magnetic beads overnight. **(A)** The precipitated material was eluted and analysed by Western blot for Flt-1/sFlt-1 using anti-Flt-1 antibody. The supernatants were collected by magnetic separation and assessed for sFlt-1 in wound healing assays. **(B)** sFlt-1/Flt-1 levels in CM measured by ELISA. **(C)** Representative images taken at time 0 and 24 h of HUVEC treated with control (DMEM/F12 medium supplemented with 2% FBS), and with proliferative, or decidual CM followed by anti-Flt-1 antibodies. **(D)** Graph showing relative mean migrated area normalised to the control. Results are mean (+/- SEM) of 2 independent experiments performed in duplicate and analysed using one-way ANOVA; *$p<0.05$; **$p<0.001$; and ***$p<0.001$.

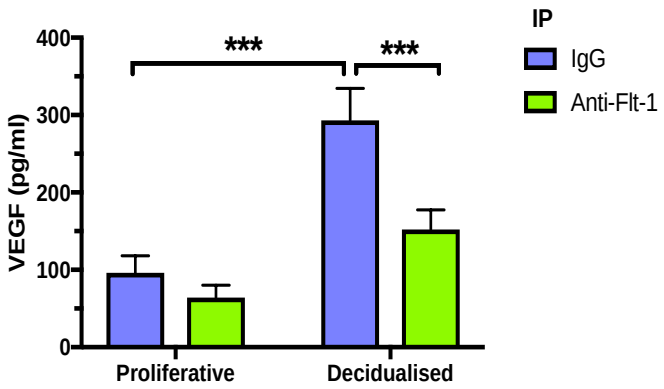

Figure 7.10: Removal of sFlt-1/Flt-1 in hESC conditioned medium (CM) reduces VEGF levels. The proliferative, and decidual hESC CM was incubated with anti-Flt-1, or control IgG antibodies with protein A/G beads overnight. The supernatants were collected by magnetic separation and the VEGF levels assessed by ELISA. Results are the mean (+/-SEM) of 5 experiments; ***p<0.001.

7.2.5 Expression of VEGF receptors in hESC

As hESC express Flt-1 receptor at their cell surface (**Figure 6.10**), the presence of other VEGF receptors was investigated. The human microvascular endothelial cell line, HMEC-1, was used as a positive control with VE-cadherin as an endothelial cell specific marker (**Figure 7.11**). VEGFR-2 was not detected in hESC during decidualisation by qPCR (data not shown) or Western Blotting (**Figure 7.11**). Interestingly, the VEGF co-receptor NRP-1 was expressed and found to increase during hESC decidualisation (**Figure 7.11 A&D**) albeit at a lower level than in HMEC-1 (**Figure 7.11 A&C**). Surprisingly, sFlt-1/Flt-1 expression was detected at very low levels in HMEC-1.

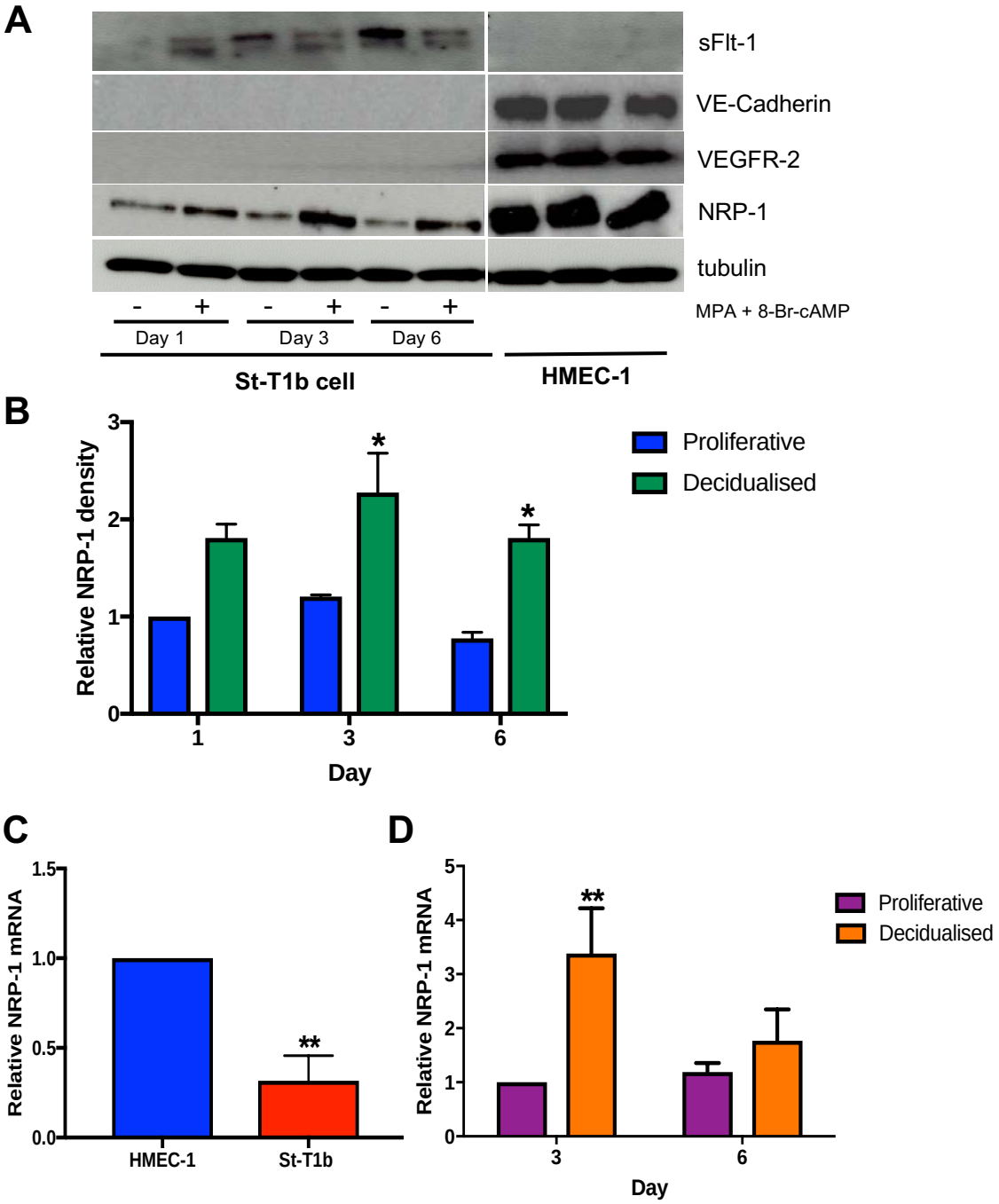

Figure 7.11: VEGF receptor expression in hESC decidualisation. St-T1b cells and HMEC-1 as a control were plated on 6-well plates. St-T1b cells were stimulated with E2 or MM1 medium over 6 days and protein lysates were harvested. **(A)** Representative Western blot showing VE-Cadherin, VEGFR-2, and NRP-1 expression with tubulin as a loading control. **(B)** Graph of densitometric analysis of NRP-1 expression in St-T1b cells during decidualisation. **(C)** Real-time qPCR of **(C)** NRP-1 mRNA expression in HMEC-1 and St-T1b cells and **(D)** NRP-1 expression in St-T1b cells stimulated with E2 or MM1 medium normalised to β-actin. Results are the mean (+/-SEM) of 3 experiments and analysed using unpaired t-test; *p<0.05; **p<0.01; ***p<0.001.

7.2.6 Effect of VEGF on hESC function

7.2.6.1 VEGF increases hESC migration

VEGF produced by hESC during decidualisation was shown to be a key regulator of endothelial cell migration and tube formation in previous section. As hESC express Flt-1 receptor on their surface (**Figure 6.10**) and we have shown that Flt-1 receptor is shed into CM, the effect of VEGF on hESC function was examined. St-T1b cells were incubated with E2 or MM1 medium for 6 days and re-plated on 12-well plates for another 18 h in low-serum medium. The pre-treated St-T1b cell monolayers were then scratch-wounded and incubated in serum-free medium supplemented with 50 ng/ml of VEGF or PIGF and eight images of each conditions were taken of each condition at 0 h and 18 h. VEGF significantly increased both the proliferative and pre-decidualised hESC migration (**Figure 7.12**) whereas, unexpectedly, no significant effect of PIGF on pre-decidualised St-T1b cell migration was observed. The migratory activity of the decidual condition cells was significantly increased compared to the proliferative control cells (**Figure 7.12**).

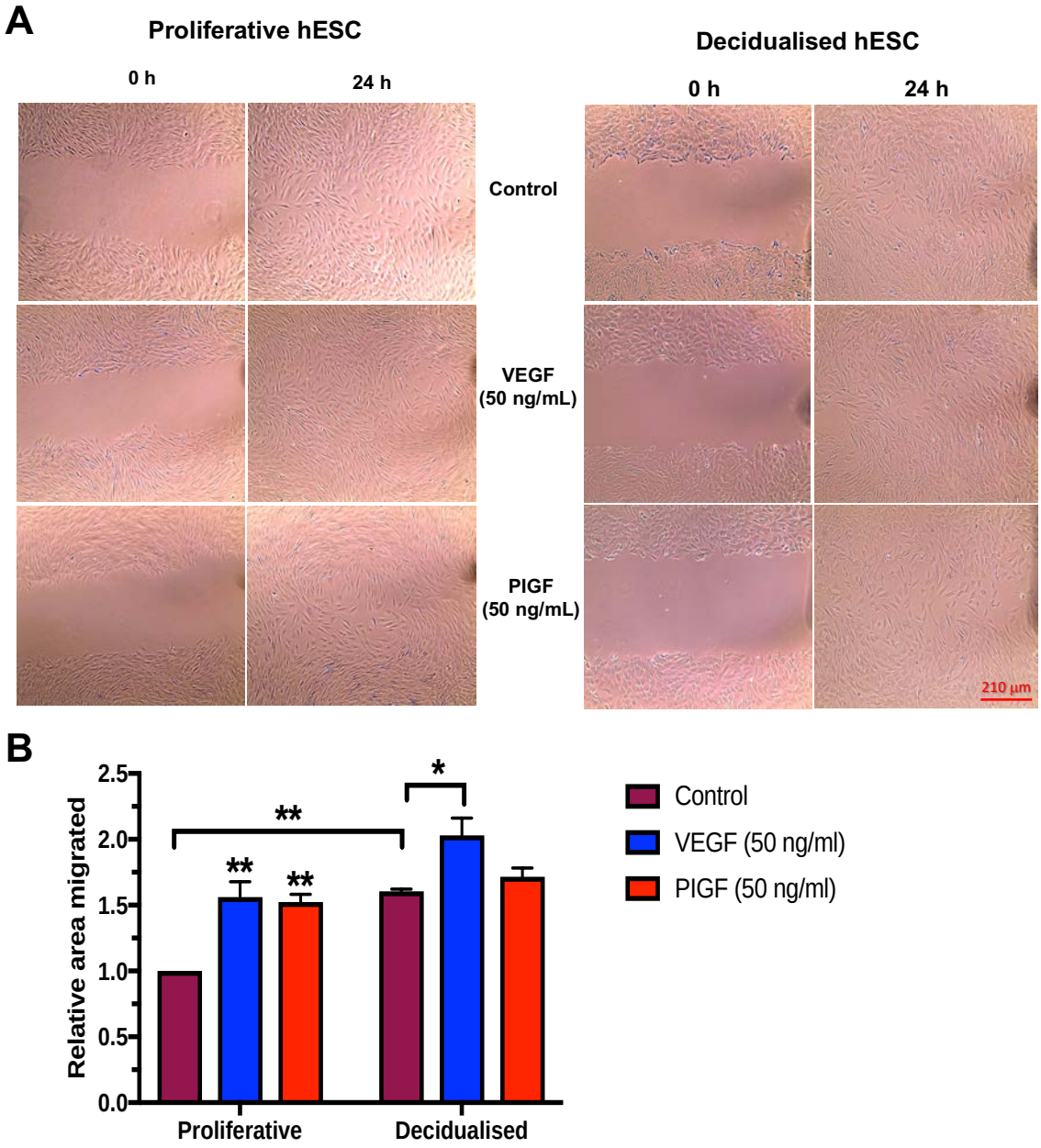

Figure 7.12: VEGF/PIGF activity increases hESC migration following decidualisation. St-T1b cells were incubated with either E2 or MM1 medium for 6 days and re-plated on 12-well plates in reduced-serum medium for 24 h. The cell monolayers were then wounded and incubated in serum-free medium supplemented with VEGF or PIGF. The wound closure was quantified using ImageJ as described in **Section 2.17.1**. **(A)** Representative images captured at 0 and 24 h using an EVOS microscope under 10 X magnification. **(B)** The mean of migrated area relative to the proliferative control cells. Results are the mean (+/- SEM) of 3 independent experiments performed in duplicate and analysed using two-way ANOVA; *$p<0.05$; **$p<0.01$.

7.2.6.2 VEGF/PIGF promotes hESC invasion

Spheroid sprouting assays were used to examine the invasive activity of hESC following decidualisation. St-T1b cells were incubated with E2 or MM1 medium for 6 days. The cells (5,000/well) were plated overnight in 96-well rounded bottom non-tissue culture-treated plates in DMEM/F12 medium supplemented with 2% FBS and 0.25% of methylcellulose. The spheroids were embedded in growth factor-reduced Matrigel on 24-well plates and DMEM/F12 basal medium supplemented with 50 ng/ml of VEGF, or PIGF as described in **Section 2.17.3** was added. Images were taken after 24 h and the mean sprout length measured using ImageJ software. Strikingly, the spheroids formed from decidual St-T1b cells were found to sprout significantly more than those formed from proliferative St-T1b cells (**Figure 7.13**). In addition, VEGF increased the invasive activity of spheroids formed from both proliferative and decidualised St-T1b cells (**Figure 7.13**) whereas, no significant increase was observed with PIGF in proliferative or decidualised St-T1b cell spheroids (**Figure 7.13**).

7.2.7 Knock-down of VEGF reduces ESC invasion

Up-regulation of VEGF activity during hESC decidualisation was observed in previous chapters and it is considered the major angiogenic factor in endometrium (Girling and Rogers, 2009). To further substantiate a role of VEGF in hESC, St-T1b cells were plated on 6-well plates and transfected with VEGF, or control siRNAs overnight. The supernatants and RNA lysates were harvested, and spheroids were formed overnight, following VEGF knock-down, using 5,000 cells/well on round bottom non-tissue culture-treated 96-well plates in DMEM/F12 medium supplemented with 2% FBS and 0.25% methylcellulose. The spheroids were embedded in Matrigel and the formation of hESC sprouts was assessed. The knock-down of VEGF was confirmed by qPCR (**Figure 7.14C**) and VEGF was significantly

reduced, by ELISA, in hESC supernatants (**Figure 7.14D**). VEGF knock-down hESC showed significantly reduced spheroid sprouting activity in Matrigel (**Figure 7.14B)** which indicates that VEGF is playing an autocrine stimulatory role on hESC invasion.

As an alternative approach to block endogenous VEGF activity, St-T1b cells were transduced with an adenovirus encoding murine sFlt-1 Ig-like loops 1-3 (Ad-sFlt-1) (Tseng *et al.*, 2002), or empty virus control (Ad-CMV) overnight before cells were used to form spheroids. Over-expression of sFlt-1 significantly reduced hESC spheroid sprouting (**Figure 7.15B)**. Endogenous sFlt-1-e15a mRNA expression did not significantly change following over-expression of sFlt-1 (**Figure 7.15C**). Surprisingly, over-expression of sFlt-1 reduced both VEGF mRNA expression (**Figure 7.15D**) and protein secretion (**Figure 7.15D**).

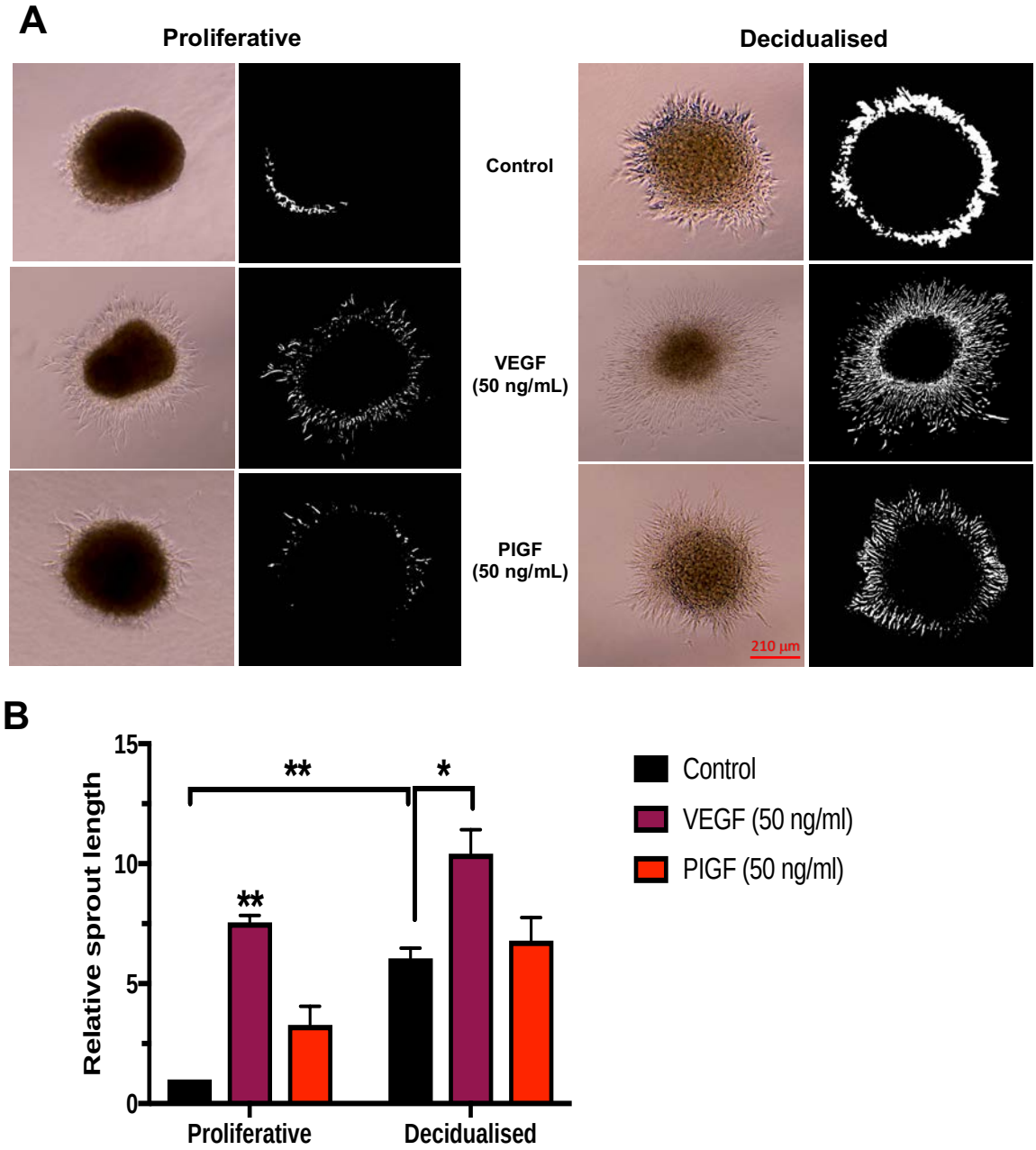

Figure 7.13: VEGF increases invasive activity in hESC. St-T1b cells were incubated in E2 or MM1 medium for 6 days and then plated on 96-well rounded bottom non-tissue culture plate in DMEM/F12 medium supplemented with 2% FBS and 0.25% methylcellulose overnight. The spheroids were then embedded in growth factor-reduced Matrigel and topped up with DMEM/F12 basal medium supplemented with VEGF or PIGF. **(A)** Representative images taken after 24 h using an EVOS microscope under 10 X objective and the mean sprout length determined using ImageJ. **(B)** Graph showing the mean of sprout length relative to the proliferative control cells. Results are the mean (+/- SEM) of 2 experiments performed in duplicate (12 replicates per well) and analysed using two-way ANOVA; *p<0.05; **p<0.01.

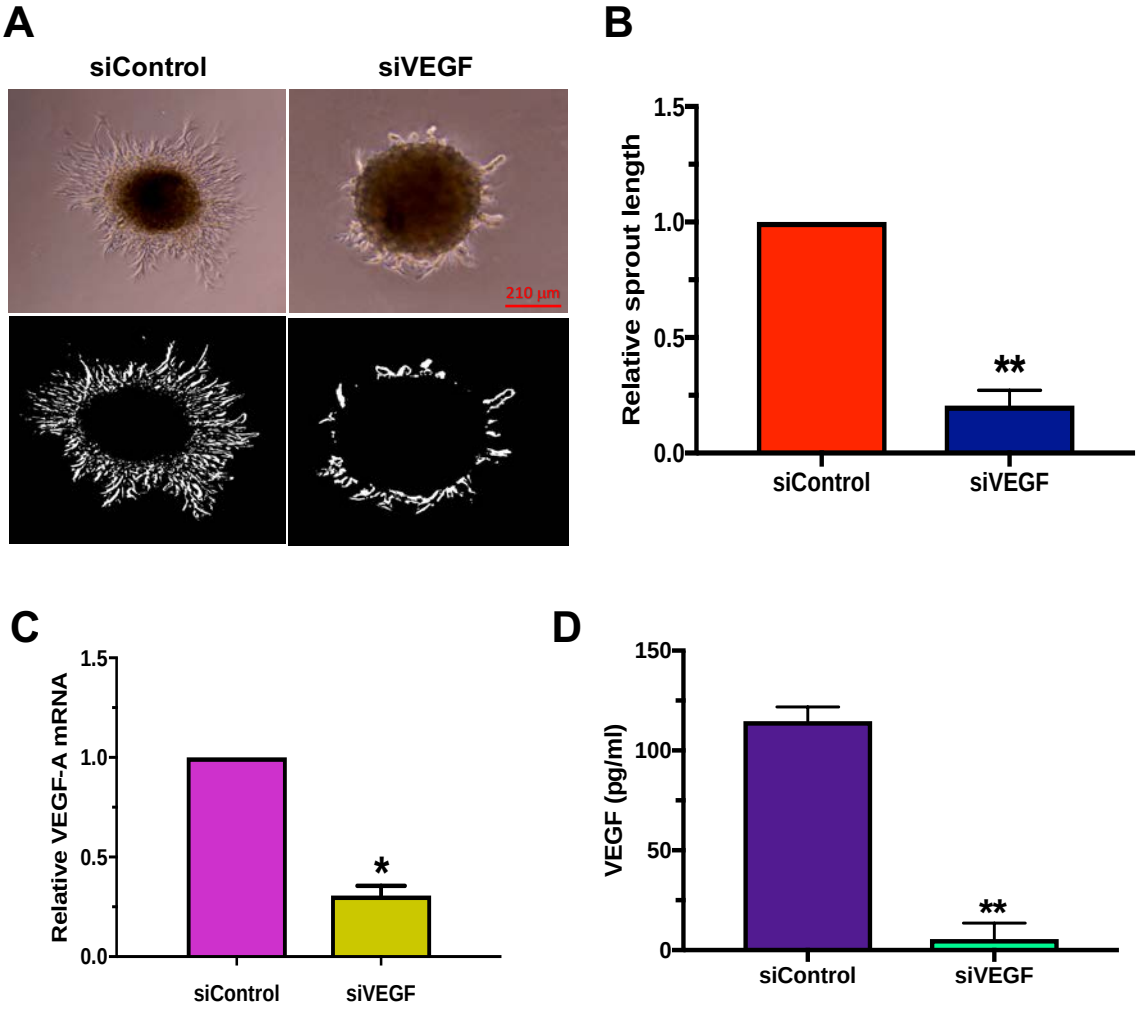

Figure 7.14: VEGF knock-down reduces hESC invasion. St-T1b cells were transfected with siRNAs targeting VEGF (siVEGF), or control (siControl) overnight. Spheroids were formed and embedded in Matrigel with the DMEM/F12 basal medium. **(A)** Representative images were taken at 24 h using an EVOS inverted phase microscope under 10 X objective and the sprout length were analysed using ImageJ. **(B)** Graph showing the mean of sprout length relative to the control. **(C)** Real-time qPCR analysis of VEGF mRNA expression normalised to β-actin. **(D)** Mean VEGF secretion from St-T1b cells by ELISA. Results are the mean (+/-SEM) of 2 experiments performed in duplicate (12 replicates per well) and using an unpaired t-test; *p<0.05, **p<0.01.

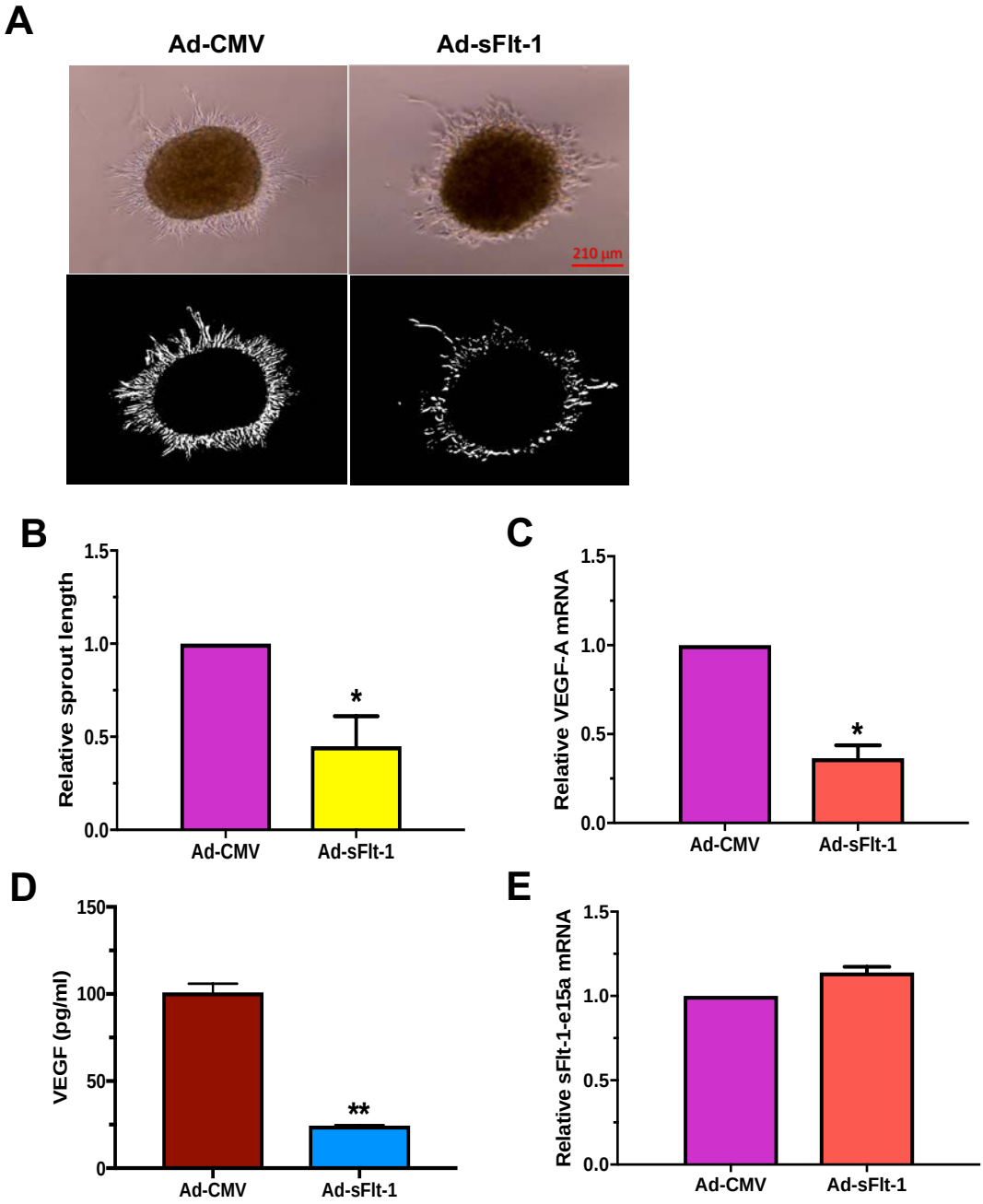

Figure 7.15: Over-expression of sFlt-1 reduces hESC invasion. St-T1b cells were transduced with adenovirus encoding murine sFlt-1-IgG-loops 1-3 (Ad-sFlt-1), or empty virus control (Ad-CMV) overnight. Spheroids were formed and embedded in Matrigel with the DMEM/F12 basal medium. **(A)** Representative images were taken using an EVOS inverted phase microscope under 10X objective and the sprout lengths were analysed using ImageJ. **(B)** Graph showing the mean of sprout lengths relative to the control. **(C)** Real-time qPCR analysis of VEGF mRNA expression. **(D)** Mean VEGF secretion from St-T1b cells by ELISA. (E) Real-time qPCR analysis of sFlt-1-e15a mRNA expression normalised to β-actin in the cells following VEGF knock-down. Results are the mean (+/-SEM) of from 2 experiments performed in duplicate (12 replicates per well); *$p<0.05$; **$p<0.01$.

7.2.8 Effect of VEGF and PIGF on phosphorylation of AKT and ERK1/2 in St-T1b cells

Although no changes of cell signalling protein activity were detected following 24 h stimulation for decidualisation (*see* **Appendix H**), it is well known that these pathways are stimulated by VEGF in endothelial cells (Takahashi *et al.,* 2003). Furthermore, Tang *et al.* (2006) reported that VEGF activates the PI3K/Akt pathway, but not ERK1/2 in normal human lung fibroblasts. Therefore, we examined the effects of VEGF and PIGF on the phosphorylation of Akt^{S473} and ERK1/2 kinases in hESC. St-T1b cells were starved overnight and treated for 0-60 mins with VEGF (50 ng/ml) or PIGF (50 ng/ml). Cell lysates were analysed by Western blotting with phospho-specific antibodies that recognise their phosphorylation at active sites of $pAkt^{S473}$, $ERK1/2^{Thr\text{-}202/Tyr\text{-}204}$ (pERK1/2) respectively. We found that $pAkt^{S473}$ and pERK1/2 was rapidly activated by VEGF, or PIGF, in a time-dependent manner, without altering the total protein levels (**Figure 7.16A**). Interestingly, unlike the PIGF-induced rapid increase in $pAkt^{S473}$ which declined after 15 min, VEGF-induced Akt phosphorylation was less rapid and sustained up to 60 mins (**Figure 7.16B**). Unlike $pAkt^{S473}$, pERK1/2 was activated after 15 min with both VEGF and PIGF treatment (**Figure 7.16C**).

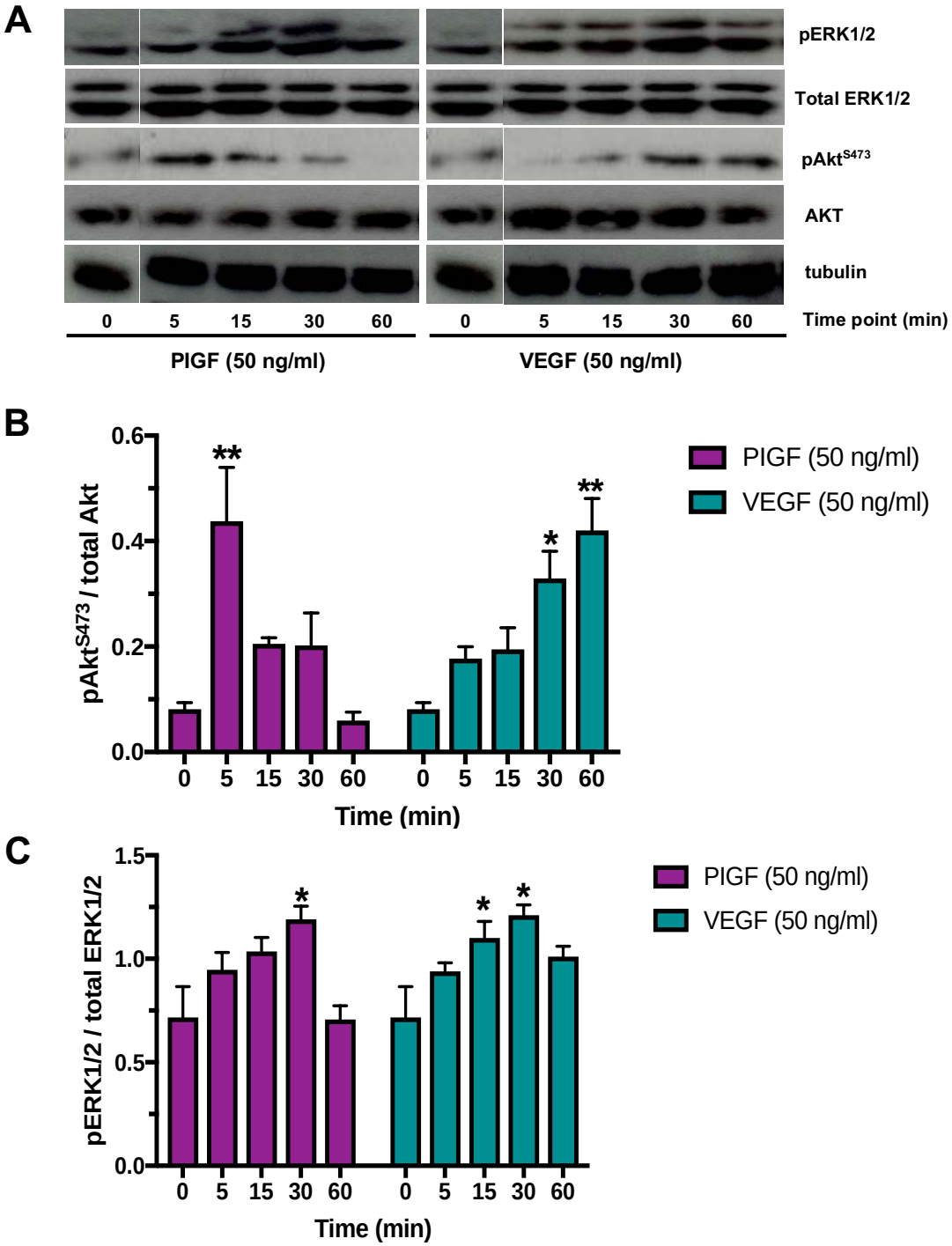

Figure 7.16: VEGF and PIGF activate Akt and ERK in hESC. Cells were treated with 50 ng/ml of PIGF or VEGF for 0-60 min. **(A)** Representative Western blots showing total Akt, pAkt^{S473}, ERK1/2, and pERK with tubulin as a control. Densitometry analysis of relative **(B)** pAkt^{S473} to total Akt and **(C)** pERK1/2 to total ERK1/2 normalised to tubulin. Results are the mean (+/- SEM) of 2 experiments and analysed using one-way ANOVA; **p<0.01; ***p<0.001.

7.2.9 Increased phosphorylation of Akt following Flt-1 knock-down

As shown in Chapter 6, VEGFR-1/Flt-1 receptor expression increased with hESC decidualisation and Flt-1 expression is reported to be required for fibroblast migration stimulated by VEGF and PIGF (Jin *et al.,* 2007). To determine whether the functional activity of Flt-1/sFlt-1 expression in hESC influences the expression of VEGF and other decidualisation related genes, Flt-1 was knocked-down with siRNAs targeting Flt-1 (siFlt-1) or control (siControl) in St-T1b cells. Flt-1 knock-down significantly suppressed the sFlt-1 isoforms in the St-T1b cells (**Figure 7.17A**). Interestingly, no significant change was observed in VEGF expression following Flt-1 knock-down (**Figure 7.17B**).

Protein expression in the cells with Flt-1 knock-down was also determined by Western blotting. Interestingly, we found increased FOXO1 protein expression (**Figure 7.18B**), but no changes in FOXO3A protein levels with Flt-1 knock-down (**Figure 7.18D**). pAkt^{S473} levels were found to increase following Flt-1 knock-down (**Figure 7.18E**) with no changes in total Akt expression (**Figure 7.18F**).

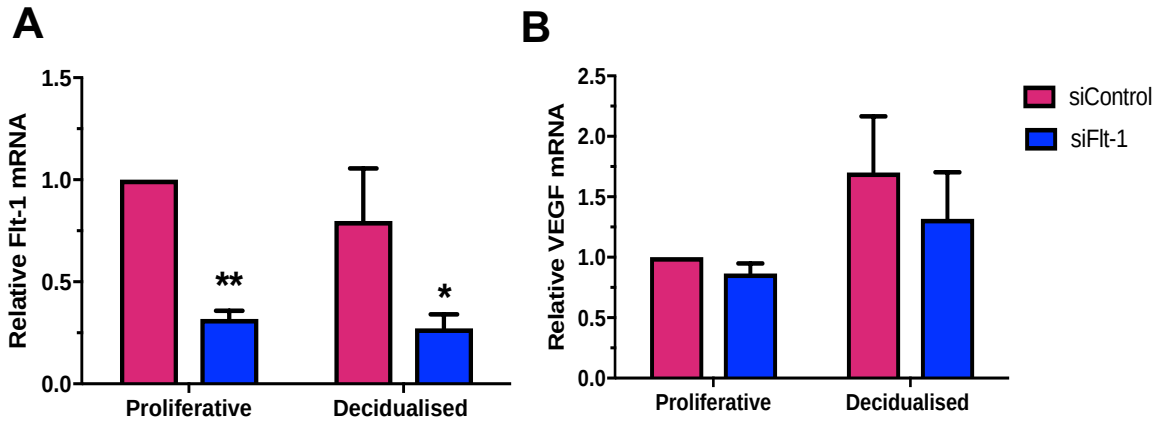

Figure 7.17: Knock-down of Flt-1 in St-T1b does not affect VEGF expression. The St-T1b cells were plated on 6-well plates and transfected with siRNAs targeting Flt-1 (siFlt-1), or control (siControl) overnight, followed by 24 h stimulation with E2 or MM1 medium. Real-time qPCR was used to measure the expression of **(A)** Flt-1 and **(B)** VEGF mRNAs. Results are the mean (+/- SEM) of 2 experiments and analysed using unpaired t-test; *p<0.05; **p<0.01.

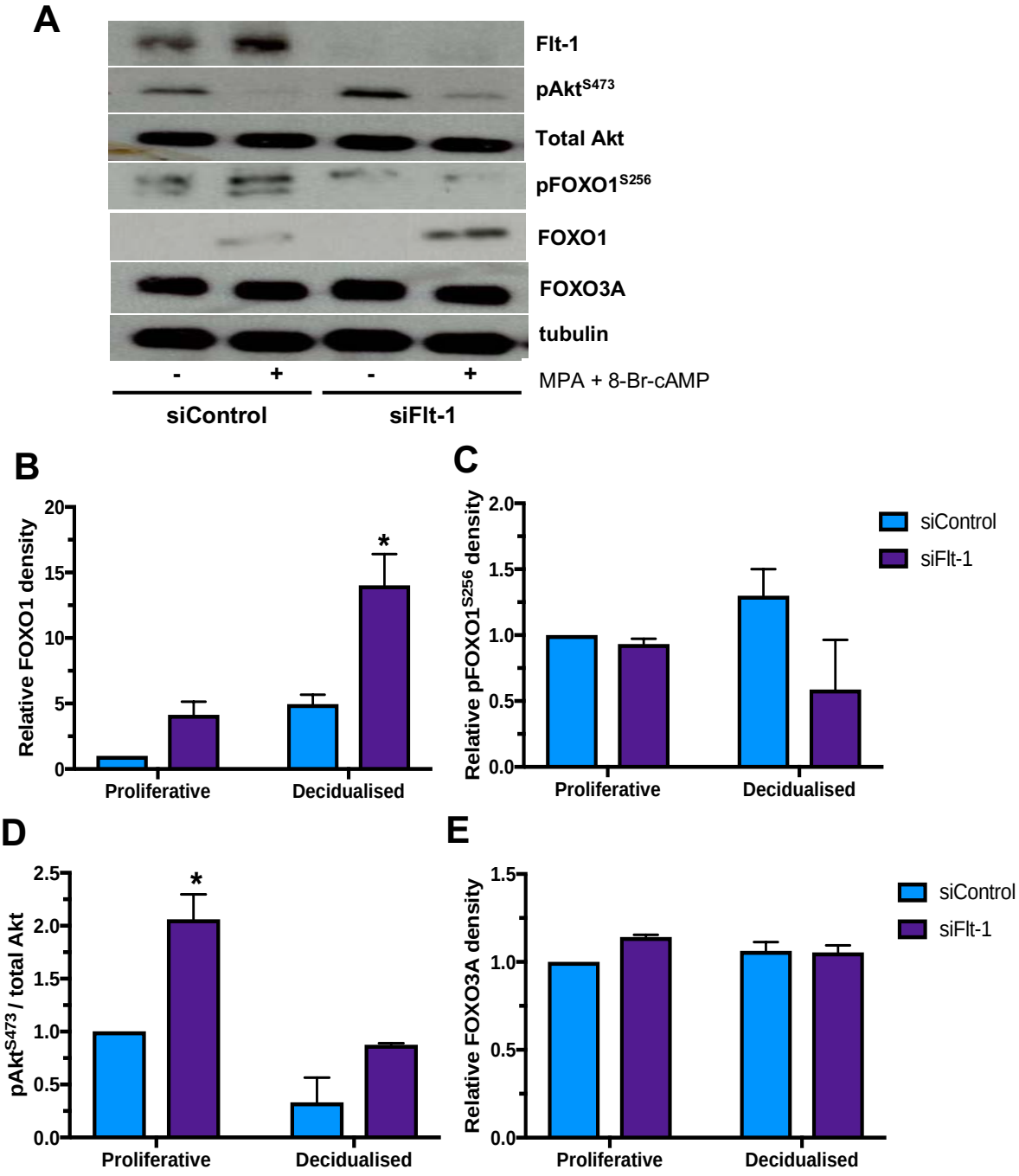

Figure 7.18: Knock-down of Flt-1 in St-T1b effects on decidualisation markers. The St-T1b cells were plated on 6-well plates and transfected with siRNAs targeting Flt-1 (siFlt-1), or control (siControl) overnight, followed by 24 h stimulation with E2 or MM1 medium. **(A)** Representative Western blot showing Flt-1, total Akt, pAkt^{S473}, FOXO1, pFOXO1^{S256}, FOXO3A with tubulin as a loading control. Graph of densitometry analysis of relative **(B)** FOXO1; **(C)** pFOXO1^{S256}, **(D)** pAkt^{S473} / total Akt, and **(E)** FOXO3A normalised to tubulin. Results are the mean (+/- SEM) of 2 experiments and analysed using unpaired t-test; *p<0.05; **p<0.01.

7.3 DISCUSSION

7.3.1 VEGF is the major angiogenic factor produced during hESC decidualisation

Angiogenesis is essential for endometrial repair and regeneration and is a critical event during decidualisation for successful pregnancy (Maybin and Critchley, 2009). Endothelial function and angiogenesis assays were carried out using St-T1b cell CM. The cells were re-stimulated with fresh medium 24 h prior to harvesting for consistency and trying to minimise the effects of nutrient depletion and accumulated waste products. Overall, decidual CM was more angiogenic than proliferative CM in endothelial cell migration, tube formation and also mixed spheroid sprouting. The angiogenic activity in proliferative CM was not significantly different from the control medium. This finding indicates that the increase in endogenous VEGF and other angiogenic factors and decrease in inhibitors produced by decidualised hESC are sufficient to stimulate endothelial cell migration, tube formation and sprouting. Furthermore, this angiogenic activity was blocked in the decidual CM by using recombinant sFlt-1, a natural inhibitor of VEGF. Endothelial cell migration and tube formation was significantly, but not fully, inhibited by the addition of recombinant sFlt-1 showing that although VEGF is the major angiogenic factor produced by decidual hESC other angiogenic factors are also produced. A range of concentrations of recombinant sFlt-1 (0, 1.0, 2.0, 3.0, 4.0 and 6.0 ng/ml) were incubated with hESC CM and VEGF levels measured by ELISA. I found a significant reduction of VEGF detected following recombinant sFlt-1 treatment (**Appendix D**). This may be due to the VEGF binding to sFlt-1 so that it is not accessible to the VEGF capture antibody. Indeed, R&D systems report that the presence of sFlt-1 can affect ELISA readings indicating that the ELISA is largely reading “free VEGF”.

In order to investigate activity of sFlt-1 in CM, sFlt-1/Flt-1 was also immunoprecipitated from the hESC CM using an anti-Flt-1 antibody. Surprisingly, CM where Flt-1 was removed by IP lead to decreased HUVEC migration in wound healing assays. Further investigation

revealed that removing sFlt-1 had also co-immunoprecipitated and removed VEGF from the CM which could be detected by ELISA (**Figure 7.10**). This was perhaps to be expected as Flt-1 has high affinity for VEGF (Shibuya, 2011). In addition, full-length Flt-1 receptor was also immunoprecipitated from CM and found to be released more in proliferative than decidual hESC which is a very surprising result. Full-length Flt-1 receptor was found on the surface of hESC (**Figure 6.10**). This suggests that the receptor is shed on micro-vesicles released into the medium. Although there are no studies in the literature characterising the release of micro-vesicles in hESC decidualisation, Tong *et al.* (2017) reported the up-regulation of Flt-1 expression on micro- and nano-vesicles in placenta from preeclampsia women compared to normal placenta. In my findings, there were higher levels of Flt-1 receptor immunoprecipitated from proliferative hESC CM suggesting proliferative hESC may produce more Flt-1 containing micro-vesicles. Taken together with the findings in Chapter 6, decidual hESC express more Flt-1 receptor, but they shed less from their cell surfaces and express less sFlt-1 leading to increased VEGF activity and potentially greater responsiveness of hESC themselves to VEGF during decidualisation.

Tong *et al.* (2017) also showed that micro-vesicle removal did not affect the total sFlt-1 secretion. Furthermore, vesicle-bound VEGF was also detected shed by placenta and removal of micro-vesicles significantly reduced VEGF levels. In decidual hESC CM there was reduced VEGF with no significant change of total sFlt-1 detected. This may be explained by the fact that Flt-1/sFlt-1 immunoprecipitation from decidual CM differentially removed vesicle-associated Flt-1 and subsequently removing vesicle-associated VEGF did not greatly affecting the already suppressed sFlt-1 levels. Total sFlt-1/Flt-1 levels were also found to significantly decrease in proliferative hESC CM, which contains significantly more sFlt-1 prior to IP than decidual hESC and suggests that micro-vesicle bound Flt-1 is being

detected in the ELISA. Therefore, further investigation is required to determine the role of micro-vesicle shedding in hESC and to examine whether VEGF and Flt-1 are vesicle-associated. Probing the Western blotted IP material for VEGF would confirm whether VEGF is co-precipitated with Flt-1.

Collectively, VEGF produced during hESC decidualisation was the main factor contributing to the pro-angiogenic activity in decidual hESC CM. This is consistent with a recent study by Wheeler *et al.* (2018) showing that VEGF in decidual primary hESC CM is one of the major factors contributing to macrophage, migration and polarisation.

7.3.2 Angiogenesis assays and mixed cell spheroid sprouting

To investigate sprouting from matrix embedded spheroids, I initially tested spheroids formed from HUVEC alone, but they did not form well and were found to break up in sprouting assays as shown in **Appendix C**, making them difficult to analyse. Therefore, mixed spheroids composed of HUVEC and St-T1b cells were used in this study. Good sprouting results were obtained with multicellular spheroids in the present study, but due to time limitations, I was not able to investigate the nature of the sprouting fully and subsequently I do not know whether the sprouts contain both endothelial or St-T1b cells. In order to answer this question, the cells could be labelled with fluorescent dyes prior to mixing for spheroids formation with cell tracer dyes visualise them under the fluorescence microscope.

7.3.3 FOXO1 and FOXO3A, pro-angiogenic factors in endothelial cell function

FOXO1 and FOXO3A have distinct roles in human endometrium, activation of FOXO3A upon prolonged oxidative stress triggers oxidative cell apoptosis, whereas FOXO1 stimulates differentiation and oxidative stress resistance during hESC decidualisation (Kajihara *et al.,* 2006). As discussed in **Chapter 5**, FOXO1 and FOXO3A were found to positively and negatively regulate VEGF expression in hESC during decidualisation. In the

present study, the CM collected from the FOXO1, or FOXO3A knock-down St-T1b cells were used to examine the role of FOXO1 and FOXO3A in the overall angiogenic activity of hESC using endothelial migration and *in vitro* tube formation assays. FOXO1 knock-down CM was found to decrease tube formation, but not migration. In contrast to FOXO1, there was no significant change in HUVEC migration and tube formation with FOXO3A knock-down CM.

Therefore, FOXO1 appears to be a key regulator of hESC pro-angiogenic activity during decidualisation. In addition to VEGF, the angiogenic factor, HGF was found to be up-regulated in decidual CM (**Chapter 3**) and is reported to be regulated by FOXO1 (Vasquez *et al.*, 2015; Potente *et al.*, 2005). Further investigation is needed to determine changes in hESC secreted angiogenic factors following FOXO1 or FOXO3A knock-down.

7.3.4 VEGF increases hESC function

In the present study, VEGF was found to increase hESC migration and invasion in both proliferative and decidual hESC. These findings are in direct contrast with previous findings by Schwenke *et al.* (2013) who reported VEGF and PIGF do not enhance hESC chemotactic and chemokinetic migration. This may be because lower concentrations of VEGF (20 ng/ml) were used for their studies compared to 50 ng/ml of VEGF in my study. VEGF activity is reported to be a highly concentration-dependent when examined in tissue environment, with different threshold concentrations required dependent on function (Ozawa *et al.*, 2004). In addition, the production of saturating amounts of VEGF, or sFlt-1, by the cultured cells might also lead to these differences between studies. PIGF was found to increase proliferative hESC migration, but not in decidual hESC. This may be due to PIGF binding to sFlt-1 and displacing VEGF in proliferative hESC and therefore promoting migration.

Decidual hESC produced lower levels of sFlt-1 therefore is less potential for VEGF displacement from sFlt-1.

Furthermore, decidualisation was found to stimulate hESC migration and invasion suggesting potential autocrine activity of VEGF in hESC function. The migration and invasion in decidual hESC was higher compared to proliferative hESC. However, a recent study in human immortalised ESC (HIESC), Fabi *et al.* (2017) found that decidual HIESC showed significantly reduced cell motility and failed to close the scratch-wounds. This may be because of differences in the decidualisation method used. In this study, St-T1b cells were decidualised with cAMP and MPA for 6 days and then re-plated before performing the wound healing assays. Whereas, Fabi *et al.* (2017) performed the wound healing assay by treating with cAMP and MPA directly on the wounded hESC without pre-decidualising the cells. One possibility is that there are differences in hESC function during decidualisation, which are not expressed within 24 h. In addition, the presence of progesterone, which has been reported to inhibit endometrial cell migration, could inhibit wound closure in hESC (Gentilini *et al.,* 2007). Furthermore, cAMP has also been reported to inhibit MEF migration (Chen *et al.*, 2008). We performed the assays in DMEM/F12 basal medium, so they were not directly influenced by the presence of oestrogen, progesterone, or high levels of exogenous cAMP.

A recent study reported that isolated human eutopic mesenchymal stem cells transduced with adenovirus encoding sFlt-1 had significantly reduced VEGF expression and lead to endometriotic lesions (Gopalakrishnan *et al.,* 2016) supporting my finding that hESC transduced with Ad-sFlt-1 show decreased VEGF mRNA expression and subsequently reduced invasion/migration. siRNA-mediated VEGF knock-down St-T1b cell and over-expression of sFlt-1 St-T1b cell spheroids using adenovirus was found to reduce the hESC

invasion activity. These findings suggest that VEGF may promote hESC invasion in an autocrine manner which needs further investigation to determine whether this is an intracrine or extracrine effect on hESC function. This could be examined through the knock-down, or over-expression of VEGF and Flt-1 and/or NRP-1 receptors and analysis of ESC function.

7.3.5 Induction of Akt and ERK1/2 phosphorylation by VEGF in ESC

In the present study, we demonstrated that VEGF stimulates the migration and invasion of hESC. Although the precise mechanism by which VEGF induces hESC migration and invasion are unknown, Gentilini *et al.* (2007) demonstrated that growth factors like PDGF-BB, and EGF are an important promoter of the dynamic behaviour of ESC and stimulate migration by activation of both PI3K/Akt and ERK1/2 pathways. Previous studies have also reported that Akt plays an important role in endometrium (Veillette *et al.,* 2013; Fabi *et al.,* 2017). In addition, the PI3K/Akt pathway was reported to be involved in the control of invasion, and chemotaxis in hESC (Schwenke *et al.*, 2013; Li *et al.,* 2012; Gentilini *et al*., 2007).

In the present study, the level of $pAkt^{S473}$ was found to be decreased in decidualisation, this is consistent with previous studies showing that Akt is activated by PI3K in response to growth factors, and that PI3K/Akt signalling pathway activity is reduced during decidualisation (Yoshino *et al*, 2003; Fabi *et al.,* 2017). However, we failed to detect changes in protein phosphorylation using phospho-kinase arrays (**Appendix H**). This is likely to be due to the sensitivity of the arrays or the fact that cells were stimulated over 24 h rather than over shorter time periods. This needs to be investigated further in the future. The $pAkt^{S473}$ and pERK1/2 (Thr202/Tyr204) was rapidly activated by exogenous VEGF and PIGF stimulation in a time-dependent manner in hESC. Our findings suggest that PI3K/Akt and ERK1/2 may mediate VEGF and PIGF-stimulated migratory responses in hESC. Further

studies are needed to determine the signalling pathways responsible for VEGF-mediated hESC migration through the use of selective PI3K/Akt and ERK1/2 pathway inhibition.

Furthermore, sFlt-1/Flt-1 knock-down was found to increase $pAkt^{S473}$ suggesting that Flt-1 activity in hESC suppresses the Akt pathway. Furthermore, knock-down of Flt-1 also increased FOXO1 activity through FOXO1 up-regulation and insignificantly decreased FOXO1 phosphorylation. Although the role of Flt-1 signalling during hESC decidualisation remains unclear, these findings suggest that Flt-1 may play a role in hESC decidualisation via suppression of the Akt pathway promoting decidualisation in hESC. This suggests that VEGF-induced migration and invasion of hESC may mediated, at least in part, through Flt-1 and not VEGFR-2/KDR as we could not detect VEGFR-2 expression in hESC. The hESC did however express the VEGF co-receptor neuropilin-1.

7.3.6 VEGF receptors in ESC

As discussed in chapter 6, Flt-1 was maintained in hESC during decidualisation consistent with the earlier studies showing that Flt-1 is expressed in ESC in the secretory phase and decreases in the late secretory phase of the menstrual cycle (Krussel *et al.*, 1999; Perrot-Applanat *et al.*, 2000; Jee *et al.*, 2009). There are many studies on VEGFR-2 expression in endometrium, but it is controversial. Sugino *et al.* (2002) isolated hESC from proliferative phase endometrium followed by *in vitro* decidualisation with oestrogen and MPA for 18 days and showed that VEGFR-2 mRNA was significantly increased, with no changes detected in Flt-1 mRNA expression. In the present study, VEGFR-2 mRNA and protein was not detected in hESC. A study in isolated mouse endometrial epithelial cells and ESC showed that only low mRNA levels of VEGFR-2 detected in ESC (Fan *et al.*, 2008).

NRP-1 was also found to be expressed in both epithelial and stromal cells with much higher expression in ESC (Fan *et al.*, 2008). My results showed that NRP-1 protein was expressed

in hESC and its expression increased with decidualisation. In contrast, one histological study in human endometrial samples obtained from healthy women in proliferative and secretory phase of menstrual cycle showed that NRP-1 expression was higher in proliferative hESC than in secretory cells (Hess *et al.*, 2009). Furthermore, a study of proliferative and secretory phase human endometrial tissue from healthy women showed a high but stable expression of NRP-1 mRNA throughout the menstrual cycle (Germeyer *et al.*, 2005). In addition, NRP-1 has been shown to interact with Flt-1 in mouse embryonic fibroblasts (NIH3T3) (Fuh *et al.,* 2000) leading to the possibility that NRP is regulating Flt-1 activity in hESC. Flt-1 also been reported as negative regulator of angiogenesis by competing with NRP-1 (Fuh *et al.,* 2000). There is also some evidence which suggests that NRP-1 may act as signalling receptor for VEGF (Becker *et al.,* 2005), however other studies dispute this fact. NRP-1 deletion in transgenic mice led to *in utero* death due to severe cardiovascular defects and defective vascular remodelling (Kawasaki *et al.,* 1999; Kitsukawa *et al.,* 1997). Further investigation is required to determine whether VEGF is acting via both NRP-1 and Flt-1 to alter hESC function.

7.3.7 Conclusion

In summary, I have demonstrated increased pro-angiogenic secretions of decidual hESC confirming that VEGF is the main angiogenic factor in these cells and concomitant changes in sFlt-1 contribute to increased VEGF activity. The angiogenic activity of decidualised CM was found to be significantly greater than proliferative CM. Furthermore, using well-established *in vitro* model systems, we demonstrate that both endogenous and exogenous VEGF can stimulate hESC migration and invasion. Akt and ERK1/2 signalling pathways were shown to be involved in VEGF-induced signal transduction in hESC decidualisation. Moreover, Flt-1 may play an important role in regulating hESC decidualisation.

CHAPTER 8:
GENERAL DISCUSSION

8.1 General discussion

The initial aim of my thesis was to characterise the *in vitro* decidualisation of the St-T1b cell line. My results clearly demonstrate that the St-T1b line behaved in a very similar manner to primary hESC and was therefore a suitable model system to investigate the underlying mechanisms regulating VEGF expression and activity during decidualisation.

8.1.1 Regulation of VEGF expression and activity in hESC decidualisation

VEGF is essential for vascular remodelling, regeneration and maturation of the endometrium, implantation and maintenance of pregnancy. This is highlighted by the fact that inappropriate expression of sFlt-1 may disrupt implantation or lead to miscarriage or fetal growth restriction in mice (Zenclussen *et al.*, 2014). Preeclampsia remains one of the most serious complications of pregnancy (Duley, 2009; Hutcheon *et al.*, 2011) and although the underlying aetiology of the disease is unknown, high levels of sFlt-1 produced by the placenta enter the maternal circulation and reduce VEGF activity, disrupting vascular homeostasis and precipitating the symptoms of preeclampsia. As decidual hESC are an important source of VEGF in the endometrium, the balance of VEGF and sFlt-1 expression in these cells is likely to be critical for a successful pregnancy.

Various transcription factors have been reported to regulate *VEGF* gene transcription such as Sp1/3, AP-2, EGR-1, STAT3 and HIF-1α (Pages and Pouyssegur, 2005). Hypoxia is the major physiological regulator of VEGF expression leading to increased HIF-1α binding to the *VEGF* promoter up-regulating VEGF mRNA expression and stabilisation (Sharkey *et al.*, 2000). In the absence of pregnancy progesterone levels decline as the corpus luteum degenerates during the late secretory phase and menstrual phase of the cycle. This triggers the inflammatory response in the endometrium to initiate menstruation (Critchley *et al.*, 1999; Maybin and Critchley, 2009). There is an increase of endometrial prostaglandin

synthesis (PGE_2) following progesterone withdrawal (Sugino *et al.*, 2004), which causes intense vasoconstriction of endometrial spiral arterioles, subsequently leading to hypoxia increasing HIF-1α stabilisation (Sharkey *et al.*, 2000; Maybin *et al.*, 2011; Maybin *et al.*, 2018). This results in up-regulation of VEGF during the menstrual and early proliferative phases (Maybin *et al.*, 2011; Maybin *et al.*, 2018). However, low HIF-1α levels were detected during the early and mid-secretory phase (Maybin *et al.*, 2018), which indicates that the up-regulation of VEGF during the secretory phase is not driven by HIF-1α.

Progesterone was reported to directly regulate VEGF in mouse primary stromal cells via progesterone receptors (Kim *et al.*, 2013). Additionally, two PREs have been identified in the VEGF promoter within a 1.9 kb fragment upstream of the transcription start site (Figure 1.10) which positively regulate VEGF expression in endometrial adenocarcinoma cells (Mueller *et al.*, 2003). However, my results contradict this, and progesterone alone did not induce VEGF in primary hESC or the St-T1b cell line even following long-term stimulation.

8.1.1.1 FOXO1 and FOXO3A regulate VEGF expression in hESC

FOXO transcription factors were found to regulate VEGF expression during hESC decidualisation *in vitro*. FOXO1 positively regulated VEGF expression, while FOXO3A negatively regulated VEGF expression during decidualisation. Thus, the balance of FOXO1 and FOXO3A activity in hESC is important for appropriate VEGF expression during decidualisation. High progesterone levels are important for establishing the decidual phenotype during the secretory phase and its maintenance during pregnancy. Progesterone signalling is important in hESC for survival through induction, translocation and inactivation of FOXO1 during decidualisation (Labied *et al.*, 2006). During decidualisation, progesterone levels up-regulate relaxin, prostaglandins and subsequently increase intracellular cAMP, activating the PKA pathway inducing the expression of FOXO1

(Christian *et al.*, 2002) (*see* **Figure 1.8**). Phosphorylation of FOXO proteins by Akt inhibits their transcriptional activity by retaining them in the cytoplasm. Since progesterone is crucial for FOXO1 activity, the effect of progesterone on *VEGF* regulation is important. Although progesterone did not directly affect VEGF expression and secretion in hESC, *VEGF* was strongly induced by cAMP indicating that the PKA pathway is important in regulating VEGF expression through FOXO1 up-regulation in hESC. This could be further explored through the use of PKA inhibitors or knock-down approaches. This is consistent with a recent RNAseq and ChIPseq study which looked at global FOXO1-dependent changes in hESC (Vasquez *et al.*, 2015). VEGF is one of the 437 genes that was identified to be regulated by FOXO1 by RNAseq although not confirmed by qPCR or Western blotting.

Three FOXO binding sites were identified in a 3 kb region of the *VEGF* promoter up-stream from the start site (*see* **Figure 5.21**). Of these sites, the greatest enrichment, indicating occupancy of FOXO1, in hESC was at the VEGF ChIP-3 site (*see* **Figure 5.21**). Interestingly, when we performed ChIP experiments in endothelial cells, FOXO1 bound to all three sites with the greatest enrichment at VEGF-ChIP-1 site (*see* **Appendix B1**). Our results are consistent with a recent study which showed that FOXO1 binds directly to the same site in the *VEGF* promoter in keratinocytes (Jeon *et al.*, 2018). In addition, Kikuchi *et al.* (2012) reported that FoxO1 binds in the same region of the mouse *VEGF* promoter in the β-cells of the pancreas.

FOXO3A bound to the same sites in the *VEGF* promoter as FOXO1 and the ChIP-3 site was also showed the greatest enrichment of FOXO3A (**Figure 5.22**). Karadedou *et al.* (2012) reported that FOXO3A negatively regulates VEGF expression by binding to the ChIP-M1 FHRE site by competing with FOXM1 in the breast carcinoma cells. Interestingly, there was no enrichment of FOXO1 or FOXO3A at this site in hESC or the HMEC-1 microvascular

endothelial cell line (*see* **Appendix B3**). My findings showed that FOXO3A knock-down increased FOXM1 expression in hESC, and FOXM1 inhibition up-regulated FOXO3A expression which may subsequently decrease VEGF expression. This could be investigated by examining the effect of over-expression, or knock-down, of FOXM1 on VEGF and FOXO3A mRNA and protein expression followed by ChIP assays to determine if there is an enrichment of FOXM1 to the *VEGF* promoter in hESC. This antagonistic relationship between FOXO1 and FOXO3A may have implications for the level of VEGF expressed in the endometrium in various pathologies which are characterised by increased oxidative stress.

8.1.2 Regulation of sFlt-1/Flt-1 expression in hESC

The sFlt-1-e15a isoform is predominantly produced by non-endothelial cells and the placenta, whereas endothelial cells express sFlt-1-i13 almost exclusively (Sela *et al.*, 2009; Jebbink *et al.*, 2011). In agreement with these studies, sFlt-1-e15a was found to be the predominant isoform produced by decidual hESC (**Appendix J**). sFlt-1 secretion was strongly down-regulated in decidual hESC consistent with a recent study (Cottrell *et al.*, 2017). Interestingly, sFlt-1-i13 and sFlt-e15a mRNAs were differentially expressed during hESC decidualisation with sFlt-1-e15a being strongly down-regulated. However, the molecular steps leading to the alternative splicing of Flt-1 mRNA to produce sFlt-1 during decidualisation have yet to be elucidated. Therefore, it is important to research this further and examine the activity of factors involved in mRNA splicing such as JMJD6 in hESC decidualisation (Palmer *et al.*, 2016). This could be investigated by determining changes in JMJD6 expression with hESC decidualisation and assessing sFlt-1 isoform expression following over-expression or knock-down of JMJD6 expression in these cells.

Flt-1 was found to be regulated by FOXO1, but not FOXO3A in hESC which is consistent with the study of Potente *et al.* (2005) performed in endothelial cells. Vasquez *et al*. (2015) also showed that Flt-1 expression is positively associated with FOXO1 activity by RNAseq in hESC (Vasquez *et al.*, 2105). However, although the full-length Flt-1 receptor is maintained during decidualisation, the level of sFlt-1, and in particular sFlt-1-e15a, decreased with FOXO1 knock-down, which indicates that FOXO1 activity is also affecting the splicing of Flt-1 mRNA.

Taken together, FOXO1 and FOXO3A play a key role in regulating VEGF levels in hESC. It will be important to confirm this activity *in vivo* using a selective endometrial FOXO1 knock-out mouse model. This could be achieved by crossing the floxed FOXO1 mice (Tanaka *et al.*, 2009) with a suitable Cre driver line such as progesterone receptor Cre mice (Hawkins *et al.*, 2012). Similar studies could then be performed using FOXO3A floxed mice. In addition to changes in VEGF and sFlt-1 levels the impact of the loss of endometrial FOXO1 and FOXO3A could then be examined on fertility, litter size and placental and fetal weight. Several attempts were made to isolate ESC from the floxed FoxO mice to extend these studies and confirm the same pattern of regulation in the mouse. Unfortunately, once isolated these cells did not proliferate in culture beyond the first passage. Recent reports have suggested a requirement for specific culture medium supplemented with growth factors to maintain mouse ESC culture (De Clercq *et al.*, 2017). In the present study, MEFs isolated from floxed FoxO mice were also used which were easy to isolate in large numbers and could be cultured for 2 to 3 passages before they started to senesce. FoxO1 was found to regulate both VEGF and Flt-1 in MEFs confirming the data obtained in hESC and underlining the broader significance of FoxO1 in regulating these genes in cells of the

fibroblast lineage. Similar MEF studies should be used for FOXO3A. This would then lead on to the examination of FOXO3A on the VEGF and sFlt-1 regulation in hESC.

8.1.3 VEGF angiogenic activity in hESC secretions

VEGF was found to be the main angiogenic factor produced by decidual hESC as the angiogenic activity in CM was almost completely blocked by sFlt-1 in *in vitro* angiogenesis assays. The CM of hESC following FOXO1 knock-down also showed reduced endothelial cell tube formation suggesting that FOXO1 up-regulation in hESC is the key factor in promoting their pro-angiogenic activity. Indeed, a number of angiogenic factors such as HGF were identified that were up-regulated in decidual hESC, and are reported to be associated with angiogenesis and wound repair driven by FoxO1 (Mori *et al.*, 2014).

8.1.4 VEGF and hESC function

I have shown that the Flt-1 receptor is present on the surface of hESC and its promoter activity up-regulated/maintained in hESC during decidualisation. Exogenous VEGF stimulated intracellular signalling and migratory activity of hESC. As I could not detect VEGFR-2 expression in hESC, Flt-1 and NRP-1 that are present must be mediating hESC migration and invasion driven by VEGF and PIGF. Flt-1 has also been reported to be expressed in other types of fibroblast, for example, human corneal fibroblasts (Berthaut *et al.*, 2009) and gingival fibroblasts (Ohshima *et al.*, 2016). Although there are many studies on the activity of Flt-1 and NRP-1, there are only limited reports in the endometrium. In agreement with my findings, Flt-1 and NRP-1 were detected in stromal cells by immunohistochemistry and up-regulated during the secretory phase (Krussel *et al.*, 1999; Fan *et al.*, 2008). The PI3K/Akt and ERK1/2 signalling pathways were found to stimulated by VEGF and PIGF in hESC. However, their full role in hESC function and decidualisation remain to be determined.

VEGF can activate many critical signalling pathways such as ERK1/2 and Akt in endothelial cells (Gerber *et al.,* 1998; Gupta *et al.,* 1999; Dimmeler and Zeiher*,* 2000; Dellinger *et al.,* 2011), Tang *et al.* (2006) reported that VEGF regulates via PI3K/Akt pathway in normal human lung fibroblasts. In the present study, VEGF was found to activate Akt and ERK1/2 in a time-dependent manner consistent with previous studies in many cell types, for example, porcine trophectoderm cells and hESC (Schwenke *et al.*, 2013). VEGF increased phosphorylation of both Akt and ERK1/2 in a time-dependent manner which was blocked by the PI3K inhibitor (LY294002) (Jeong *et al.*, 2014). While Schwenke *et al.* (2013) demonstrated that inhibition of PI3K/Akt pathway with Wortmannin inhibits the chemokinesis and chemotaxis in hESC. Many studies have demonstrated that the PI3K/Akt signalling pathway plays a central role in mesenchymal cell proliferation, migration, differentiation and angiogenesis (Chen *et al.*, 2013). VEGF was found to regulate hESC migration and sprouting/invasion. However, its direct effect on hESC function and decidualisation remains to be determined. Therefore, it is important to selectively inhibit the PI3K/Akt or ERK1/2 pathway to determine which signalling pathway is involved in hESC migration and sprouting.

Surprisingly, both Akt and ERK1/2 activity were found to be up-regulated in unstimulated hESC following Flt-1 knock-down in hESC demonstrating that activation of these signalling pathways is mediated by Flt-1. Moreover, Akt activity rapidly decreased after 5 min of VEGF treatment. ERK1/2 activity also decreased slightly after 15 min of VEGF treatment and this suppression was only sustained until 30 min of treatment. These results suggest that Flt-1 signalling may be important in hESC function. However, further studies are needed to determine whether Flt-1 mediates these effects on cell signalling alone or requires the presence of NRP-1. NRP-1 has been shown to interact with Flt-1 in mouse embryonic

fibroblasts (NIH3T3) (Fuh *et al.,* 2000) leading to the possibility that NRP-1 is regulating or contributing to Flt-1 activity in hESC. Furthermore, Flt-1 has been proposed to act as a negative regulator of angiogenesis in NIH3T3 by preventing NRP-1 binding to VEGF165 (Fuh *et al.*, 2000). To access this, experiments should be performed examine VEGF-mediated signalling and function in hESC following Flt-1 receptor or NRP-1 knock-down.

8.2 Limitations and future directions

8.2.1 Complexity of cellular interactions in cycling human endometrial tissue and models for research

Endometrial tissue homeostasis, cellular proliferation, metabolism and reproductive function are mediated by the orchestrated crosstalk between these diverse cell populations via paracrine and endocrine pathways (Kurita *et al.*, 1998; Chen *et al.*, 2013; Li *et al.*, 2005). Histologic analysis of the cycling endometrial microenvironment consistently reveals luminal and glandular epithelial cells supported by ESC, and a complex vascular bed composed primarily of spiral arterioles and capillaries that undergo remodelling processes during the menstrual cycle to provide the nutrition and oxygen to the tissue maintaining homeostasis (Herington *et al.*, 2011). Although ESC represent a large component of human endometrium, there are epithelial cells and a dynamic flux of resident or infiltrating immune cells. The immune cell component of the endometrium is composed of both resident and recruited leukocytes that primarily include macrophages, uNK cells, T cells and neutrophils (Russell *et al.*, 2011). The relative numbers of these immune cell types is hormonally regulated within the endometrium throughout the menstrual cycle and the withdrawal of P4 induces a sharp increase in immune cell infiltration during menstruation (Russell *et al.*, 2011). The immunological axis of endometrial function plays a critical role in protecting this open tissue from infectious pathogens, while being permissive to the invasion of an allogenic

embryo. Thus, the relative somatic cell numbers, proliferative states, architectural complexity and immune cell ratios within the endometrium vary significantly across each phase of the menstrual cycle further adding another level of complexity to endometrial research related to health and disease. Unfortunately, much of current knowledge of the human endometrial microenvironment relies on histological analysis of the endometrium and an analytical bandwidth that limits ability to fully understand the complex multi-cellular interactions and intrinsic molecular signatures that are necessary to maintain reproductive health.

Appropriate tissue acquisition and characterisation protocols are essential for clinical and basic science research settings and coupled with accurate histological examination, allows researchers to obtain specific cell populations for designing *in vitro* studies. Clinical endometrial research has focused almost exclusively on the histological and pathological analysis of biomarkers of disease from examination of *ex vivo* tissues (Aplin, 1989). Alternatively, isolated human cells can be used prospectively for *in vitro* culture studies. Several protocols to obtain primary human endometrial cells (*e.g.* epithelial glands and stroma), as well as endothelial cells, from endometrial biopsies using enzyme digestion of the tissue have been established. The ability to culture hESC *in vitro* culture has greatly advanced our understanding of implantation. However, the technical simplicity of current cell culture models often fails to recapitulate the complex tissue microenvironment to which cells are exposed *in vivo*. The intra-patient variability between tissue samples has hindered the reproducibility of many studies and therefore investigations are often limited to single cell type *in vitro* studies, typically focusing on either the biology of epithelial cells or stromal fibroblasts, and to a much lesser extent the vascular and immune components (Albrecht, 2003; Sha *et al.*, 2007). Specifically, current models fail to mimic fully the physiological

changes that occur within the endometrium within a typical 28-day menstrual cycle in response to endocrine signals and the complex inter-cellular communication that regulate endometrial function. These experimental constraints have limited our understanding of the cellular and molecular mechanisms that drive reproductive function.

Due to ethical considerations and the complexity of interspecies *in vivo* studies, experiments with endometrial implants and explants or *in vitro* culture of isolated ESC would be preferable. The most informative experimental set up, in my opinion, would involve human and mouse ESC, which should identify any interspecies variability and provide complimentary results. Future studies would aim to validate the findings of this thesis in hESC decidualisation *in vitro* using mouse decidualisation models. Mouse models have been widely utilised to investigate the process of decidualisation *in vivo*. However, the reproductive cycles of non-human mammals vary widely, particularly in the murine species which do not have a menstrual cycle, but rather an oestrous cycle (Ramathal *et al.*, 2010). This issue with rodent models is a point of concern because they are the most widely used as *in vivo* models throughout drug development and toxicology. One of the reasons why human menstruation is not fully understood is the fact that this process has proved difficult to model experimentally. Menstruation only occurs in a few species including old world monkeys, apes and, of course, humans (Cameron *et al.*, 1998). The most similar *in vivo* model to human endometrium is currently the macaque, but high costs, low throughput and ethical issues have limited the use of these animals for advancing reproductive biology (Greaves *et al.*, 2017). In contrast, the relative low cost, easy maintenance and utility of murine models has been essential to the growth of biomedical research. Although mice do not menstruate and are not susceptible to endometrial conditions like endometriosis, the regulation of uterine function essentially mirrors that in women with cell proliferation during

an E2-dominated phase (proestrous) and functional maturation during a P4-dominated phase leading to development of a "window of uterine receptivity" stimulated by the action of E2 on the P4 primed uterus (Paria *et al.*, 2002; Bruner-Tran *et al*., 2018). To accomplish murine to human translation it is critically important to replicate and validate murine findings using murine models which better recapitulate the human condition *in vivo*. The development of humanized murine models or robust *in vitro* human models may each provide an alternative to overcome the issues discussed above. The ease of genetic manipulation in the mouse and commercial availability of genetically engineered murine models provides a clear advantage for *in vivo* research. Specifically, the grafting of human tissues or cells in immunodeficient mice and the ability to selectively control sex steroids provides suitable *in vivo* models for studying human endometrial processes.

8.2.2 Further investigation of the regulation of VEGF and implications for endometrial and pregnancy-related disorders

Total VEGF mRNA expression and protein secretion was observed in this thesis. The pattern of total VEGF mRNA expression differed from that of VEGF protein secretion in hESC under some conditions. This may be a result of alternative VEGF isoform expression. For example, if relative $VEGF_{121}$ and $VEGF_{165}$ mRNA increased and $VEGF_{189}$ mRNA decreased, this may result in no significant overall change in total VEGF mRNA levels, but increased VEGF protein secretion may be detected by ELISA due to the relative increase in soluble isoforms which the ELISA assay detects in cell supernatants and a decrease in the largely cell/ECM associated $VEGF_{189}$. Moreover, the primers for total VEGF will detect the inhibitory $VEGF_{xxx}b$ isoforms (Gu *et al.*, 2013) as well as the more common active $VEGF_{xxx}a$ isoforms. Therefore, if $VEGF_{xxx}a$ mRNA increased and $VEGF_{xxx}b$ mRNA decreased, no overall change in total VEGF mRNA and protein secretion would be observed,

although there may be greater overall VEGF activity. Therefore, to further our understanding of VEGF expression in ESC, VEGF isoform-specific changes should be investigated using real-time qPCR as previously published (Walter *et al.*, 2010) and isoform specific ELISAs. Furthermore, ELISA assays were used to detect the VEGF, or sFlt-1 protein released into culture supernatants. Therefore, if $VEGF_{121}$ and $VEGF_{165}$ are bound to Flt-1 on ESC, or sFlt-1 in solution, then the levels of VEGF detected would be lower than the total amount produced by the cells. To overcome this issue and gain a better understanding of total VEGF levels and isoforms present in the ESC during decidualisation, Western blotting using antibodies that detect all VEGF protein isoforms, as well as antibodies selective for each isoform should also be performed.

In the current study, it was also demonstrated that FOXO1 and FOXO3A differentially regulate VEGF in hESC. Further confirmation of the regulation of VEGF on the ESC using rodent models complemented by studies on human samples could shed light on the mechanisms underlying their effects on decidualisation, infertility and pathologies such as endometriosis and preeclampsia. The first step would involve murine models of decidualisation to determine the pattern of expression of FoxO1, Vegf and Flt-1 in wild-type mice. The use of uterine-specific mouse CRE lines, such as the P4 Cre line (Hawkins *et al.*, 2012), to target and ablate the FoxO1 and/or FoxO3a genes in the endometrium would be required to fully elucidate the interplay of FoxO1 and FoxO3a in decidualisation *in vivo*. These models also can be used to determine the relationship of FoxO1 and FoxO3A, and its expression in VEGF and Flt-1 regulation in suitable models of pathology such as endometriosis, or the restricted uterine perfusion model of preeclampsia (Fushima *et al.*, 2016).

The complex nature of infertility and pregnancy related complications (preeclampsia, IUGR, miscarriage)-associated infertility has been the focus of study for many years. For examples, treatments for the chronic pain suffered by women with endometriosis, such as progesterone analogues, may result in menstruation cessation and a contraceptive effect which will not be desirable for all women. As discussed earlier in Chapter 1, several reports have demonstrated a decreased of FOXO1, HOXA10 and VEGF expression during ESC decidualisation in women with infertility problems. VEGF is crucial for vascular remodelling in the endometrium and perturbation of VEGF activity can lead to infertility, recurrent miscarriage and preeclampsia (Maynard *et al.*, 2003; Jakovljevic *et al.*, 2016). While the level of sFlt-1 was found to increase in preeclampsia and recurrent miscarriage (Jakovljevic *et al.*, 2016). In this thesis, VEGF levels were found to increase during hESC decidualisation and concomitant decrease in sFlt-1 secretion. Therefore, it is important to understand the relationship between VEGF and sFlt-1 levels in the patients with disorders related to decidualisation impairment for example endometriosis, preeclampsia, recurrent miscarriage and IUGR which may help in the identification of novel therapeutics for the concomitant treatment of pain and infertility associated with this disorder. Therefore, a full understanding of the specific roles of this transcription factors and during ESC decidualisation would allow a better understanding of cellular cross-talk and the control of functional processes in reproductive function in health and disease and may provide a basis for the development of new treatment modalities.

8.3 Conclusion

The findings in this thesis contribute to our understanding of the mechanisms underlying the up-regulation of VEGF activity during hESC decidualisation. Importantly, they identify the significance of FOXO1 in driving VEGF expression and the concomitant decrease in sFlt-1

expression in hESC decidualisation, therefore, leading to a net increase in VEGF activity. It also identifies for the first time the antagonistic relationship of FOXO1 and FOXO3A in regulating VEGF expression during hESC decidualisation (**Figure 8.1**).

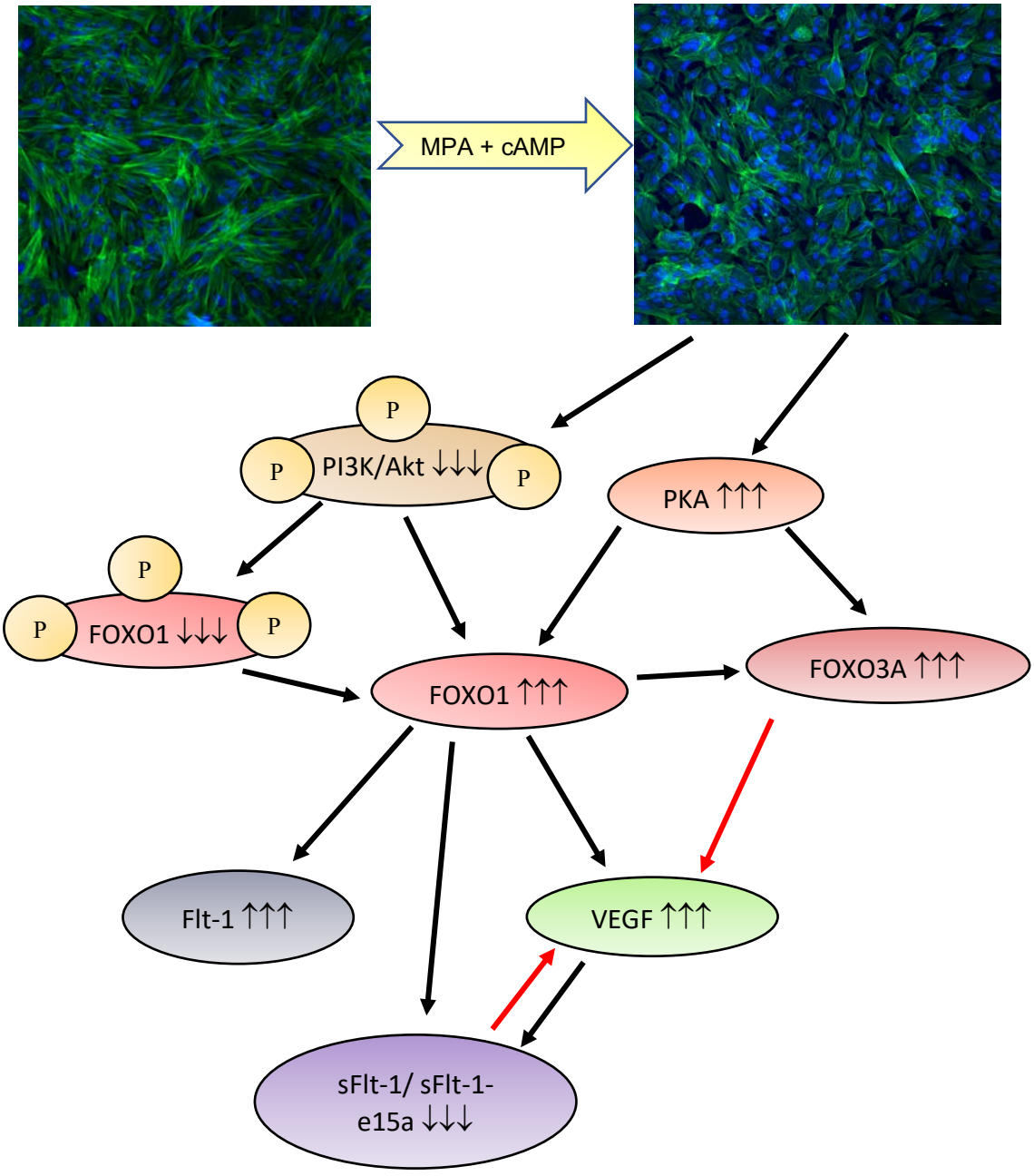

Figure 8.1: Summary diagram of the findings in this thesis.

APPENDICES

Appendix A: Plasmid transfection in St-T1b cells

The hESC were found to be difficult to transfect limiting the approaches that could be used to determine the signalling pathways and transcriptional regulation leading to increased VEGF expression upon decidualisation. Various transfection reagents were tested to try to improve the transfection efficiency of the hESC (**Table I**). The St-T1b cell line was seeded on 12-well plates following manufacturer's guidelines and pcDNA3-EGFP plasmid (1 µg/well) was used to transfect cells in order to determine the transfection efficiency by counting GFP positive cells and the total number of cells following Hoescht 33342 nuclear counterstaining. Various transfection reagents and conditions were used, and TransIT-2020 reagent was found to give the highest transfection efficiency (~24%) in the St-T1b cells (**Figure I**).

TRANSFECTION REAGENT	TRANSFECTION EFFICIENCY	
	St-T1b	
	DNA (µg): Reagent (µl)	Percentage (%)
LIPOFECTAMINE® 2000 (INVITROGEN)	1: 3	~ 1%
	1:5	~ 1%
JETPRIME (POLYPLUS)	1:2	~ 8%
	1:3	~ 1%
K2 (BIONTEX)	1:3	~2%
	1:4	~1.5%
HAPPYFECT (TECREA LTD)	1:2.5	0%
POLYETHYLENIMINE (PEI), SIGMA	1:6	~1%
TRANSIT-X2 (GENEFLOW)	1:2	~6%
	1:3	~11%
TRANSIT-2020 (GENEFLOW)	1:2	~24%
	1:3	~16%
	1:4	~14%
VIROMER BLUE (LIPOCALYX)	1.0x	~8%
	1.5x	~11%

Table I: The transfection efficiency using various reagents and conditions used in the St-T1b cells.

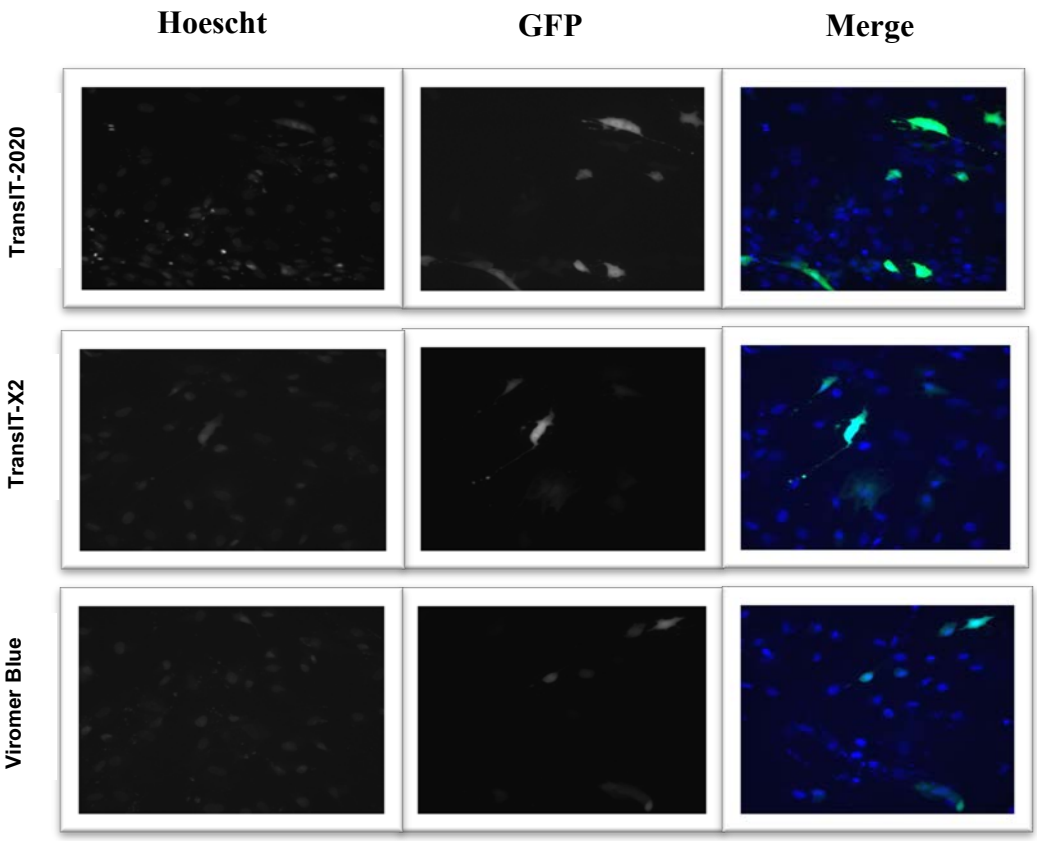

Figure I: Transfection of the St-T1b with GFP plasmids using various reagents. Cells were transfected with pcDNA3-EGFP (green) using TransIT-2020, TransIT-X2 and Viromer Blue, counterstained with Hoescht 33442 (blue) and the images taken of five random fields with a fluorescence microscope under the 10 X objective.

Appendix B: ChIP

B1: FOXO1 binds to human *VEGF* promoter in HMEC-1

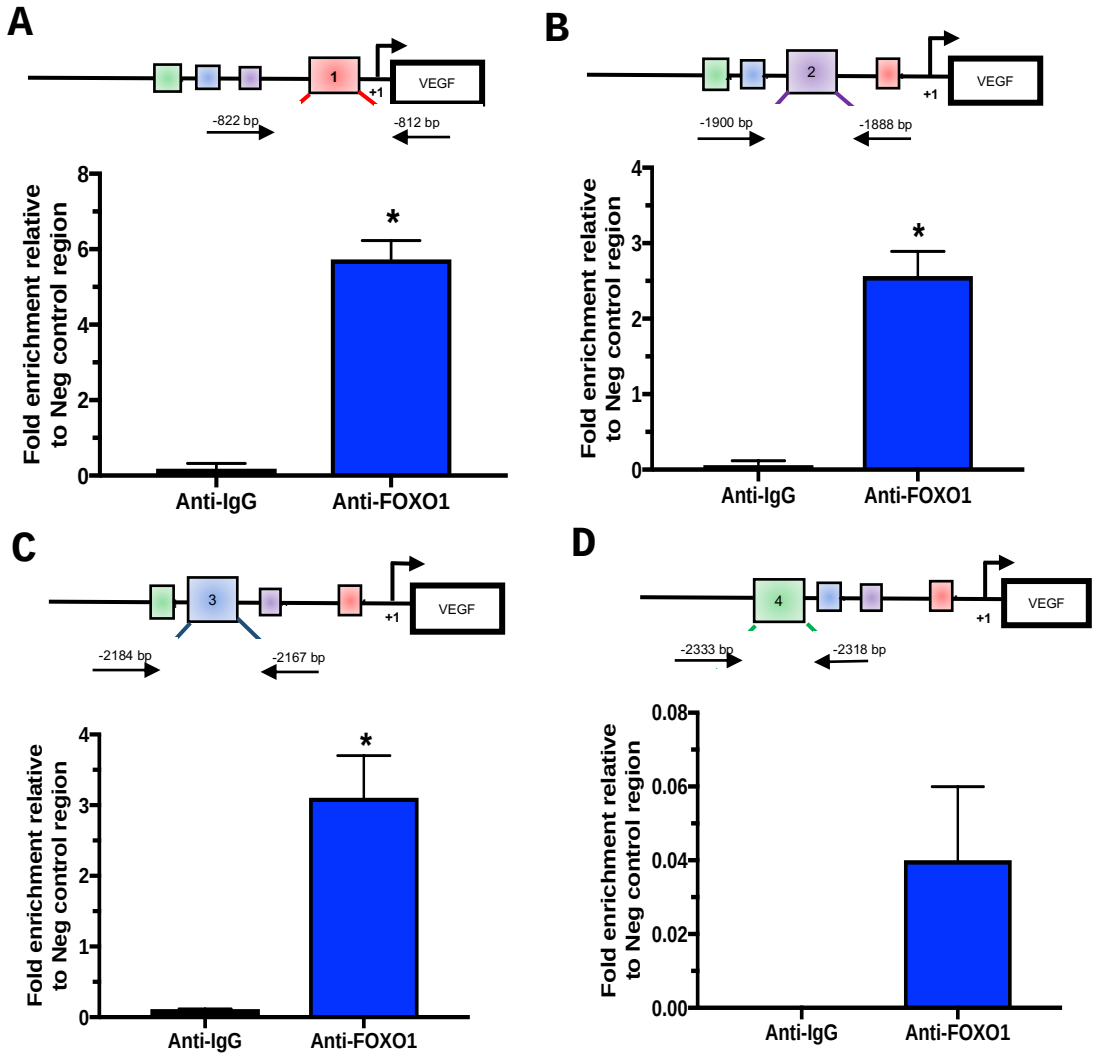

Figure II: FOXO1 binds directly to *VEGF* promoter in HMEC-1. ChIP assays were performed in HMEC-1 and immunoprecipitated with anti-FOXO1 or control IgG antibodies. The % Input was used to determine the enrichment of VEGF binding. The fold enrichment of FOXO1 binding to the VEGF **(A)** ChIP-1, **(B)** ChIP-2, **(C)** ChIP-3, and **(D)** ChIP-4 sites to the NegC regions was determined by real-time qPCR. Results are the mean (+/- SEM) of two independent ChIP experiments; *p<0.05; **p<0.01.

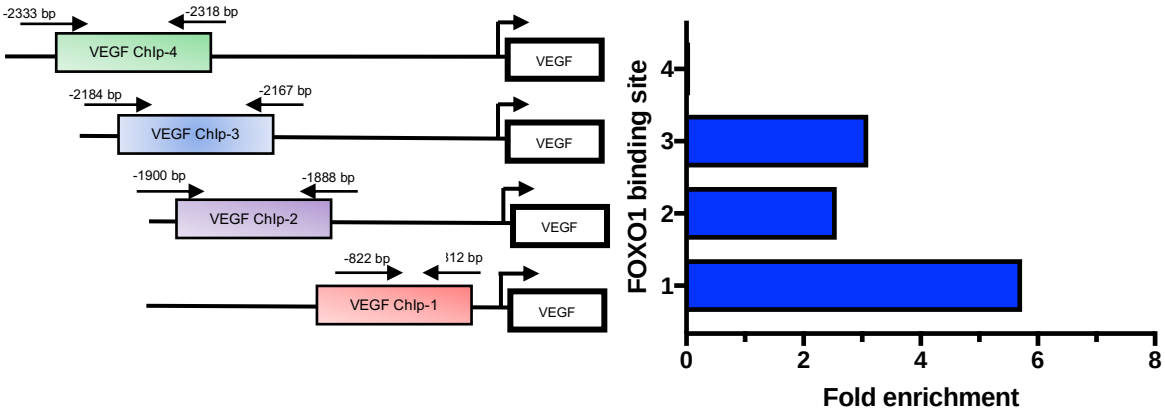

Figure III: FOXO1 binding sites identified by ChIP analysis in the human *VEGF* promoter in HMEC-1. Graph showing the degree of enrichment of FOXO1 binding normalised to input DNA and NegC regions in HMEC-1.

B2: FOXO1 binds to *IGFBP-1* in hESC

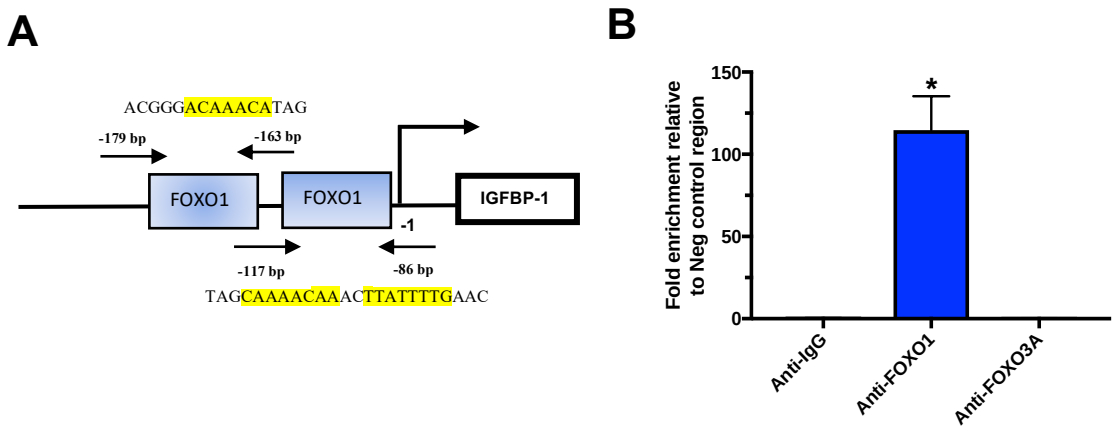

Figure IV: FOXO1 binds directly to *IGFBP-1* promoter in hESC. (A) Schematic representative of *IGFBP-1* promoter containing three FOXO1 binding sites. ChIP assays were performed in St-T1b cells with anti-FOXO1, anti-FOXO3A, or control IgG antibodies to determine binding to FHRE in the *IGFBP-1* promoter region. **(B)** The % Input was used to determine the enrichment of IGFBP-1 binding. The fold enrichment of *IGFBP-1* binding normalised to NegC regions by real-time qPCR analysis. Results are mean (+/- SEM) of two ChIP experiments; *p<0.05.

B3: FOXO1 binds to human HMG-box protein-1 (*HBP-1)* promoter in HMEC-1

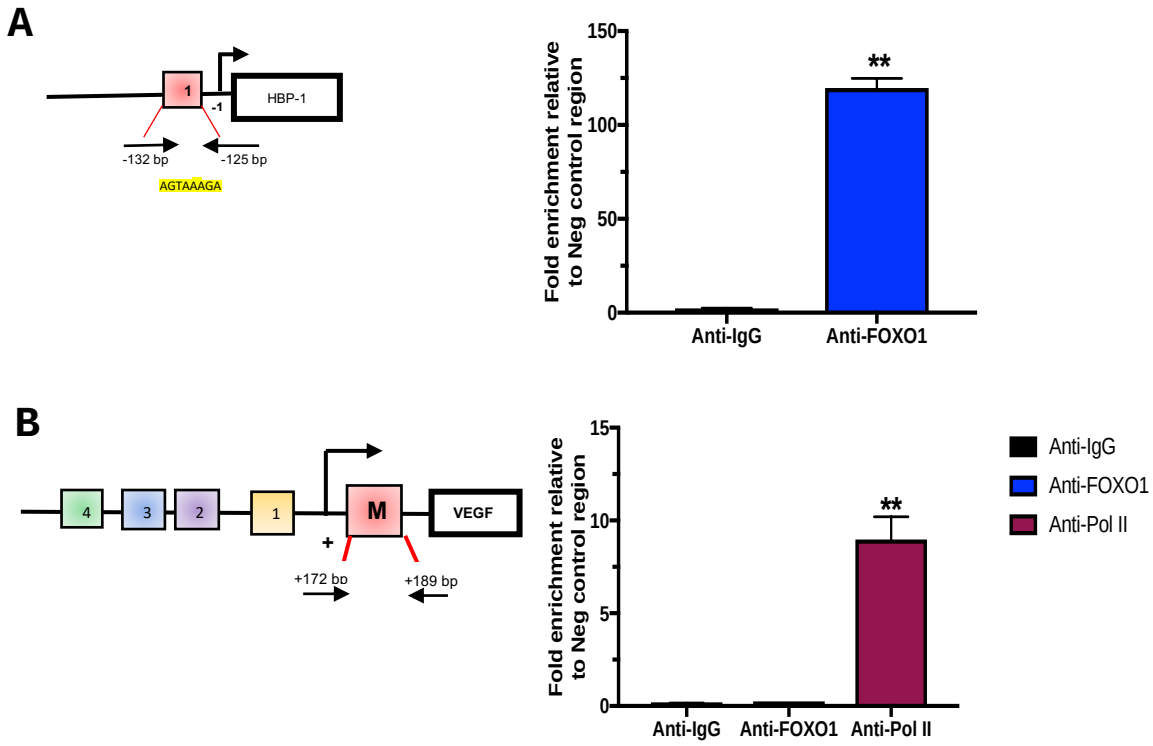

Figure V: FOXO1 binds directly to *HBP-1* promoter in HMEC-1. ChIP assays were performed in HMEC-1 cells and immunoprecipitated with anti-FOXO1, or control IgG antibodies and Pol II antibodies as positive control to determine the enrichment of binding to the *HBP-1* and *VEGF* promoter region. The % Input was used to determine the enrichment of FOXO1 or Pol II binding to **(A)** HBP-1 and **(B)** VEGF-FOXM1 binding normalised to NegC regions by real-time qPCR. Results are mean (+/- SEM) of 2 ChIP experiments; **p<0.01.

B4: FOXO1 binds to *Flt-1* promoter in HMEC-1

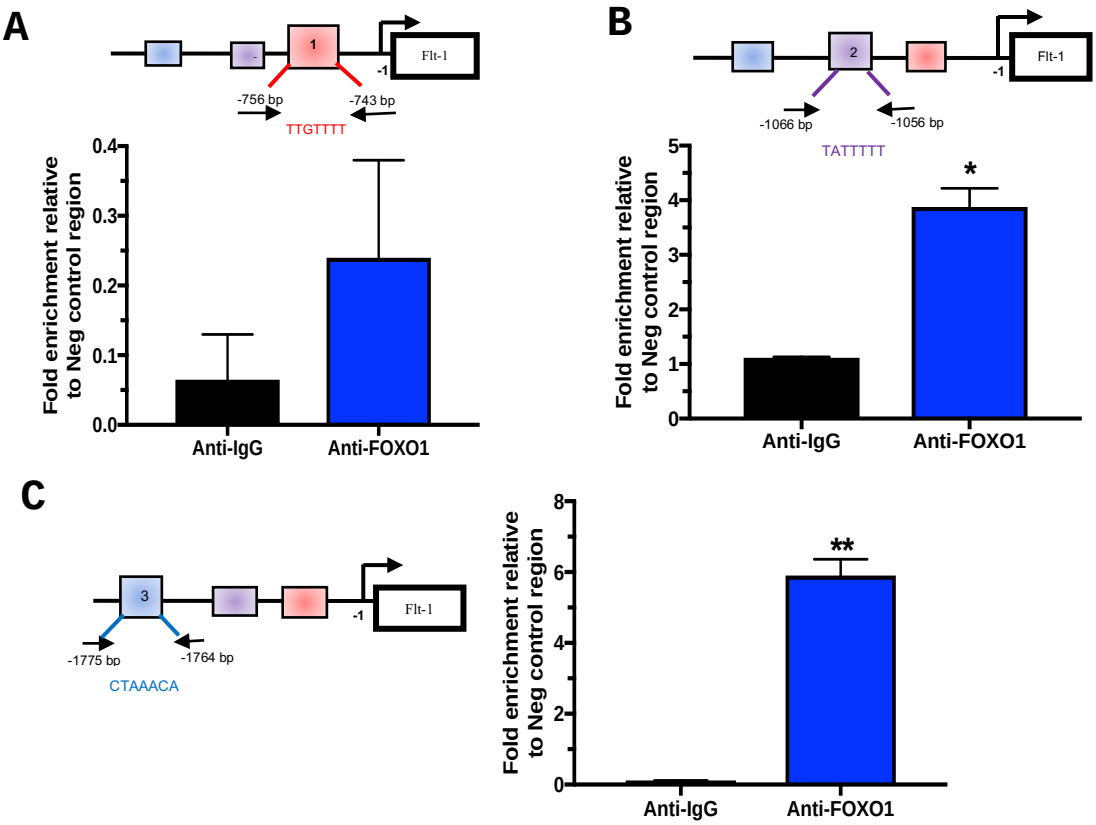

Figure VI: FOXO1 binds directly to *Flt-1* promoter in HMEC-1. ChIP assays were performed in HMEC-1 and immunoprecipitated with anti-FOXO1, or control IgG antibodies. The % Input was used to determine the fold enrichment of FOXO1 binding to the Flt-1 **(A)** ChIP-1, **(B)** ChIP-2, and **(C)** ChIP-3 sites relative to the NegC regions determined by real-time qPCR. Results are mean (+/- SEM) of 2 ChIP experiments; *p<0.05; **p<0.01.

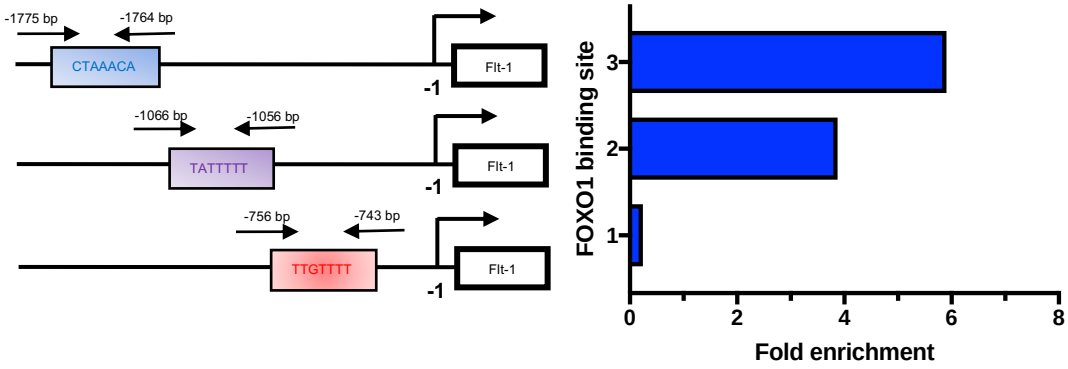

Figure VII: FOXO1 binding sites identified by ChIP analysis in human *Flt-1* promoter in HMEC-1. Graph showing the degree of enrichment of FOXO1 binding normalised to input DNA and NegC regions in HMEC-1.

Appendix C: Spheroid sprouting

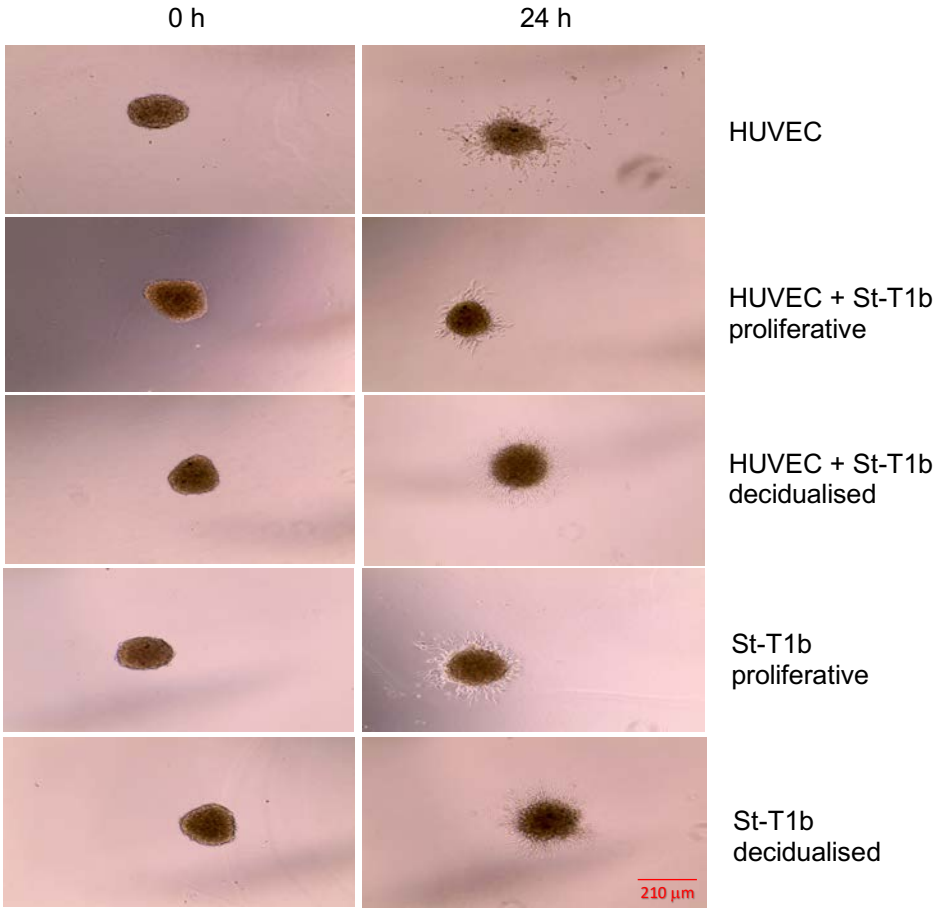

Figure VIII: Formation of spheroid from different cell types. Spheroids were formed using HUVEC and/or St-T1b cells (5,000 cells/spheroid) overnight and embedded into the growth factor-reduced Matrigel in DMEM/F12 medium consisting of 2% FBS and 50 ng/ml VEGF 24 h. Representative images of spheroids taken with an EVOS under 10 X objectives at 0 and 24 h.

Appendix D: sFlt-1 may mask the detection of VEGF in the ELISA

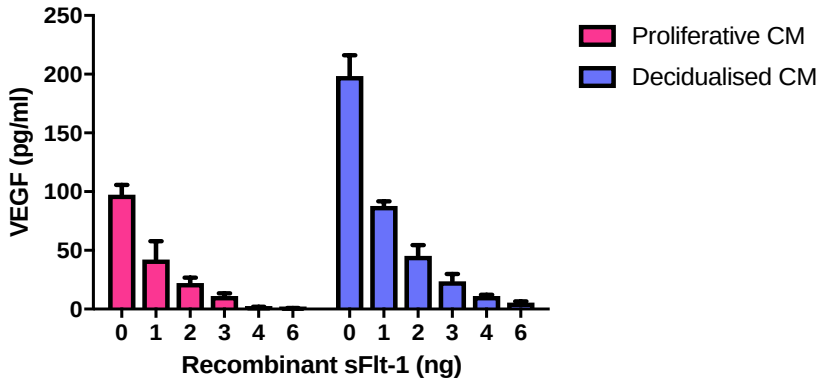

Figure IX: Decreased VEGF detection in hESC conditioned medium (CM) following incubation with recombinant sFlt-1. Proliferative hESC CM or decidualised hESC CM were incubated with relatively high levels of recombinant sFlt-1 for 1 h at room temperature and VEGF levels assessed by ELISA.

Appendix E: Time course of siRNA knock-down in St-T1b cells

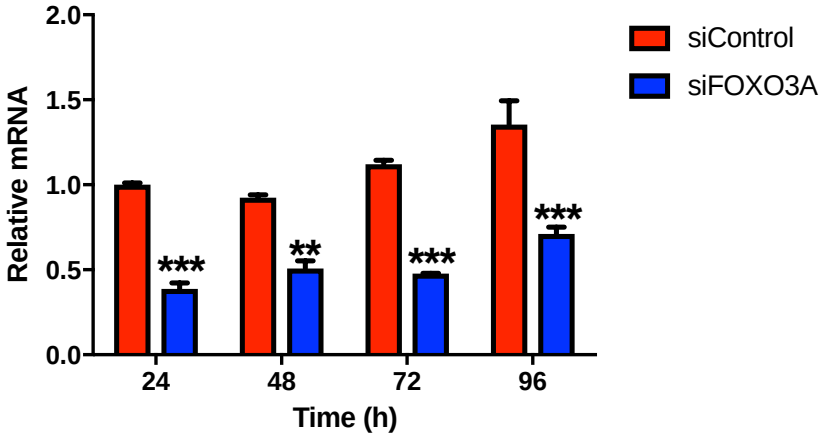

Figure XI: Time course of FOXO3A siRNA knock-down in St-T1b cells. St-T1b cells were plated on 6-well plates and transfected with siRNA targeting FOXO3A (siFOXO3A) or control (siControl). The cell lysate was harvested every 24 h up to 4 days and relative FOXO3A mRNA levels assessed by real-time qPCR and normalised to β-actin.

Appendix F: Effect of sFlt-1 expression in hESC following VEGF knock-down

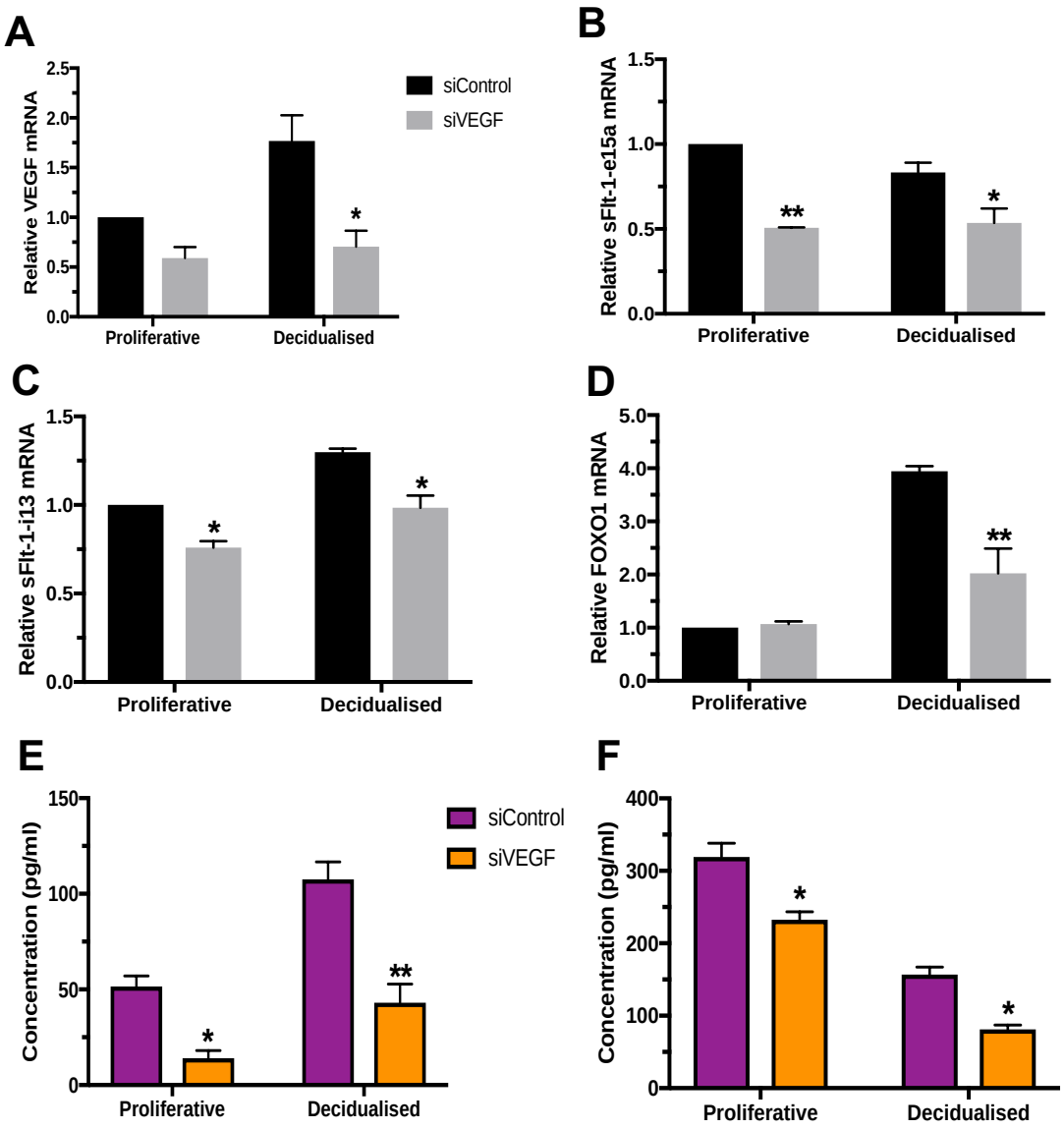

Figure XII: VEGF knock-down decreases sFlt-1 and FOXO1 expression in decidual hESC. St-T1b cells were plated on 6-well plates and transfected with siRNA targeting VEGF (siVEGF) or control (siControl) overnight and stimulated with E2 or MM1 medium for 24 h. Real-time qPCR analysis of **(A)** VEGF, **(B)** sFlt-1-e15a, **(C)** sFlt-1-i13 and **(D)** FOXO1 mRNA expression normalised to β-actin. **(E)** VEGF and **(F)** sFlt-1 protein levels in the supernatant were accessed by ELISA. Results are the mean (+/- SEM) of 2 experiments; *p<0.05; **p<0.01.

Appendix G: Effect of H_2O_2 on FOXO1/O3A and VEGF expression in hESC

FOXO1 and FOXO3A expression was found to increase dramatically in St-T1b cells treated with H_2O_2 during decidual conditions. Therefore, the effect of H_2O_2 on VEGF expression was determined in the St-T1b cells under proliferative and decidual conditions. The cells were grown to confluence and incubated with E2 or MM1 medium for 24 h before treatment with 200 µM H_2O_2 for a further 24 h. **Figure XIII** shows that there was a significant increase of VEGF protein secretion in both proliferative and decidual cells. VEGF secretion in proliferative cells stimulated with H_2O_2 was significantly greater than decidualised cells treated with H_2O_2.

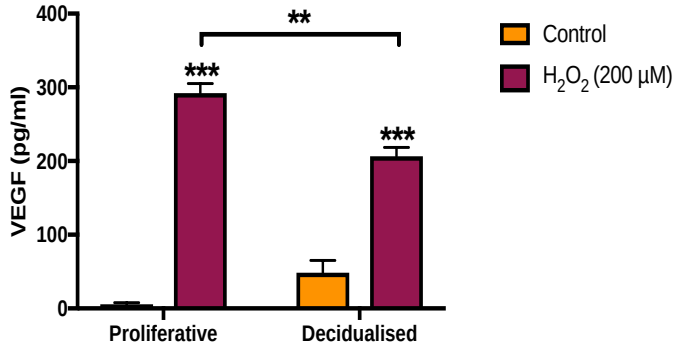

Figure XIII: Effect of H2O2 on VEGF secretion in hESC during decidualisation. St-T1b cells were plated in 6-well plates overnight and incubated with E2 and MM1 medium for 24 h followed by 24 h. Supernatants were collected after 24 h exposure to 200 µM H_2O_2. VEGF protein levels in the supernatant were assessed by ELISA. Results are the mean (+/- SEM) of 2 experiments; *p<0.05; **p<0.01; ***p<0.001.

Appendix H: Changes in signalling activity in hESC decidualisation

The $pAkt^{S473}$ was reported to be reduced in decidualised hESC compared to control cells (Yoshino *et al.*, 2003) as my results confirmed in **Section 4.3.6**. Therefore, I wanted to determine changes in other cell signalling pathways involved in hESC decidualisation. Confluent St-T1b cells were treated with DMEM/F12 containing 2% FBS for 24 h followed by 6 h of stimulation with E2 or MM1, medium. The cell lysates were harvested to test on a human phospho-kinase arrays as described in **Section 2.11.2**. However, there were no significant changes in target protein phosphorylation between control and decidualised cells (**Table II & Figure XIV**).

Target	Phosphorylation site	St-T1b	
		Proliferative	**Decidualised**
p38α	T180/Y182	0.51	0.33
ERK1/2	T202/Y204, T185/Y187	0.72	0.45
JNK1/2/3	T183/Y185, T221/Y223	0.60	0.60
GSK-3α/β	S21/S9	0.65	0.67
EGF R	Y1086	0.53	0.44
MSK1/2	S376/S360	0.70	0.53
AMPKα1	T183	0.58	0.54
Akt 1/2/3	S473	0.38	0.41
TOR	S2448	0.42	0.37
CREB	S133	0.54	0.55
HSP27	S78/S82	0.51	0.42
AMPKα2	T172	0.77	0.72
β-Catenin	-	0.75	0.41
Src	Y419	0.62	0.53
Lyn	Y397	0.55	0.43
Lck	Y394	0.27	0.17
STAT2	Y689	0.93	0.89
STAT5a	Y694	0.36	0.34
Fyn	Y420	0.43	0.33
Yes	Y426	0.68	0.64
Fgr	Y412	0.25	0.22
STAT6	Y641	0.84	0.71
STAT5b	Y699	0.47	0.44
Hck	Y411	0.51	0.48
Chk-2	T68	0.67	0.57
FAK	Y397	0.73	0.68
PDGFRβ	Y751	0.70	0.55
STAT5a/b	Y694/Y699	0.63	0.59
PRAS40	T246	0.92	0.87
P53	S392	0.14	0.19
Akt 1/2/3	T308	0.31	0.25
P53	S46	0.26	0.27
P70 S6 kinase	T389	0.11	0.05
P53	S15	0.08	0.03
c-Jun	S63	0.40	0.28
P70 S6 Kinase	T421/S424	0.22	0.17
RSK1/2/3	S380/S386/S377	0.16	0.10
eNOS	S1177	0.10	0.01
STAT3	Y705	0.24	0.14
P27	T198	0.03	0.00
PLC-γ1	Y783	0.13	0.05
STAT3	S727	0.12	0.05
WNK1	T60	0.57	0.43
PYK2	Y402	0.16	0.05
HSP60	-	0.61	0.52

Table II: List of human phosphor-kinase that expressed in St-T1b cells during decidualisation. Signal densities were quantified using ImageJ software after exposure to film. Integrated densities of each spot were corrected using the negative control spots and normalised to positive control.

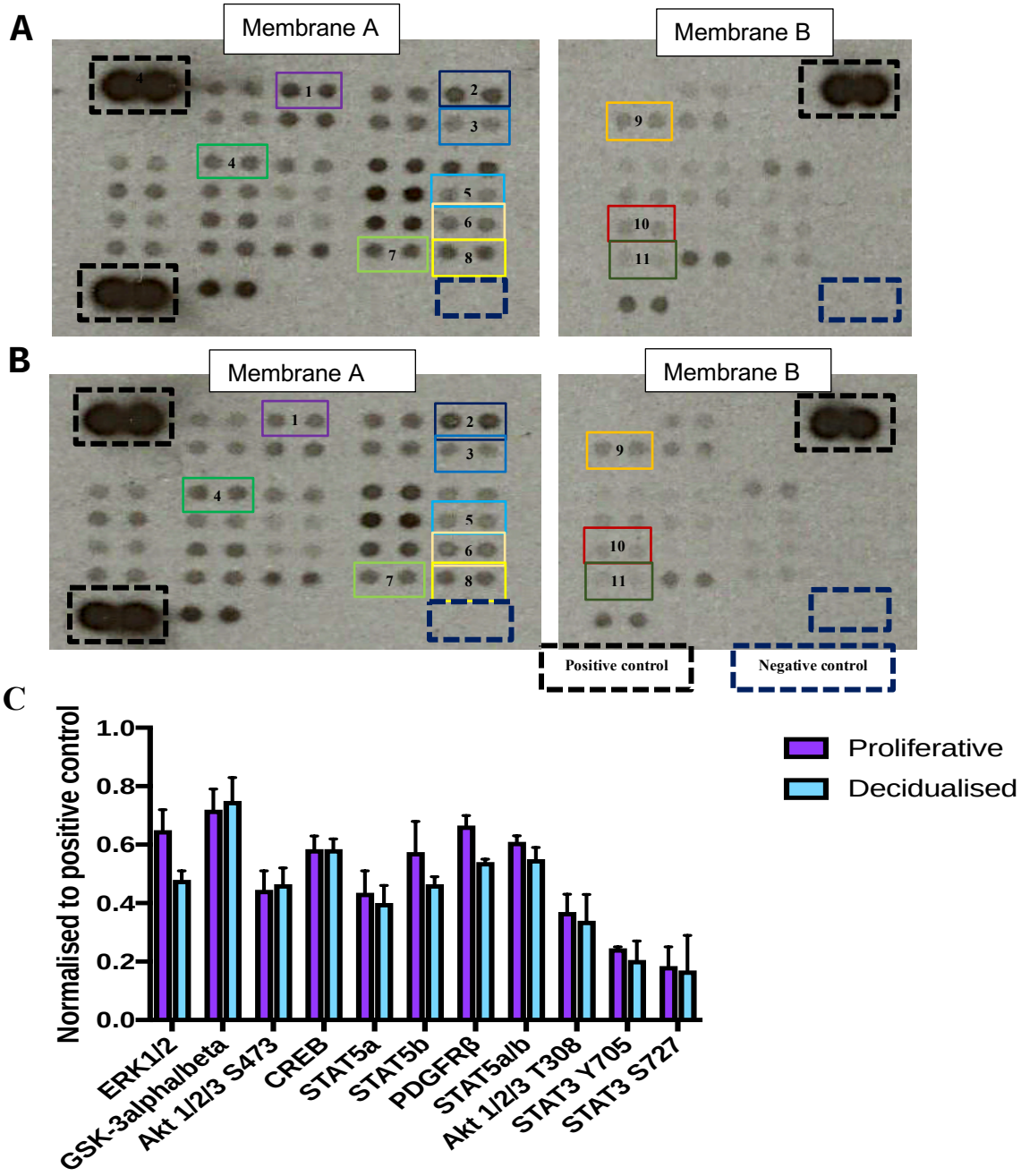

Figure XIV: Changes in cell signalling protein phosphokinase activity during decidualisation in St-T1b cells. St-T1b cells (2.4×10^6) were plated on 10 cm ∅ tissue culture dishes for 24 h. The cells were then treated with **(A)** 2% FBS medium or **(B)** MM1 medium for 6 h and the cell lysate was harvested and run on phospho-kinase protein arrays. The density was measured by densitometry using Image J and the results were normalised to positive control spots after the background was substracted. **(C)** Graph showing the results of target kinases that have been indicated with the numbered boxes on the membrane decidualisation. Results are the mean (+/- SEM) of 2 experiments.

Appendix I: FOXO1 and FOXO3A expression in hESC treated with only 8-Br-cAMP

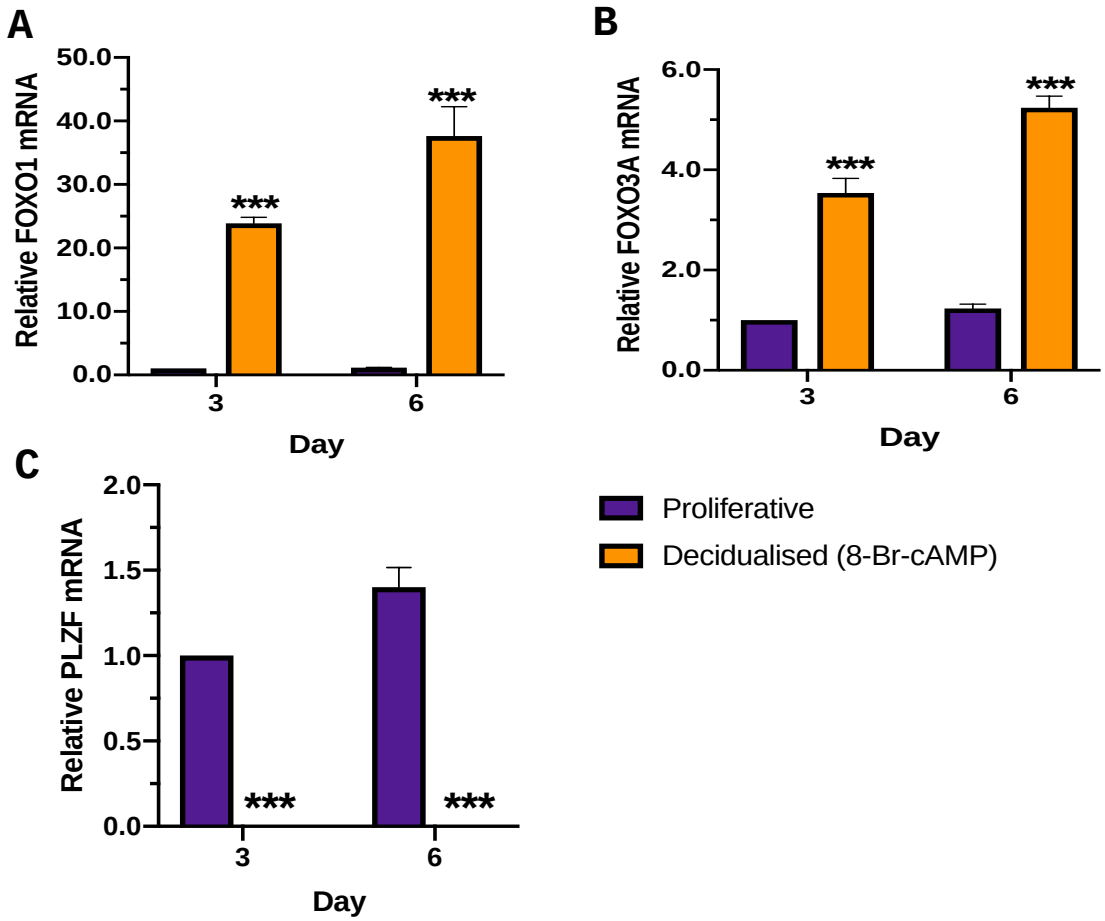

Figure XV: MPA does not affect the FOXO expression in decidual hESC. St-T1b cells were plated on 6-well plates overnight and stimulated with E2 or MM1 medium with only 0.5 mM 8-Br-cAMP up to 6 days. Real-time qPCR analysis of **(A)** FOXO1, **(B)** FOXO3A, and **(C)** PLZF mRNA expression normalised to β-actin. Results are the mean (+/- SEM) of 3 experiments and analysed using two-way ANOVA with multiple comparisons; ***p<0.001.

Appendix J: sFlt-1-e15a is the predominant isoform expressed in decidual hESC

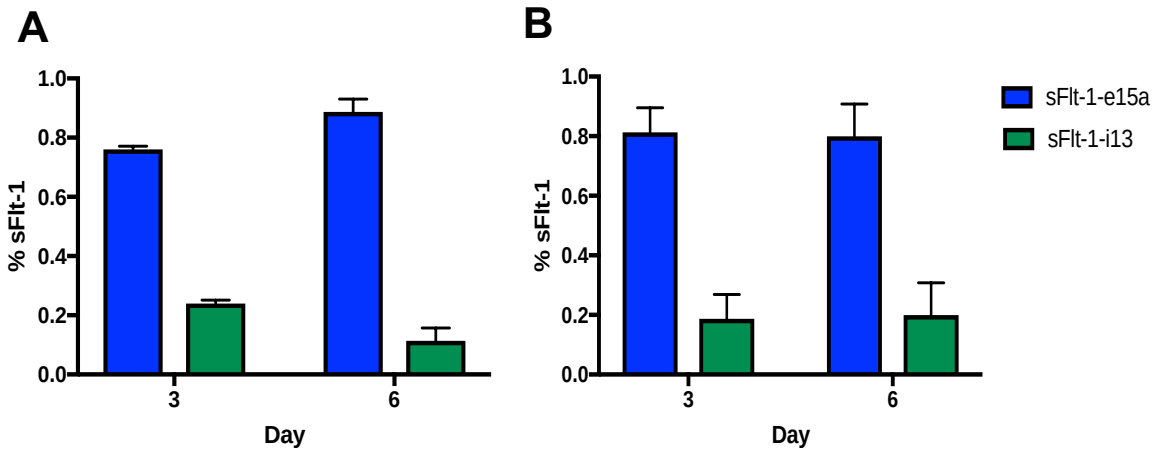

Figure XVI: sFlt-1-e15a is the predominant isoform expressed in decidual hESC. Percentage of sFlt-1-e15a and sFlt-1-i13 isoforms expression in (A) primary hESC and (B) St-T1b cell was measured from the densitometry analysis.

Bibliography

Achache H, and Revel A. Endometrial receptivity markers, the journey to successful embryo implantation. *Hum Reprod Update*, 2006; **12**(6): 731-46.

Ades EW, Candal FJ, Swerlick RA, *et al.* HMEC-1: establishment of an immortalized human microvascular endothelial cell line. *J Invest Dermatol.* 1992; **99**(6): 683-90.

Afshar Y, Jeong J, Roqueiro D, *et al*. Notch1 mediates uterine stromal differentiation and is critical for complete decidualisation in the mouse. *The FASEB Journal*, 2012; **26**(1): 282-294.

Aghajanova L, Hamilton A, Kwintkiewicz J, *et al*. Steroidogenic enzyme and key decidualisation marker dysregulation in endometrial stromal cells from women with versus without endometriosis. *Biol Reprod*., 2009; **80**(1): 105-14.

Aghajanova L, Horcajadas JA, Weeks JL, *et al*. The protein kinase A pathway-regulated transcriptome of endometrial stromal fibroblasts reveals compromised differentiation and persistent proliferative potential in endometriosis. *Endocrinology,* 2010; **151**(3): 1341-55.

Aghajanova L, Tatsumi K, Horcajadas JA, *et al*. Unique transcriptome, pathways, and networks in the human endometrial fibroblast response to progesterone in endometriosis. *Biol Reprod*., 2011; **84**(4): 801-15.

Ahmad S, Hewett PW, Al-Ani B, *et al.* Autocrine activity of soluble Flt-1 controls endothelial cell function and angiogenesis. *Vasc Cell.,* 2011;**3**(1):15.

Ahmed A, and Cudmore MJ. Can the biology of VEGF and haem oxygenases help solve pre-eclampsia? *Biochem. Soc. Trans.*, 2009; **37**: 1237-1242.

Albrecht ED, Pepe GJ. Estrogen regulation of placental angiogenesis and fetal ovarian development during primate pregnancy. *Int J Dev Biol.*, 2010; **54**: 397–408.

Alessi DR, Andjelkovic M, Caudwell FB, *et al*. Mechanism of activation of protein kinase B by insulin and IGF-1. *EMBO J.*, 1996; **15**(23): 6541-51.

Anacker J, Segerer SE, Hagemann C, *et al*. Human decidua and invasive trophoblasts are rich sources of nearly all human matrix metalloproteinases. *Mol Hum Reprod.*, 2011; **17**(10): 637-52.

Andraweera PH, Dekker GA, Laurence JA, *et al*. Placental expression of VEGF family mRNA in adverse pregnancy outcomes. *Placenta*. 2012; **33**: 467-472.

Aoyagi Y, Nasu K, Kai K, *et al*. Decidualisation differentially regulates microRNA expression in eutopic and ectopic endometrial stromal cells. *Reprod Sci.*, 2017; **24**(3): 445-455.

Araujo J, Breuer P, Dieringer S, *et al*. FOXO4-dependent upregulation of superoxide dismutase-2 in response to oxidative stress is impaired in spinocerebellar ataxia type 3. *Hum Mol Genet.,* 2011; **20**: 2928-41.

Arganda-Carreras I, Kaynig V, Rueden C, *et al.* Trainable weka segmentation: a machine learning tool for microscopy pixel classification. *Bioinformatics*, 2017; **33** (15).

Ashkar AA, Black GP, Wei Q, *et al*. Assessment of requirements for IL-15 and IFN regulatory factors in uterine NK cell differentiation and function during pregnancy. *J Immunol.*, 2003; **171**(6): 2937-2944.

Autiero M, Waltenberger J, Communi D, *et al*. Role of PIGF in the intra- and intermolecular cross talk between the VEGF receptors Flt1 and Flk1. *Nat Med.*, 2003; **9**(7): 936-43.

Bagot CN, PJ T, HS T. Alteration of maternal Hoxa10 expression by in vivo gene transfection affects implantation. *Gene Therapy*, 2000; **7**: 1378-84.

Bansal R, Ford B, Bhaskaran S, *et al*. Elevated levels of serum vascular endothelial growth factor-A are not related to NK cell parameters in recurrent IVF failure. *J Reprod Infertil.*, 2017; **18**(3): 280-287.

Barleon B, Sozzani S, Zhou D, *et al.* Migration of human monocytes in response to vascular endothelial growth factor (VEGF) is mediated via the VEGF receptor flt-1. *Blood*, 1996; **87**(8): 3336-43.

Barthel A, Schmoll D, Unterman TG. FoxO proteins in insulin action and metabolism. *Trends in Endocrinol Metab.*, 2005; **16**: 183-9.

Bartscha O, Ivell R. Relaxin and phosphodiesterases collaborate during decidualisation. *Ann N Y Acad Sci*., 2004; **1030**(1): 479-492.

Becker PM, Waltenberger J, Yachechko R, *et al*. Neuropilin-1 regulates vascular endothelial growth factor-mediated endothelial permeability. *Circ Res*., 2005; **96**: 1257-1265.

Bell SC, Jackson JA, Ashmore J, *et al*. Regulation of insulin-like growth factor-binding protein-1 synthesis and secretion by progestin and relaxin in long term cultures of human endometrial stromal cells. *J Clin Endocrinol Metab.*, 1991; **72**(5): 1014-24.

Bellomo D, Headrick JP, Silins GU, *et al*. Mice lacking the vascular endothelial growth factor-B gene (vegfb) have smaller hearts, dysfunctional coronary vasculature, and impaired recovery from cardiac ischemia. *Circ Res.*, 2000; **86**(2): e29-e35.

Benson GV, Lim H, Paria BC, *et al*. Mechanisms of reduced fertility in Hoxa-10 mutant mice: uterine homeosis and loss of maternal Hoxa-10 expression. *Development,* 1996; **122**: 2687-96.

Berthaut A, Mirshahi P, Benabbou N, *et al.* Vascular endothelial growth factor receptor-1 (VEGFR-1) expression in human corneal fibroblast decreased with age. *Molecular vision*, 2009; **15**: 1997-2007.

Boeckel JN, Guarani V, Koyanagi M, *et al*. Jumonji domain- containing protein 6 (Jmjd6) is required for angiogenic sprouting and regulates splicing of VEGF-receptor 1. *Proc Natl Acad Sci USA*, 2011; **108**:3276–3281.

Bole-Feysot C, Goffin V, Edery M, *et al*. Prolactin (PRL) and its receptor: actions, signal transduction pathways and phenotypes observed in PRL receptor knockout mice. *Endocr Rev.,* 1998; **19**: 225- 268.

Boura E, Silhan J, Herman P, *et al*. Both the N-terminal loop and wing W2 of the forkhead domain of transcription factor Foxo4 are important for DNA binding. *J. Biol. Chem*., 2007; **282**: 8265-8275.

Bourdiec A, Ahmad S, Lachhab A, *et al*. Regulation of inflammatory and angiogenesis mediators in a functional model of decidualized endometrial stromal cells. *Reprod Biomed Online*, 2016; **32**: 85-95.

Brar AK, Frank GR, Kessler CA, *et al*. Progesterone-dependent decidualisation of the human endometrium is mediated by cAMP. *Endocrine*, 1997; **6**: 301-307.

Brar AK, Handwerger S, Kessler CA, *et al*. Gene induction and categorical reprogramming during in vitro human endometrial fibroblast decidualisation. *Physiological Genomics,* 2001; **7**: 135-48.

Brent MM, Anand R, Marmorstein R. Structural basis for DNA regconition by FoxO1 and its regulation by posttranslational modification. *Stucture*, 2008; **16**: 1407-1416.

Brosens I, Pijnenborg R, Vercruysse L, *et al*. The "Great obstetrical syndromes" are associated with disorders of deep placentation. *Obstet Gynecol*., 2011; **204**(3): 193-201.

Brosens JJ, Gellersen B. Death or survival – progesterone-dependent cell fate decisions in the human endometrial stroma. *J Mol Endocrinol*., 2006; **36**(3): 389-398.

Brosens JJ, Hayashi N, and White JO. Progesterone receptor regulates decidual prolactin expression in differentiating human endometrial stromal cells. *Endocrinology*, 1999; **140**(10): 4809-20.

Brosens JJ, Parker MG, Mclndoe A, *et al*. A role for menstruation in preconditioning the uterus for successful pregnancy. *Am J Obstet Gynecol*., 2009; **200**(6): 615 e1-6.

Brosens JJ, Pijnenborg R, Brosens IA. The myometrial junctional zone spiral arteries in normal and abnormal pregnancies: A review of the literature. *Obstet Gynecol*. 2002; **187**(5): 1416-1423.

Brownawell AM, Kops GJ, Macara IG, *et al*. Inhibition of nuclear import by protein kinase B (Akt) regulates the subcellular distribution and activity of the forkhead transcription factor AFX. *Mol. Cell Biol*., 2001; **21**: 3534-3546.

Brunet A, Bonni A, Zigmond MJ, *et al*. Akt promotes cell survival by phosphorylating and inhibiting a Forkhead transcription factor. *Cell*, 1999; ***96***: 857-868.

Bruner-Tran KL, Mokshagundam S, Herington JL, *et a*l. Rodent models of experimental endometriosis: identifying mechanisms of disease and therapeutic targers. *Current Women's Health Reviews*, 2018; **14**: 172-188.

Bryant-Greenwood GD, Rutanen EM, Partanen S, *et al*. Sequential appearance of relaxin, prolactin and IGFBP- 1 during growth and differentiation of the human endometrium. *Mol Cell Endocrinol.*, 1993; **95**: 23-29.

Burney RO, Talbi S, Hamilton AE, *et al*. Gene expression analysis of endometrium reveals progesterone resistance and candidate susceptibility genes in women with endometriosis. *Endocrinology*, 2007; **148**(8): 3814-26.

Burton GJ, Jauniaux E, Watson AL. Maternal arterial connections to the placental intervillous space during the first trimester of human pregnancy: the Boyd collection revisited. *Am J Obstet Gynecol*., 1999; **181**(3): 718-24.

Bussolino F, Di Renzo MF, Ziche M, *et al*. Hepatocyte growth factor is a potent angiogenic factor which stimulates endothelial cell motility and growth. *J Cell Biol*., 1992; **119**(3): 629-641.

Buzzio OL, Lu Z, Miller CD, *et al*. FOXO1A differentially regulates genes of decidualisation. *Endocrinology*, 2006; **147**(8): 3870-6.

Cakmak H, Taylor HS. Implantation failure: molecular mechanisms and clinical treatment. *Hum Reprod Update,* 2011; **17**: 242-53.

Calnan DR, and Brunet A. The FoxO code. *Oncogene*, 2008; **27**: 2276-2288.

Carmeliet P and Jain RK. Molecular mechanisms and clinical applications of angiogenesis. *Nature*, 2011; **473**(7347): 298-307.

Carmeliet P, Ferreira V, Breier G, *et al*. Abnormal blood vessel development and lethality in embryos lacking a single VEGF allele. *Nature*, 1996; **380**(6573): 435-439.

Carmeliet P, Moons L, Luttun A, et al. Synergism between vascular endothelial growth factor and placental growth factor contributes to angiogenesis and plasma extravasation in pathological conditions. *Nat Med*, 2001; **7**(5): 575-583.

Cartharius K, Frech K, Grote K. MatInspector and beyond: promoter analysis based on transcription factor binding sites. *Bioinformatics*, 2005; **21**(13): 2933-42.

Cermik D, Selam B, Taylor HS. Regulation of HOXA-10 expression by testosterone in vitro and in the endometrium of patients with polycystic ovary syndrome. *J Clin Endocrinol Metab*, 2003; **88**(1): 238-43.

Chan RW, Schwab KE, and Gargett CE. Clonogenicity of human endometrial epithelial and stromal cells. *Biol Reprod*, 2004; **70**(6): 1738-50.

Chapdelaine P, Kang J, Boucher-Kovalik S, *et al*. Decidualisation and maintenance of a functional prostaglandin system in human endometrial cell lines following transformation with SV40 large T antigen. *Mol hum reprod*, 2006; **12**(5): 309-319.

Chatzaki E, Kouimtzoglou E, Margioris AN, *et al*. Transforming growth factor ß1 exerts an autocrine regulatory effect on human endometrial stromal cell apoptosis, involving the FasL and bcl-2 apoptotic pathways. *Mol Hum Reprod.*, 2003; **9**(2): 91-95.

Chegini N. Uterine microRNA signature and consequence of their dysregulation in uterine disorders. *Anim Reprod*., 2010; **7**(3): 117-128.

Chen J, Crawford R, Chen C, *et al*. The key regulatory roles of the PI3K/Akt signalling pathway in the functionalities of mesenchymal stem cells and applications in tissue regeneration. *Tissue Eng*, 2013; **19**(6): 516-528.

Chen JC and Roan NR. Isolation and culture of human endometrial epithelial cells and stromal fibroblasts. *Bio Protoc.*, 2015; **5**(20).

Chen L, Zhang JJ, and Huang X. cAMP inhibits cell migration by interfering with Rac-induced Lamellipodium formation. *J Biol Chem*, 2008; **283**(20): 13799-13805.

Chen Z, Xiao Y, Zhang J, *et al*. Transcription factors E2A, FOXO1 and FOXP1 regulate recombination activating gene expression in cancer cells. *PLoS One*, 2011; **6**: e20475.

Cheon Y, Li Q, Xu X, *et al*. A genomic approach to identify novel progesterone receptor regulated pathways in the uterus during implantation. *Mol Endocrinol*., 2002; **16**(12): 2853-2871.

Cho H, Thorvaldsen JL, Chu Q, *et al*. Akt1/PKBalpha is required for normal growth but dispensable for maintenance of glucose homeostasis in mice. *J biol chem.*, 2001; **276**: 38349-38352.

Chobotova K, Karpovich N, Carver J, *et al*. Heparin-binding epidermal growth factor and its receptors mediate decidualisation and potentiate survival of human endometrial stromal cells. *J Clin Endocrinol Metab.*, 2005; **90**(2): 913-9.

Choi SS, and Diehl AM. Epithelial-to-mesenchymal transitions in the liver. *Hepatology*, 2009; **50**: 2007-2013.

Christian M, lam EW, Wilson Ms, *et al*. FOXO transcription factors and their role in disorders of the female reproductive tract. *Curr Drug Targets*, 2011; **12**: 1291-302.

Christian M, Zhang X, Schneider-Merck T, *et al*. Cyclic AMP-induced forkhead transcription factor, FKHR, cooperates with CCAAT/Enhancer-binding protein ß in differentiating human endometrial stromal cells. *J Biol Chem*., 2002; **277**(23): 20825-20832.

Chung J-Y, Song Y, Wang Y, *et al*. Differential expression of vascular endothelial growth factor (VEGF), endocrine gland derived-VEGF, and VEGF receptors in human placentas from normal and preeclamptic pregnancies. *J Clin Endocrinol Metab.*, 2004; **89**: 2484-2490.

Claesson-Welsh L. VEGF receptor signal transduction – A brief update. *Vascul Pharmacol.*, 2016; **86**: 14-17.

Classen-Linke I, Alfer J, Krusche CA, *et al*. Progestins, progesterone receptor modulators, and progesterone antagonists change VEGF release of endometrial cells in culture. *Steroids,* 2000; **65:** 763–771.

Clifford RL, John AE, Brightling CE, *et al*. Abnormal Histone Methylation Is Responsible for Increased Vascular Endothelial Growth Factor 165a Secretion from Airway Smooth Muscle Cells in Asthma. *J Immunol.*, 2012; **189**: 819.

Cloke B, Fusi L, Brosens J eds. 2010 Decidualisation: Cambridge University Press.

Connolly DT. Regulation of vascular function by vascular permeability factor. *Plenum Press, New York*, 1991.

Coomans de Brachène A, Bollaert E, Eijkelenboom A, *et al*. The expression of the tumour suppressor HBP1 is down-regulated by growth factors via the PI3K/PKB/FOXO pathway. *Biochem J.*, 2014; **460**: 25.

Corbacho A, Martinez De, La Escalera G, *et al*. Roles of prolactin and related members of the prolactin/growth hormone/placental lactogen family in angiogenesis. *J Endocrinol.*, 2002; **173**(2): 219-238.

Cortés F, Debacker C, Péault B, *et al*. Differential expression of KDR/VEGFR-2 and CD34 during mesoderm development of the early human embryo. *Mech Dev*, 1999; **83**: 161-164.

Cottrell HN, Wu JJ, Rimawi BH, *et al*. Human endometrial stromal cell plasticity: Reversible sFlt1 expression negatively coincides with decidualisation. *Hypertension in Pregnancy*, 2017; **36**(2): 204-211.

Critchley HO, and Saunders PT. Hormone receptor dynamics in a receptive human endometrium. *Reprod Sci.*, 2009; **16**:191-199.

Critchley HO, Jones RL, Lea RG, *et al*. Role of inflammatory mediators in human endometrium during progesterone withdrawal and early pregnancy. *J Clin Endocrinol Metab.*, 1999; **84**: 240–248.

Cross MJ, Dixelius J, Matsumoto T, *et al*. VEGF-receptor signal transduction. *Trends Biochem Sci*. 2003; **28**(9): 488-494.

Crossey PA, Pillai CC, Miell JP. Altered placental development and intrauterine growth restriction in IGF binding protein-1 transgenic mice. *J Clin Invest.* 2002; **110**(3): 411-418.

Curry TE, and Osteen KG. The matrix metalloproteinase system: Changes, regulation, and impact throughout the ovarian and uterine reproductive cycle. *Endocr Rev*., 2003; **24**(4): 428-465.

Daftary GS, Troy PJ, Bagot CN, *et al*. Direct regulation of beta3-integrin subunit gene expression by HOXA10 in endometrial cells. *Mol Endocrinol.*, 2002; **16**(3): 571-9.

De Clercq K, Hennes A, Vriens J. Isolation of Mouse Endometrial Epithelial and Stromal Cells for *In Vitro* Decidualization. *J. Vis. Exp.,* 2017; **121**; e55168.

Dewerchin M, and Carmeliet P. PlGF: a multitasking cytokine with disease-restricted activity. *Cold Spring Harb Perspect Med*., 2012; **2**(8): a011056.

de Ziegler D, Fanchin R, de Moustier B, *et al*. The hormonal control of endometrial receptivity: estrogen (E2) and progesterone. *J Reprod Immunol.,* 1998*;* **39**: 149- 166.

Dellinger MT, and Brekken RA. Phosphorylation of Akt and ERK1/2 is required for VEGF-A/VEGFR2-induced proliferation and migration of lymphatic endothelium. *PLoS ONE*, 2011; **6**(12): e28947.

Dey SK, Lim H, Das SK, *et al*. Molecular cues to implantation. *Endocr Rev*. 2004; **25**(3): 341-373.

Diedrich K, Fauser BCJM, Devroey P, *et al*. The role of the endometrium and embryo in human implantation. *Hum Reprod Update*, 2007; **13**(4):365-377.

Dimitriadis E, Nie G, Hannan NJ, *et al*. Local regulation of implantation at the human fetal-maternal interface. *Int J Dev Biol.* 2010; **54**(2-3): 313-322.

Dimitriadis E, Robb L, and Salamonsen LA. Interleukin 11 advances progesterone-induced decidualisation of human endometrial stromal cells. *Mol Hum Reprod*., 2002; **8**(7): 636-643.

Dimitriadis E, Stoikos C, Baca M, *et al*. Relaxin and prostaglandin E2 regulate interleukin 11 during human endometrial stromal cell decidualisation. *J Clin Endocrinol Metab.*, 2005; **90**(6): 3458-3465.

Dimitriadis E, White CA, Jones RL, *et al*. Cytokines, chemokines and growth factors in endometrium related to implantation. *Hum Reprod Update.* 2005; **11**(6):613-630.

Dimmeler S, and Zeiher AM. Akt takes center stage in angiogenesis signaling. *Circ Res.*, 2000; **86**: 4–5.

Dor Y, Porat R, Keshet E. Vascular endothelial growth factor and vascular adjustments to perturbations in oxygen homeostasis. *Am J Physiol.,* 2001; **280**: C1367–C1374.

Douglas NC, Tang H, Gomez R, *et al*. Vascular endothelial growth factor receptor 2 (VEGFR-2) functions to promote uterine decidual angiogenesis during early pregnancy in the mouse. *Endocrinology*, 2009; **150**: 3845- 3854.

DuBridge RB, Tang P, Hsia HC, *et al*. Analysis of mutation in human cells by using an Epstein-Barr virus shuttle system. *Mol Cell Biol.*, 1987; **7**: 379-87.

Duley L. The global impact of pre-eclampsia and eclampsia. *Semin Perinatol*, 2009; **33**(3): 130-7.

Dunn CL, Kelly RW, Critchley HO. Decidualisation of the human endometrial stromal cell: an enigmatic transformation. *Reprod Biomed Online,* 2003; **7**: 151-61.

Easton RM, Cho H, Roovers K, *et al*. Role for Akt3/protein kinase Bgamma in attainment of normal brain size. *Mol Cell Biol.*, 2005; **25**: 1869-1878.

El-Zenneni H, Moustafa R, Abdel-Hafeez M, *et al*. Assessment of uterine, subendometrial blood flows and endometrial gland vascular endothelial growth factor (EG-VEGF) in women with unexplained infertility. *Middle East Fertility Society Journal,* 2015; **20**: 119-26.

Ericson K, Gan C, Cheong I, *et al*. Genetic inactivation of AKT1, AKT2, and PDPK1 in human colorectal cancer cells clarifies their roles in tumor growth regulation. *Proc Nat Acad Sci.*, 2010; **107**: 2598-603.

Essaghir A, Dif N, Marbehant CY, *et al*. The transcription of FOXO genes is stimulated by FOXO3 and repressed by growth factor. *J Biol Chem.,* 2009; **284**(16): 10334-10342.

Essers MA, Weijzen S, de Vries-Smits AM, *et al*. FOXO transcription factor activation by oxidative stress mediated by the small GTPase Ral and JNK. *EMBO J*., 2004; **23**: 4802-4812.

Fabi F, Grenier K, Parent S, *et al*. Regulation of the PI3K/Akt pathway during decidualisation of endometrial stromal cells. *PLoS ONE*, 2017; **12**(5): e0177387.

Fan X, Krieg S, Kuo CJ, *et al*. VEGF blockade inhibits angiogenesis and reepithelialisation of endometrium. *FASEB J*., 2008; **22**(10): 3571-80.

Fan X, Rai A, Kambham N, *et al*. Endometrial VEGF induces placental sFLT1 and leads to pregnancy complications. *J Clin Invest.*, 2014; **124**: 4941–4952.

Farrer-Brown G, Beilby JO, Tarbit MH. The blood supply of the uterus arterial vasculature. *J Obstet Gynaecol Br Commonw*., 1970; **77**: 673-681.

Fazleabas AT, Kim JJ, Strakova Z. Implantation: Embryonic signals and the modulation of the uterine Environment—A review. *Placenta*. 2004; **25**, Supplement: S26-S31.

Fearnley GW, Smith GA, Harrison MA, *et al*. Vascular endothelial growth factor-A regulation of blood vessel sprouting in health and disease. *OA Biochemistry*, 2013; **1**(1): 5.

Felekkis K, TOuvana E, Stefanou Ch, *et al.* Review: microRNAs: a newly described class of encoded molecules that play a role in health and disease. *Hippokrata*, 2010; **14**(4): 236-240.

Ferrara N. Binding to the extracellular matrix and proteolytic processing: two key mechanisms regulating vascular endothelial growth factor action. *Mol. Biol. Cell*, 2010; **21**: 687-690.

Ferrara N, Carver-Moore K, Chen H, *et al*. Heterozygous embryonic lethality induced by targeted inactivation of the VEGF gene. *Nature*. 1996; **380**(6573):439-442.

Ferrara N, Chen H, Davis-Smyth T, *et al*. Vascular endothelial growth factor is essential for corpus luteum angiogenesis. *Nat Med.,* 1998; **4**: 336–340.

Ferrara N, and Henzel WJ. Pituitary follicular cells secrete a novel heparin-binding growth factor specific for vascular endothelial cells. *Biochem Biophys Res Commun*., 1989; **161**(2): 851-858.

Ferrara N. History of discovery: Vascular endothelial growth factor. *Arterioscler Thromb Vasc Biol*. 2009; **29**: 789-791.

Ferrara N. Vascular endothelial growth factor: Basic science and clinical progress. *Endocr Rev*., 2004; **25**(4): 581-611.

Filigheddu N, Gregnanin I, Porporato PE, *et al*. Differential expression of microRNAs between eutopic and ectopic endometrium in ovarian endometriosis. *J Biomed Biotechnol.*, 2010; **2010**: 369549.

Fisher SJ. Why is placentation abnormal in preeclampsia? *Am J Obstet Gynecol.*, 2015; **213**(4): S115–S122.

Fong GH, Rossant J, Gertsenstein M, *et al*. Role of the Flt-1 receptor tyrosine kinase in regulating the assembly of vascular endothelium. *Nature*, 1995; **376**: 66-70.

Fong GH, Zhang L, Bryce DM, *et al*. Increased hemangioblast commitment, not vascular disorganization, is the primary defect in flt-1 knock-out mice. *Development*, 1999; **126**(13): 3015-3025.

Frank GR, Brar AK, Cedars MI, *et al*. Prostaglandin E2 enhances human endometrial stromal cell differentiation. *Endocrinology*, 1994; **134**(1): 258-263.

Frank S, Hubner G, Breier G, *et al*. Regulation of VEGF expression in cultured keratinocytes. Implications for normal and impaired wound healing. *J Biol Chem*., 1995; **270**: 12607–12613.

Fraser HM, and Wulff C. Angiogenesis in the corpus luteum. *Reprod Biol Endocrinol.*, 2003; **1**:88.

Fuh G, Li B, Crowley C, *et al*. Requirements for binding and signaling of the kinase domain receptor for vascular endothelial growth factor. *J Biol Chem*., 1998; **273**(18): 11197-11204.

Fuh G, Garcia KC, de Vos AM. The interaction of neuropilin-1 with vascular endothelial growth factor and its receptor flt-1. *J Biol Chem.*, 2000; **275**(35): 26690-5.

Furuyama T, Kitayama K, Shimoda Y, *et al*. Abnormal angiogenesis in Foxo1 (Fkhr)-deficient mice. *J Biol Chem*., 2004; **279**: 34741-34749.

Furuyama T, Nakazawa T, Nakano I, *et al*. Identification of the differential distribution patterns of mRNAs and consensus binding sequences for mouse DAF-16 homologues. *Biochem. J.*, 2000; **349**: 629-634.

Fushima T, Sekimoto A, Minato T, *et al*. Reduced uterine perfusion pressure (RUPP) model of preeclampsia in mice. *PLoS ONE*, 2016; **11**(5): e0155426.

Gagnon R. Placental insufficiency and its consequences. *Eur J Obstet Gynecol Reprod Biol.,* 2003;**110**(1): S99–S107.

Gao F, Bian F, Ma X, *et al*. Control of regional decidualisation in implantation: role of FoxM1 downstream of Hoxa10 and cyclin D3. *Sci Rep.*, 2015; **5**:13863.

Gao J, Mazella J, Tang M, *et al*. Ligand-activated progesterone receptor isoform hPR-A is a stronger transactivator than hPR-B for the expression of IGFBP-1 (insulin-like growth factor binding protein-1) in human endometrial stromal cells*. Mol Endocrinol*., 2000; **14**(12): 1954-61.

Gao JG, Mazella J, Tseng L. Activation of the human IGFBP-1 gene promoter by progestin and relaxin in primary culture of human endometrial stromal cells. *Mol Cell Endocrinol.*, 1994; **104**: 39-46.

Garofalo RS, Orena SJ, Rafidi K, *et al*. Severe diabetes, age-dependent loss of adipose tissue, and mild growth deficiency in mice lacking Akt2/PKB beta. *J Clin Invest.*, 2003; **112**: 197-208.

Garrido-Gomez T, Dominguez F, Lopez JA, *et al*. Modeling human endometrial decidualisation from the interaction between proteome and secretome. *J Clin Endocrinol Metab.*, 2011; **96**: 706-716.

Garzia E, Borgato S, Cozzi V, *et al*. Lack of expression of endometrial prolactin in early implantation failure: A pilot study. *Hum Reprod*, 2004; **19**(8): 1911-1916.

Gelfand MV, Hagan N, Tata A, *et al*. Neuropilin-1 functions as a VEGFR2 co-receptor to guide developmental angiogenesis independent of ligand binding. *Elife,* 2014; **22**(3): e03720.

Gellersen B, and Brosens JJ. Cyclic decidualisation of the human endometrium in reproductive health and failure. *Endocr Rev*, 2014; **35**(6): p. 851-905.

Gellersen B, Brosens IA, Brosens JJ. Decidualisation of the human endometrium: mechanisms, functions, and clinical perspectives. *Semin Reprod Med*., 2007; **25**: 445-453.

Gellersen B, Reimann K, Samalecos A, *et al*. Invasiveness of human endometrial stromal cells is promoted by decidualisation and by trophoblast-derived signals. *Hum Reprod*., 2010; **25**: 862 – 873.

Gellersen B, Wolf A, Kruse M, *et al*. Human endometrial stromal cell-trophoblast interactions: mutual stimulation of chemotactic migration and promigratory roles of cell surface molecules CD82 and CEACAM1. *Biol Reprod.*, 2013; **88**(3): 80, 1-13.

Gellersen B, and Brosens JJ. Cyclic AMP and progesterone receptor cross-talk in human endometrium: a decidualizing affair. *J Endocrinol.*, 2003; **178**(3): p. 357-72.

Gentilini D, Busacca M, Francesco SD, *et al*. PI3K/Akt and ERK1/2 signalling pathways are involved in endometrial cell migration induced by 17β-estradiol and growth factors. *Mol Hum Reprod.*, 2007; **13**(5): 317-322.

Gerber HP, McMurtrey A, Kowalski J, *et al*. Vascular endothelial growth factor regulates endothelial cell survival through the phosphatidylinositol 3-kinase/Akt signal transduction pathway: requirement for Flk-1/KDR activation. *J Biol Chem.*, 1998; **273**: 30336–30343.

Germeyer A, Hamilton AE, Laughlin LS, *et al*. Cellular expression and hormonal regulation of neuropilin-1 and -2 messenger ribonucleic Acid in the human and rhesus macaque endometrium. *J Clin Endocrinol Metab*., 2005; **90**(3):1783–90.

Gilbert SF. Developmental biology. 9th ed., Sunderland, Mass.: *Sinauer Associates*. 2010; xxi, 711, 80 p.

Gille H, Kowalski J, Yu L, *et al*. A repressor sequence in the juxtamembrane domain of Flt-1 (VEGFR-1) constitutively inhibits VEGF-dependent PI3 kinase activation and endothelial cell migration. *EMBO J*., 2000; **19**: 4064-4073.

Gilles C. Contribution: Angiogenesis Analyser. *ImageJ News*, 2012.

Girling JE, Rogers PAW. Regulation of endometrial vascular remodelling: role of the vascular endothelial growth factor family and the angiopoietin–TIE signalling system. *Reproduction*, 2009; **138**: 883-93.

Giudice LC, Lamson G, Rosenfeld RG, *et al*. Insulin-like growth factor-II (IGF-II) and IGF binding proteins in human endometrium. *Ann N Y Acad Sci.*, 1991; **626**: 295-307.

Giudice LC, Mark SP, Irwin JC. Paracrine actions of insulin-like growth factors and IGF binding protein-1 in non-pregnant human endometrium and at the decidual–trophoblast interface1. *J Reprod Immunol*., 1998; **39**(1–2): 133-148.

Giudice LC. Maternal-fetal conflict — lessons from a transgene. *J Clin Invest.*, 2002; **110**(3): 307-309.

Giudice LC. Microarray expression profiling reveals candidate genes for human uterine receptivity. *Am J Pharmacogenomics*, 2004; **4**:299-312.

Gleeson LM, Chakraborty C, McKinnon T, *et al*. Insulin-like growth factor-binding protein 1 stimulates human trophoblast migration by signaling through α5β1 integrin via mitogen-activated protein kinase pathway. *J Clin Endocrinol Metab.*, 2001; **86**(6): 2484-2493.

Gluckman PD, Hanson MA, Cooper C, Thornburg KL. Effect of *in utero* and early-life conditions on adult health and disease. *N Engl J Med.,* 2008; **359**(1): 61–73.

Gnoth C, Godehardt E, Frank-Herrmann P, *et al*. Definition and prevalence of subfertility and infertility. *Hum Reprod.*, 2005; **20**(5): 1144-1147.

Godbole G and Modi D. Regulation of decidualisation, interleukin-11 and interleukin-15 by homeobox A 10 in endometrial stromal cells. *J Reprod Immunol*., 2010; **85**(2): 130-139.

Goldenberg RL, Culhane JF, Iams JD, *et al*. Epidermiology and causes of preterm birth. *Lancet*, 2008; **371**: 75-84.

Gonzalez M, Neufeld J, Reimann K, *et al*. Expansion of human trophoblastic spheroids is promoted by decidualized endometrial stromal cells and enhanced by heparin-binding epidermal growth factor-like growth factor and interleukin-1 beta. *Mol Hum Reprod*., 2011; **17**(7): 421-33.

Gopalakrishnan ARK, Pandit H, Metkari SM, *et al*. Ademoviral vector encoding soluble Flt-1 engineered human endometrial mesenchymal stem cells effectively regress endometriotic lesions in NOD/SCID mice. *Gene Therapy*, 2016; **23**: 580-591.

Gordon JD, Shiferen JL, Foulk RA, *et al*. Angiogenesis in the human female reproductive tract. *Obstet Gynecol Sur.*, 1995; **50**(9): 688-697.

Graham FL, Smiley J. Characteristics of a Human Cell Line Transformed by DNA from Human Adenovirus Type 5. *J Gener Virol.*, 1977; **36**: 59-74.

Grant KS, Wira CR. Effect of mouse uterine stromal cells on epithelial cell transepithelial resistance (TER) and TNFalpha and TGFbeta release in culture. *Biol Reprod.,* 2003; **69**: 1091-8.

Greaves E, Critchley HOD, Horne AW, *et al*. Relevant human tissue resources and laboratory models for use in endometriosis research. *Acta Obstet Gynecol Scand*, 2017; **96** (6): 644-58.

Greening DW, Nguyen HP, Elgass K, *et al*. Human endometrial exosomes contain hormone-specific cargo modulating trophoblast adhesive capacity: insights into endometrial-embryo interactions. *Biol Reprod.*, 2016; **94**(2): 38.

Greenwood JD, Minhas K, di Santo JP, *et al*. Ultrastructural studies of implantation sites from mice deficient in uterine natural killer cells. *Placenta*, 2000; **21**:693 – 702.

Grinius L, Kessler C, Schroeder J, *et al*. Forkhead transcription factor FOXO1A is critical for induction of human decidualisation. *J Endocrinol*., 2006; **189**(1): 179-87.

Gu Y, Lewis DF, Wang Y. Placental productions and expressions of soluble endoglin, soluble fms-like tyrosine kinase receptor-1, and placental growth factor in normal and preeclamptic pregnancies', *J Clin Endocrinol Metab.*, 2008; **93**(1): 260- 6.

Gu F, Li X, Kong J, *et al*. VEGF111b, a new member of VEGFxxxb isoforms and induced by mitomycin C, inhibits angiogenesis. *Biochemical and Biophysical Research Communications*, 2013; **441**: 18-24.

Gui Y, Zhang J, Yuan L, *et al*. Regulation of HOXA-10 and its expression in normal and abnormal endometrium. *Mol Hum Reprod*. 1999; **5**(9): 866-873.

Gupta K, Kshirsagar S, Li W, *et al*. VEGF prevents apoptosis of human microvascular endothelial cells via opposing effects on MAPK/ERK and SAPK/JNK signaling. *Exp Cell Res*, 1999; **247**: 495–504.

Gupta MB, Shehab MA, Nygard K, *et al.* IUGR is associated with marked hyperphosphorylation of decidual and maternal plasma IGFBP-1. *J Clin Endocrinol Metab.*, 2019; **104**: 408-422.

Hanna J, Goldman-Wohl D, Hamani Y, *et al*. Decidual NK cells regulate key developmental processes at the human fetal-maternal interface. *Nat. Med.*, 2006; **12**(9): 1065-74.

Hannan NJ, Paiva P, Dimitriadis E, *et al*. Models for study of human embryo implantation: Choice of cell lines? *Biol Reprod*., 2010; **82**(2): 235-245.

Haouzi D, Dechaud H, Assou S, *et al*. Insights into human endometrial receptivity from transcriptomic and proteomic data. *Reprod Biomed Online*, 2012; **24**(1): 23-34.

Harper MJ. The implantation window. *Baillieres Clin Obstet Gynaecol.*, 1992; **6**(2): 351-71.

Hawkins SM, Andreu-Vieyra CV, Kim TH, *et al.* Dysregulation of uterine signalling pathways in progesterone receptor-cre knockout of Dicer. *Mol Endocrinol.*, 2012; **26**(9): 1552-1566.

He Y, Du M, Guo P, *et al*. Regulation of C-C motif chemokine ligand 2 and its receptor in human decidual stromal cells by pregnancy-associated hormones in early gestation. *Hum Reprod.*, 2007; **22**(10): 2733-2742.

He Y, Smith SK, Day KA, *et al*. Alternative splicing of vascular endothelial growth factor (VEGF)-R1 (FLT-1) pre-mRNA is important for the regulation of VEGF activity. *Mol Endocrinol*., 1999; **13**(4): 537- 45.

Herington J, Bruner-Tran KL, Lucas JA, *et al*. Immune interactions in endometriosis. *Expert Rev Clin Immunol.*, 2011; **7:** 611-626.

Hess AP, Schanz A, Batson-Buest DM, *et al*. Expression of the vascular endothelial growth factor neuropilin-1 in the human endometrium. *J Reprod Immunol.*, 2009; **79**: 129-136.

Heydarian M, McCaffrey T, Florea L, *et al*. Novel splice variants of sFlt1 are upregulated in preeclampsia. *Placenta,* 2009; **30**: 250-5.

Hiratsuka S, Minowa O, Kuno J, *et al*. Flt-1 lacking the tyrosine kinase domain is sufficient for normal development and angiogenesis in mice. *Proc Natl Acad Sci USA,* 1998; **95:** 9349–9354.

Hills FA, English J, Chard T. Circulating levels of IGF-I and IGF- binding protein-1 throughout pregnancy: relation to birthweight and maternal weight. *J Endocrinol*., 1996; **148**(2): 303–309.

Hod T, Cerdeira AS, Karumanchi SA. Molecular mechanisms of preeclampsia. *Cold Spring Harb Perspect Med.*, 2015; **5**: 1–21.

Horseman ND, Zhao W, Montecino-Rodriguez E, *et al*. Defective mammopoiesis, but normal hematopoiesis, in mice with a targeted disruption of the prolactin gene. *The EMBO Journal.,* 1997; **16**(23): 6926-6935.

Houck KA, Ferrara N, Winer J, *et al***.** The vascular endothelial growth factor family: identification of a fourth molecular species and characterization of alternative splicing of RNA. *Mol Endocrinol.*, 1991; **5**: 1806- 1814.

Houser BL. Decidual macrophages and their roles at the maternal-fetal interface. *Yale J. Biol. Med.,* 2012; **85**: 105–118.

Huang JC, Liu DY, Dawood MY. The expression of vascular endothelial growth factor isoforms in cultured human endometrial stromal cells and its regulation by 17beta-oestradiol. *MHR: Basic sci of reprod med.*, 1998; **4**: 603-7.

Hull ML, Charnock-Jones D, Chan CLK, *et al*. Antiangiogenic agents are effective inhibitors of endometriosis. *J Clin Endocrinol Metab.*, 2003; **88**(6): 2889-2899.

Hutcheon JA, Lisonkova S, Joseph KS. Epidemiology of pre-eclampsia and the other hypertensive disorders of pregnancy. *Best Pract Res Clin Obstet Gynaecol.*, 2011; **25**(4): 391-403.

Huyen DV, and Bany BM. Evidence for a conserved function of heart and neural crest derivatives expressed transcript 2 in mouse and human decidualisation. *Reproduction*, 2011; **142**(2): 353-368.

Inada K, Iiavashi S, Iguchi T, *et al*. Establishment of a Primary Culture Model of Mouse Uterine and Vaginal Stroma for Studying In Vitro Estrogen Effects. *Soc Exp Biol Med.*, 2006; **231**: 303-10.

Jakovljevic A, Bogavac M, Lozanov-Crvenkovic Z, *et al*. Early pregnancy angiogenic proteins levels and pregnancy related hypertensive disorders. *J Matern Fetal Neonatal Med*., 2017; **30**(5): 534-539.

Jebbink J, Keijser R, Veenboer G, *et al*. Expression of placental FLT1 transcript variants relates to both gestational hypertensive disease and fetal growth. *Hypertension*, 2011; **58**:70–76.

Jee BD, Suh CS, Kim KC, *et al*. Expression of vascular endothelial growth factor -A and its receptor-1 in a luteal endometrium in patients with repeated in vitro fertilization failure. *Fert Steril.*, 2009; **91**: 528-34.

Jeon HH, Yu Q, Lu Y, *et al*. FOXO1 regulates VEGFA expression and promotes angiogenesis in healing wounds. *J Pathol.*, 2018; **245**(3): 258-264.

Jeong W, Kim J, Bazer FW, *et al*. Stimulatory effect of vascular endothelial growth factor on proliferation and migration of porcine trophectoderm cells and their regulation by the phosphatidylinositiol-3-kinase-AKT and Mitogen-activated protein kinase cell signaling pathways. *Biol Reprod.*, 2014; **90**(3): 1-10.

Jiang G, Qi Y. Detection of MMP-9 and TIMP-3 mrna ex- pression in the villi of patients undergoing early sponta- neous abortion: A report of 30 cases. *Exp Ther Med*., 2015; **9**: 1939–43.

Jiang Y, Liao Y, He H, *et al*. FoxM1 directs STAT3 expression essential for human endometrial stromal decidualisation. *Sci Rep.,* 2015; **5**: 13735.

Jiang Y, Yan G, Zhang H, *et al*. Activation of matrix metalloproteinase-26 by HOXA10 promotes embryo adhesion *in vitro. Biochem Biophys Res Commun*., 2014; **445**(3): 622-8.

Jiang ZY, Zhou QL, Holik J, *et al*. Identification of WNK1 as a substrate of Akt/Protein kinase B and a negative regulator of insulin-stimulated mitogenesis in 3T3-L1 cells. *J Biol Chem.*, 2005; **280**(22): 21622-21628.

Jin E, Liu J, Suehiro J, *et al*. Differential roles for ETS, CREB, and EGR binding sites in mediating VEGF receptor 1 expression in vivo. *Blood*, 2009; **114**(27): 5557-66.

Johns A, Freay AD, Fraser W, et al. Disruption of estrogen receptor gene prevents 17β-estradiol-induced angiogenesis in transgenic mice. *Endocrinology*, 1996; **137**: 4511–4513.

Johnson MH and Everitt BJ. Essential Reproduction. Sixth Edition. Oxford. Blackwell Publishing, 2007.

Jones RL, Critchley HO, Brooks J, *et al*. Localization and temporal expression of prolactin receptor in human endometrium. *J Clin Endocrinol Metab*., 1998; **83**(1): 258-62.

Jones RL, Findlay JK, Farnworth PG, *et al*. Activin A and inhibin A differentially regulate human uterine matrix metalloproteinases: Potential interactions during decidualisation and trophoblast invasion. *Endocrinology*, 2006; **147**(2): 724-732.

Jones RL, Salamonsen LA, Findlay JK. Activin A promotes human endometrial stromal cell decidualisation in vitro. *J Clin Endocrinol Metab.*, 2002; **87**(8): 4001-4004.

Kaestner KH, Knochel W, Martinez DE. Unified nomenclature for the winged helix/forkhead transcription factors. *Genes Dev*., 2000; **14**: 142–146.

Kaiserman-Abramof IR, and Padykula HA**.** Angiogenesis in the postovulatory primate endometrium: the coiled arteriolar system. *Anat Rec*., 1989; **224**: 479-489.

Kaitu'u-Lino TJ, Morison NB, Salamonsen LA. Estrogen is not essential for full endometrial restoration after breakdown: lessons from a mouse model. *Endocrinology*, 2007; **148**: 5105–5111.

Kajihara T, Brosens JJ, Ishihara O. The role of FOXO1 in the decidual transformation of the endometrium and early pregnancy. *Med Mol Morphol.* 2013; **46**(2):61-68.

Kajihara T, Jones M, Fusi L, *et al*. Differential expression of FOXO1 and FOXO3a confers resistance to oxidative cell death upon endometrial decidualisation. *Mol Endocrinol.,* 2006; **20**: 2444-55.

Kalantaridou SN, Makrigiannakis A, Mastorakos G, *et al*. Roles of reproductive corticotropin-releasing hormone. *Ann N Y Acad Sci*., 2003; **997**(1):129-135.

Kane NM, Jones M, Brosens JJ, *et al*. TGFβ1 attenuates expression of prolactin and IGFBP-1 in decidualized endometrial stromal cells by both SMAD-dependent and SMAD-independent pathways. *PLoS ONE*, 2010; **5**(9): e12970.

Kao LC, Germeyer A, Tulac S, *et al*. Expression profiling of endometrium from women with endometriosis reveals candidate genes for disease-based implantation failure and infertility. *Endocrinology*, 2003; **144**(7): 2870-81.

Karadedou CT, Gomes AR, Chen J, *et al*. FOXO3a represses VEGF expression through FOXM1-dependent and -independent mechanisms in breast cancer. *Oncogene*, 2012; **31**(14):1845-58.

Karkkainen MJ, Haiko P, Sainio K, *et al*. Vascular endothelial growth factor C is required for sprouting of the first lymphatic vessels from embryonic veins. *Nat Immunol.,* 2004; **5**(1): 74-80.

Kawamori D, Kaneto H, Nakatani Y, *et al*. The forkhead transcription factor Foxo1 bridges the JNK pathway and the transcription factor PDX-1 through its intracellular translocation. *J Biol Chem.*, 2006; **281**(2): 1091-1098.

Kawasaki T, Kitsukawa T, Bekku Y, *et al*. A requirement for neuropilin-1 in embryonic vessel formation. *Development*, 1999; **126**: 4895-4902.

Keck PJ, Hauser SD, Krivi G, *et al*. Vascular permeability factor, an endothelial cell mitogen related to PDGF. *Science*. 1989; **246**(4935): 1309-1312.

Kendall RL, and Thomas KA. Inhibition of vascular endothelial cell growth factor activity by an endogenously encoded soluble receptor. *Proc Natl Acad Sci U S A,* 1993; **90**(22): 10705-10709.

Kessler CA, Moghadam KK, Schroeder JK, *et al*. Cannabinoid receptor I activation markedly inhibits human decidualisation. *Mol Cell Endocrinol*., 2005; **229**(1–2): 65-74.

Khong TY, De Wolf F, Robertson WB, *et al*. Inadequate maternal vascular response to placentation in pregnancies complicated by pre-eclampsia and by small-for-gestational age infants. *Br J Obstet Gynaeco.,* 1986; **93**: 1049–1059.

Kietzmann T, Mennerich D, and Dimova EY. Hypoxia-inducible factors (HIFs) and phosphorylation: impact on stability, localization, and transactivity. *Front. Cell Dev. Biol*., 2016; **4**: 11.

Kikuchi O, Kobayashi M, Amano K, *et al*. FoxO1 gain of function in the pancreas cause glucose intolerance, polycystic pancreas, and islet hypervascularization. *PLoS One*, 2012; **7**(2): e32249.

Kim JJ, Taylor HS, Akbas GE, *et al*. Regulation of insulin-like growth factor binding protein-1 promoter activity by FKHR and HOXA10 in primate endometrial cells. *Biol Reprod*., 2003; **68**(1): 24-30.

Kim JJ, Buzzio OL, Lu Z. Role of FOXO1A in the regulation of insulin-like growth factor binding protein-1 in human endometrial cells: Interaction with progesterone receptor. *Biol Reprod.*, 2005; **73**(4): 833-839.

Kim JJ, Taylor HS, Lu Z, *et al*. Altered expression of HOXA10 in endometriosis: potential role in decidualisation. *Mol Hum Reprod.,* 2007; **13**: 323-32.

Kim M, Park HJ, Seol JW, *et al*. VEGF-A regulated by progesterone governs uterine angiogenesis and vascular remodelling during pregnancy. *EMBO Mol Med.*, 2013; **5**: 1415-1430.

Kitsukawa T, Shimizu M, Sanbo M, *et al*. Neuropilin-semaphorin III/D-mediated chemorepulsive signals play a crucial role in peripheral nerve projection in mice. *Cell Press*, 1997; **19**(5): 995-1005.

Kolodkin AL, Levengood DV, Rowe EG, *et al*. Neuropilin is a semaphoring III receptor. *Cell*, 1997; **90**: 753-762.

Kolte D, McClung JA, Aronow WS. Vasculogenesis and Angiogensis. *Translational Research in Coronary Artery Disease*, 2016.

Kommagani R, Szwarc MM, Vasquez YM, *et al*. The promyelocytic leukemia zinc finger transcription factor is critical for human endometrial stromal cell decidualisation. *PLoS Genet.,* 2016; **12**: e1005937.

Koopman LA, Kopcow HD, Rybalov B, *et al*. Human decidual natural killer cells are a unique NK cell subset with immunomodulatory potential. *J Exp Med*., 2003; **198**: 1201-1212.

Koressaar T, and Remm M. Enhancements and modifications of primer design program Primer3. *Bioinformatics*, 2007; **23**(10): 1289-91.

Krikun, G., Mor, G., Alvero, A., *et al*. A novel immortalized human endometrial stromal cell line with normal progestational response. *Endocrinology*, 2004; **145**: 2291-2296.

Krishna U, Bhalerao S. Placental insufficiency and fetal growth restriction. *J Obstet Gynaecol India*, 2011; **61**(5): 505–511.

Krussel JS, Casan EM, Raga F, *et al*. Expression of mRNA for vascular endothelial growth factor trans- membraneous receptors Flt1 and KDR, and the soluble receptor sFlt in cycling human endometrium. *Mol Hum Reprod.*, 1999; **5**: 452–458.

Kurita T, Lee K, Saunders PTK, *et al*. Regulation of progesterone receptors and decidualisation in uterine stroma of the estrogen receptor-α knockout mouse. *Biol Reprod.*, 2001; **64**(1): 272-283.

Kusama K, Yoshie M, Tamura K, *et al*. Regulation of decidualisation in human endometrial stromal cells through exchange protein directly activated by cyclic AMP (Epac). *Placenta*, 2013. **34**(3): 212-21.

Labied S, Kajihara T, Madureira PA, *et al*. Progestins regulate the expression and activity of the forkhead transcription factor FOXO1 in differentiating human endometrium. *Mol Endocrinol.*, 2006; **20**(1): 35-44.

Lacey H, Haigh T, Westwood M, *et al.* Mesenchymally- derived insulin-like growth factor 1 provides a paracrine stimu- lus for trophoblast migration. *BMC Dev Biol.*, 2002; **2**(1): 5.

Lalmansingh AS, Karmarkar S, Jin Y, et al. Multiple modes of chromatin remodelling by forkhead box proteins. *Biochimica et Biophysica Acta: Gene Regulatory Mechanisms,* 2012; **1819**(7): 707-715.

Laoukili J, Stahl M, and Medema RH. FoxM1: at the crossroads of ageing and cancer. *Biochim Biophys Acta*., 2007; **1775**(1): 92-102.

Large MJ, Wetendorf M, Lanz RB, *et al*. The Epidermal Growth Factor Receptor Critically Regulates Endometrial Function during Early Pregnancy. *PLoS Genetics,* 2014; **10**: e1004451.

Lash GE, Schiessi B, Kirkley, *et al*. Expression of angiogenic growth factors by uterine natural killer cells during early pregnancy. *J Luekoc Biol.*, 2006; **80**(3): 572-80.

Leach RE, Kilburn B, Wang J, *et al*. Heparin-binding EGF-like growth factor regulates human extravillous cytotrophoblast development during conversion to the invasive phenotype. *Dev Biol*., 2004; **266**: 223-237.

Lecce G, Meduri G, Ancelin M, *et al*. Presence of estrogen receptor β in the human endometrium through the cycle: Expression in glandular, stromal, and vascular cells. *J Clin Endocrinol Metab.*, 2001; **86**(3): 1379-1386.

Ledee N, Chaouat G, Serazin V, *et al*. Endometrial vascularity by three-dimensional power Doppler ultrasound and cytokines: a complementary approach to assess uterine receptivity. *J Reprod Immunol.*, 2008**; 77**:57-62.

Lee J, Oh JS, Cho C. Impaired expansion of trophoblast spheroids cocultured with endometrial cells overexpressing cellular retinoic acid-binding protein 2. *Fertil Steril*., 2011; **95**(8): 2599-2601.

Lee KY, and DeMayo FJ. Animal models of implantation. *Reproduction*. 2004; **128**(6): 679-695.

Lekstrom-Himes J and Xanthopoulos KG. Biological role of the CCAAT/enhancer-binding protein family of transcription factors. *J Biol Chem.*, 1998; **273**(44): 28545-8.

Lengner CJ, Lepper C, van Wijnen AJ, *et al*. Primary mouse embryonic fibroblasts: a model of mesenchymal cartilage formation. *J Cell Physiol*., 2004; **200**: 327-33.

Lessey BA, Gui Y, Apparao KB, *et al*. Regulated expression of heparin-binding EGF-like growth factor (HB-EGF) in the human endometrium: a potential paracrine role during implantation. *Mol Reprod Dev*., 2002; **62**(4): 446-55.

Leung DW, Cachianes G, Kuang WJ, *et al*. Vascular endothelial growth factor is a secreted angiogenic mitogen. *Science*. 1989; **246**(4935): 1306-1309.

Li H, Li H, Bai L, *et al*. Lefty inhibits *in vitro* decidualisation by regulating p57 and cyclin D1 expressions. *Cell Biochem Funct*., 2014; **32**: 657-664.

Li MQ, Luo XZ, Meng YH, *et al*. CXCL8 enhances proliferation and growth and reduces apoptosis in endometrial stromal cells in an autocrine manner via a CXCR1-triggered PTEN/AKT signa pathway. *Hum Reprod.*, 2012; **27**(7): 2107-16.

Li Q, Kannan A, Wang W, *et al*. Bone morphogenetic protein 2 functions via a conserved signaling pathway involving Wnt4 to regulate uterine decidualisation in the mouse and the human. *J Biol Chem.*, 2007; **282**(43): 31725-31732.

Li XF, Charnock-Jones DS, Zhang E, *et al*. Angiogenic growth factor messenger ribonucleic acids in uterine natural killer cells. *J Clin Endocrinol Metab.*, 2001; **86**: 1823-1834.

Li Y, Zhu H, Klausen C, *et al.* Vascular endothelial growth factor-A (VEGF-A) mediates activin A-induced human trophoblast endothelial-like tube formation. *Endocrinol.*, 2015; **156**: 4257-4268.

Licht P, Russu V, Wildt L. On the role of human chorionic gonadotropin (hCG) in the embryo-endometrial microenvironment: Implications for differentiation and implantation. *Semin Reprod Med.,* 2001; **19**(1): 37-47.

Lim H, Ma L, Ma WG, *et al*. Hoxa-10 regulates uterine stromal cell responsiveness to progesterone during implantation and decidualisation in the mouse*. Mol Endocrinol.*, 1999; **13**(6): 1005-17.

Lim HJ and Dey SK. HB-EGF: a unique mediator of embryo uterine interactions during implantation. *Exp Cell Res*, 2009; **315**: 619-626.

Lin J and Gu Y. Effect of monocyte chemoattractant protein-1 and estradiol on the secretion of vascular endothelial growth factor in endometrial stromal cells in vitro. *Fert Steril.*, 2005; **84**(6): 1793-1796.

Lockwood CJ, Krikun G, Hickey M, *et al*. Decidualized human endometrial stromal cells mediate hemostasis, angiogenesis and abnormal uterine bleeding. *Reprod Sci.*, 2009; **16**(2): 162-170.

Lockwood CJ, Krikun G, Koo AB, *et al*. Differential effects of thrombin and hypoxia on endometrial stromal and glandular epithelial cell vascular endothelial growth factor expression. *J Clin Endocrinol Metab.*, 2002; **87**: 4280–4286.

Lockwood CJ, Krikun G, Rahman M, *et al*. The role of decidualisation in regulating endometrial hemostasis during the menstrual cycle, gestation, and in pathological states. *Semin Thromb Hemost*., 2007; **33**(10): 111-7.

Lockwood CJ, Matta P, Krikun G, *et al*. Regulation of monocyte chemoattractant protein-1 expression by tumor necrosis factor-α and interleukin-1β in first trimester human decidual cells. *Am J Pathol., 2006*; **168**(2).

Loke YW, King A, and Burrows TD. Decidua in human implantation. *Hum Reprod*, 1995; **10**(2): 14-21.

Long J, Yang C, He J, *et al*. FOXO3a is essential for murine endometrial decidualisation through cell apoptosis during early pregnancy. *J Cell Physiol.*, 2018; 1-13.

Loots G, and Ovcharenko I. rVista 2.0: evolutionary analysis of transcription factor binding sites. *Nucleic Acids Research*, 2004; **32**(Web Server Issue): W217-W221.

Lu Z, Hardt J, and Kim JJ. Global analysis of genes regulated by HOXA10 in decidualisation reveals a role in cell proliferation. *Mol Hum Reprod.*, 2008; **14**(6): 357-366.

Lydon JP, DeMayo FJ, Funk CR, *et al*. Mice lacking progesterone receptor exhibit pleiotropic reproductive abnormalities. *Genes Dev.*, 1995; **9**: 2266-2278.

Lynch VJ, Brayer K, Gellersen B, *et al*. HoxA-11 and FOXO1A cooperate to regulate decidual prolactin expression: Towards inferring the core transcriptional regulators of decidual genes. dey SK, ed. *PLoS ONE*, 2009; **4**(9): e6845.

Macer ML, and Taylor HS. Endometriosis and infertility: a review of the pathogenesis and treatment of endometriosis-associated infertility. *Obster Gynecol Clin North Am.*, 2012; **39**(4): 535-49.

Macklon NS and Brosens JJ. The human endometrium as a sensor of embryo quality. *Biol Reprod*., 2014; **91**(4): 98.

Mak IY, Brosens JJ, Christian M, *et al*. Regulated expression of signal transducer and activator of transcription, Stat5, and its enhancement of PRL expression in human endometrial stromal cells in vitro. *J Clin Endocrinol Metab*., 2002; **87**(6): 2581-8.

Mälarstig A, Tenno T, Jossan S, *et al.* A quantitative real-time PCR for tissue factor mRNA. *Thrombosis Research*, 2003; **112**(3): 175-183.

Mangioni S, Viganò P, Florio P, *et al*. Effect of activin A on tumor necrosis factor-α/intercellular adhesion molecule-1 pathway in endometrial stromal cells. *Eur J Obstet Gynecol Reprod Biol.*, 2005; **123**(2): 218-223.

Mantena SR, Kannan A, Cheon Y, *et al*. C/EBPβ is a critical mediator of steroid hormone-regulated cell proliferation and differentiation in the uterine epithelium and stroma. *PNAS*, 2006; **103**(6): 1870-1875.

Maru Y, Yamaguchi S, Shibuya M. Flt-1, a receptor for vascular endtothelial growth factor, has transforming and morphogenic potentials. *Oncogene*, 1998; **16**: 2585-2595.

Maruyama T, and Yoshimura Y. Molecular and cellular mechanisms for differentiation and regeneration of the uterine endometrium. *Endocr J.* 2008; **55**(5):795-810.

Maruyama T, Yamamoto Y, Shimizu A, *et al*. Pyrazolo pyrimidine-type inhibitors of src family tyrosine kinases promote ovarian steroid-induced differentiation of human endometrial stromal cells in vitro. *Biol Reprod*., 2004; **70**(1): 214-221.

Maslar ILAA, Powers-Craddock P, Ansbacher R. Decidual prolactin production by organ cultures of human endometrium: Effects of continuous and intermittent progesterone treatment. *Biol reprod.*, 1986; **34**:741-750.

Masuda H, Matsuzaki Y, Hiratsu E, *et al*. Stem cell-like properties of the endometrial side population: implication in endometrial regeneration. *PLoS One*, 2010; **5**: e10387.

Matsui N, Kawano Y, Nakamura S, *et al*. Changes in vascular endothelial growth factor production associated with decidualisation by human endometrial stromal cells in vitro. *Acta obstetricia et gynecol Scand*, 2004; **83**: 138-43.

Matsumoto H, Sakai K, and Iwashita M. Insulin-like growth factor binding protein-1 induces decidualisation of human endometrial stromal cells via alpha 5 beta 1 integrin. *Mol Hum Reprod*., 2008; **14**(8): 485-9.

Matsuoka A, Kizuka F, Lee L, *et al*. Progesterone increases manganese superoxide dismutase expression via a cAMP-dependent signaling mediated by noncanonical Wnt5a pathway in human endometrial stromal cells. *J Clin Endocrinol Metab*., 2010; **95**(11): E291-E299.

Matsuzaki S, Canis M, Darcha C, *et al*. HOXA-10 expression in the mid-secretory endometrium of infertile patients with either endometriosis, uterine fibromas or unexplained infertility. *Hum Reprod*., 2009; **24**(12): 3180-7.

Maybin J and Critchley. Review: Repair and regeneration of the human endometrium. *J Exp Rev Obstet Gynecol.*, 2009; **4**(3): 283-298.

Maybin JA, Hirani N, Brown P, *et al*. The regulation of vascular endothelial growth factor by hypoxia and prostaglandin F2{alpha} during human endometrial repair. *J Clin Endocrinol Metab.*, 2011; **96**:2475 – 2483.

Maybin JA, Murray AA, Saunders PTK, *et al*. Hypoxia and hypoxia inducible factors-1α are required for normal endometrial repair during menstruation. *Nat Comm.*, 2018; **9**: 295.

Maynard S, Min J, Merchan J, *et al*. Excess placental soluble fms-like tyrosine kinase 1 (sFlt-1) may contribute to endothelial dysfunction, hypertension, and proteinuria in pre-eclampsia. *J Clin Invest.*, 2003; **111**(5): 649-58.

McConnell MJ, Durand L, Langley E, *et al*. Post transcriptional control of the epigenetic stem cell regulator PLZF by sirtuin and HDAC deacetylases. *Epi Chrom.*, 2015; **8**: 38.

McLaren J, Prentice A, Charnock-Jones DS, *et al*. Vascular endothelial growth factor is produced by peritoneal fluid macrophages in endometriosis and is regulated by ovarian steroids. *J Clin Invest.,* 1996; **98**(2): 482-489.

Meduri G, Bausero P, Perrot-Applanat M. Expression of vascular endothelial growth factor receptors in the human endometrium: modulation during the menstrual cycle. *Biology of Reproduction*, 2000; **62**: 439-447.

Menkhorst E, Salamonsen LA, Zhang J, *et al*. Interleukin 11 and activin A synergise to regulate progesterone-induced but not cAMP-induced decidualisation. *J Reprod Immunol*., 2010; **84**(2): 124-132.

Micalizzi DS, Farabaugh SM, Ford HL. Epithelial-mesenchymal transition in cancer: parallels between normal development and tumor progression. *J Mammary Gland Biol Neoplasia*, 2010; **15**: 117-134.

Mihm M, Gangooly S, Muttukrishna S. The normal menstrual cycle in women. *Anim Reprod Sci*. 2011; **124**(3–4): 229-236.

Miquerol L, Langille BL, Nagy A. Embryonic development is disrupted by modest increases in vascular endothelial growth factor gene expression. *Development*, 2000; **127**(18): 3941-3946.

Mori R, Tanaka K, Kerckhove Md, et al. Reduced FOXO1 expression accelerates skin wound healing and attenuates scarring. *Am J Pathol*., 2014; **184**(9): 2465-2479.

Mote PA, Balleine RL, McGowan EM, *et al*. Colocalization of progesterone receptors A and B by dual immunofluorescent histochemistry in human endometrium during the menstrual cycle. *J Clin Endocrinol Metab*, 1999; **84**(8): 2963-71.

Mueller MD, Vigne J-L, Minchenko A, *et al*. Regulation of vascular endothelial growth factor (VEGF) gene transcription by estrogen receptors α and β. *Proc Natl Aca Sci U S A*, 2000; **97**: 10972-7.

Mueller MD, Vigne JL, Pritts EA, *et al*. Progestins activate vascular endothelial growth factor gene tran- scription in endometrial adenocarcinoma cells. *Fertil Steril.*, 2003; **79**: 386 – 92.

Muy-Rivera M, Vadachkoria S, Woelk G, *et al*. Maternal plasma VEGF, sVEGF-R1, and PIGF concentrations in preeclamptic and normotensive pregnant Zimbabwean women. *Physiol Res.*, 2005; **54**: 611.

Myatt SS, Wang J, Monteiro LJ, *et al*. Definition of microRNAs that repress expression of the tumor suppressor gene FOXO1 in endometrial cancer. *Cancer Res.*, 2010; **70**: 367–377.

Neufeld G, Cohen T, Gengrinovitch S, *et al*. Vascular endothelial growth factor and its receptors. *FASEB J*., 1999; **13**: 9– 22.

Nikuei P, Malekzadeh K, Rajaei M, *et al*. The imbalance in expression of angiogenic facotrs as candidate predictive biomarker in preeclampsia. *Iran J Reprod Med.*, 2015; **13**(5): 251-262.

Nishizawa H, Ota S, Suzuki M, *et al*. Comparative gene expression profiling of placentas from patients with severe preeclampsia and unexplained fetal growth restriction. *Reprod Biol Endocrinol.*, 2011; **9**: 107.

Norwitz ER, Schust DJ, Fisher SJ. Implantation and the survival of early pregnancy. *N Engl J Med*., 2001; **345**(19): 1400-1408.

Obsil T, and Obsilova V. Strutural basis for DNA recognition by FOXO proteins. *Biochimica et Biophysica Acta (BBA) - Mol Cell Res.*, 2011; **1813**(11): 1946-1953.

Obsilova V, Vecer J, Herman P, *et al*. 14-3-3 Protein interacts with nuclear localization sequence of forkhead transcription factor FoxO4. *Biochem.*, 2005; **44**: 11608-11617.

Ohshima M, Yamaguchi Y, Ambe K, *et al.* Fibroblast VEGF-receptor 1 expression as molecular target in periodontitis. *J Clin Periodontol*., 2016; **43**: 128–137.

Okada H, Okamoto R, Tsuzuki T, *et al*. Progestins inhibit estradiol-induced vascular endothelial growth factor and stromal cell-derived factor 1 in human endometrial stromal cells. *Fertil Steril*, 2011; **96**(3): 786-91.

Okada H, Tsutsumi A, Imai M, *et al*. Estrogen and selective estrogen receptor modulators regulate vascular endothelial growth factor and soluble vascular endothelial growth factor receptor 1 in human endometrial stromal cells. *Fertil Steril.*, 2010; **93**:2680–2686.

Okada H, Tsuzuki T, Murata H. Review: Decidualisation of the human endometrium. *Reprod Med Biol.*, 2017; 1-8.

Okada H, Tsuzuki T, Shindoh H, *et al*. Regulation of decidualisation and angiogenesis in the human endometrium: Mini review. *J Obstet Gynaecol Res*., 2014; **40**(5): 1180-1187.

Oliver C, Montes MJ, Galindo JA, *et al*. Human decidual stromal cells express alpha-smooth muscle actin and show ultrastructural similarities with myofibroblasts. *Hum Reprod.,* 1999; **14**:1599-1605.

Olofsson B, Korpelainen E, Pepper MS, *et al*. Vascular endothelial growth factor B (VEGF-B) binds to VEGF receptor-1 and regulates plasminogen activator activity in endothelial cells. *Proc Natl Acad Sci.*, 1998; **95**(20): 11709-11714.

Ozawa CR, Banfi A, Glazer NL, *et al*. Microenvironmental VEGF concentration, not total dose, determines a threshold between normal and aberrant angiogenesis. *J Clin Invest*., 2004; **113**(4):516–27.

Ozbilgin K, Karaca F, Turan A, *et al*. The higher heparin-binding epidermal growth factor (HB-EGF) in missed abortion. *Taiwanese J Obstet Gynecol.*, 2015; **54**(1): 13-18.

Pabona JMP, Simmen FA, Nikiforov MA, *et al*. Krüppel-like factor 9 and progesterone receptor coregulation of decidualizing endometrial stromal cells: Implications for the pathogenesis of endometriosis. *J Clin Endocrinol Metab.,* 2012; **97**(3): E376-E392.

Pfaffl MW. Quantification strategies in real-time PCR. In: Bustin SA, editor. The Real-Time PCR Encyclopedia A–Z of Quantitative PCR. *International University Line; La Jolla, CA*, 2004; 87-112.

Pagès G and Pouysségur J. Transcriptional regulation of the Vascular Endothelial Growth Factor gene-a concert of activating factors. *Cardiovascular Res.*, 2005; **65**(3): 564-573.

Paik J, Kollipara R, Chu G, *et al*. FoxOs are lineage-restricted redundant tumor suppressors and critical regulators of endothelial cell homeostasis. *Cell*, 2007; **128**(2): 309-323.

Palmer KR, Tong S, Tuohey L, *et al*. Jumonji domain containing protein 6 is decreased in human preeclamptic placentas and regulates sFlt-1 splice variant production. *Biol Reprod*, 2016; **94**(3): 59, 1-9.

Pang L, Wei Z, Li Q, *et al*. An increase in vascular endothelial growth factor (VEGF) and VEGF soluble receptor-1 (sFlt-1) are associated with early recurrent spontaneuous abortion. *PLoS ONE*, 2013; **8**(9): e75759.

Paria BC, Reese J, Das SK, *et al*. Deciphering the cross-talk of implantation: advances and challenges. *Science*, 2002; **296**(5576): 2185-2188.

Park J, Keller G, Ferrara N. The vascular endothelial growth factor (VEGF) isoforms: differential deposition into the subepithelial extracellular matrix and bioactivity of extracellular matrix bound VEGF. *Mol Biol Cell***,** 1993; **4**: 1317-1326.

Park JE, Chen HH, Winer J, *et al*. Placenta growth factor potentiation of vascular endothelial growth factor bioactivity, in vitro and in vivo, and high affinity binding to flt-1 but not to flk-1/KDR. *J Biol Chem.*, 1994; **269**(41): 25646-25654.

Patel B, Elguero S, Thakore S, *et al*. Role of nuclear progesterone receptor isoforms in uterine pathophysiology. *Hum Reprod Update*, 2015; **21**(2): 155-73.

Perrot-Applanat M, Ancelin M, Buteau-Lozano H, *et al*. Ovarian steroids in endometrial angiogenesis. *Steroids*, 2000; **65**: 599-603.

Pertovaara L, Kaipainen A, Mustonen T, *et al*. Vascular endothelial growth factor is induced in response to transforming growth factor-beta in fibroblastic and epithelial cells. *J Biol Chem*., 1994; **269**: 6271–6274.

Pillai R.S. MicroRNA function: Multiple mechanisms for a tiny RNA? *RNA*, 2005; **11**: 1753–1761.

Plaisier M. Decidualisation and angiogenesis. *Best Prac Res Clin Obstet Gynaecol.*, 2011; **25**(3):259-271.

Plante BJ, Kanna A, Bagchi MK, *et al*. Cyclic regulation of transcription factor C/EBP beta in human endometrium. *Reprod Biol Endocrinol.*, 2009; **7**:15.

Poliseno L, Tuccoli A, Mariani L, *et al*. MicroRNAs modulate the angiogenic properties of HUVECs. *Blood*, 2006; **108**: 3068–3071.

Poljak B, Agarwal U, Jackson R, *et al.* Diagnostic accuracy of individual antenatal tools for prediction of small-for- gestational age at birth. *Ultrasound Obstet Gynecol.,* 2017; 49(4): 493–499.

Pallotto EK, Kilbride HW. Perinatal outcome and later implications of intrauterine growth restriction. *Clin Obstet Gynecol.,* 2006; **49**(2): 257–269.

Poltorak Z, Cohen T, Sivan R, *et al*. VEGF145, a secreted vascular endothelial growth factor isoform that binds to extracellular matrix. *J. Biol. Chem*., 1997; **272**: 7151-7158.

Potente M, Urbich C, Sasaki K, *et al*. Involvement of Foxo transcription factors in angiogenesis and postnatal neovascularization. *J Clin Invest.*, 2005; **115**(9): 2382-2392.

Qian K, Hu L, Chen H, *et al*. Hsa-miR-222 is involved in differentiation of endometrial stromal cells *in vitro*. *Endocrinology*, 2009; **150**: 4734–4743.

Quante M, Raskopf E, Stahl S, *et al.* No functional and transductional significance of specific neuropilin 1 siRNA inhibition in colon carcinoma cell lines lacking VEGF receptor 2. *Oncology Reports*, 2009; **21**: 1161-1168.

Rabaglino MB, Uiterweer EDP, Jeyabalan A, *et al*. A bioinformatics approach reveals evidence for impaired endometrial maturation before and during early pregnancy in women who developed preeclampsia. *Hypertension*, 2015; **65**(2): 421-429.

Rajakumar A, Powers R W, Hubel CA, *et al*. Novel soluble Flt-1 isoforms in plasma and cultured placental explants from normotensive pregnant and preeclamp- tic women. *Placenta,* 2009; **30**: 25–34.

Ramaswamy S, Nakamura N, Sansal I, *et al*. A novel mechanism of gene regulation and tumor suppression by the transcription factor FKHR. *Cancer Cell*, 2002; **2**(1): 81-91.

Ramathal C, Bagchi I, Taylor R, *et al.* Endometrial decidualisation: of mice and men. *Semin Reprod Med*., 2010; **28**(1): 17-26.

Reem GH, Ray DW, Davis JR. The human prolactin gene upstream promoter is regulated in lymphoid cells by activators of T-cells and by cAMP. *J Mol Endocrinol.*, 1999; **22**: 285-292.

Rein DT, Schmidt T, Bauerschmitz G, *et al*. Treatment of endometriosis with a VEGF-targeted conditionally replicative adenovirus. *Fertil Steril*., 2010; **93**(8): 2687-94.

Reis FM, Maia AL, Ribeiro MF, *et al*. Progestin modulation of c-fos and prolactin gene expression in the human endometrium. *Fertil Steril*., 1999; **71**: 1125-1132.

Ribatti D. The crucial role of vascular permeability factor/vascular endothelial growth factor in angiogenesis: A historical review. *Br J Haematol*., 2005; **128**(3): 303-309.

Rider V. Progesterone and the control of uterine cell proliferation and differentiation. *Front Biosci*., 2002; **7**: 1545-1555.

Roberts JM, and Cooper DW. Pathogenesis and genetics of pre-eclampsia. *Lancet,* 2001; **357**: 53–56.

Roberts JM, Rajakumar A. Preeclampsia and Soluble fms-Like Tyrosine Kinase 1. *J Clin Endocrinol Metab*., 2009; **94**(7): 2252-2254.

Rocha ALL, Carrarelli P, Novembri R, *et al*. Activin A stimulates interleukin 8 and vascular endothelial growth factor release from cultured human endometrial stromal cells: possible implications for the pathogenesis of endometriosis. *Reprod Sci.*, 2012; **19**(8): 832-838.

Rogers PA, and Gargett CE. Endometrial angiogenesis. *Angiogenesis*, 1998; **2**:287-294.

Rogers PA. Structure and function of endometrial blood vessels. *Hum Reprod Update*, 1996. **2**(1): 57-62.

Roupé KM, Veerla S, Olson J, *et al*. Transcription Factor Binding Site Analysis Identifies FOXO Transcription Factors as Regulators of the Cutaneous Wound Healing Process. *PLoS ONE*, 2014; **9**(2): e89274.

Russell P, Anderson L, Lierberman D, *et al.* The distribution of immune cells and macrophages in the endometrium of women with recurrent reproductive failure I: techniques. *J Reprod Immunol.*, 2011; **91**(1-2): 90-102.

Sakai N, Maruyama T, Sakurai R, *et al*. Involvement of histone acetylation in ovarian steroid-induced decidualisation of human endometrial stromal cell. *J Biol Chem.*, 2003; **278**(19): 16675-16682.

Salamonsen LA, Hannan NJ, and Dimitriadis E. Cytokines and chemokines during human embryo implantation: roles in implantation and early placentation. *Semin Reprod Med*., 2007; **25**(6): 437-44.

Salker M, Teklenburg G, Molokhia M, *et al*. Natural selection of human embryos: impaired decidualisation of endometrium disables embryo-maternal interactions and causes recurrent pregnancy loss. *PLoS One*, 2010; **5**: e10287.

Salker MS, Nautiyal J, Steel JH, *et al*. Disordered IL-33/ST2 activation in decidualizing stromal cells prolongs uterine receptivity in women with recurrent pregnancy loss. *PLoS One*, 2012; **7**(12): e52252.

Samalecos A, Reinmann K, Wittmann S, *et al*. Characterization of a novel telomerase-immortalised human endometrial cell line St-T1b. *Reprod Bio Endocrinol*., 2009; **7**:76.

Saravelos SH, and Regan L. Unexplained recurrent pregnancy loss. *Obstet Gynecol Clin North Am*, 2014; **41**(1): 157-66.

Satokata I, Benson G, and Maas R. Sexually dimorphic sterility phenotypes in Hoxa10-deficient mice. *Nature*, 1995. **374**(6521): 460-3.

Schoolcraft WB, and Katz-Jaffe MG. Comprehensive chromosome screening of trophectoderm with vitrification facilitates elective single-embryo transfer for infertile women with advanced maternal age. *Fertil Steril*., 2013; **100**(3): 615-619.

Schroeder JK, Kessler CA, Handwerger S. Critical role for TWIST1 in the induction of human uterine decidualisation. *Endocrinology*, 2011; **152**(11): 4368-4376.

Schultz JR, Petz LN, Nardulli AM. Estrogen receptor α and Sp1 regulation progesterone receptor gene expression. *Mol Cell Endorinol.*, 2003; **201**: 165-175.

Schwenke M, Knofler M, Velicky P, *et al*. Control of human endometrial stromal cell motility by PDGF-BB, HB-EGF and trophoblast-secreted factors. *PLoS One*, 2013; **8**: e54336.

Scott Jr. RT, Upham KM, Forman EJ, *et al*. Blastocyst biopsy with comprehensive chromosome screening and fresh embryo transfer significantly increases in vitro fertilization implantation and delivery rates: A randomized controlled trial. *Fertil Steril*., 2013; **100**(3): 697-703.

Sela S, Itin A, Natanson-Yaron S, Greenfield C, *et al*. A Novel Human-Specific Soluble Vascular Endothelial Growth Factor Receptor 1: Cell Type-Specific Splicing and Implications to Vascular Endothelial Growth Factor Homeostasis and Preeclampsia. *Circ Res.*, 2008; **102**(12): 1566-74.

Semenza G. Angiogenesis in ischemic and neoplastic disorders. *Annu Rev Med*., 2003; **54**: 17–28.

Senger DR, Galli SJ, Dvorak AM, *et al*. Tumor cells secrete a vascular permeability factor that promotes accumulation of ascites fluid. *Science*, 1983; **219**(4587): 983-985.

Sferruzzi-Perri AN, Owens JA, Standen P, *et al.* Early treatment of the pregnant guinea pig with IGFs promotes placental transport and nutrient partitioning near term. *Am J Physiol Endocrinol Metab.*, 2007; **292**(3): E668–E676.

Sha G, Wu D, Zhang L, *et al.* Differentially expressed genes in human endometrial endothelial cells derived from eutopic endometrium of patients with endometriosis compared with those from patients without endometriosis. *Hum Reprod.*, 2007; **22**(12): 3159-3169.

Shalaby F, Rossant J, Yamaguchi TP, *et al*. Failure of blood-island formation and vasculogenesis in flk-1-deficient mice. *Nature*. 1995; **376**(6536): 62-66.

Shapiro BS, Daneshmand ST, Garner FC, *et al*. Evidence of impaired endometrial receptivity after ovarian stimulation for in vitro fertilization: A prospective randomized trial comparing fresh and frozen–thawed embryo transfer in normal responders. *Fertil Steril*., 2011; **96**(2): 344-348.

Sharkey AM, Day K, McPherson A, *et al*. Vascular endothelial growth factor expression in human endometrium is regulated by hypoxia. *J Clin Endocrinol Metab.*, 2000; **85**: 402–409.

Shazand K, Baban S, Prive C, *et al*. FOXO1 and c-jun transcription factors mRNA are modulated in endometriosis. *Mol Hum Reprod*., 2004; **10**(12): 871-7.

Shehab MA, Damerill I, Shen T, *et al.* Liver mTOR controls IGF-I bioavailability by regulation of protein kinase CK2 and IGFBP-1 phosphorylation in fetal growth restriction. *Endocrinology*, 2014; **155**(4): 1327–1339.

Shehab MA, Biggar K, Singal SS, *et al.* Exposure of decidualized HIESC to low oxygen tension and leucine deprivation results in increased IGFBP- 1 phosphorylation and reduced IGF-I bioactivity. *Mol Cell Endocrinol.*, 2017; **452**: 1–14.

Sherafat-Kazemzadeh R, Schroeder J, Kessler CS. Parathyroid hormone-like hormone (PTHLH) represses decidualisation of human uterine fibroblast cells by an Autocrine/Paracrine mechanism. *J Clin Endocrinol Metab.,* 2011; **96**(2): 509-514.

Shibuya M, Yamaguchi S, Yamane A, *et al*. Nucleotide sequence and expression of a novel human receptor-type tyrosine kinase gene (flt) closely related to the fms family. *Oncogene*, 1999; **5**(4): 519-24.

Shibuya M, Yamaguchi S, Yamane A, *et al*. Nucleotide sequence and expression of a novel human receptor-type tyrosine kinase gene (flt) closely related to the fms family. *Oncogene*, 1990; **5**: 519-524.

Shibuya M. Vascular Endothelial Growth Factor (VEGF) and Its Receptor (VEGFR) Signaling in Angiogenesis: A Crucial Target for Anti- and Pro-Angiogenic Therapies. *Genes Cancer,* 2011; **2**: 1097-105.

Shifren JL, Tseng JF, Zaloudek CJ, *et al*. Ovarian steroid regulation of vascular endothelial growth factor in the human endometrium: implications for angiogenesis during the menstrual cycle and in the pathogenesis of en- dometriosis. *J Clin Endocrinol Metab.*, 1996; **81**: 3112–3118.

Shiozawa T, Shih H, Miyamoto T, *et al*. Cyclic changes in the expression of steroid receptor coactivators and corepressors in the normal human endometrium. *J Clin Endocrinol Metab.*, 2003; **88**(2): 871-878.

Shuya LL, Menkhorst EM, Yap J, *et al*. Leukemia inhibitory factor enhances endometrial stromal cell decidualisation in humans and mice. *PLoS ONE*. 2011; **6**(9): e25288.

Sievers F, Wilm A, Dineen D, *et al.* Fast, scalable generation of high-quality protein multiple sequence alignments using Clustal Omega. *Mol. Syst. Biol.*, 2011; **7**:539.

Simone ND, Nicuolo FD, Castellani R, *et al*. Low-molecular-weight heparins induce decidual heparin-binding epidermal growth factor-like growth factor expression and promote survival of decidual cells undergoing apoptosis. *Fertil Steril*., 2012; **97**(1); 169-177.

Singal SS, Nygard K, Gratton R, *et al.* Increased insulin-like growth factor binding protein-1 phosphorylation in decidualised stromal mesenchymal cells in human intrauterine growth restriction placentas. *J Histochem Cytochem.*, 2018; **66**: 617-630.

Singh M, Chaudhry P, Asselin E. Bridging endometrial receptivity and implantation: Network of hormones, cytokines, and growth factors. *J Endocrinol*, 2011; **210**(1): 5-14.

Singh N, Prasad P, Das B, *et al*. Involvement of matrix metalloproteinases and their inhibitors in endometrial extracellular matrix turnover in Clamydia trachomatis-infected recurrent spontaneous aborters. *Pathogen and Disease*, 2017; **75**(1): 1-8.

Skrzypczak J, Wirstlein P, Mikolajczyk M, *et al*. TGF superfam- ily and MMP2, MMP9, TIMP1 genes expression in the en- dometrium of women with impaired reproduction. *Folia His- tochem Cyto.*, 2007; **45**: 43–8.

Smith MK, Peters MC, Richardson TP, *et al*. Locally enhanced angiogenesis promotes transplanted cell survival. *Tissue Eng.*, 2004; **10**(1-2): 63-71.

Smith SK. Regulation of angiogenesis in the endometrium. *Trends Endocrinol Metab.*, 2001; **12**(4):147-151.

Smith SK. Vascular endothelial growth factor and the endometrium. *Hum Reprod.*, 1996; **11**: 56–61.

Soker S, Miao HQ, Nomi M, *et al*. VEGF165 mediates formation of complexes containing VEGFR-2 and neuropilin-1 that enhance VEGF165-receptor binding. *J. Cell Biochem.*, 2002; **85**: 357-368.

Soker S, Takashima S, Miao HQ, *et al*. Neuropilin-1 is expressed by endothelial and tumour cells as an isoform-specific receptor for vascular endothelial growth factor. *Cell,* 1998*;* **92**: 735–745.

Stefanoska I, Jovanović Krivokuća M, Vasilijić S, *et al*. Prolactin stimulates cell migration and invasion by human trophoblast in vitro. *Placenta*. 2013; **34**(9): 775-783.

Stewart SA, Dykxhoom DM, Palliser D, *et al*. Lentivirus-delivered stable gene silencing by RNAi in primary cells. *RNA*, 2003; **9**(4): 493-501.

Strakova Z, Mavrogianis P, Meng X, *et al*. In vivo infusion of interleukin-1beta and chorionic gonadotropin induces endometrial changes that mimic early pregnancy events in the baboon. *Endocrinology*, 2005; **146**(9): 4097-104.

Su RW, Strug MR, Joshi NR, *et al*. Decreased Notch pathway signaling in the endometrium of women with endometriosis impairs decidualisation. *J Clin Endocrinol Metab.*, 2015; **100**(3): E433-42.

Sugawara K, Hamatani T, Yamada M, *et al*. Derivation of human decidua-like cells from amnion and menstrual blood. *Sci Rep.*, 2014; **4**:4599.

Sugino N, Karube-Harada A, Taketani T, *et al*. Withdrawal of ovarian steroids stimulates prostaglandin F2α production through nuclear factor-κB activation via oxygen radicals in human endometrial stromal cells: potential relevance to menstruation. *J Reprod Dev.*, 2004; **50**: 215–225.

Sugino N, Kashida S, Karube-Harada A, *et al*. Expression of vascular endothelial growth factor (VEGF) and its receptors in human endometrium throughout the menstrual cycle and in early pregnancy. *Reproduction*. 2002; **123**(3): 379-387.

Sugino N, Shimamura K, Takiguchi S, *et al*. Changes in activity of superoxide dismutase in the human endometrium throughout the menstrual cycle and in early pregnancy. *Hum Reprod.*, 1996; **11**(5): 1073- 1078.

Suzuki T, Sugino N, Fukaya T, *et al*. Superoxide dismutase in normal cycling human ovaries: immunohistochemical localization and characterization. *Fertil Steril.*, 1999; **72** (4): 720-726.

Szwarc MM, Hai L, Gibbon WE, *et al*. Human endometrial stromal cell decidualisation requires transcriptional reprogramming by PLZF. *Biol Reprod.*, 2018; **98**(1): 15-27.

Tabibzadeh S. Isolation, characterization, and function of EBAF/LEFTY B: Role in infertility. *Ann N Y Acad Sci*., 2011; **1221**(1):98-102.

Takagi H, King GL, Aiello LP. Identification and characterization of vascular endothelial growth factor receptor (Flt) in bovine retinal pericytes. *Diabetes*, 1996; **45**: 1016–1023.

Takahashi M, Matsui A, Inao M, *et al*. ERK/MAPK-dependent PI3K/Akt phosphorylation through VEGFR-1 after VEGF stimulation in activated hepatic stellate cells. *Hepatology Research*, 2003; **26**: 232-236.

Takano M, Lu Z, Goto T, *et al*., Transcriptional cross talk between the forkhead transcription factor forkhead box O1A and the progesterone receptor coordinates cell cycle regulation and differentiation in human endometrial stromal cells. *Mol Endocrinol.*, 2007; **21**(10): 2334-49.

Takashima SM, Kitakaze M, Asakura M, *et al*. Targeting of both mouse neuropilin-1 and neuropilin-2 genes severely impairs developmental yolk sac and embryonic angiogenesis. *Proc Natl Acad Sci U S A,* 2002; **99**(6): 3657-62.

Takei Y, Kadomatsu K, Yuzawa Y, et al. A small interfering RNA targeting vascular endothelial growth factor as cancer therapeutics. *Cancer Research*, 2004; **64**: 3365-3370.

Takena N, Maemura K, Imai Y, *et al.* Endothelial PAS domain protein 1 gene promotes angiogenesis through the transactivation of both vascular endothelial growth factor and its receptor, Flt-1. *Circ Res.*, 2004; **95**: 146-153.

Tamura I, Asada H, Maekawa R, *et al*. Induction of IGFBP-1 Expression by cAMP Is Associated with Histone Acetylation Status of the Promoter Region in Human Endometrial Stromal Cells. *Endocrinology*, 2012; **153**: 5612-21.

Tamura I, Ohkawa Y, Sato T, *et al*. Genome-Wide Analysis of Histone Modifications in Human Endometrial Stromal Cells. *Mol Endocrinol.*, 2014a; **28**: 1656-69.

Tamura I, Sato S, Okada M, *et al*. Importance of C/EBPβ Binding and Histone Acetylation Status in the Promoter Regions for Induction of IGFBP-1, PRL, and Mn-SOD by cAMP in Human Endometrial Stromal Cells. *Endocrinology*, 2014b; **155**: 275-86.

Tanaka J, Qiang L, Banks AS, *et al*. Foxo1 links hyperglycemia to LDL oxidation and endothelial nitric oxide synthase dysfunction in vascular endothelial cells. *Diabetes*, 2009; **58**: 2344-54.

Tanaka N, Miyazaki K, Tashiro H, *et al*. Changes in adenylyl cyclase activity in human endometrium during the menstrual cycle and in human decidua during pregnancy. *J Reprod Fertil.*, 1993; **98**:33-39.

Tang B, and Gurpide E. Direct effect of gonadotropins on decidualisation of human endometrial stromal cells. *J Steroid Biochem Mol Biol*., 1993; **47**(1–6): 115-121.

Tang B, Guller S, and Gurpide E. Cyclic adenosine 3',5'-monophosphate induces prolactin expression in stromal cells isolated from human proliferative endometrium. *Endocrinology*, 1993; **133**(5): 2197-203.

Tang ED, Nuñez G, Barr FG, *et al*. Negative Regulation of the Forkhead Transcription Factor FKHR by Akt. *J Biol Chem*, 1999; **274**: 16741-6.

Tang M, Naidu D, Hearing P, *et al*. LEFTY, a member of the transforming growth factor-β superfamily, inhibits uterine stromal cell differentiation: A novel autocrine role. *Endocrinology*, 2010; **151**(3):1320-1330.

Tang Y, Nakada MT, Rafferty P, *et al*. Regulation of vascular endothelial growth factor expression by EMMPRIN via the PI3K-Akt Signalling pathway. *Mol Cancer Res*., 2006; **4**(6): 371-377.

Tawadros N, Salamonsen LA, Dimitriadis E, *et al*. Facilitation of decidualisation by locally produced ghrelin in the human endometrium. *Mol Hum Reprod*., 2007; **13**: 483-9.

Taylor HS, Arici A, Olive D, *et al*. HOXA10 is expressed in response to sex steroids at the time of implantation in the human endometrium. *J Clin Invest*., 1998; **101**(7): 1379-84.

Taylor HS, Vanden-Heuvel GB, and Igarashi P. A conserved Hoxa10 is in the mouse and human female reproductive system: late establishment and persistent adult expression of the Hoxa cluster genes. *Biol Reprod*., 1997; **57**(6): 1338-45.

Teklenburg G, Salker M, Molokhia M, *et al*. Natural selection of human embryos: decidualizing endometrial stromal cells serve as sensors of embryo quality upon implantation. *PLoS One*, 2010; **5**: e10258.

Telgmann R, and Gellersen B. Marker genes of decidualisation: Activation of the decidual prolactin gene. *Hum Reprod Update*, 1998; **4**(5): 472-479.

Telgmann R, Maronde E, Tasken K, *et al*. Activated protein kinase A is required for differentiation-dependent transcription of the decidual prolactin gene in human endometrial stromal cells. *Endocrinology*, 1997; **138**:929- 937.

Terman BI, Carrion ME, Kovacs E, *et al*. Identification of a new endothelial cell growth factor receptor tyrosine kinase. *Oncogene*, 1991; **6**: 1677-1683.

Thomas CP, Andrews JI, Liu KZ. Intronic polyadenylation signal sequences and alternate splicing generate human soluble Flt1 variants and regulate the abundance of soluble Flt1 in the placenta. *FASEB J*., 2007; **21**: 3885–3895.

Thomas CP, Andrews JI, Raikwar NS, *et al*. A recently evolved novel trophoblast-enriched secreted form of fms-like tyrosine kinase-1 variant is up-regulated in hypoxia and preeclampsia. J *Clin Endocrinol Metab.,* 2009; **94**:2524–2530.

Tierney EP, Tulac S, Huang SJ, *et al*. Activation of the protein kinase A pathway in human endometrial stromal cells reveals sequential categorical gene regulation. *Physiol. Genomics*, 2003; **16**: 47-66.

Timeva T, Shterev A, Kyurkchiev S. Recurrent implantation failure: The role of the endometrium. *J Reprod Infertil*., 2014; **15**(4): 173-183.

Tischer E, Mitchell R, Hartman T, *et al*. The human gene for vascular endothelial growth factor. *J Biol Chem.*, 1991; **266**: 11947–54.

Tochigi H, Kajihara T, Mizuno Y, *et al*. Loss of miR-542-3p enhances IGFBP-1 expression in decidualising human endometrial stromal cells. *Sci Rep.*, 2017; **7**: 40001.

Tong M, Chen Q, James JL, *et al*. Micro- and Nano-vesicles from first trimester human placentae carry Flt-1 and levels are increased in severe preeclampsia. *Endocrinology.*, 2017; **8**: 174.

Tory DS, Leavenworth J, Chang M, Maheshwari V, Groesch K, Ball ER, Torry RJ. Angiogenesis in implantation. *J Assist Reprod Genet.,* 2007; **24**: 303–315.

Tseng L, Gao JG, Chen R, *et al*. Effect of progestin, antiprogestin, and relaxin on the accumulation of prolactin and insulin-like growth factor-binding protein-1 messenger ribonucleic acid in human endometrial stromal cells. *Biol Reprod*, 1992; **47**: 441-450.

Tseng L, Mazella J. Prolactin and its receptor in human endometrium. *Semin Reprod Endocrinol.*, 1999; **17**: 23-27.

Tsui KH, Chen LY, Shieh ML, *et al*. Interleukin-8 can stimulate progesterone secretion from a human trophoblast cell line, *BEWO*. *In Vitro Cell. Dev. Biol.-Animal*., 2004; **40**: 331-336.

Tsuzuki T, Okada H, Cho H, *et al*. Divergent regulation ofangiopoietin-1, angiopoietin-2, and vascular endothelialgrowth factor by hypoxia and female sex steroids in human endometrial stromal cells. *Eur J Obstet Gynecol Reprod Biol.*, 2013; **168**: 95–101.

Turton KB, Annis DS, Rui L, *et al*. Ratios of Four STAT3 Splice Variants in Human Eosinophils and Diffuse Large B Cell Lymphoma Cells. *PLoS ONE*, 2015; **10**: e0127243.

Tzivion G, Dobson M, Ramakrishnan G. FoxO transcription factors; Regulation by AKT and 14-3-3 proteins. *Biochimica et Biophysica Acta (BBA) - Mol Cell Res.,* 2011; **1813**: 1938-45.

Ujvari D, Jakson I, Babayeva S, *et al*. Dysregulation of In Vitro Decidualisation of Human Endometrial Stromal Cells by Insulin via Transcriptional Inhibition of Forkhead Box Protein O1. *PLoS ONE,* 2017; **12**: e0171004.

Valko M, Leibfritz D, Moncol J, *et al*. Free radicals and antioxidants in normal physiological functions and human disease. *Int J Biochem Cell Biol*., 2007; **39**(1): 44-84.

van Mourik MSM, Macklon NS, Heijnen CJ. Embryonic implantation: Cytokines, adhesion molecules, and immune cells in establishing an implantation environment. *J Leukocyte Biol.*, 2009; **85**(1): 4-19.

Vasquez YM, Mazur EC, Li X, *et al*. FOXO1 is Required for Binding of PR on IRF4, Novel Transcriptional Regulator of Endometrial Stromal Decidualisation. *Mol Endocrinol.,* 2015; **29**: 421-33.

Vassilev V, Pretto CM, Cornet PB, *et al*. Response of matrix metalloproteinases and tissue inhibitors of metalloproteinases messenger ribonucleic acids to ovarian steroids in human endometrial explants mimics their gene- and phase-specific differential control in vivo. *J Clin Endocrinol Metab.*, 2005; **90**(10): 5848-5857.

Veillette A, Grenier K, Brasseur K, *et al*. Regulation of the PI3-K/Akt survival pathway in the rat endometrium. *Biol Reprod.*, 2013; **79**: 1-11.

Venners SA, Wang X, Chen C, *et al*. Paternal smoking and pregnancy loss: A prospective study using a biomarker of pregnancy. *Am J Epidemiol.*, 2004; **159**(10): 993-1001.

Verdi J, Tan A, Shoae-Hassani A, *et al*. Endometrial stem cells in regenerative medicine. *J Biol Eng.*, 2014; **8**: 20.

Vincenti V, Cassano C, Rocchi M, *et al*. Assignment of the vascular endothelial growth factor gene to human chromosome 6p21.3. *Circ.*, 1996; **93**: 1493-1495.

Vuorela P, Carpen O, Tulppala M, *et al*. VEGF, its receptors and the Tie receptors in recurrent miscarriage. *Mol Hum Reprod*., 2000; **6** (3):276-282.

Wang W, Taylor RN, Bagchi IC, *et al*. Regulation of human endometrial stromal proliferation and differentiation by C/EBPβ involves cyclin E-cdk2 and STAT3. *Mol Endocrinol.*, 2012; **26**(12): 2016-30.

Wang Y, Lv Y, Gao S, *et al*. MicroRNA profiles in spontaneous decidualized menstrual endometrium and early pregnancy decidua with successfully implanted embryos*. PLoS ONE*, 2016; **11**(1): e0143116.

Wang Y, Zhou Y, Graves DT. FOXO Transcription Factors: Their Clinical Significance and Regulation. *BioMed Res Int.,* 2014; **2014**: 13.

Watanabe H, Nonoguchi K, Sakurai T, *et al*. A novel protein Depp, which is induced by progesterone in human endometrial stromal cells activates Elk-1 transcription factor. *Mol Hum Reprod.*, 2005; **11**(7): 471-6.

Watson H, Franks S, Bonney R. Regulation of epidermal growth factor receptor synthesis by ovarian steroids in human endometrial cells in culture. *J Reprod Fertil.*, 1996; **107**: 199-205.

Weigel D, Jurgens G, Kuttner F, *et al*. The homeotic gene fork head encodes a nuclear protein and is expressed in the terminal regions of the Drosophila embryo. *Cell*, 1989; **57**(4): 645-58.

Weigelt J, Climent I, Dahlman-Wright K, et al. Solution structure of the DNA binding domain of the human forkhead transcription factor AFX (FOXO4). *Biochemistry*, 2001; **40**(20): 5861-5869.

Weimar CH, Kavelaars A, Brosens JJ, *et al*. Endometrial stromal cells of women with recurrent miscarriage fail to discriminate between high- and low-quality human embryos. *PLoS One*, 2012. **7**(7): e41424.

Wen DX, Xu YF, Mais DE, *et al*. The A and B isoforms of the human progesterone receptor operate through distinct signaling pathways within target cells. *Mol Cell Biol.*, 1994; **14**: 8356-8364.

Wenger RH, Stiehl DP, and Camenisch G. Integration of oxygen signaling at the consensus HRE. *Sci. STKE,* 2005*;* **2005**: re12.

Wheeler KC, Jena MK, Pradhan BS, *et al*. VEGF may contribute to macrophage recruitment and M2 polarization in the decidua. *PLoS ONE*, 2018; **13**(1): e0191040.

Whitehead CL, Palmer KR, Nilsson U, *et al*. Placental expression of a novel primate-specific splice variant of sFlt-1 is upregulated in pregnancies complicated by severe early onset pre-eclampsia. *BJOG*, 2011; **118**(10): 1268-71.

Wilcox AJ, Baird DD, and Weinberg CR. Time of implantation of the conceptus and loss of pregnancy. *N Engl J Med.*, 1999; **340**(23): 1796-9.

Winn VD, Gormley M, Fisher SJ. The impact of preeclampsia on gene expression at the maternal-fetal interface. *Pregnancy Hypertens*., 2011; **1**: 100–108.

Wu Y, Halverson G, Basir Z, *et al*. Aberrant methylation at HOXA10 may be responsible for its aberrant expression in the endometrium of patients with endometriosis. *Obstet Gynecol*., 2005; **193**(2): 371-380.

Wynn RM. Ultrastructural development of the human decidua. *Am J Obstet Gynecol.*, 1974; **118**(5): 652-670.

Xiao Z, Li S, Yu Y, *et al*. VEGF-A regulates sFlt-1 production in trophoblasts through both Flt-1 and KDR receptors. *Mol Cell Biochem.,* 2018. https://doi.org/10.1007/s11010-018-3337-5.

Xie Y, Cui D, Kong Y. FoxM1 influences embryo implantation and is regulated by 17 beta-estradiol and progesterone in mouse uteri and endometrium cells. *Int J Clin Exp Pathol.*, 2014; **7**(10): 6585-6595.

Xu G, Guimond M, Chakraborty C, *et al*. Control of proliferation, migration, and invasiveness of human extravillous trophoblast by decorin, a decidual product. *Biol Reprod.*, 2002; **67**(2): 681-689.

Yang H, Zhou Y, Edelshain B, *et al*. FKBP4 is regulated by HOXA10 during decidualisation and in endometriosis. *Reproduction*, 2012; **143**: 531-8.

Yang ZZ, Tschopp O, Di-Poi N, *et al*. Dosage-dependent effects of Akt1/protein kinase Balpha (PKBalpha) and Akt3/PKBgamma on thymus, skin, and cardiovascular and nervous system development in mice. *Mol Cell Biol.*, 2005; **25** (785): 10407-10418.

Yoshie M, Kusama K and Tamura K. Molecular mechanisms of human endometrial decidualisation activated by cyclic adenosine monophosphate signaling pathways. *J Mammal Ova Res.*, 2015; **32**(3): 95-102.

Yoshino O, Osuga Y, Hirota Y, *et al*. Akt as a possible intracellular mediator for decidualisation in human endometrial stromal cells. *Mol Hum Reprod*., 2003; **9**(5): 265-269.

Yoshino O, Osuga Y, Hirota Y, *et al*. Endometrial stromal cells undergoing decidualisation down-regulate their properties to produce proinflammatory cytokines in response to interleukin-1β via reduced p38 mitogen-activated protein kinase phosphorylation. *J Clin Endocrinol Metab*., 2003b; **88**(5): 2236-2241.

Yuan Z, Lehtinen MK, Merlo P, *et al*. Regulation of neuronal cell death by MST1-FOXO1 signaling. *J Biol Chem*., 2009; **284**: 11285-11292.

Yuhki M, Kajitani T, Mizuno T, *et al*. Establishment of an immortalized human endometrial stromal cell line with functional responses to ovarian stimuli Munehiro. *Reprod Biol Endocrinol*, 2011; **9**: 104.

Zenclussen ML, Linzke N, Schumacher A, *et al.* Heme oxygenase-1 is critically involved in placentation, spiral artery remodelling, and blood pressure regulation during murine pregnancy. *Front Pharmacol.*, 2014; **5**: 291.

Zhang L, Rees MCP and Bicknell R. The isolation and long-term culture of normal human endometrial epithelium and stroma. Expression of mRNAs for angiogenic polypeptides basally and on oestrogen and progesterone challenges. *J Cell Sci.*, 1995; **108**: 323-331.

Zhang P, Tang M, Zhong T, *et al*. Expression and function of Kisspeptin during mouse decidualisation. *PLoS ONE,* 2014; **9**(5): e97647.

Zhang S, Lin H, Kong S, *et al*. Physiological and molecular determinants of embryo implantation. *Mol Aspects Med.,* 2013; **34**: 939-80.

Zhang X, Gan L, Pan H, *et al*. Phosphorylation of serine 256 suppresses transactivation by FKHR (FOXO1) by multiple mechanism. *J Biol Chem.*, 2002; **277**(47): 45276-45284.

Zhang X, Tang N, Hadden TJ, *et al*. Akt, FoxO and regulation of apoptosis. *Biochim Biophys Acta*, 2011; **1813**: 1978-86.

Zhou J, Dsupin BA, Giudice LC, *et al*. Insulin-like growth factor system gene expression in human endometrium during the menstrual cycle. *J Clin Endocrinol Metab.,* 1994*;* **79**: 1723-173.

Zhou Y, Damsky CH, Fisher SJ. Preeclampsia is associated with failure of human cytotrophoblasts to mimic a vascular adhesion phenotype. One cause of defective endovascular invasion in this syndrome? *J Clin Invest*, 1997; **99**: 2152–2164.

Zhu WL, Tong H, Teh JT, *et al*. Forkhead Box Protein O3 Transcription Factor Negatively Regulates Autophagy in Human Cancer Cells by Inhibiting Forkhead Box Protein O1 Expression and Cytosolic Accumulation. *PLoS ONE*, 2014; **9**(12): e115087.

Presentations and posters related to this Thesis

ICVS Away Day
24th June 2016, Birmingham, UK
Poster Presentation: Regulation of Vascular Endothelial Growth Factor-A (VEGF) Activity during Endometrial Stromal Cell Decidualisation
Ling Ting, Sarah Conner and Peter Hewett

ICVS Away Day
9th June 2017, Birmingham, UK
Poster Presentation: FoxO3a Antagonises FoxO1-driven VEGF Expression During Endometrial Stromal Cell Decidualisation.
Ling Ting, Sarah Conner and Peter Hewett

4th World Congress of Reproductive Biology (WCRB)
27-29th September 2017, Okinawa, Japan
Poster Presentation: Vascular Endothelial Growth Factor-A (VEGF) Activity and Regulation in Decidualised Endometrial Stromal Cells.
Ling Ting, Sarah Conner and Peter Hewett

Fertility 2018 Conference
3-6th January 2018, Liverpool, UK
Poster Presentation: Soluble Fms-like Tyrosine Kinase-1 (sFlt-1) Secretion Decreases During Endometrial Stromal Cell Decidualisation.
Ling Ting, Sarah Conner and Peter Hewett

ICVS and Reproductive Biology and Genetics (RBG) Seminar
16th and 17th May 2018, Birmingham, UK
Oral Presentation: Regulation of Vascular Endothelial Growth Factor-A (VEGF) Activity in Human Endometrial Stromal Cell Decidualisation.
Ling Ting